UNIVERSITÀ DEGLI STUDI DI NAPOLI FEDERICO II

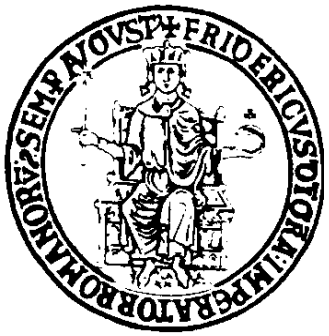

Scuola Politecnica e delle Scienze di Base

Dipartimento di Ingegneria Civile, Edile e Ambientale

DOTTORATO DI RICERCA IN INGEGNERIA DEI SISTEMI CIVILI
XXXIV CICLO

Ph.D. Thesis

"DARK AND PHOTO FERMENTATION FOR MIXED CULTURE BIOREFINERY: ENERGY AND CHEMICALS PRODUCTION FROM WASTE"

Grazia Policastro

Ph.D. Coordinator
Prof. Eng. Andrea Papola

Promotor
Prof. Eng. Massimiliano Fabbricino
Co-Promotor
Dr. Eng. Vincenzo Luongo

Contents

Abstract **iv**

PART 1: Valorisation of agri-food feedstocks by mixed culture fermentation into lactic acid

Chapter 1 – Dark and photo fermentation for mixed culture biorefinery: Energy and chemicals production from waste **1**

1.1.Introduction 2

References 7

Chapter 2 - Repeated-batch fermentation of cheese whey for semi-continuous lactic acid production using mixed cultures at uncontrolled pH **10**

2.1. Introduction 11

2.2. Materials and methods 13

2.3. Results 15

2.4. Discussion 20

2.5. Conclusions 24

References 25

PART 2: Photo fermentation of agri-food feedstocks and dark fermentation effluents for hydrogen and PHAs production

Chapter 3 - A preliminary study on a novel bioaugmentation technique enhancing lactic acid production by mixed cultures fermentation **29**

3.1. Introduction 30

3.2. Materials and methods 32

3.3. Results and discussion 35

3.4. Conclusions 45

References 46

Chapter 4 - Carbon Catabolite Repression occurrence in photo fermentation of ethanol-rich substrates: effect of the ethanol to glycerol ratio **52**

4.1. Introduction 53

4.2. Materials and methods 54

4.3. Results and discussion 57

4.4. Conclusions 67

References 69

Chapter 5 - Enhancing hydrogen production by photo fermentation of ethanol rich dark fermentation effluents **73**

5.1. Introduction 74
5.2. Materials and methods 77
5.3. Results and discussion 80
5.4. Conclusions 88
References 90
Chapter 6 - Biohydrogen and poly-β-hydroxybutyrate production by winery wastewater photo fermentation: Effect of substrate concentration and nitrogen source 98
6.1. Introduction 99
6.2. Materials and methods 101
6.3. Results 104
6.4. Discussion 108
6.5. Conclusions 113
References 115
Chapter 7 - Mixed cultures enhance hydrogen production in single stage photo fermentation processes 121
7.1. Introduction 122
7.2. Materials and methods 123
7.3. Results and discussion 127
7.4. Conclusions 132
References 133
Chapter 8 - A comprehensive review of mathematical models of photo fermentation 138
8.1. Introduction 139
8.2. Environmental factors affecting photo fermentation 141
8.3. Kinetic models 142
8.4. Parametric models 151
8.5. Non-ideal reactor models 156
8.6. Models comparison and future perspectives 163
References 166
Appendix A 174
Appendix B 178
PART 3: Other biorefinery processes
Chapter 9 - Improving biological production of poly(3-hydroxybutyrate-co-3-hydroxyvalerate) (PHBV) co-polymer: a critical review 181

9.1. Introduction 182
9.2. PHBV biosynthesis processes, characteristics and applications 185
9.3. Techno-economic analysis and production strategies 188
9.4. Microorganisms as production strategy 201
9.5. Strategies related to substrates 206
9.6. Combination of different strategies 214
9.7. Operating conditions 216
9.8. Discussion 220
9.9. Conclusions 223
References 225
Chapter 10 - A chemostat enrichment system to induce lipids accumulation in microalgae 239
10.1. A chemostat enrichment system to induce lipids accumulation in microalgae 240
10.2. Materials and methods 248
References 251
Chapter 11 – Conclusions and perspectives 254

Abstract

Over the last decades, the interest of sustainable alternative technologies for energy and chemicals production is dramatically increasing. Contextually, the waste production is driving governments to promote more efficient processes to reduce the amount of residues and favour a more sustainable bioeconomy. In this context, biorefining systems, based on waste utilisation, are promising alternative to fossil fuels-based processes for biofuel and/or chemicals production. The use of waste biomass requires bioconversions to be performed by mixed cultures rather than pure ones. Mixed cultures with the desired metabolic capacity have the advantage to not require sterilization of the inflow, to confer higher robustness and lower costs to processes and can prevent inhibition phenomena. However, little is known about mixed cultures applications, based on the adoption of a selecting environment rather than a pure culture. In this thesis, different mixed culture biotechnologies have been studied and applied to improve by-products valorisation in a biorefinery concept. The thesis consists of three different parts related to: i) Valorisation of agri-food feedstocks by mixed-culture fermentation into lactic acid; ii) Photo fermentation of agri-food feedstocks and dark fermentation effluents for hydrogen and PHAs production; iii) Other biorefinery processes. In detail, different applications of the dark fermentation process have been tested, including lactic acid production and hydrogen production. Moreover, the generation of dark fermentation effluents rich in ethanol has been studied as a strategy to enhance the hydrogen production in the photo fermentative step of two stages dark and photo fermentation processes. Also, the photo fermentation process has been studied as a single stage process, under both experimental and modelling approaches. The photo fermentative concomitant generation of hydrogen and PHAs has been investigated. Moreover, strategies to produce PHBV have been extensively studied, as this specific co-polymer can represent one of the most interesting future applications to valorise dark fermentation effluents. Finally, lipids induction in continuous microalgal cultivation systems has been tested. Results show how to optimize operational conditions, to create selective environments in which mixed cultures displaying a desired functionality are enriched. Moreover, the feasibility and the advantages of mixed cultures applications over pure ones has been demonstrated. The main findings of this thesis represent a step forward in the field of mixed cultures biotechnologies and interesting starting points for many possible future research directions aimed at the scale up of the studied processes.

Chapter 1

Dark and photo fermentation for mixed culture biorefinery:

Energy and chemicals production from waste

Dark and photo fermentation for mixed culture biorefinery: Energy and chemicals production from waste

1.1 Introduction

To contrast greenhouse gases (GHG) emissions, global warming and natural resources depletion, international policies are promoting an alternative "bioeconomy", based on biorefining systems [1]. The most exhaustive definition of biorefinery was introduced by the International Energy Agency (IEA) Bioenergy Task 42, established in 2007 to acknowledge the increasing relevance of biorefinery in a sustainable bioenergy research context: "*Biorefining is the sustainable processing of biomass into a spectrum of marketable products and energy*".

Traditionally, biomass is a generic term to define all materials derived from plants. However, in the last decades, the definition of biomass has moved from a simple ecological concept to a biorefinery-oriented concept, as indicated by the 2009/28/EC Directive of the European Parliament: "*The biomass is the biodegradable fraction of products, waste and residues from biological origin from agriculture (including vegetal and animal substances), forestry and related industries including fisheries and aquaculture, as well as the biodegradable fraction of industrial and municipal waste.*" [2].

The use of waste biomass feedstocks in biorefining systems represent an appropriate strategy for the green production of commercial products and sustainable energy, contextually with the cost-efficient use of bioresources, the reduction and valorisation of wastes [3]. In this context, biological anaerobic processes represent a promising technology to produce value added chemicals and green energy from wastes. The increasing interest on anaerobic processes from both academia and industries relies on their versatility in terms of substrate application range and integration in developed biorefining systems [4].

Anaerobic digestion (AD) is one of the most well-known and established processes for the stabilization and valorisation of organic wastes. In this process, organic compounds can be degraded into a methane-rich biogas and a stable digestate via a series of sequential biological reactions operated by specific bacterial species [5].

Over the last decades, increasing attention has been directed towards the study of an alternative anaerobic process, named Dark Fermentation (DF). DF is a modification of the AD process, aimed at the conversion of organic compounds to a hydrogen-rich biogas and/or valuable chemicals [6]. Mixed culture DF can result in a wide range of intermediates and by-products, depending on the operational conditions that influence the microbial community structure [7], such as: i) substrate characteristics; ii) loading rate; iii) temperature, pH, and other operating and environmental conditions. One of the most studied DF applications is the production of biohydrogen, which has gained considerable interests in the energy and environmental sector. Indeed, compared to other biofuels, hydrogen own the highest specific energy content (122 MJ/kg) and clean combustion properties [8]. Usually, when the substrate bioconversion is addressed to hydrogen production, the dark fermentation effluent (DEF) contains a mix of volatile fatty acids (VFAs), such as acetic, butyric and propionic acid [9]. However, alternative metabolic pathways can lead to a limited or null hydrogen production and the generation of DFEs containing other high purity chemicals. For instance, species communities such as *Bacillus* spp. or *Lactobacillus* spp. can lower the hydrogen yield, directing the substrate bioconversion to lactic acid (LA) generation [7]. This alternative application is also gaining a considerable interest. Indeed, LA is a valuable chemical, as it can be used in pharmaceutical, food and chemical industries and for the production of polylactic acid (PLA) polymers, with the aim of replacing petrolchemical plastics [10]. In the case of fermentative LA production, the main challenge for large scale applications is the production of a high purity effluent and elevate LA concentration, in order to allow for a low-cost extraction [11]. On the other hand, the key challenge of DF aimed at hydrogen production relies on the valorisation of the VFAs mix, remaining as major fermentation by-products within the bulk liquid [9].

Many authors underlined that the DF process aimed at hydrogen production could be perfectly integrated in many biorefining systems, as the DF by-products could be used in subsequent biological processes for the production of fuels and/or chemicals [12,13]. A striking example of an integrated biorefining system is represented by the combination of the DF process with a consequent photo fermentation (PF) stage. The combined DF–PF process not only results in a higher hydrogen productivity compared to the DF alone, but also in obtaining a stable liquid effluent. Indeed, the organic acids usually present in DFEs are suitable carbon sources for purple non sulfur bacteria (PNSB), performing the PF

process [9]. Under anaerobic conditions, PNSB carry out the photosynthesis using light and reduced carbon sources to produce hydrogen. The use of light as energy source is regulated by the photosystem I of PNSB, which allows for the accumulation of photons within the cell membrane and a consequent formation of an energy gradient towards the liquid phase. On the other hand, the assimilation of the substrate leads to a proton gradient formation, which stimulates the production of energy in the form of ATP, allowing for the final hydrogen production [14].

Along with hydrogen generation, PNSB are also able to store polyhydroxybutyrate (PHB) in their cytoplasm [15]. PHAs are valuable biopolymers, which represent the most promising candidates for the production of totally biodegradable plastic materials. Over the last few years, the combined production of energy and materials from waste is gaining great attention. This new approach can replace fossil fuels with organic matter as a source of both biofuels and bioplastics [16]. The production of PHAs represents an added value in the PF processes and a very interesting option in the valorization of DFEs. In particular, the use of DFEs rich in propionic acid for PHAs production, can lead to the generation of a co-polymer, the polyhydroxybutyrate-co-hydroxyvalerate (PHBV), that owns better thermal and mechanical properties compared to and all other PHAs [17].

Due to the wide variety of organic compounds which can be assimilated by PNSB (e.g. short chain acids, alcohols, sugars), PF can be conducted as a single stage process, as well. In this case, the main challenges are related to the presence of complex and/or toxic compounds in the waste substrates and the optimization of the hydrogen productivity [18]. Currently, the complex mechanism of PF is far from being completely elucidated. Therefore, more studies are required to clarify the behaviour of PNSB under different environmental and feed conditions, both under single stage PF and two stage DF-PF. To this attempt, the use of mathematical models could be helpful to effectively understand and control the process. Mathematical models can simulate the influence of different environmental and operational conditions, therefore decreasing the load of the experimental tests, which are costly and time-consuming [19].

Another interesting option for biofuels production from waste are the third generation biorefining systems, based on microalgae [20]. Indeed, via the photosynthesis process, microalgae can convert CO_2 into organic compounds with high energy content [21]. The organic compounds accumulated by microalgae are starch and lipids, which are, respectively, precursors of bioethanol and biodiesel. Among the mentioned compounds,

lipids production is a preferable option due to the higher energy density and lower downstream energy cost [22]. Microalgae derived biodiesel can be used in existing systems, with little modifications of vehicle engines and represent a suitable renewable alternative to the petroleum derived diesel. [23]. However, more efforts are required to find a suitable lipids induction technique in microalgae.

Currently, one of the main drawbacks to the scale-up of all the mentioned biological systems is the wide use of pure cultures, which require aseptic environments and carefully controlled conditions, to avoid contamination issues. Nevertheless, focusing on a desired characteristic rather than on a specific strain, the issue of contamination can become a value [24]. By manipulating the bioprocess operation or varying the inoculum source, it is possible to enrich a suitable mixed culture, based on the natural selection. The mixed cultures with the desired metabolic capacity have the advantage not to require the sterilization of the inflow [25]. Moreover, mixed cultures confer higher robustness and lower costs to processes and can adapt to a wider range of conditions, preventing inhibition phenomena [26]. However, little is known about the conditions to apply to obtain suitable selective environments for the mentioned bioprocesses and the effectiveness of such technologies under the use of mixed cultures. Therefore, the leading research question of this work is: ***How to efficiently apply the use of mixed cultures to produce energy and valuable chemicals via dark and photo fermentation of waste biomass?***

This thesis deals with waste biomass valorisation via mixed cultures biological processes. Different applications of the DF process have been studied, including lactic acid production and hydrogen production. Particular attention has been given to the valorisation of the DFEs resulting from the hydrogen production process, via the double stage DF-PF process. The production of DFEs rich in ethanol has been studied as a strategy to enhance the hydrogen production in the PF step. The PF process has been studied as a single stage process, as well. A particular focus has been given to the concomitant generation of both hydrogen and PHAs, and a comprehensive literature study of PF mathematical models has been performed. Moreover, strategies to produce PHBV have been extensively studied, as this specific co-polymer can represent one of the most interesting future applications to valorise DFEs. Finally, lipids induction in continuous microalgal cultivation systems has been studied. **Figure 1.1** shows the structure of the thesis.

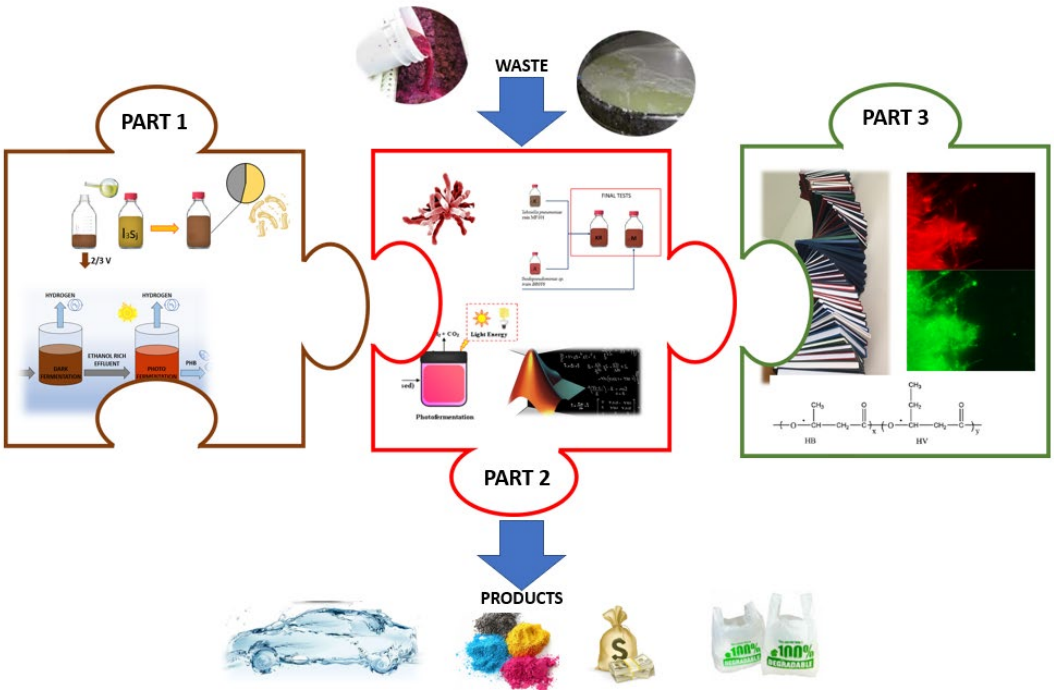

Figure 1.1. Graphic reproduction of the thesis structure

In detail, the overall structure of the thesis takes the following form:

PART 1: **Valorisation of agri-food feedstocks by mixed-culture fermentation into lactic acid**

Chapter 2 introduces the fermentative lactic acid production from cheese whey, studying the optimization of a semi-continuous reactor;

Chapter 3 presents a preliminary study on a bioaugmentation technique to select a mixed culture producing lactic acid from digestate;

PART 2: Photo fermentation of agri-food feedstocks and dark fermentation effluents for hydrogen and PHAs production

Chapter 4 elucidates the behaviour of PNSB in the presence of mixed substrates representative of a DFE containing ethanol and glycerol;

Chapter 5 shows the applicability of a sequential DF-PF process, promoting ethanol production in the dark fermentation stage and minimizing the DFE pre-treatments;

Chapter 6 introduces the single stage photo fermentation process and focuses on the optimization of conditions to promote the contextual production of hydrogen and polyhydroxybutyrate (PHB) from winery wastewater;

Chapter 7 compares hydrogen and PHB production of pure dark and photo fermentative bacteria and mixed cultures containing both dark and photo fermentative bacteria, under photo fermentative conditions;

Chapter 8 presents a comprehensive literature study on mathematical models of the photo fermentation process;

PART 3: Other biorefinery processes

Chapter 9 presents a literature study on strategies to improve PHBV production;

Chapter 10 introduces a technique to enrich a lipid storing microalgal community in chemostat systems;

Chapter 11 highlights the major findings and implications of the research and provides perspectives

References

[1] de Jong E, Jungmeier G. Biorefinery Concepts in Comparison to Petrochemical Refineries. Elsevier B.V.; 2015. https://doi.org/10.1016/B978-0-444-63453-5.00001-X.

[2] Directive 2009/28/EC of the European Parliament and of the Council of 23 April 2009 on the promotion of the use of energy from renewable sources and amending and subsequently repealing Directives 2001/77/EC and 2003/30/EC. Official Journal of the European Union, 5, p.2009.

[3] Sillanpää M., Ncibi C. (2017) Biomass: The Sustainable Core of Bioeconomy. In: A Sustainable Bioeconomy. Springer, Cham. https://doi.org/10.1007/978-3-319-55637-6_3

[4] Cherubini F. The biorefinery concept: Using biomass instead of oil for producing energy and chemicals. Energy Convers Manag 2010;51:1412–21. https://doi.org/10.1016/j.enconman.2010.01.015.

[5] Ariunbaatar, J., Panico, A., Esposito, G., Pirozzi, F., & Lens, P. N. (2014). Pretreatment methods to enhance anaerobic digestion of organic solid waste. *Applied energy*, *123*, 143-156.

[6] Boshagh, F., & Rostami, K. (2020). A review of application of experimental design techniques related to dark fermentative hydrogen production. *Journal of Renewable Energy and Environment*, *7*(2), 27-42.

[7] Ghimire A, Frunzo L, Pirozzi F, Trably E, Escudie R, Lens PNL, et al. A review on dark fermentative biohydrogen production from organic biomass: Process parameters and use of by-products. Appl Energy 2015;144:73–95. https://doi.org/10.1016/j.apenergy.2015.01.045.

[8] Policastro G, Luongo V, Fabbricino M. Biohydrogen and poly-β-hydroxybutyrate production by winery wastewater photofermentation: Effect of substrate concentration and nitrogen source. J Environ Manage 2020;271:111006. https://doi.org/10.1016/j.jenvman.2020.111006.

[9] Luongo V, Ghimire A, Frunzo L, Fabbricino M, d'Antonio G, Pirozzi F, et al. Photofermentative production of hydrogen and poly-β-hydroxybutyrate from dark

fermentation products. Bioresour Technol 2017;228:171–5. https://doi.org/10.1016/J.BIORTECH.2016.12.079.

[10] Liang S, McDonald AG, Coats ER. Lactic acid production from potato peel waste by anaerobic sequencing batch fermentation using undefined mixed culture. Waste Manag 2015;45:51–6. https://doi.org/10.1016/J.WASMAN.2015.02.004.

[11] Ahmad, A., Banat, F., & Taher, H. (2020). A review on the lactic acid fermentation from low-cost renewable materials: Recent developments and challenges. *Environmental Technology & Innovation*, 101138.

[12] Bastidas-Oyanedel, J.R., Bonk, F., Thomsen, M.H. and Schmidt, J.E., 2015. Dark fermentation biorefinery in the present and future (bio) chemical industry. Reviews in Environmental Science and Bio/Technology, 14(3), pp.473-498.

[13] Dahiya, S., Chatterjee, S., Sarkar, O., & Mohan, S. V. (2021). Renewable hydrogen production by dark-fermentation: Current status, challenges and perspectives. *Bioresource Technology*, *321*, 124354.

[14] Tiang, M. F., Hanipa, M. A. F., Abdul, P. M., Jahim, J. M., Mahmod, S. S., Takriff, M. S., ... & Wu, S. Y. (2020). Recent advanced biotechnological strategies to enhance photo-fermentative biohydrogen production by purple non-sulphur bacteria: an overview. *International Journal of Hydrogen Energy*, *45*(24), 13211-13230.

[15] Monroy, I., & Buitrón, G. (2020). Production of polyhydroxybutyrate by pure and mixed cultures of purple non-sulfur bacteria: A review. *Journal of biotechnology*, *317*, 39-47.

[16] Pagliano G, Ventorino V, Panico A, Pepe O. Integrated systems for biopolymers and bioenergy production from organic waste and by-products: A review of microbial processes. Biotechnol Biofuels 2017;10:1–24. https://doi.org/10.1186/s13068-017-0802-4.

[17] Tebaldi ML, Maia ALC, Poletto F, de Andrade FV, Soares DCF. Poly(-3-hydroxybutyrate-co-3-hydroxyvalerate) (PHBV): Current advances in synthesis methodologies, antitumor applications and biocompatibility. J Drug Deliv Sci Technol 2019;51:115–26. https://doi.org/10.1016/j.jddst.2019.02.007.

[18] Eroğlu E, Gündüz U, Yücel M, Türker L, Eroğlu I. Photobiological hydrogen production by using olive mill wastewater as a sole substrate source. Int J Hydrogen Energy 2004. https://doi.org/10.1016/S0360-3199(03)00110-1.

[19] Basak N, Jana AK, Das D. CFD modeling of hydrodynamics and optimization of photofermentative hydrogen production by Rhodopseudomonas palustris DSM 123 in annular photobioreactor. Int J Hydrogen Energy 2016;41:7301–17. https://doi.org/10.1016/j.ijhydene.2016.02.126.

[20] Behera B, Unpaprom Y, Ramaraj R, Maniam GP, Govindan N, Paramasivan B. Integrated biomolecular and bioprocess engineering strategies for enhancing the lipid yield from microalgae. Renew Sustain Energy Rev 2021;148:111270. https://doi.org/10.1016/j.rser.2021.111270.

[21] Mooij PR, Stouten GR, Tamis J, Van Loosdrecht MCM, Kleerebezem R. Survival of the fattest. Energy Environ Sci 2013;6:3404–6. https://doi.org/10.1039/c3ee42912a.

[22] Li T, Gargouri M, Feng J, Park JJ, Gao D, Miao C, et al. Regulation of starch and lipid accumulation in a microalga Chlorella sorokiniana. Bioresour Technol 2015;180:250–7. https://doi.org/10.1016/j.biortech.2015.01.005.

[23] Mata TM, Martins AA, Caetano NS. Microalgae for biodiesel production and other applications: A review. Renew Sustain Energy Rev 2010;14:217–32. https://doi.org/10.1016/j.rser.2009.07.020.

[24] Mooij PR. On the use of selective environments in microalgal cultivation. 2016.

[25] Kleerebezem R, van Loosdrecht MC. Mixed culture biotechnology for bioenergy production. Curr Opin Biotechnol 2007;18:207–12. https://doi.org/10.1016/j.copbio.2007.05.001.

[26] Sali, S., & Mackey, H. R. (2021). The application of purple non-sulfur bacteria for microbial mixed culture polyhydroxyalkanoates production. *Reviews in Environmental Science and Bio/Technology*, *20*(4), 959-983.

PART 1

Valorisation of agri-food feedstocks by mixed culture fermentation into lactic acid

Chapter 2

Repeated-batch fermentation of cheese whey for semi-continuous lactic acid production using mixed cultures at uncontrolled pH

This chapter has been published as: Luongo, V., Policastro, G., Ghimire, A., Pirozzi, F., and Fabbricino, M. (2019). Repeated-batch fermentation of cheese whey for semi-continuous lactic acid production using mixed cultures at uncontrolled pH. Sustainability, 11(12), 3330.

Repeated-batch fermentation of cheese whey for semi-continuous lactic acid production using mixed cultures at uncontrolled pH

Abstract

The paper investigates mixed-culture lactate (LA) fermentation of cheese whey, in order to verify the possibility of using waste materials as feedstock to produce a high economical potential product. Fermentation performances of two reactors operating in repeated-batch mode at uncontrolled pH conditions were evaluated in terms of LA production, varying the hydraulic retention time and the feeding conditions. Five experimental phases were conducted. The hydraulic retention time (HRT) was varied from 1 to 4 d to verify its effect on process performances. Best results, corresponding to maximum LA concentration (20.1 g LA/L), and maximum LA yield (0.37 g $COD_{(LA)}$/g $COD_{(CW)}$) were reached feeding the reactors with cheese whey alone, setting the HRT to 2 d. The maximum value of extracted lactic acid mass (10.6 g LA/L d) was observed, instead, decreasing the HRT to 1.

2.1. Introduction

Waste biomass from food processing industries can be seen as an abundant source for biorefineries aimed at industrial production of biofuels and value-added chemicals [1]. Dairy industries, for example, makes an important contribution to the production of liquid effluents, rich in organic substances characterized by significant contents of lactose (0.18 - 60 kg/m^3), protein (1.4 -33.5 kg/m^3) and fats (0.08 -10.58 kg/m^3) [2,3]. The generation of a liquid effluent, i.e. cheese whey (CW), is estimated at 0.8 - 0.9 L per liter of treated milk, or 9 kg per kg of produced cheese [2,4,5]. The total amount of produced CW worldwide is estimated around 180-190 million tons per year, and only half of this by-product is successively used for food or feed production [4]. On the other hand, around 100 million tons per year are typically discarded as a waste by-product in the environment, representing a significant issue for traditional wastewater treatment plants. Moreover, different functional proteins with high nutritional and therapeutic properties can be obtained from CW purification, using a wide variety of separation techniques [5]. The chemical composition and the characteristics of the CW depend on the type of milk as well as on the adopted cheese production technique. However, generally, CW has a minerals content of about 0.46 ± 10%, and a concentration of total suspended solids ranging between 0.1 - 22 g/L. Other typical characteristics are: pH in the range 3.3 - 9.0, phosphorus content of 0.006 - 0.5 g/L, total Kjeldahl nitrogen (TKN) of 0.01 - 1.7 g/L, chemical oxygen demand (COD) values in the interval 0.8 - 102 g/L and biological

oxygen demand (BOD) values in the range 0.6 - 60 g/L [2,3]. Therefore, while CW processing in conventional wastewater treatment plants can be quite challenging, this waste biomass could be conveniently used as valuable feedstocks for the production of bio-fuels and biochemicals.

A sustainable route for the production of biofuels and biochemicals is the development of biorefineries based on renewable biomass sources [6]. This is why anaerobic fermentation-based bioprocesses, such as dark fermentation (DF) and anaerobic digestion (AD), have been widely tested an applied for the production of bio-hydrogen (H_2), bio-methane (CH_4) and several biochemicals, including high-value organic acids (i.e. acetate, lactate, butyrate) [7]. Among others, lactic acid is probably one of the most interesting products of anaerobic fermentation, being widely used in food industries as preservative compound, curing agent, and flavoring agent, in cosmetics and pharmaceuticals such as skin care products. Moreover, lactic acid can be chemically treated for the production of biological plastics, a natural alternative to petrochemical plastics that represents, as well known, a significant, environmental problem [7–9]. Even though most of the lactic acid used today is derived from biological routes, its production cost could be much more competitive if the used feedstock, which accounts for more than 70% of the production costs [10,11], is represented by organic wastes. To this aim, CW can serve as an excellent feedstock for the production of lactic acid. However, several past studies have been carried out on pure cultures under axenic conditions [12–15]. To the best of our knowledge, only a few studies used mixed culture inoculum and complex substrates as fermentation feedstock [16,17]. The maintenance operation for axenic conditions and the use of a pH buffer may have significant cost implications on the lactic acid production economy [18]. Therefore, the use of mixed culture and real waste feedstock were adopted in this study, as they represent crucial aspects for the development and application of a sustainable waste based biorefinery.

The aim of this paper is to assess the application of dark fermentative lactic acid production using CW mediated by mixed cultures. Among other biological conversion technologies, DF is considered particularly interesting, as it allows the production of multiple biofuels and other platform chemicals from waste biomasses [10–14]. The study also aims at maximizing the lactate yields along with optimal process stability at the natural pH of the substrate. Different managing techniques have been adopted using two lab-scale fermentative bioreactors for lactic acid production from CW. The effect of digestate addition on lactic acid production and fermentation performances has been highlighted. The presented results constitute an interesting starting point for scaled-up

applications in the field of CW valorisation and lactic acid production by mixed cultures fermentation.

2.2. Materials and Methods

2.2.1. Substrate and inoculum

The substrate used in the present study was obtained from the dairy company La Perla del Mediterraneo, located in Capaccio (Salerno, Italy). The company exports a wide variety of products in different European and extra European countries (i.e. USA and Asia) being one of the larger company of the area of Salerno. After sampling, CW was immediately frozen at -20° C to keep its characteristic as unaltered as possible.

The anaerobic digestate used as inoculum for the DF was collected from the full-scale treatment plant of the same facility, adopted for the anaerobic co-digestion of CW and buffalo manure. The digestate was pre-treated at 105 °C for 1.5 hours to inhibit methanogenic species, which are more sensitive to heat shocks than acetogenic and fermentative bacteria [22].

The main characteristics of the adopted substrate and inoculum were evaluated in triplicate and are reported in Table 1.

Table 1.1. Characteristics of the used cheese whey and inoculum. CW= cheese whey

	TS (g/L)	**VS (g/L)**	**COD (gCOD/L)**	**pH (-)**	**Soluble Carbohydrates (g/L)**
CW	47.0±0.5	39±1	49±2	5.6	37±5
Inoculum	50±4	30±2	41±3	7.5	-

2.2.2. Experimental setup and operational conditions

2.2.2.1 Dark fermentation bioreactor

DF process was conducted using two 2 L glass reactors, maintained under mesophilic conditions (35 ± 1 °C) and operated in repeated-batch mode aimed at semi-continuous lactic acid production. Constant stirring conditions of 250 rpm were adopted for both the reaction units. Differently from fed-batch reactors, repeated-batch feeding mode ensure a constant reaction volume in bioreactors, which is more similar to the real-scale feeding

strategy usually adopted for wet anaerobic treatment plants. The feeding strategy is deeply connected to the sampling strategy as they are contextual at each feeding day. This allows for a semi-continuous production of lactic acid being the reactors operated continuously for the whole experimental time. The reactors were equipped with three different ports. The first one was connected to an external tank, and used to feed the CW. The second one was utilized for effluent extraction. The last one, placed on the top of the reactor, was devoted to biogas extraction and to head-space gas analysis. Glass tube and gaskets were used for the junctions. Sealing joints were controlled filling up each reactor, before use, with water and pressurized air.

2.2.2.2 Experimental conditions

The experimental test was conducted for 136 days, with no pH correction, and was characterized by five distinct operative phases, as indicated in Table 2. Phase 1 (start-up phase) was conducted in batch mode, assigning a substrate to inoculum ratio equal to 1.9 gVS/gVS. The other phases, instead, were conducted in repeated-batch mode, varying, for each of them, the value of the hydraulic retention time (HRT). 400 mL of inoculum was added to the reactor at the beginning of phase 2 and phase 3, and after each HRT of these phases. No inoculum addition was operated, instead, before or during phase 4 and phase 5. This choice was adopted to simulate the management of a real-scale anaerobic digester operating in wet condition. According to the assigned operative conditions, the organic loading rate (OLR) increased during the experimental operations (Table 2). At selected times, small volumes of the influent and the effluent from the two reactors were sampled to check the pH value and to measure the concentration of organic acids (OAs) and ethanol (EtOH). Moreover, the characteristics of the used cheese whey were analyzed daily to monitor their variation.

Table 2.2. Operative conditions of the different experimental phases.

Phase	**1**	**2**	**3**	**4**	**5**
OLR (kg VS/m^3/d)	batch	19.6	32.4	32.4	49
HRT (d)	batch	4	2	2	1
Time length (d)	18	31	11	53	10

2.2.3 Analytical methods

OAs and ethanol concentrations were determined by high-pressure liquid chromatography (HPLC). Samples were analyzed using a LC 25 Chromatography Oven (Dionex, USA) equipped with an Organic Acids column (Metrohom, Switzerland) and an UVD 340U detector (Dionex, USA). 1 mM H_2SO_4 solution was used as eluent and pumped at the rate of 0.7 mL/min by a GD 500 Gradient Pump (Dionex, USA). pH values were measured using an inoLab pH meter (WTW, Germany). COD concentrations were measured trough the optical density value by colorimetric analysis, according to the Standard Methods (APHA, 2005), using a Photolab Spektral spectrophotometer (WTW, Germany). According to other studies [1,25], TS and VS content was determined by oven drying at 105°C and 550°C, respectively. The composition of the biogas produced during the process was analysed using a Varian Star 3400 gas chromatograph equipped with Shin-Carbon ST 80/100 column and a thermal conductivity detector, following the indications reported elsewhere [23]. The separation was conducted using Argon as carrier gas.

2.3. Results

CW fermentation was performed in two identical biological units operating in the same condition to achieve averaged values of all the investigated parameters. Standard deviations between the two measures, corresponding to the variation range in this special case, were indicated by error bars, reported for lactic acid alone, for clarity of representation.

During the start-up phase, high F/M ratio and anaerobic conditions led to an increasing organic acids production (Figure 1a) and a corresponding gradual decrease of pH from 6 to 4.5 (Figure 1b). Ethanol was detected as significant fermentation by-product, and its concentration reached a maximum value of 5.5 g/L. It showed an increasing trend with low concentration until day 7. Acetic acid showed an opposite trend reaching a stable low concentration (around 2 g/L) at day 10. Moreover, a normalized hydrogen volume of 103 mL H_2 was produced within 20 days of fermentation (data not shown).

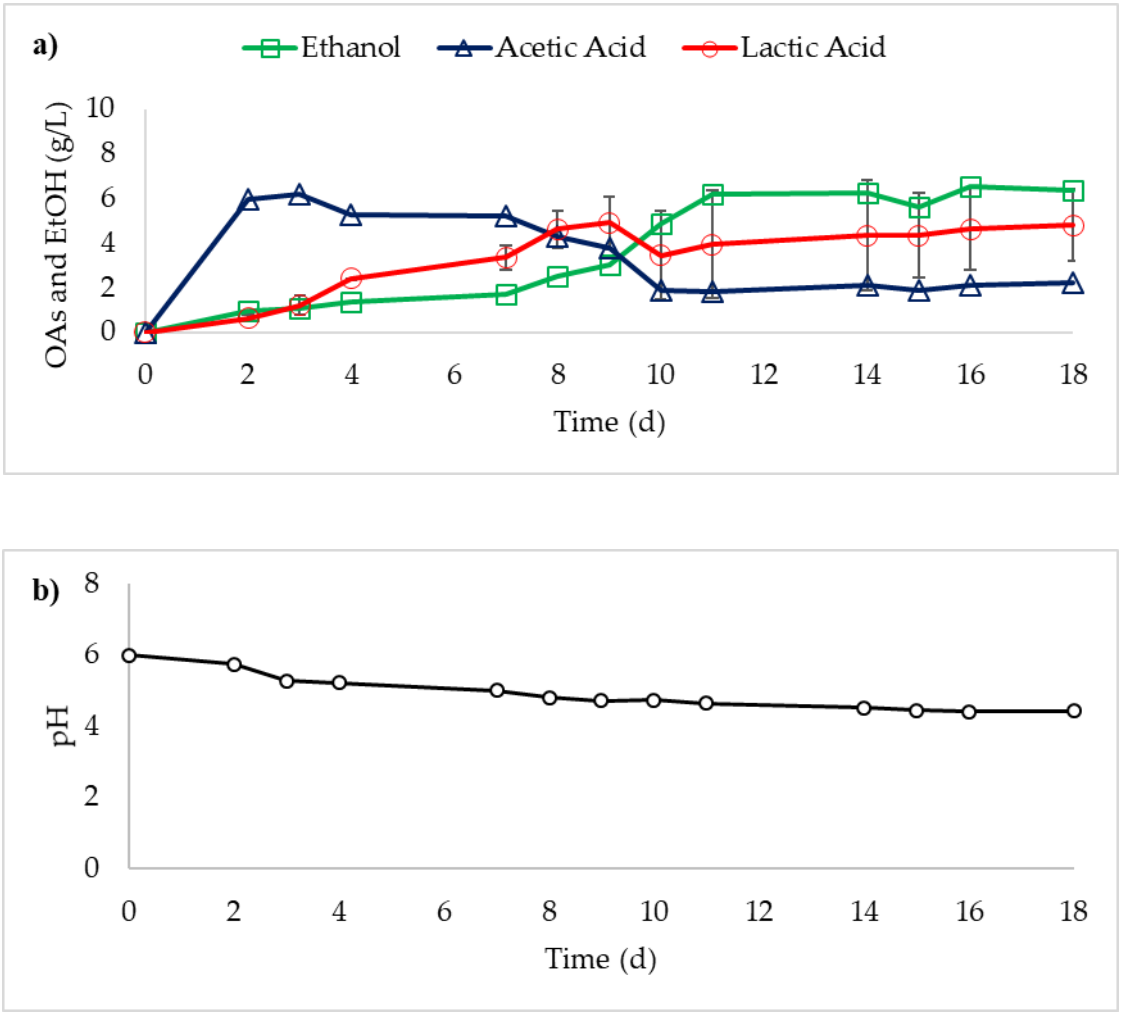

Figure 2.1. Trends of the main organic compounds (a) and pH (b) during phase 1.

During phase 2 (day 22-53) the adoption of 4 d HRT resulted in an increase in OAs generation (Figure 2a). Increasing lactic acid production led to lower pH values (Figure 2b). The registered pH dropped from 4.5 to 3.8 at the end of phase 2. As shown in Figure 2a, acetic acid and ethanol are still present in the reactor. Acetic acid increases until reaching a constant concentration around 4.5 g/L, while, again, an opposite trend is exhibited by ethanol, whose concentration is very low during the last days of phase 2.

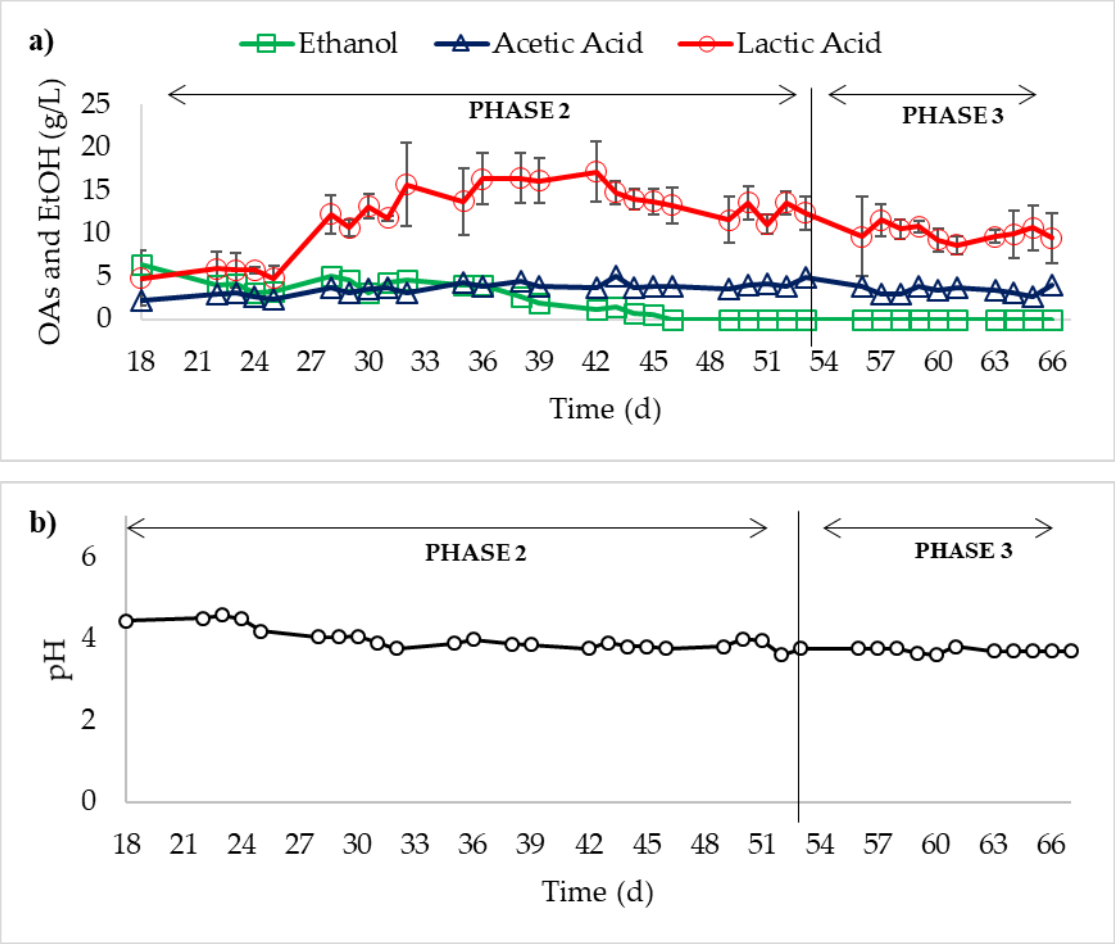

Figure 2.2. Process monitoring during phases 2 and 3, with inoculum addition: a) OAs and EtOH; b) pH.

During phase 3 (day 56-67), lactic acid and acetic acid were the main by-products, and their concentration remained quite unchanged. The adopted HRT allowed a fermentative process producing the maximum lactic acid concentration (11.6 g/L), which, nonetheless, was lower than the maximum value obtained during phase 2 (17.2 g/L). Acetic acid concentration kept constant (≈ 3 g/L) and no ethanol production was observed.

During phase 4 (day 70-123), the digestate was no longer added, and the HRT was not varied compared to the previous phase (HRT = 2 d). In these conditions the pH varied between 3.6 and 3.4, remaining almost stable for the whole phase length, while the production of acetic acid slightly increased (Figure 3).

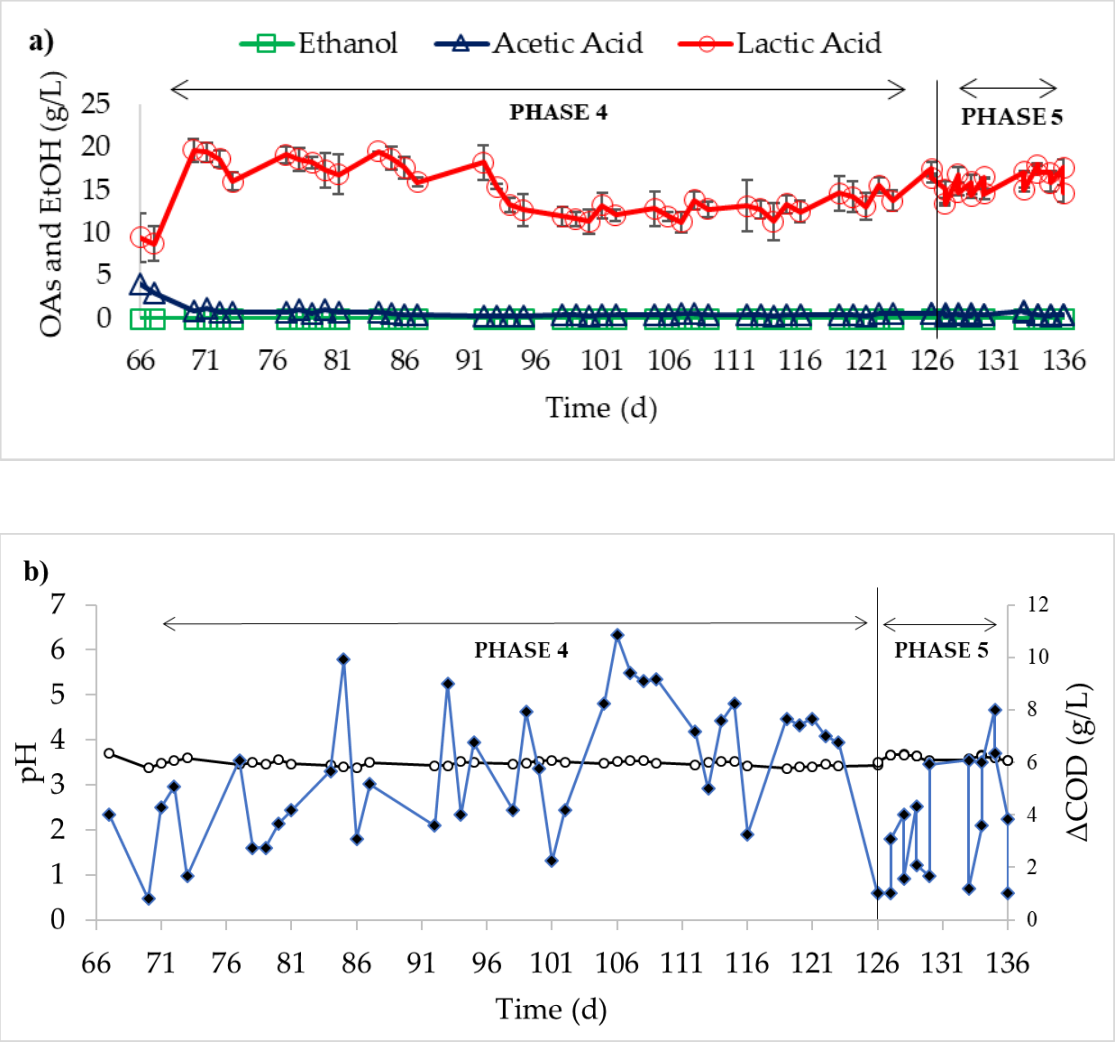

Figure 2.3. Process monitoring during phases 4 and 5, without inoculum addition: a) OAs and EtOH; b) pH.

Finally, the minimum HRT (1 d) adopted in phase 5 (day 126-136), corresponding to the maximum OLR of 32.43 g COD/L/d, had negligible effects on lactic acid accumulation within the effluent (Figure 3a). The pH value varied between 3.6 and 3.4 as in the previous phase (Figure 3b). A maximum lactic acid concentration of 17.6 g/L was reached, which was lower than those reached during phase 4.

For mass balance purposes, Figure 3b additionally shows the trend of consumed soluble COD during phase 4 and 5. The reported values have been calculated as the net soluble COD variation between the influent and effluent soluble COD values. The maximum soluble COD variation of around 11 g/L was registered at day 106 during phase 4. Moreover, Figure 4 shows the daily specific yield of lactic acid (Y^*) during the same operation phases, evaluated as mols of accumulated COD in form of lactic acid by mols of net consumed soluble COD. The latter was calculated by removing lactic acid

contribution to the influent and effluent soluble COD value. The results showed a maximum and minimum yield of 0.33 and 0.10 mol LA / mol COD in phase 4 and phase 5, respectively.

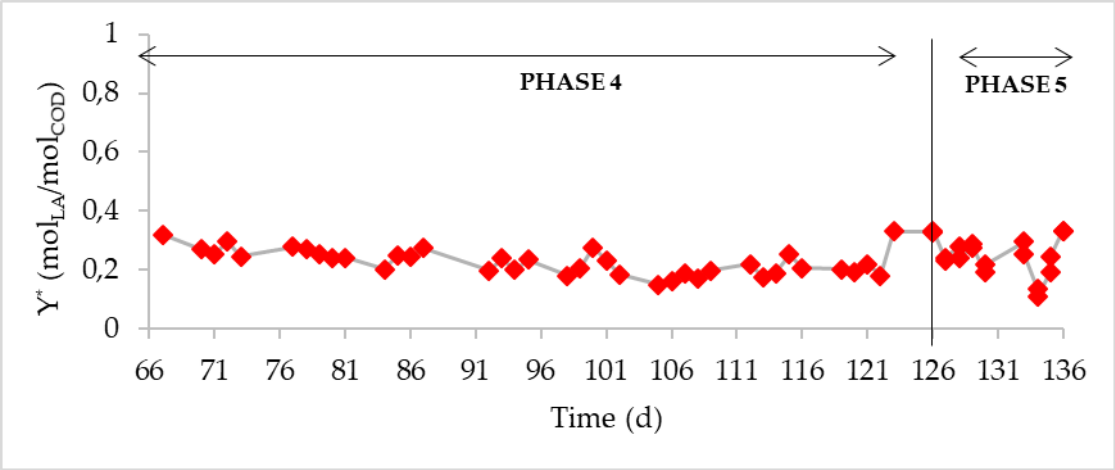

Figure 2.4. Daily specific lactic acid yields (Y^*) during the last operational phases.

Hydrogen production was also detected during the initial phases of fermentation. The cumulative hydrogen generated during phase 1 and 2 reached a total normalized volume of 299 mL until day 40 (data not shown). The hydrogen yields achieved during these phases were very low compared to other literature studies [22,26,27], but the aim of this work was far to H_2 production optimization. After that period only CO_2 was generated. Such a result is in agreement with the observed trend of pH values. After phase 2, pH value was always below 4, which generally correspond to inhibiting conditions for hydrogen generation studies [24].

Finally, Figure 5 illustrates the average lactic acid yields obtained per unit of fed substrate in terms of soluble COD. Each bar corresponds to a single HRT and different colours are related to each operation phases. The main results are later summarized in Table 3, in which the average (Y) and the maximum (Y_{max}) value of the yield, and the average (P) and the maximum (P_{max}) lactic acid production rate (daily amount of lactic acid produced per litre) have been reported. All the showed values refer to the net converted soluble COD, obtained by subtracting the influent lactic acid contribution already contained in the cheese whey. Standard deviations related to each phase (Table 3) refer to the averaged values of all the specified parameters during the different HRT constituting a single phase.

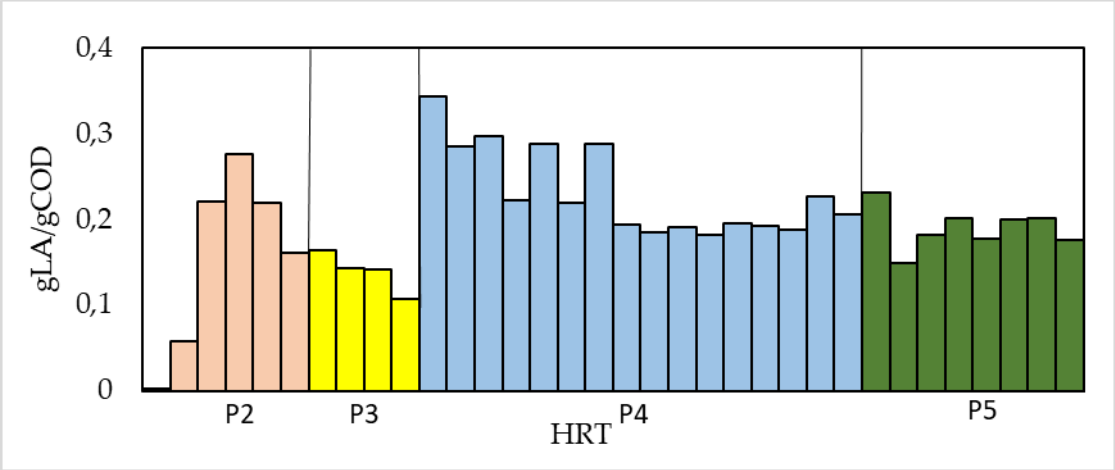

Figure 2.5. Lactic acid yields during the different operational phases (P1, P2, P3, P4 and P5 represent the five phases).

Table 2.3. Yield and production of lactic acid for the phases operated in repeated-batch mode. CW= cheese whey; LA= lactic acid

Phase	Y ($gCOD_{(LA)}/gCOD_{(CW)}$)	P (gLA/L)	Y_{MAX} ($gCOD_{(LA)}/gCOD_{(CW)}$)	P_{MAX} (gLA/L)	Y^*_{MAX} %
2	0.199±0.09	2.262±1.017	0.33	3.75	-
3	0.148±0.02	3.407±0.287	0.2	4.55	-
4	0.247±0.05	5.675±0.626	0.37	8.55	0.33
5	0.200±0.02	9.190±0.289	0.23	10.6	0.33

It is evident that after 16 cycles (during phase 4), conducted with different operational conditions, the reactors reached a stable performance until the end of the last phase (18 more HRT turnovers) even if a HRT change was adopted between phase 4 and phase 5. During phase 4, the maximum yield of 0.37 g $COD_{(LA)}$ g/$COD_{(CW)}$ was reached, while the maximum value of extracted lactic acid mass of 10.6 g LA/L/d was observed during the last phase.

2.4. Discussion

The high organic carbon content and the prevalent rapidly biodegradable COD fraction of CW allows for a promising conversion of this liquid effluent in dark fermentative bioreactors [29,30]. During the start-up phase of continuous bioreactors, digestate from

anaerobic digestion is normally used as inoculum for dark fermentation experiments, as it contains high concentration of fermentative anaerobic bacteria performing the first stages of anaerobic digestion process [31,32]. Different pre-treatment strategies have been introduced during the last years [22], which lead to methanogenic activity inhibition by favoring acidogenic and acetogenic species [25]. The significant amount of digestate used as inoculum for CW conversion had an important buffering effect during the start-up phase, and limited the pH drop (Figure 1b) due to acids generation [26]. Hydrogen production was low, while ethanol was the main fermentation by-product. Such a result was related to the fact that alcohol production processes (i.e. solventogenesis) are usually associated to the presence of acetic acid, which is produced by the Wood-Ljungdahl pathway using hydrogen as electron acceptor [27]. However, the concomitant presence of ethanol and acetic acid could also have been due to the presence of heterofermentative bacteria. Heterofermentation, in fact, is one of the different pathways that lactic acid bacteria can follow, leading to lactic acid, carbon dioxide, ethanol and acetic acid production [28,29]. As consequence of the mentioned conversion processes low lactic acid concentrations characterized phase 1. The maximum measured lactic acid concentration value, in fact, resulted below 5 g/L.

Lactic acid concentration clearly increased in the second phase of operation. The adoption of a repeated-batch feeding strategy, which was different from the start-up phase, strongly affected lactic acid concentration and yields. In industrial scale applications, lactic acid is generally produced in batch mode, and by using pure cultures, whose growth is optimized by the addition of significant amount of chemicals [13]. Previous studies [21-23] attested that the adoption of a repeated-batch mode can give higher yield than the adoption of a single batch mode [10,24,25]. During the same phase, high concentrations of acetic and lactic acid were reached, and the pH profile indicated that the buffering capacity due to digestate addition did not affect the pH evolution.

During the third phase, the more stable OAs concentrations suggested that the microbial community was more acclimated to the CW conversion. Although the lactic acid production rate was more stable, the higher ORL led to a lower substrate conversion rate, reducing bioreactor performances. This could be due to the reduced time for slower biological reactions contributing to lactic acid production during phase 2.

Acetic acid concentration, which varied between 2 and 4 g/L during the digestate addition phases (1, 2 and 3), drastically decreased to 1 g/L at the beginning of phase 4. Digestate is rich in acetogenic bacteria, which are able to convert organic compounds in acetic acid [31,32]. The lower presence of acetogenic microorganisms in the feeding cheese whey

led to their progressive washing-out during phase 4 and 5. Conversely, lactic acid production considerably increased, and a maximum concentration of 20.1 g/L was obtained. This result was probably due to the prevalence of autochthonous lactic bacteria, which led to a higher lactic acid percentage compared to the previous phases [28]. Indeed, lactic acid bacteria are more acid-tolerant than other fermentative bacteria as they are able to regulate their intracellular pH [34-36]. Moreover, they are able to grow at extremely low pH [14,37]. In previous studies, acidic pre-treatments on fermentation inoculum were adopted to favor lactic acid bacteria growth and proliferation [14,38]. This procedure limited the production of undesirable compounds in the fermentation broth increasing the purity of the produced lactic acid.

It is worth noting that the lactic acid concentration measured during phase 4 and 5 (without inoculum addition) did not reach the peaks characteristics of phase 2 (operated with inoculum addition). Nonetheless, the concentration fluctuations were restrained (Figure 3a) suggesting that the process was more stable along the different feeding cycles. As far as concern the effect of the HRT variation, it could be observed that the adoption of lower values did not strongly affect the lactic acid concentration, which decreased only by few g/L from phase 2 to phase 3 and from phase 4 to phase 5. As reported by other authors [29], when low HRTs were adopted (12 h and 8 h), it was possible to reach a high extracted lactic acid mass in presence of low lactic acid concentrations. HRT variations affected both the yield and the mass of extracted lactic acid from the bioreactors. The yield was higher when a higher HRT was adopted while the production increased for lower HRT values. Therefore, it seems more convenient to use lower HRTs, in order to extract a higher lactic acid amount in terms of daily mass.

Different studies also demonstrated that the optimum pH value for lactic acid production was between 5.5 and 5.9 [13,39,40]. The adoption of lower values led to low lactic acid concentrations (below 5 g/L) [14,31,38]. In contrast, the results achieved in this study showed that it was possible to produce a high lactic acid amount (20.1 g/L) at low pH, under the adopted uncontrolled pH conditions. This result is highly relevant as uncontrolled pH conditions are usually unfavorable for lactic acid production. Perez et al. [13], for instance, studied CW fermentation by *Lactobacillus Helveticus* at uncontrolled pH conditions in batch mode. The maximum observed concentration value was about 15 g/L, while the same species was able to accumulate around 60 g/L at a fixed pH of 5.9, and 80 g/L with the supplementary addition of yeast extract. Liang et al. performed another example of uncontrolled pH fermentation in 2014 [16]. The authors used potato peel waste as substrate and mixed culture in batch mode. The maximum concentration of

14.7 g/L of lactic acid was observed. Wu et al. [30], studied acidogenic fermentation of fruit and vegetables wastes. In order to improve the lactic acid production, they varied the pH value of a CSTR reactor from 4 to 5 by external addition of a NaOH solution. The maximum concentration of about 15 g/L was reached, which was again lower the maximum concentration achieved in the present study. Regarding the lactic acid yields (Y and Y_{MAX} in Table 3), expressed as g of produced lactic acid (in terms of COD) per g of fed COD to the reactors, the higher Y_{MAX} value was reached by Choi et al., 2016 [29], using CW and performing the fermentation at a fixed pH of 5.5. When the same reactor was operated at pH 3, the average yields were below the value of 0.1. In this study, the values of Y ranged between 0.2 and 0.37, similarly to the case presented by Whu et al. in 2015 with different wastes [30].

Other authors evaluate the yield in terms of mol of produced lactic acid per mol of consumed lactose, carbohydrates or soluble sugars consumed during the fermentation process [31–33]. This add a qualitative information about the biological conversion and refers to the percentage of the feeding organic compound effectively converted into lactate. Ghaly et al. [31], studied the batch fermentation of cheese whey using pure cultures and nutrient supplementation. They reached the yields (in terms of g of lactic acid per g of lactose) between 0.56 and 0.72. Different strains were tested by Joudeikiene et al. [32], who performed pure-cultures cheese whey batch fermentation at 37 °C under stationary optimized conditions. The results showed significant lactic acid yields ranging between 0.33 and .065. In this study, the g of lactic acid (in terms of COD) per g of converted COD were evaluated in repeated-batch conditions. The maximum yield of 0.37 was achieved during phase 4, which was lower than the values reported in batch conditions using pure cultures.

No important pH variation was detected from the second phase to the end of the process, as the pH remained around the lactic acid pKa due to the prevalence of this compound in the culture medium. It was more convenient to feed the reactor with the cheese whey alone as it was possible to extract higher amounts of lactic acid, which had higher purity compared to the previous phases where other fermentation by-products were detected. The presented results demonstrated that mixed culture CW fermentation represents a promising alternative to pure culture fermentation processes usually adopted for biological lactic acid production. This study represents a preliminary base for successive higher-scale applications and for mathematical modeling of mixed culture fermentation processes [34,35].

2.5. Conclusions

Semi-continuous lactic acid production from cheese whey under repeated-batch conditions was investigated using mixed microbial cultures at uncontrolled pH. Two reactors were operated for 5 operational phases and 136 days. Different HRT and ORL values were tested to evaluate lactic acid yields and fermentation performances. The results showed the maximum LA concentration of 20.1 g/L and the maximum yield of 0.37 g of lactic acid per g fed COD, which were achieved with the HRT of 2 d. Conversely, the maximum value of extracted lactic acid mass (10.6 g/L/d) was obtained when 1 d HRT was adopted. The results represent an interesting base for higher scale application of mixed-culture fermentation with uncontrolled pH conditions.

References

[1] Ghimire A, Frunzo L, Salzano E, Panico A, Lens PNL, Pirozzi F. Biomass Enrichment and Scale-up Implications for Dark Fermentation Hydrogen Production with Mixed Cultures. Chem Eng Trans 2015;43:391–6. https://doi.org/10.3303/CET1543066.

[2] Carvalho F, Prazeres AR, Rivas J. Cheese whey wastewater: Characterization and treatment. Sci Total Environ 2013;445–446:385–96. https://doi.org/10.1016/j.scitotenv.2012.12.038.

[3] Prazeres AR, Carvalho F, Rivas J. Cheese whey management: A review. J Environ Manage 2012;110:48–68. https://doi.org/10.1016/j.jenvman.2012.05.018.

[4] Ibarruri J, Hernández I. Valorization of cheese whey and orange molasses for fungal biomass production by submerged fermentation with Rhizopus sp. Bioprocess Biosyst Eng 2019. https://doi.org/10.1007/s00449-019-02127-4.

[5] Kaur N, Sharma P, Jaimni S, Kehinde BA, Kaur S. Recent developments in purification techniques and industrial applications for whey valorization: A review. Chem Eng Commun 2019;0:1–16. https://doi.org/10.1080/00986445.2019.1573169.

[6] Cherubini F. The biorefinery concept: Using biomass instead of oil for producing energy and chemicals. Energy Convers Manag 2010;51:1412–21. https://doi.org/10.1016/j.enconman.2010.01.015.

[7] Eş I, Mousavi Khaneghah A, Barba FJ, Saraiva JA, Sant'Ana AS, Hashemi SMB. Recent advancements in lactic acid production - a review. Food Res Int 2018;107:763–70. https://doi.org/10.1016/j.foodres.2018.01.001.

[8] Dorgan JR, Lehermeier HJ, Palade L-I, Cicero J. Polylactides: Properties and Prospects of an Environmentally Benigh Plastic from Renewable Resources. Macromol Symp 2001;175:55–66.

[9] Bogaert J-C, Coszach P. Poly(lactic acids)- a potential solution to plastic waste dilemma. Macromol Symp 2000;153:287–303.

[10] Abdel-Rahman MA, Tashiro Y, Sonomoto K. Recent advances in lactic acid production by microbial fermentation processes. Biotechnol Adv 2013;31:877–902. https://doi.org/10.1016/j.biotechadv.2013.04.002.

[11] Tan J, Mohamed Ali Abdel-Rahman A, Sonomoto K. Biorefinery-Based Lactic Acid Fermentation: Microbial Production of Pure Monomer Product. Adv Polym Sci 2018;279:27–66. https://doi.org/10.1007/12.

[12] Shahbazi A, Mims MR, Li Y, Shirley V, Ibrahim SA, Morris A. Lactic Acid

Production from Cheese Whey by Immobilized Bacteria. Appl Biochem Biotechnol 2005;122:0529–40. https://doi.org/10.1385/abab:122:1-3:0529.

[13] Soriano-Perez S, Flores-Velez L, Alonso-Davila P, Cervantes-Cruz G, Arriaga S. Production of lactic acid from cheese whey by batch cultures of Lactobacillus helveticus. Ann Microbiol 2012;62:313–7. https://doi.org/10.1007/s13213-011-0264-z.

[14] Itoh Y, Tada K, Kanno T, Horiuchi JI. Selective production of lactic acid in continuous anaerobic acidogenesis by extremely low pH operation. J Biosci Bioeng 2012;114:537–9. https://doi.org/10.1016/j.jbiosc.2012.05.020.

[15] Pradhan N, Dipasquale L, D'Ippolito G, Panico A, Lens PNL, Esposito G, et al. Hydrogen production by the thermophilic bacterium Thermotoga neapolitana. Int J Mol Sci 2015;16:12578–600. https://doi.org/10.3390/ijms160612578.

[16] Liang S, McDonald AG, Coats ER. Lactic acid production from potato peel waste by anaerobic sequencing batch fermentation using undefined mixed culture. Waste Manag 2015;45:51–6. https://doi.org/10.1016/J.WASMAN.2015.02.004.

[17] Bonk F, Bastidas-Oyanedel JR, Yousef AF, Schmidt JE, Bonk F. Exploring the selective lactic acid production from food waste in uncontrolled pH mixed culture fermentations using different reactor configurations. Bioresour Technol 2017;238:416–24. https://doi.org/10.1016/j.biortech.2017.04.057.

[18] Tejayadi S, Cheryan M. Lactic acid from cheese whey permeate. Productivity and economics of a continuous membrane bioreactor. Appl Microbiol Biotechnol 1995;43:242–8.

[19] Motte JC, Sambusiti C, Dumas C, Barakat A. Combination of dry dark fermentation and mechanical pretreatment for lignocellulosic deconstruction: An innovative strategy for biofuels and volatile fatty acids recovery. Appl Energy 2015;147:67–73. https://doi.org/10.1016/j.apenergy.2015.02.042.

[20] Bastidas-Oyanedel J-R, Bonk F, Thomsen MH, Schmidt JE. Dark fermentation biorefinery in the present and future (bio) chemical industry. Rev Environ Sci Bio/Technology 2015;14:473–98.

[21] Ghimire A, Trably E, Frunzo L, Pirozzi F, Lens PNL, Esposito G, et al. Effect of total solids content on biohydrogen production and lactic acid accumulation during dark fermentation of organic waste biomass. Bioresour Technol 2018;248:180–6. https://doi.org/10.1016/j.biortech.2017.07.062.

[22] Ghimire A, Frunzo L, Pirozzi F, Trably E, Escudie R, Lens PNL, et al. A review on dark fermentative biohydrogen production from organic biomass: Process

parameters and use of by-products. Appl Energy 2015;144:73–95. https://doi.org/10.1016/j.apenergy.2015.01.045.

[23] Luongo V, Ghimire A, Frunzo L, Fabbricino M, d'Antonio G, Pirozzi F, et al. Photofermentative production of hydrogen and poly-β-hydroxybutyrate from dark fermentation products. Bioresour Technol 2017;228:171–5.

[24] Ghimire A, Sposito F, Frunzo L, Trably E, Escudié R, Pirozzi F, et al. Effects of operational parameters on dark fermentative hydrogen production from biodegradable complex waste biomass. Waste Manag 2016;50:55–64. https://doi.org/10.1016/j.wasman.2016.01.044.

[25] Maharaj BC, Mattei MR, Frunzo L, Hullebusch ED va., Esposito G. ADM1 based mathematical model of trace element complexation in anaerobic digestion processes. Bioresour Technol 2019;276:253–9. https://doi.org/10.1016/j.biortech.2018.12.064.

[26] Ghimire A, Luongo V, Frunzo L, Pirozzi F, Lens PNL, Esposito G. Continuous biohydrogen production by thermophilic dark fermentation of cheese whey: Use of buffalo manure as buffering agent. Int J Hydrogen Energy 2017;42:4861–9. https://doi.org/10.1016/j.ijhydene.2016.11.185.

[27] Ragsdale SW. Enzymology of the Wood-Ljungdahl pathway of acetogenesis. Ann N Y Acad Sci 2008;1125:129–36. https://doi.org/10.1196/annals.1419.015.

[28] Colombo B, Sciarria TP, Reis M, Scaglia B, Adani F. Polyhydroxyalkanoates (PHAs) production from fermented cheese whey by using a mixed microbial culture. Bioresour Technol 2016;218:692–9. https://doi.org/10.1016/j.biortech.2016.07.024.

[29] Choi G, Kim J, Lee C. Effect of low pH start-up on continuous mixed-culture lactic acid fermentation of dairy effluent. Appl Microbiol Biotechnol 2016;100:10179–91. https://doi.org/10.1007/s00253-016-7871-3.

[30] Wu Y, Ma H, Zheng M, Wang K. Lactic acid production from acidogenic fermentation of fruit and vegetable wastes. Bioresour Technol 2015;191:53–8. https://doi.org/10.1016/j.biortech.2015.04.100.

[31] Ghaly AE, Tango MSA, Mahmoud NS, Avery AC. Batch propagation of Lactobacillus helveticus for production of lactic acid from lactose concentrated cheese whey with microaeration and nutrient supplementation. World J Microbiol Biotechnol 2004;20:65–75. https://doi.org/10.1023/B:WIBI.0000013313.44873.83.

[32] Juodeikiene G, Zadeike D, Bartkiene E, Klupsaite D. Application of acid tolerant

Pedioccocus strains for increasing the sustainability of lactic acid production from cheese whey. LWT - Food Sci Technol 2016;72:399–406. https://doi.org/10.1016/j.lwt.2016.05.023.

[33] Tango MSA, Ghaly AE. Effect of nutrient addition on batch production of lactic acid from cheese whey using Lactobacillus helveticus. 1998;16:26 pp.

[34] Frunzo L, Fermoso FG, Luongo V, Mattei MR, Esposito G. ADM1-based mechanistic model for the role of trace elements in anaerobic digestion processes. J Environ Manage 2019;241:587–602. https://doi.org/10.1016/j.jenvman.2018.11.058.

[35] Mattei MR, Frunzo L, D'Acunto B, Pechaud Y, Pirozzi F, Esposito G. Continuum and discrete approach in modeling biofilm development and structure: a review. J Math Biol 2018;76:945–1003. https://doi.org/10.1007/s00285-017-1165-y.

Chapter 3

A preliminary study on a novel bioaugmentation technique enhancing lactic acid production by mixed culture fermentation

This chapter has been published as: Policastro, G., Carraturo, F., Compagnone, M., Giugliano, M., Guida, M., Luongo, V., Napolitano, R. and Fabbricino, M. (2021). A preliminary study on a novel bioaugmentation technique enhancing lactic acid production by mixed cultures fermentation. Bioresource Technology, 340, 125595.

A preliminary study on a novel bioaugmentation technique enhancing lactic acid production by mixed cultures fermentation

Abstract

The chapter is a preliminary study on the selection of lactic acid producing microorganisms from a mixed microbial population via bioaugmentation. The bioaugmentation technique is based on pH sudden variations occurring in sequential batch steps of a dark fermentation process applied to simple substrates. Different conditions are tested and compared. The structure of microbial communities and concentrations of metabolic intermediates are analyzed to study the possible substrate conversion routes. Obtained results indicate that the initial mixed culture produced a lactic acid percentage of 5% in terms of $COD_{LA}/COD_{PRODUCTS}$. In the most favourable conditions, the selected culture produced a lactic acid percentage of 59%. The analysis of the composition of microbial communities before and after the bioaugmentation processes, indicates that lactic acid production mainly results from the population change to bacteria belonging to the genus *Bacillus.* Indeed, the relative abundance of *Bacilli* increased from 0.67%, to 8.40% during the bioaugmentation cycle.

3.1. Introduction

The development of new strategies for an efficient production of lactic acid (LA) is of great interest, due to the wide application of this product in chemical, pharmaceutical and food industries[1]. Moreover, LA can be used to produce a polymer (polylactic acid) able to replace petrochemical plastics in several applications [2]. This is why LA market is supposed to reach 9.8 billion USD by 2025 [3], with an annual growth rate of almost 19% [4].

Among different LA production alternatives, microbial fermentation is gaining increasing attention, being the less expensive and the most environmental friendly solution [5].

Currently, pure bacterial fermentations account for 90% of LA production worldwide [4], although the use of mixed cultures would be more attractive, because of its intrinsic economical and operational advantages, including the possibility of using waste material as bacterial substrates, with no need of sterilisation [6]. Indeed, the use of mixed culture fermentation for LA production is still challenging to date. Recently, it has been reported that LA may result as the dominant product of mixed microbial fermentations if specific

substrates are used. Rombout at al. [3] studying mixed fermentation for LA production, observed that the microbial community could be dominated by lactic acid bacteria (LAB) (*e.g. Lactococcus* and *Lactobacillus* species) using a rich medium containing peptides and B vitamins. On the contrary, employing a simple mineral medium, the substrate is mainly fermented to acetate and butyrate by species belonging to the *Clostridia* class. Luongo et al., [1] observed that indigenous cultures of cheese whey allow obtaining LA as the main fermentation product. At the same time, the authors proved that the use of an external inoculum for LA production from cheese whey at uncontrolled pH, resulted in acetic acid and ethanol production. The study also demonstrated that LAB are able to grow at extremely low pH [1]. The external pH decrease do not constitute an acid shock as LAB are naturally able to acidify the external medium [7]. Moreover, LAB are more acid-tolerant than other fermentative bacteria [8,9]. Consequently, various researchers adopted acidic pre-treatments to favour LAB proliferation in mixed culture fermentation. This procedure limited the production of other catabolites, and increased the lactic acid percentage in the fermentation broth [10,11].

Generally, a rapid change of the external pH represents a stressful situation for microorganisms. However, differently from most non-lactic acids producing bacteria, LAB are able to regulate their intercellular pH as an adaptation strategy [7]. When the external pH decrease, neutrophilic bacteria maintain an internal pH that is close to 7. The high internal-external pH difference generates large proton gradients, which is disadvantageous for fermentative bacteria. Indeed, proton translocation requires energy [12]. On the other hand, many acid-tolerant microorganisms, such as LAB, have developed a different strategy: The internal pH decreases as the external pH decreases to maintain a constant pH gradient rather than a constant internal pH [7]. Several possible methods which can be used by bacteria to regulate the internal pH have been studied, such as the synthesis of cytoplasmic buffer, proton symport systems, production of acid or bases and proton pumps [13].

Akao et al. [14] showed that acidic pre-treatments are able to promote the selection of LAB from mixed cultures, although, in that sense, even better results can be obtained through a swing pH control of the system [15].

Starting from these results, the present chapter proposes a preliminary study on an innovative operative strategy to improve the selection of LAB from an external inoculum, in order to maximize LA production from a simple medium. The proposed strategy, indicated as bioaugmentation cycle, is based on the development of three sequential fermentative steps, conducted in batch conditions. The selection of LAB simply occurs as consequence of pH variations, induced by the applied organic charge and by the punctual pH corrections effectuated at the beginning of each step. To optimize the bioaugmentation efficiency, various Food to Microorganisms (F/M) ratios are tested. No nutrient addition is operated, as the study is aimed at developing a technique which could be applied in the presence of simple substrates. Therefore, the present study represents an indication to address future researches aimed at producing lactic acid from both unrelated substrates and external inocula, acting on operational conditions only.

3.2.Materials and Methods

3.2.1. Experimental apparatus and materials

Experimental tests were conducted in batch mode, at mesophilic temperature (35 ± 1 °C), using 500 mL glass reactors (400 mL working volume). The reactors were equipped with two different ports, used for liquid and gas sampling operations. Plastic tubes and gaskets were used for junctions. Before use, sealing joints were controlled, filling each reactor with water and pressurized air. High purity chemicals were used for substrate preparation and all analytical determinations. Adopted glassware were soaked overnight in a nitric acid bath (2% v/v) and rinsed several times with bi-distilled water.

3.2.2. Bioaugmentation cycle

The bioaugmentation cycle was composed by three successive fermentative steps, each conducted using, as inoculum ($I_{i=1-3}$), the biomass selected in the previous step. The external mixed culture, used as initial inoculum (I_1), was sampled from a full-scale anaerobic treatment plant located in Casal di Principe (South of Italy), processing the organic fraction of municipal solid waste. The characteristic of the digestate were: COD= 77.30±0.08 g/L, pH=8. Before use, the inoculum was pre-treated by heat shock, as detailed described elsewhere [1]. Used substrate for each fermentation step was a synthetic glucose solution, prepared dissolving the solid compound in bi-distilled water.

Five different operative conditions were tested, corresponding to five different initial concentrations of the substrate ($S_{j\ =\ 1\text{-}5}$), as summarized in Table 1. Substrate concentrations were calculated setting different initial F/M ratios. Each condition was conducted in triplicates. For simplicity, experiments are reported as I_iS_j, where I= inoculum and i= 1-3 is the step number. S= substrate and j=1-5 represent the five different substrate concentrations.

Table 3.1. Operative conditions of fermentative steps (I_iS_j).

Cycle #	Step 1	Step2	Step3	F/M ratio (mgCOD/mgCOD)	Substrate concentration (g/L)
1	I_1S_1	I_2S_1	I_3S_1	0.025	0.60
2	I_1S_2	I_2S_2	I_3S_2	0.5	1.20
3	I_1S_3	I_2S_3	I_3S_3	0.1	2.40
4	I_1S_4	I_2S_4	I_3S_4	0.25	6.01
5	I_1S_5	I_2S_5	I_3S_5	0.5	12.03

The reactor adopted for the first step was filled with the external inoculum, and the substrate maintaining a 1:2 volumetric ratio (v/v). The reactor was operated until no increase in terms of lactic acid production was detected. The obtained fermented mixture was used as inoculum of the second fermentative step. This latter was performed keeping the same volumetric ratio of the previous step between inoculum and substrate, and the same substrate concentration. The reactor was operated in the new conditions until no increase in terms of lactic acid production was detected. Once more the obtained fermented mixture was used as inoculum of the subsequent and last step, keeping the volumetric ratio between inoculum and substrate equal to 1:2. At the beginning of each step the pH value was adjusted to 6.0 ±0.01, using a 1M NaOH solution. No pH correction was operated, instead, during the fermentation period. At selected time (24 h), organic acids (OAs) concentration, hydrogen production and pH variation were measured. Moreover, a microbial characterization was conducted on the initial inoculum and on the fermented mixtures obtained at the end of the bioaugmentation cycle.

3.2.3 Lactic acid production tests

The fermented mixtures produced at the end of the five bioaugmentation cycles corresponding to the five tested F/M conditions, were used as inoculum for LA production tests (I-$PT_{j=1-5}$). The fermented mixture from the reactor I_3S_1 was used as inoculum for the test I-PT_1 and so on. LA production tests were conducted using once more glucose as substrate, keeping the volumetric ratio between inoculum and substrate equal to 1:2 (v/v). The substrate concentration was fixed to 24.06 g/L in order to compare the performances of the different cycles adopting the same operative conditions. A blank test (I-PT_0) using, as inoculum, the initial mixed culture (I_1) was performed too. In all cases, the initial pH was adjusted to 6.0 ±0.01. At selected time (24 h), OAs concentrations, hydrogen production and pH variation were measured.
Table 2 summarizes the composition of the reactors adopted for LA production tests.

3.2.4. Analytical methods and Instruments

OAs concentration was determined by high-pressure liquid chromatography (HPLC), using a LC 25 Chromatography Oven (Dionex, USA) equipped with an Organic Acids column (Metrohom, Switzerland) and an UVD 340U detector (Dionex, USA). pH was measured using an inoLab pH meter (WTW, Germany). COD concentration was measured by colorimetric analysis, according to the Standard Methods (APHA, 2005). Biogas quantitative determination was performed by water displacement, according to Policastro et al., [16]. Biogas composition was successively analyzed by gas chromatography, using a Varian Star 3400 gas chromatograph equipped with Shin-Carbon ST 80/100 column and a thermal conductivity detector.
The extraction of the total DNA was carried out to sequence the genome of the whole microbiota, employing the Next Generation Sequencing (NGS) technology, targeting bacterial 16S rRNA gene. For each sample under analysis, 10 g were aliquoted and centrifuged to extract DNA from the supernatant. Supernatant was transferred into sterile 2 mL vials containing 0.5 g glass beads. CTAB extraction protocol (Doyle, 1990) was carried out to recover total DNA from the samples. The extracted DNA samples were amplified with PCR using the V3 and V4 primers (V3: TCGTCGGCAGCGTCAGATGTGTATAAGAGACAGCCTACGGGNGGCWCGAG; V4:
GTCTCGTGGGCTCGGAGATGTGTATAAGAGACAGGACTACHVGGGTATCTA

ATCC), complementary to V3-V4 variable region of the bacterial 16S rRNA gene (500 bp). Sequencing was conducted with a MiSeq Illumina platform, using 2 × 300 bp paired end, 600 cycles, following the manufacturer's instructions (Illumina MiSeq, USA). Differences in the group's communities retrieved from Illumina experiment were assessed by anosim using weighted UniFrac distance, and Anova using Bray Curtis distance [17].

3.3. Results and Discussion

Figure 3.1 and Figure 3.2 report the percentages of fermentation products (i.e. OAs and hydrogen) calculated as ($COD_{SINGLE\ PRODUCT}/COD_{TOTAL\ PRODUCTS}$)*100, obtained during the first step of the bioaugmentation cycle ($I_1S_{j=1-5}$) and the LA production tests ($I\text{-}PT_{j=0-5}$). The OAs percentages reported for the LA production tests represent the net productions.

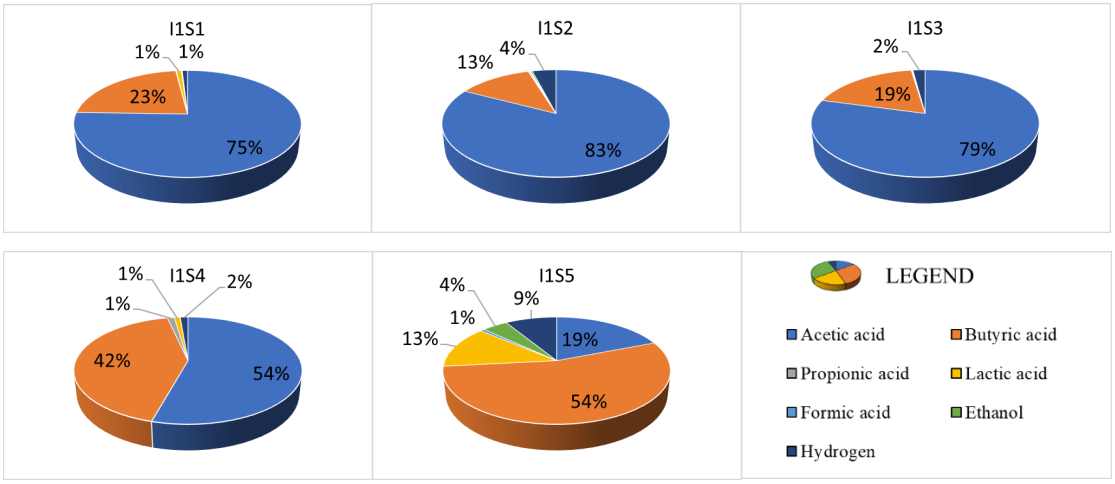

Figure 3.1. Fermentation products of the first step (I_1S_j) of the bioaugmentation cycles.

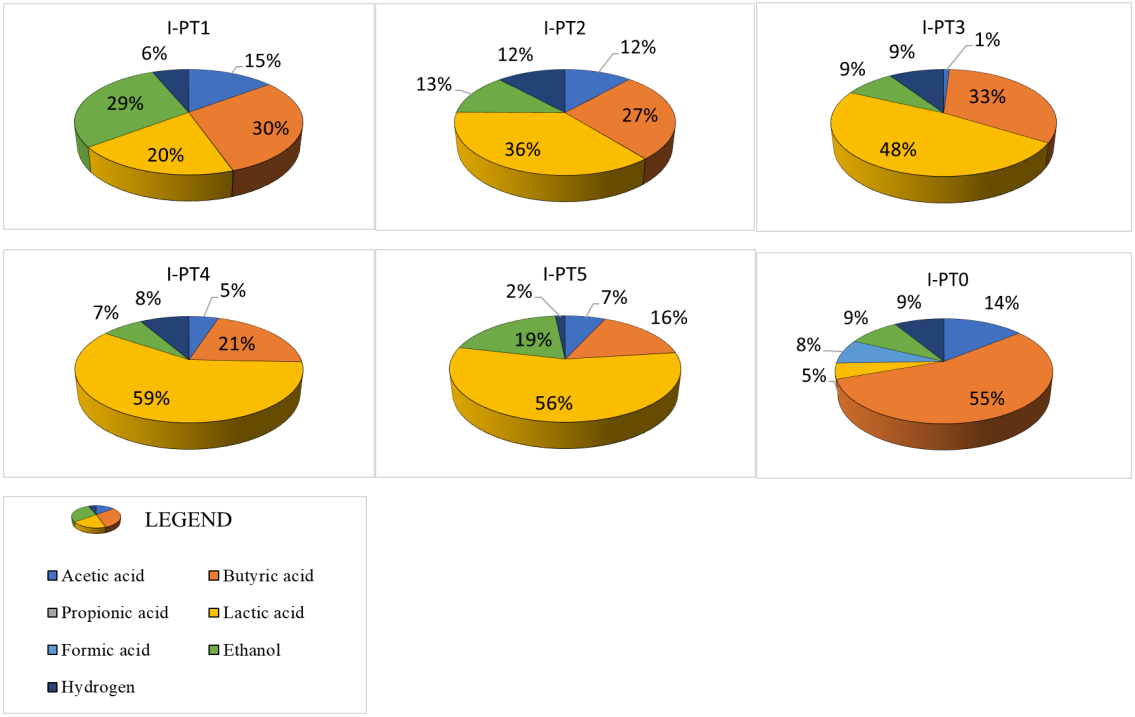

Figure 3.2. Fermentation products of the lactic acid production tests (I-PT$_j$).

The obtained results indicate that acetic acid (A) and butyric acid (B) were the main soluble products of the fermentation process, during the first step of the bioaugmentation cycles. Such results were in agreement with previous studies on mixed cultures fermentation processes [18,19]. In particular, acetic acid was prevalent in I_1S_1, I_1S_2, I_1S_3 and I_1S_4 sets, while butyric acid was prevalent at higher glucose concentrations. During the LA production tests, a strong decrease of the acetic acid and butyric acid concentrations occurred. Moreover, the ratio between butyric and acetic acid (B/A) increased during these tests, compared to the first step of the bioaugmentation cycles. No propionic acid was ever detected. Probably, the heat shock pre-treatment might have inhibited non-spore-forming propionate producers [20]. On the other hand, ethanol production was almost negligible in the first step of the bioaugmentation cycles (except I_1S_4 set) and increased in the LA production tests, suggesting that microorganisms principally followed the heterolactic fermentation pathway [3].

In terms of biogas production, no methane was ever detected. Conversely, hydrogen was produced both during the I_1S_j steps and during the I-PT$_j$ tests. Hydrogen yield was strongly related to the presence of butyric acid. A general reduction of both hydrogen

production and butyric acid was observed during the LA production tests, principally for cultures selected at higher glucose concentrations.

Lactic acid production was observed only in I_1S_3 reactor. However, in the I-PT_j tests, all sets of reactors produced a considerable percentage of lactic acid as a result of the bioaugmentation technique. The most efficient set was the I-PT_4 one, suggesting that the adopted condition was the most appropriate for lactic acid bacteria selection. The I-PT_4 set produced the higher lactic acid percentage (59%) corresponding to 0.51 $g_{LA}/g_{CONSUMED\ GLUCOSE}$. The only exception was represented by the blank test (I-PT_0), which produced a low amount of lactic acid (5%) corresponding to 0.04 $g_{LA}/g_{CONSUMED\ GLUCOSE}$.

Figure 3.3 reports the lactic acid and the pH trends during the three steps of the bioaugmentation cycles (I_iS_j) and during the LA production tests (I-PT_j).

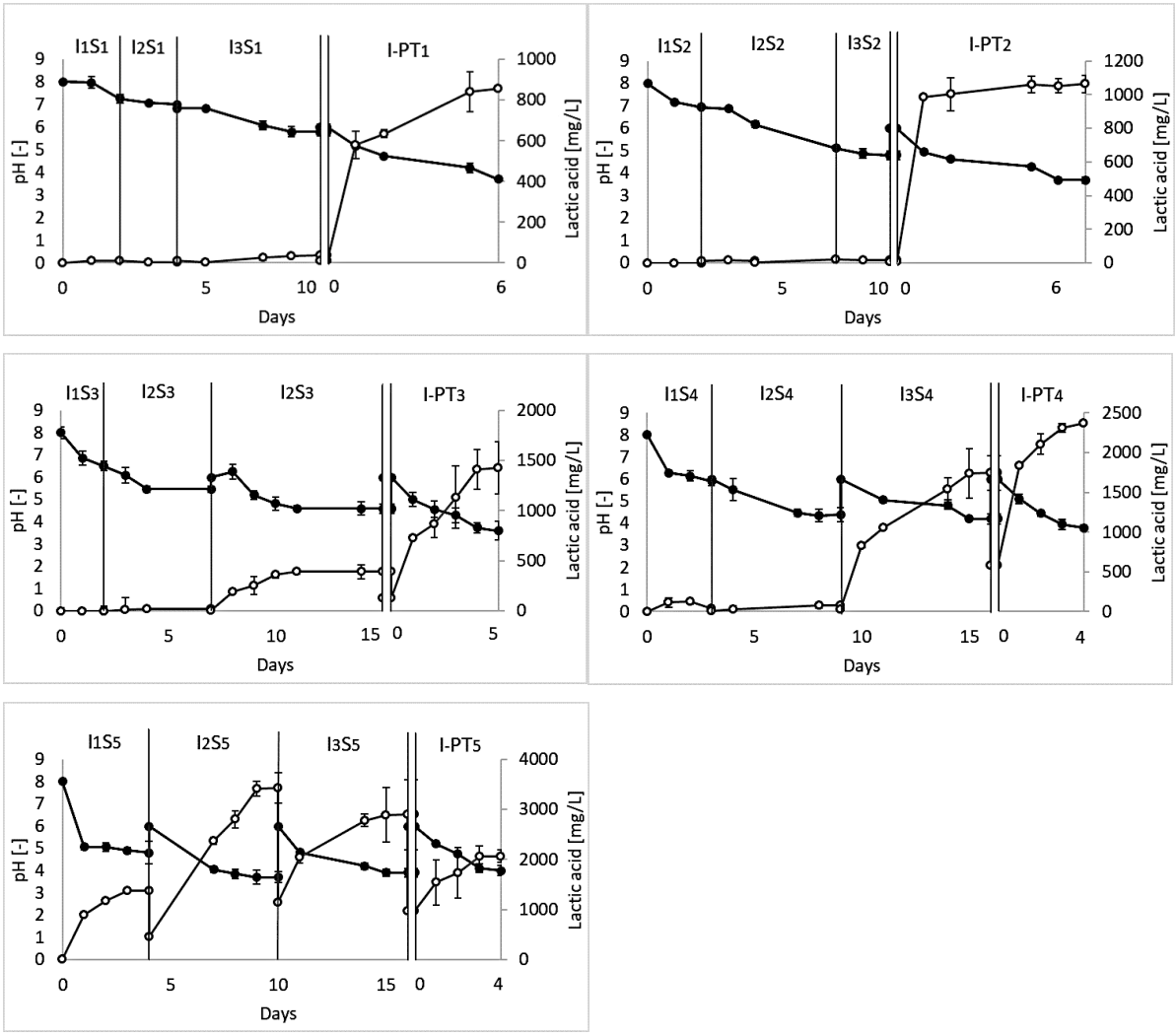

Figure 3.3. Lactic acid concentration and pH trend during the 3 steps of the bioaugmentation cycle (I_iS_j) and the final LA production tests (I-PT_j).

The initial pH value was 8 for all the experimental sets. During the first step, the conversion of glucose to OAs generated a pH drop. As expected, the higher the glucose concentration the more the pH dropped. pH decrease varied from 10% (I_1S_1) to 50% (I_1S_5). Lactic acid was not detected in I_1S_1, I_1S_2 and I_1S_3 reactors. On the other hand, it was produced in the I_1S_4 and I_1S_5 sets, which were the only ones that reached a pH lower than 6. Therefore, at the end of the first step, the pH correction to 6 was performed only for sets I_1S_4 and I_1S_5. During the second step, a slight pH decrement was observed for reactors I_2S_1, I_2S_2 and I_2S_3. However, lactic acid production was not significant. The same result was observed for reactor I_2S_4. Reactors I_2S_4 did not produce significative lactic acid amounts, even though the pH dropped from 6 to 4.8. On the other hand, I_2S_5 produced a lactic acid amount which was more than doubled with respect to the first cycle. At the end of the second cycle, the pH correction was performed for reactors I_2S_3, I_2S_4 and I_2S_5. At the third step, a relevant increase of the lactic acid production was observed for reactors I_3S_3 and I_3S_4, while a reduction was detected for I_3S_5. As for reactors I_3S_1 and I_3S_2, the lactic acid concentrations were registered mainly at the same not significant values of the previous steps. At the end of the third step, the pH of all reactors was lower than 6: thus, pH correction was applied within all sets. During the LA production tests, lactic acid production increased in all sets of reactors. A concomitant pH drop was observed. However, the production of the I-PT_5 set was lower, compared to that observed during the two previous steps of the bioaugmentation cycle. Such results suggest that lactic acid production was related to sudden pH changes more than to an acidic pH environment. Indeed, before the first pH correction, only when pH decreased suddenly, it was sudden produced lactic acid. Otherwise, the most significative lactic acid increase was observed after the first pH correction. To support this hypothesis, control experiments were performed at uncontrolled pH. In this case, lactic acid production was significative only during the I-PT_j tests, when the glucose concentration was high enough to cause a rapid accumulation of acids and, therefore, a rapid pH drop (data not shown). These results agree with previous studies reporting that acidic conditions are able to promote

the selection of LAB from mixed cultures, even though, better results can be obtained through a swing pH control of the system [15].

To control the change of the microbial community due to the bioaugmentation cycle, microbial composition analysis was performed. The analysis was conducted on the fermented mixtures sampled from reactors I_3S_1 and I_3S_4 (used as inoculum respectively for reactor I-PT_1 and reactor I-PT_4) and the initial inoculum. The selected fermented mixtures corresponded to the bioaugmentation cycles, which resulted more performant during the LA production tests.

Among the most abundant species detected in the initial inoculum, 3 Firmicutes phylotypes and 17 Euryarchaeota phylotypes were identified. Firmicutes phylotypes were related to bacteria in the classes of Clostridia and Tissirellia. The 17 Euryarchaeota phylotypes belonged to Methanomicrobiaceae, Metanotrichaceae, Methanospirillaceae and Methanoregulaceae Families. Methanomicrobiaceae, Methanospirillaceae and Methanoregulaceae are known to as methanogens, exploiting H_2/CO_2 or formate to produce methane [21,22]. Hence, microorganisms belonging to the Methantrichaceae Family, resulting most dominant in the analysed samples, are classified as acetoclastic methanogens [22]. The microbial composition of the initial inoculum is in agreement with previous analysis of anaerobic digestion effluents [22].

Bacterial communities resulting from the two bioaugmentation cycles showed higher diversity at Phylum and Genus level compared to the initial inoculum. Indeed, Firmicutes, Actinobacteria, Bacteroidetes, and Proteobacteria were found to be abundant in both I_3S_1 and I_3S_4, while they were not dominant in the initial inoculum. Notably all the most abundant species contained in the selected fermented mixtures were different compared to the initial inoculum, confirming the effectiveness of the bioaugmentation technique. The changes in the relative abundance of the most common species detected in all the three different samples are reported in Figure 3.4.

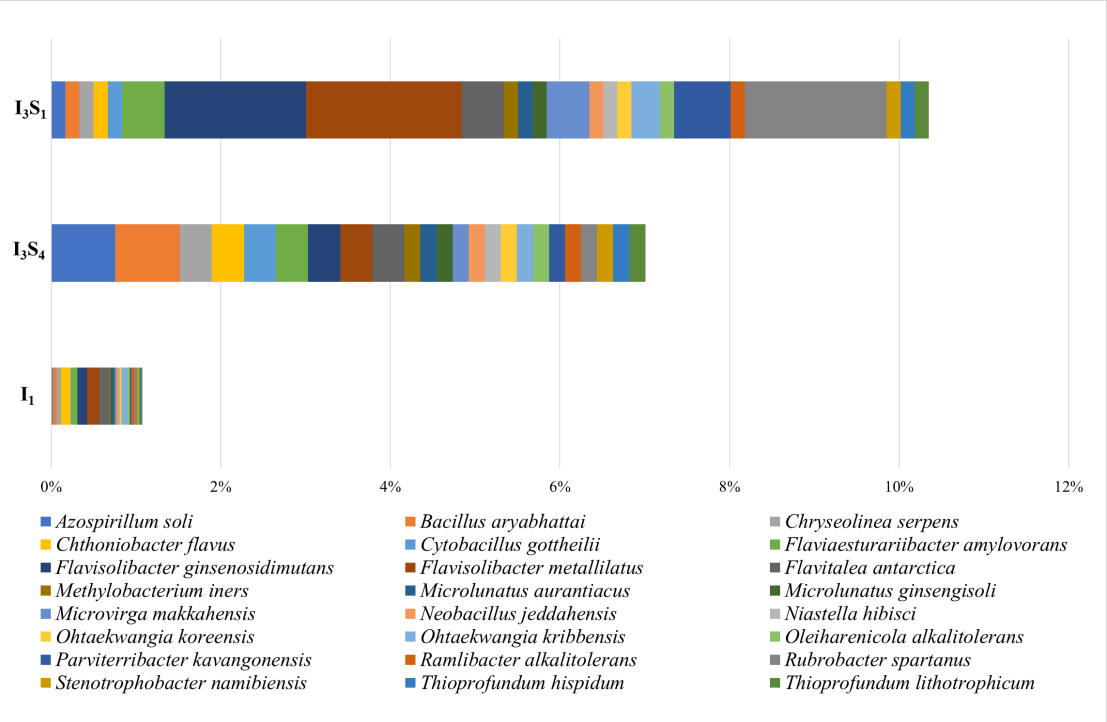

Figure 3.4. Barplot at species level analysing common microorganisms detected in samples I_1, I_3S_1 and I_3S_4.

The relative abundance of all the studied species increased during the bioaugmentation cycle. In particular, *Azospirillum soli, Bacillus aryabhattai, Chryseolinea serpens, Chthoniobacter flavus* and *Cytobacillus gottheilii* were more abundant in the I_3S_4 sample compared to the I_3S_1 one. Conversely, *Flaviaesturariibacter amylovorans, Flavisolibacter ginsenosidimutans, Flavisolibacter metallilatus, Flavitalea Antarctica, Ohtaekwangia kribbensis, Microvirga makkahensis, Parviterribacter kavangonensis and Rubrobacter spartanus* were present in higher relative abundance in the sample I_3S_1, compared to the I_3S_4 one. The remaining species were detected in similar percentages in both samples. It is worth noting that the abundance of species belonging to the genus bacillus was higher in the I_3S_4 sample. Comparing microbiological results obtained in this study with other works on lactic acid production by mixed cultures, it can be stated that acidic pre-treatments operated at constant pH are efficient when LAB such as species from *Lactobacillus*, *Lactococcus* or *Pediococcus* genera are present in the culture [14,23]. In this study, these species were absent in all the analyzed samples. However, the composition of the microbial cultures selected in this study was similar to those reported in other studies on fermentation processes producing lactic acid [10,24].

Considering all microorganisms detected in the three samples, the phylotypes that contribute to the presence of genes encoding the enzymes for lactate generation were *Bacillus* and *Corynebacterium*. The percentages of the genus *Bacillus* were: i) 0.67% in the initial inoculum; ii) 8.40% in the I_3S_4 sample; and iii) 1.77% in the I_3S_1 sample. The percentages of the genus *Corynebacterium* were, instead: 0.74% in the initial inoculum; ii) 0.94% in the I_3S_4 sample; and iii) 0.83% in the I_3S_1 sample.

3.3.1. Effect of the substrate concentration and the bioaugmentation technique on the fermentation process

Despite the abundant presence of methanogens, no methane was detected during the first step of the bioaugmentation cycle, demonstrating the efficiency of the heat shock pre-treatment. In general, the aim of inoculum pre-treatments is to create extreme conditions which are favourable to spore-forming fermentative bacteria, and hostile to non-spore-forming methanogens [25,26]. Of course, methanogens are only temporarily inhibited by the pre-treatment. Usually, in long-term processes (e.g. continuous fermentations), methanogenic archaea populations re-establish their activity [26]. In this study, the absence of methanogens in I_3S_1 and I_3S_4 samples and the absence of methane production in the LA production tests demonstrate that the bioaugmentation technique was effective for the methanogens wash out. The results were consistent with the high sensitivity of methanogens to pH values [27].

The prevalence of acetic acid and butyric acid in reactor I_1S_j indicates that microorganisms principally followed the acetate and butyrate pathways, rather than a mixed fermentation pathway. Moreover, as reported in previous studies, the fermentative metabolism of *Clostridium* species, which were abundant in the initial inoculum, produces mainly butyrate and acetate as primary soluble metabolites [28].

The observed dominance of the butyric acid pathway at increasing glucose concentration, also reported by Garcia et al. [29], probably indicates a stress condition due to the pH drop. Indeed, being glucose a rapidly biodegradable sugar, its bioconversion to hydrogen and organic acid was fast.

Very peculiar are the results related to hydrogen production. Usually, hydrogen yield increases at increasing B/A ratios [30]. In this study, however, hydrogen production is more strongly related to the presence of butyric acid rather than to the B/A ratio. From a

theoretical point of view, the metabolic route from glucose to acetate produces higher hydrogen yields compared to the pathway from glucose to butyrate [31]. However, acetate can also be a product of hydrogen consumers, such as homoacetogens belonging to the *Clostridium* genus. Since homoacetogenesis can occur concomitantly with biohydrogen production, such an event might have promoted hydrogen consumption to produce acetate [29,32]. Conversely, the butyrate pathway is inevitably linked to hydrogen production in mixed culture [33]. Due to the microbial selection, a lower acetic acid concentration was detected in the LA production tests, indicating a limited acetogenesis. This hypothesis is also supported by the higher B/A ratios observed in I-PT_j tests compared to the I_1S_j ones.

During the I_1S_i step, lactic acid production was observed only in reactors operated at high substrate concentrations. This result was attributed to the sudden pH drop, due to the higher initial glucose concentration. Nevertheless, lactic acid was detected in all the I-PT_j tests, suggesting that a shift to lactate production pathway occurred during the selection cycles. As previously mentioned, the concomitant presence of ethanol may indicate that microorganisms principally followed the heterolactic fermentation pathway [3].

3.3.2. Influence of the pH on lactic acid production

As mentioned before, the analysis of the pH and lactic acid trends lead to the evidence that lactic acid production was related to sudden pH changes more than to an acidic pH environment. The most efficient set was the I-PT_4 one, suggesting that the adopted condition guaranteed the most appropriate pH oscillation. The bioaugmentation technique operated at lower substrate concentrations was not efficient enough, while the higher glucose concentration of 12.03 (corresponding to the initial F/M ratio of 0.5) led to the progressive inhibition of the overall microbial community.

Among the microorganisms detected in the analyzed samples, the phylotypes that contribute to the presence of genes encoding the enzymes for lactate generation were *Bacillales* and *Corynebacteriales* [15,34–36]. *Corynebacteriales* relative abundance kept at almost the same percentages in I_3S_1, I_3S_4 an I_1 samples, suggesting that they were not affected by the bioaugmentation technique. Therefore, *Corynebacteriales* could have partially contributed to the lactic acid production. Conversely, microorganisms belonging to the genus *Bacillus* were present in higher relative abundance after the selection. In particular, the higher percentage was detected in the I_3S_4 fermented mixtures, which

showed the best performances in term of lactic acid production. Most likely, the pH variation obtained using a substrate concentration of 6.01 g/L (corresponding to an initial 0.25 F/M ratio) and intermittent pH adjustments determined a selection of lactic acid producing bacteria belonging to the *Bacillus* genus. Results also suggest that the pH oscillation was beneficial for *Bacillus* growth, more than a less variable acidic pH.

Compared to other lactic acid producing bacteria, *Bacillus* species have several advantages that could have helped their selection and proliferation in the conditions adopted in this study. Indeed, literature studies report that *Bacillus* species can grow and produce lactic acid using poor media instead of nutrient-rich and expensive media [37]. Moreover, they are able to produce lactic acid at both low and/or high pH [38]. Such characteristics are also advantageous in terms of process management and costs. Indeed, the risk of the contamination during the fermentation is reduced and the costs related to nutrients and sterilization are avoided. Moreover, as reported by other authors, it is also possible that the other fermentative species had a metabolic change to the lactic acid production pathway [28,33]. Indeed, Lin et al., [28] showed that when glucose was limiting, *Clostridium butyricum* shifted from the acetate/butyrate pathway to the lactate/ethanol one. Even when glucose was further supplied, the metabolic routes did not return to initial production pathways. The metabolic shift could have been facilitated by the present of glucose [29]. Indeed, under sugars availability, an accumulation of the intermediate pyruvate can occur. Pyruvate conversion to lactate represent a single step transformation that channels the surplus of electrons generated by fermentable sugars availability besides yielding reducing power to fermentative microorganisms [39]. Moreover, Corcoran et al., [40] observed that the inclusion of carbohydrates which could be utilized by *L. rhamnosus* GG resulted in enhanced survival, while the survival effect was lost in cultures containing nonmetabolizable sugars, thereby establishing a relationship between glycolysis and enhanced survival in acidic conditions.

Chemical results reported in this study are in agreement with previous studies, performed on operating conditions of mixed culture fermentation processes. Temudo et al., [41] investigated the influence of operational conditions on open mixed culture fermentation and observed that lactic acid was detected in higher concentrations during transient states, such as a rapid increase of the substrate concentration, changes of the dilution rate or pH variations. Moreover, Sakai et al., [42] observed that the intermittent pH neutralization

led to a stable and reproducible lactic acid production and inhibited the non-lactic acid bacteria growth. Finally, Tashiro et al., [15] demonstrated that the pH constant control throughout fermentation did not improve lactic acid production. Conversely, a pH control strategy consisting in a switch from swing control to constant control promoted the lactic acid production pathway.

All described results are congruent with the Biplot diagram reported in Figure 5, representing the 2D representation of the Principal Component Analysis, generated employing the data set corresponding to the LA production tests I-PT_0, I-PT_1 and I-PT_2.

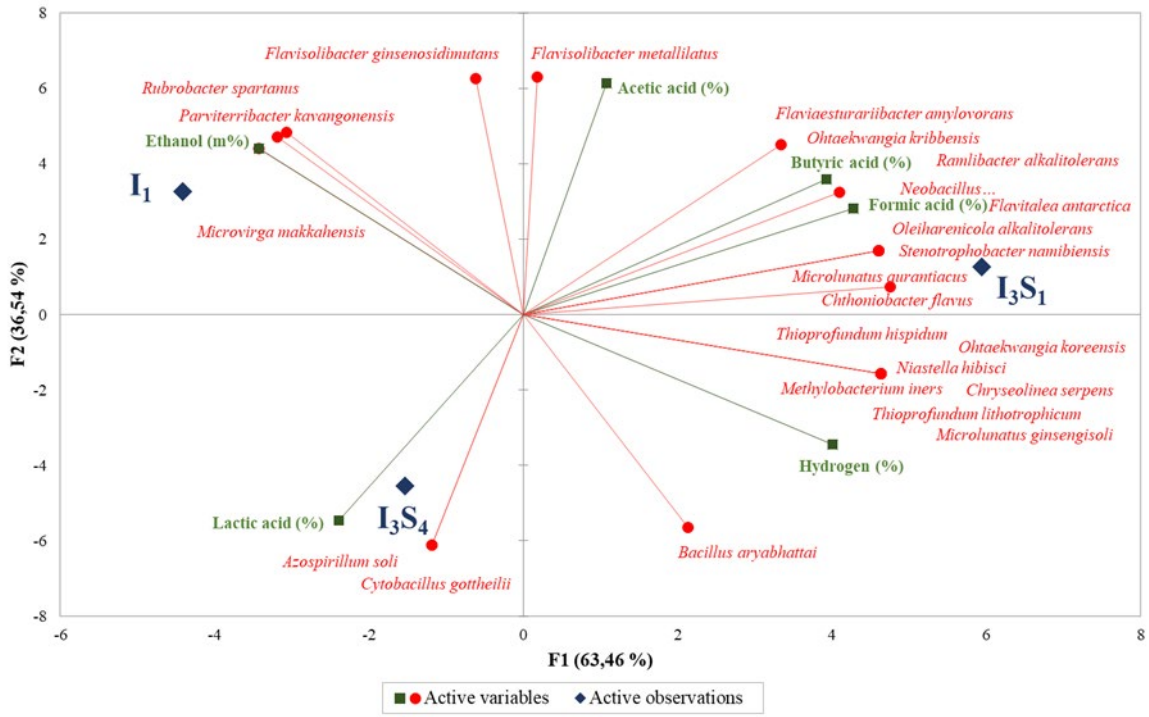

Figure 3.5. Principal Component Analysis (axes F1 and F2: 100,00%)

As an example, according to the directions of the microorganisms' vectors, and considering measured chemical parameters, LA production may depend on *Bacillus* sp., *Cytobacillus* sp., *Azospirillum* sp.

3.4. Conclusions

The study represents a first step on the development of a novel bioaugmentation technique for the selection of mixed cultures producing lactic acid. The technique may be applied to external inocula, and to any waste substrate rich in fermentable carbohydrates, without additional requirements in terms of macro and micro-nutrients availability.

The technique guarantees a pH oscillation, that enhance the selection of mixed microbial cultures producing lactic acid. The metabolites and microbial community analysis suggest that lactic acid production results from the population change to lactic acid producing bacteria belonging to the genus *Bacillus* and/or a metabolic shift of fermentative bacteria.

References

[1] Luongo V, Policastro G, Ghimire A, Pirozzi F, Fabbricino M. Repeated-Batch Fermentation of Cheese Whey for Semi-Continuous Lactic Acid Production Using Mixed Cultures at Uncontrolled pH. Sustainability 2019;11:3330. https://doi.org/10.3390/su11123330.

[2] Liang S, McDonald AG, Coats ER. Lactic acid production from potato peel waste by anaerobic sequencing batch fermentation using undefined mixed culture. Waste Manag 2015;45:51–6. https://doi.org/10.1016/J.WASMAN.2015.02.004.

[3] Rombouts JL, Kranendonk EMM, Regueira A, Weissbrodt DG, Kleerebezem R, van Loosdrecht MCM. Selecting for lactic acid producing and utilising bacteria in anaerobic enrichment cultures. Biotechnol Bioeng 2020;117:1281–93. https://doi.org/10.1002/bit.27301.

[4] Oliveira RA de, Komesu A, Vaz Rossell CE, Wolf Maciel MR, Maciel Filho R. A study of the residual fermentation sugars influence on an alternative downstream process for first and second-generation lactic acid. Sustain Chem Pharm 2020;15:100206. https://doi.org/10.1016/j.scp.2019.100206.

[5] Rawoof SAA, Kumar PS, Vo DVN, Devaraj K, Mani Y, Devaraj T, et al. Production of optically pure lactic acid by microbial fermentation: a review. Environ Chem Lett 2021;19:539–56. https://doi.org/10.1007/s10311-020-01083-w.

[6] Regueira A, Rombouts JL, Wahl SA, Mauricio-Iglesias M, Lema JM, Kleerebezem R. Resource allocation explains lactic acid production in mixed-culture anaerobic fermentations. Biotechnol Bioeng 2021;118:745–58. https://doi.org/10.1002/bit.27605.

[7] Siegumfeldt H, Rechinger KB, Jakobsen M. Dynamic changes of intracellular pH in individual lactic acid bacterium cells in response to a rapid drop in extracellular pH. Appl Environ Microbiol 2000;66:2330–5. https://doi.org/10.1128/AEM.66.6.2330-2335.2000.

[8] Padmavathi T, Bhargavi R, Priyanka PR, Niranjan NR, Pavitra PV. Screening of

potential probiotic lactic acid bacteria and production of amylase and its partial purification. J Genet Eng Biotechnol 2018;16:357–62. https://doi.org/10.1016/j.jgeb.2018.03.005.

[9] Wang C, Cui Y, Qu X. Mechanisms and improvement of acid resistance in lactic acid bacteria. Arch Microbiol 2018;200:195–201. https://doi.org/10.1007/s00203-017-1446-2.

[10] Choi G, Kim J, Lee C. Effect of low pH start-up on continuous mixed-culture lactic acid fermentation of dairy effluent. Appl Microbiol Biotechnol 2016;100:10179–91. https://doi.org/10.1007/s00253-016-7871-3.

[11] Itoh Y, Tada K, Kanno T, Horiuchi JI. Selective production of lactic acid in continuous anaerobic acidogenesis by extremely low pH operation. J Biosci Bioeng 2012;114:537–9. https://doi.org/10.1016/j.jbiosc.2012.05.020.

[12] Kobayashi H, Suzuki T, Unemoto T. Streptococcal cytoplasmic pH is regulated by changes in amount and activity of a proton-translocating ATPase. J Biol Chem 1986;261:627–30. https://doi.org/10.1016/s0021-9258(17)36138-0.

[13] Hutkins RW, Nannen NL. pH Homeostasis in Lactic Acid Bacteria. J Dairy Sci 1993;76:2354–65. https://doi.org/10.3168/JDS.S0022-0302(93)77573-6.

[14] Akao S, Tsuno H, Horie T, Mori S. Effects of pH and temperature on products and bacterial community in l-lactate batch fermentation of garbage under unsterile condition. Water Res 2007;41:2636–42. https://doi.org/10.1016/j.watres.2007.02.032.

[15] Tashiro Y, Inokuchi S, Poudel P, Okugawa Y, Miyamoto H, Miayamoto H, et al. Novel pH control strategy for efficient production of optically active l-lactic acid from kitchen refuse using a mixed culture system. Bioresour Technol 2016;216:52–9. https://doi.org/10.1016/j.biortech.2016.05.031.

[16] Policastro G, Luongo V, Fabbricino M. Biohydrogen and poly-β-hydroxybutyrate production by winery wastewater photofermentation: Effect of substrate concentration and nitrogen source. J Environ Manage 2020;271:111006. https://doi.org/10.1016/j.jenvman.2020.111006.

[17] Corniello A, Guida M, Stellato L, Trifuoggi M, Carraturo F, Del Gaudio E, et al. Hydrochemical, isotopic and microbiota characterization of telese mineral waters (Southern Italy). Environ Geochem Health 2021;4. https://doi.org/10.1007/s10653-021-00806-4.

[18] González-Cabaleiro R, Lema JM, Rodríguez J. Metabolic energy-based modelling explains product yielding in anaerobic mixed culture fermentations. PLoS One 2015;10:1–17. https://doi.org/10.1371/journal.pone.0126739.

[19] Khanal SK, Chen WH, Li L, Sung S. Biological hydrogen production: Effects of pH and intermediate products. Int J Hydrogen Energy 2004;29:1123–31. https://doi.org/10.1016/j.ijhydene.2003.11.002.

[20] Ghimire A, Frunzo L, Pontoni L, d'Antonio G, Lens PNL, Esposito G, et al. Dark fermentation of complex waste biomass for biohydrogen production by pretreated thermophilic anaerobic digestate. J Environ Manage 2015;152:43–8. https://doi.org/https://doi.org/10.1016/j.jenvman.2014.12.049.

[21] Garrity GM, Holt JG, Whitman WB, Keswani J, Boone DR, Koga Y, et al. Phylum All. Euryarchaeota phy. nov. BT - Bergey's Manual® of Systematic Bacteriology: Volume One : The Archaea and the Deeply Branching and Phototrophic Bacteria. In: Boone DR, Castenholz RW, Garrity GM, editors., New York, NY: Springer New York; 2001, p. 211–355. https://doi.org/10.1007/978-0-387-21609-6_17.

[22] Qiao JT, Qiu YL, Yuan XZ, Shi XS, Xu XH, Guo RB. Molecular characterization of bacterial and archaeal communities in a full-scale anaerobic reactor treating corn straw. Bioresour Technol 2013;143:512–8. https://doi.org/10.1016/j.biortech.2013.06.014.

[23] Juodeikiene G, Zadeike D, Bartkiene E, Klupsaite D. Application of acid tolerant Pedioccocus strains for increasing the sustainability of lactic acid production from cheese whey. LWT - Food Sci Technol 2016;72:399–406. https://doi.org/10.1016/j.lwt.2016.05.023.

[24] Xu Z, Zhang S, Zhang R, Li S, Kong J. The changes in dominant lactic acid bacteria and their metabolites during corn stover ensiling. J Appl Microbiol 2018;125:675–85. https://doi.org/10.1111/jam.13914.

[25] Kraemer JT, Bagley DM. Improving the yield from fermentative hydrogen production. Biotechnol Lett 2007;29:685–95. https://doi.org/10.1007/s10529-006-9299-9.

[26] Luo G, Karakashev D, Xie L, Zhou Q, Angelidaki I. Long-term effect of inoculum pretreatment on fermentative hydrogen production by repeated batch cultivations: Homoacetogenesis and methanogenesis as competitors to hydrogen production. Biotechnol Bioeng 2011;108:1816–27. https://doi.org/10.1002/bit.23122.

[27] Leitão RC, Van Haandel AC, Zeeman G, Lettinga G. The effects of operational and environmental variations on anaerobic wastewater treatment systems: A review. Bioresour Technol 2006;97:1105–18. https://doi.org/10.1016/j.biortech.2004.12.007.

[28] Lin PY, Whang LM, Wu YR, Ren WJ, Hsiao CJ, Li SL, et al. Biological hydrogen production of the genus Clostridium: Metabolic study and mathematical model simulation. Int J Hydrogen Energy 2007;32:1728–35. https://doi.org/10.1016/j.ijhydene.2006.12.009.

[29] García-Becerra M, Macías-Muro M, Arellano-García L, Aguilar-Juárez O. Bio-hydrogen production from tequila vinasses: Effect of detoxification with activated charcoal on dark fermentation performance. Int J Hydrogen Energy 2019;44:31860–72. https://doi.org/10.1016/j.ijhydene.2019.10.059.

[30] Hawkes FR, Hussy I, Kyazze G, Dinsdale R, Hawkes DL. Continuous dark fermentative hydrogen production by mesophilic microflora: Principles and progress. Int J Hydrogen Energy 2007;32:172–84. https://doi.org/10.1016/j.ijhydene.2006.08.014.

[31] Ghimire A, Frunzo L, Pirozzi F, Trably E, Escudie R, Lens PNL, et al. A review on dark fermentative biohydrogen production from organic biomass: Process parameters and use of by-products. Appl Energy 2015;144:73–95. https://doi.org/10.1016/J.APENERGY.2015.01.045.

[32] Siriwongrungson V, Zeng RJ, Angelidaki I. Homoacetogenesis as the alternative pathway for H2 sink during thermophilic anaerobic degradation of butyrate under suppressed methanogenesis. Water Res 2007;41:4204–10.

https://doi.org/10.1016/j.watres.2007.05.037.

[33] Guo XM, Trably E, Latrille E, Carrere H, Steyer JP. Predictive and explicative models of fermentative hydrogen production from solid organic waste: Role of butyrate and lactate pathways. Int J Hydrogen Energy 2014;39:7476–85. https://doi.org/10.1016/j.ijhydene.2013.08.079.

[34] Mugnai G, Borruso L, Mimmo T, Cesco S, Luongo V, Frunzo L, et al. Dynamics of bacterial communities and substrate conversion during olive-mill waste dark fermentation: Prediction of the metabolic routes for hydrogen production. Bioresour Technol 2021;319:124157. https://doi.org/10.1016/j.biortech.2020.124157.

[35] Ohara H, Yahata M. L-lactic acid production by Bacillus sp. in Anaerobic and aerobic culture. J Ferment Bioeng 1996;81:272–4. https://doi.org/10.1016/0922-338X(96)82222-7.

[36] Poudel P, Tashiro Y, Sakai K. New application of Bacillus strains for optically pure L-lactic acid production: General overview and future prospects. Biosci Biotechnol Biochem 2016;80:642–54. https://doi.org/10.1080/09168451.2015.1095069.

[37] Wang Q, Zhao X, Chamu J, Shanmugam KT. Isolation, characterization and evolution of a new thermophilic Bacillus licheniformis for lactic acid production in mineral salts medium. Bioresour Technol 2011;102:8152–8. https://doi.org/10.1016/j.biortech.2011.06.003.

[38] Abdel-Rahman MA, Tashiro Y, Sonomoto K. Recent advances in lactic acid production by microbial fermentation processes. Biotechnol Adv 2013;31:877–902. https://doi.org/10.1016/j.biotechadv.2013.04.002.

[39] Elbeshbishy E, Dhar BR, Nakhla G, Lee HS. A critical review on inhibition of dark biohydrogen fermentation. Renew Sustain Energy Rev 2017;79:656–68. https://doi.org/10.1016/j.rser.2017.05.075.

[40] Corcoran BM, Stanton C, Fitzgerald GF, Ross RP. Survival of probiotic lactobacilli in acidic environments is enhanced in the presence of metabolizable

sugars. Appl Env Microbiol:3060–7. https://doi.org/10.1128/AEM.71.6.3060.

[41] Temudo MF, Muyzer G, Kleerebezem R, Van Loosdrecht MCM. Diversity of microbial communities in open mixed culture fermentations: Impact of the pH and carbon source. Appl Microbiol Biotechnol 2008;80:1121–30. https://doi.org/10.1007/s00253-008-1669-x.

[42] Sakai K, Murata Y, Yamazumi H, Tau Y, Mori M, Moriguchi M, et al. Selective Proliferation of Lactic Acid Bacteria and Accumulation of Lactic Acid during Open Fermentation of Kitchen Refuse with Intermittent pH Adjustment. Food Sci Technol Res 2000;6:140–5. https://doi.org/10.3136/fstr.6.140.

PART 2

Photo fermentation of agri-food feedstocks and dark fermentation effluents for hydrogen and PHAs production

Chapter 4

Carbon Catabolite Repression occurrence in photo fermentation of ethanol-rich substrates: Effect of the ethanol to glycerol ratio

This chapter has been published as: Policastro, G., Giugliano, M., Luongo, V., Napolitano, R. and Fabbricino, M. (2021). Carbon catabolite repression occurrence in photo fermentation of ethanol-rich substrates. Journal of Environmental Management, 297, 113371.

Carbon Catabolite Repression occurrence in photo fermentation of ethanol-rich substrates

Abstract

The chapter investigates the phenomenon of Carbon Catabolite Repression occurring during photo fermentation of ethanol-rich effluents, which usually contain ethanol as main carbon source, and glycerol as secondary one. The study was conducted using mixed phototrophic cultures, adopting, as substrate, the effluent produced by the alcoholic fermentation of sugar cane bagasse. In order to elucidate the phenomenon, experimental tests were carried out using two different ethanol to glycerol ratios. Results were compared with those resulting from pure ethanol and glycerol conversion. According to the obtained data, as a result of Carbon Catabolite Repression occurrence, the presence of glycerol negatively affects hydrogen production. Indeed, part of the ethanol source is converted to biomass and polyhydroxybutyrate rather than to hydrogen. In more details, the presence of glycerol determines a drop of the hydrogen production, which goes from 12% to 32%, according to the ethanol/glycerol ratio, compared to the production obtained from fermentation of ethanol alone. Therefore, to promote the hydrogen production, it is advisable to apply strategies to produce low glycerol concentrations in the ethanol production stage.

4.1. Introduction

Hydrogen is the most attractive alternative fuel, due to its high energy content and clean combustion properties [1]. In the past decade, biological hydrogen production processes have attracted increasing attention as a tool to reverse greenhouse gas emissions. Among biological processes, photo fermentation (PF) has been acknowledged as an effective and environmentally-friendly process for biohydrogen production [2]. Photo fermentative microorganisms, known as purple non sulfur bacteria (PNSB), are able to utilize various organic compounds as feedstock, including dark fermentation effluents (DFEs) [3,4]. The photo conversion of DFEs is particularly interesting, as it allows combining two different anaerobic biological processes (Dark fermentation and Photo fermentation). Consequently, it is possible to enhance hydrogen yields via the photo conversion of the organic matter contained in DFEs. [5]. Moreover, additional valuable by-products are produced as consequence of PNSB metabolic activity, so increasing the overall convenience of the transformation. Indeed, PNSB are able to accumulate polyhydroxybutyrate (PHB), a precursor of totally biodegradable plastic materials. This

allows energy to be obtained from organic waste together with valuable chemicals for bio-plastic production. DFEs contain various types of organic compounds, mainly belonging to the class of organic acids (e.g. acetic acid, butyric acid, propionic acid, lactic acid) and alcohols (e.g. ethanol, butanol) [6,7]. Therefore, when DFEs are used as substrates for the PF process, photo fermentative bacteria access to multiple carbon sources. Such an event may compromise the efficiency of biohydrogen production. In fact,.in a multi-substrate environment, the presence of a preferred carbon source often prevents the use of other available sources for the same metabolic conversion [8]. Specifically, it has been observed that, during fermentation processes, a preferred substrate is used for hydrogen production, while the others are used for biomass production. This phenomenon, named Carbon Catabolite Repression (CCR), is regulated at genetic level [9].

Unfortunately, there is a lack of studies related to the development of CCR phenomenon during PF of DFEs. Although some authors have reported that glucose may act as a catabolite repressor [10], no other information is available related to other carbon sources, to date. Therefore, the question is worth of additional research efforts, especially referring to the photo fermentative conversion of ethanol-rich effluents, which are poorly investigated, despite their importance for practical applications. Ethanol-rich effluents, in fact, are always obtained as a result of the alcoholic fermentation of sugar-rich substrates [11]. This process generates ethanol as main compound and glycerol as secondary one. Almost 4–5% of the initial amount of substrate can go toward glycerol synthesis [12]. Therefore, glycerol is the major by-products of ethanol production.

The aim of the present study was to verify the occurrence of CCR phenomenon during PF of DFEs, testing the effect of glycerol presence in ethanol-rich effluents, on the overall production of biohydrogen. The study was conducted using mixed phototrophic cultures on a synthetic substrate simulating the effluent resulting from bagasse alcoholic fermentation [11]. PHB accumulation, as alternative result of the conversion process, was also explored, to better elucidate the effect of CCR phenomenon.

4.2.Materials and methods

4.2.1. Materials and experimental set up

The inoculum was sampled from a mixed culture PF reactor operating at laboratory scale, used for previous experiments [1]. Before use, microorganisms were enriched using ethanol (2 mL/L) as substrate, a nutrient rich-medium and a trace elements solution. The

nutrient-rich medium was prepared as follows: $NaC_5NO_4H_8$ (sodium glutamate), 400 mg/L; $MgSO_4.7H_2O$ (magnesium sulphate heptahydrate), 200 mg/L; yeast extract, 300 mg/L; $C_6H_5FeO_7$ (ferric citrate), 24.5 mg/L; NaCl (sodium chloride), 400 mg/L; K_2HPO_4 (potassium hydrogen phosphate), 600 mg/L; KH_2PO_4 (potassium dihydrogen phosphate), 300 mg/L; $NaHCO_3$ (sodium hydrogen carbonate), 700 mg/L; $CaCl_2.2H_2O$ (calcium chloride dihydrate), 75 mg/L. Micronutrients were provided by adding 10 mL/L of the following trace element solution: $ZnCl_2$ (zinc chloride), 70 mg/L; $MnCl_2$ $4H_2O$ (magnesium chloride tetrahydrate), 100 mg/L; H_3BO_3 (boric acid), 60 mg/L; $CoCl_2.6H_2O$ (cobalt(II) chloride hexahydrate), 200 mg/L; $CuCl_2.2H_2O$ (copper(II) chloride dihydrate), 20 mg/L; $NiCl_2.6H_2O$ (nickel(II) chloride hexahydrate), 20 mg/L; $NaMoO_4.2H_2O$ (sodium molybdate dihydrate), 40 mg/L; HCl 25% (hydrogen chloride), 1 mL L^{-1}.

The synthetic substrate was prepared reproducing the composition of one of the fermentation effluents reported in the study by Wang et al., [11]. The mentioned effluent was obtained from the fermentation process of sugars released from pre-treated sugar cane bagasse, using a co-culture of *Escherichia coli* LW419 and turbo yeast. The synthetic effluent was diluted to contain the feeding Chemical Oxygen Demand (COD) under inhibiting threshold values. COD values above 1.5 g_{COD} L^{-1} have been reported to reduce the hydrogen productivity [1]. The dilution was performed using the same nutrient-rich medium and the trace elements solution, adopted for the re-activation phase. The chemicals used for all analytical determinations were high purity degree. Only bi-distilled water was adopted as reagent water. Before each use, glassware was soaked overnight in a concentrated nitric acid bath (2% v/v) and rinsed carefully.

Two experimental sets, each composed by three different experiments, were carried out. Each experiment was performed in triplicate. Regarding the first set, the first experiment was prepared using ethanol and glycerol as substrate. Such experiment will be called Etoh-gly 1. The ethanol to glycerol ratio of 12.5 was set in accordance to the fermentative effluent of the sugar cane bagasse reported by Wang et al., [11]. The other two experiments were carried out with ethanol and glycerol as sole substrates. Such experiment will be called Etoh 1 and Gly 1, respectively. Ethanol and glycerol concentrations in the second and the third experiment, were equal to those used in the first experiment. Etoh 1 and Gly 1 experiments were conducted in order to compare the hydrogen production of the set Etoh-gly 1 with the sum of productions obtained from reactors prepared using ethanol and glycerol alone (overlapping effects). The second set was prepared using the same designing criteria adopted for the first one and changing the ethanol to glycerol ratio. Such set was conducted to investigate the effect of the ethanol

to glycerol ratio on the overlapping effects. The characteristics of experiments are summarized in **Table 1**.

Table 4.1. Characteristics of the experimental set-up

Experiment #	COD (mg L^{-1})	Ethanol (mg L^{-1})	Glycerol (mg L^{-1})	Ethanol to glycerol mass ratio
Set 1				
Etoh-gly 1	1000	457	37	12.5
Etoh 1	955	457	-	-
Gly 1	45	-	37	-
Set 2				
Etoh-gly 2	1000	417	105	4
Etoh 2	870	417	-	-
Gly 2	130	-	105	-

Photo bioreactors were built using transparent borosilicate glass bottles with a total volume of 500 mL and a working volume of 400 mL. The working volume was filled with 395 mL of culture medium and 5 mL of inoculum. Reactors were hermetically sealed with plastic caps, equipped with two sampling tubes. Oxygen and nitrogen gas absence was ensured by initial flushing with argon gas. Each reactor was placed on a magnetic stirrer, adjusting the rotation speed to 250 rpm. Temperature was kept to 25±2°C using a climatic chamber and the initial pH value was fixed to 7, using a KOH solution.

The light energy was provided by flexible light emitting diode (LED) strips, positioned between reactors. The light intensity was kept at about 4000 lux for the entire duration of the tests.

4.2.3. Analytical methods and equipment

Gas production was quantified trough water displacement. Successively, gas samples were analyzed via gas chromatography to determine hydrogen and carbon dioxide content. Gas chromatography was performed using a Varian Star 3400 gas chromatograph equipped with Shin Carbon ST 80/100 column. Argon was utilized as carrier gas with 20 psi front and rear end pressure. Organic acids (OAs), Volatile Fatty Acids (VFAs), glycerol and ethanol concentrations were determined by high pressure liquid chromatography, using a Dionex (Sunnyvale, USA) LC 25 Chromatography Oven equipped with a Metrohom (Herisau, Switzerland) Organic Acids column (Metrosep

Organic Acids - 250/7.8), a Dionex (Sunnyvale, USA) GD 500 Gradient Pump and two different detectors. The first one was a Dionex (Sunnyvale, USA) UVD 340U detector and was used for Oas and VFAs determination. The second one, a Jasco (Cremella, Italy) RI-2031, was used for ethanol and glycerol detection. The eluent was a 5 mM H_2SO_4 solution, pumped at a rate of 0.7 mL/min. The temperature was 50°C. PHB concentration was determined by chloroform extraction and successive gas chromatography and mass spectrometry analysis. Gas chromatography and mass spectrometry were conducted using a GC-MS with a ZB Semi Volatiles Zebron column (Phenomenex, Torrance, USA). Helium was used as carrier gas. For the PHB extraction, samples were preliminarily lyophilized, using a Martin Christ ALPHA 2-4 LSC plus freeze dryer (Osterode am Harz, Germany). Biomass growth was quantified measuring the total suspended solids (TSS) concentration via the optical density (OD) at 660 nm. The optical density was measured via a Photolab Spektral, WTW (Wheilheim, Germany) spectrophotometer (6600 UV vis). Light intensity was checked using a Lutron-LX-107 light meter (Coopersburg, USA).

4.3. Results and Discussion

4.3.1. Photo Fermentation experiments

Figures 4.1 to 4.3 illustrate the time-course profiles of the parameters monitored during the first set of experiments.

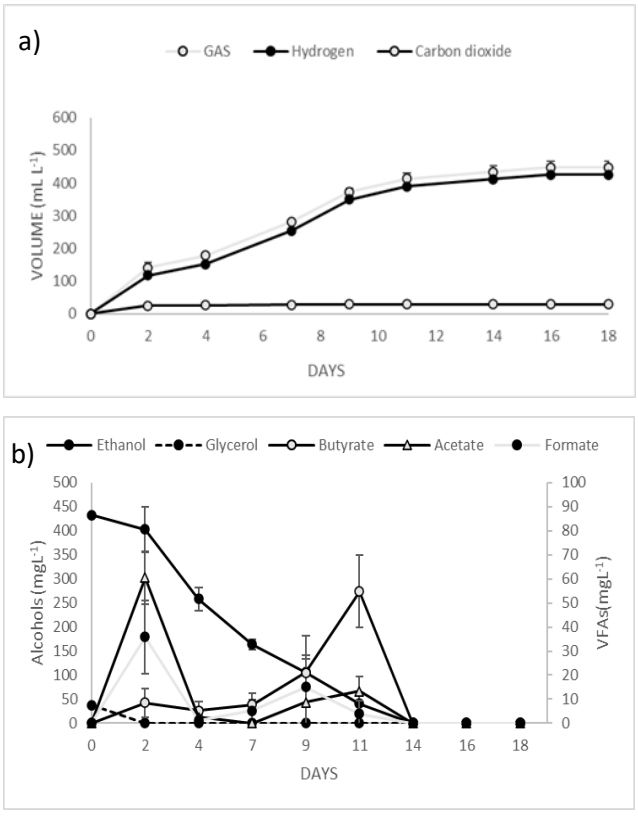

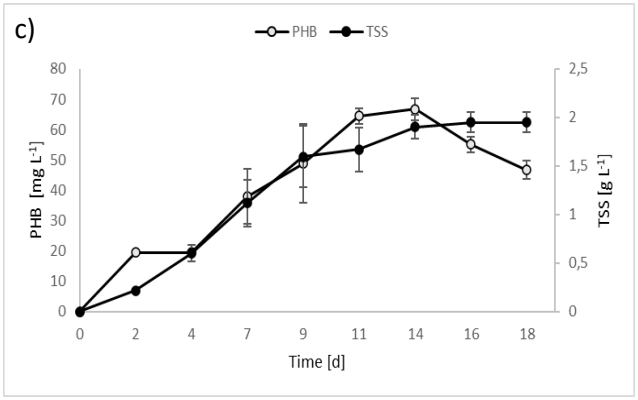

Figure 4.1. Experimental results for reactors Etoh-gly 1. a) Hydrogen, carbon dioxide and total biogas cumulative production (standard temperature and pressure conditions). b) Ethanol, glycerol and organic acids concentration. c) PHB and TSS concentration.

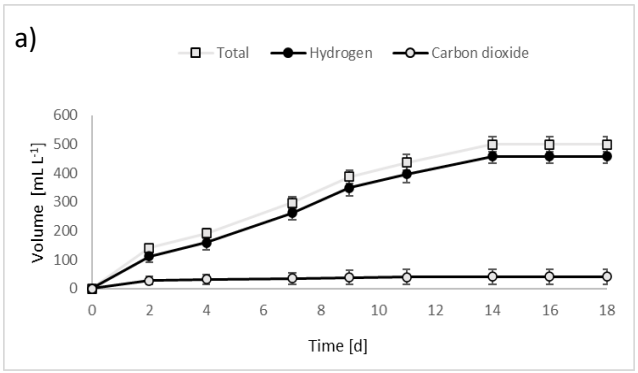

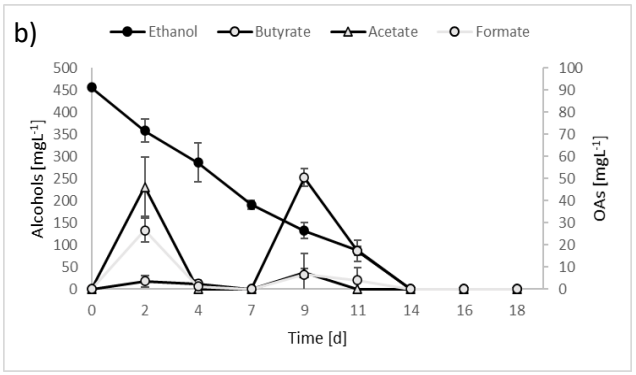

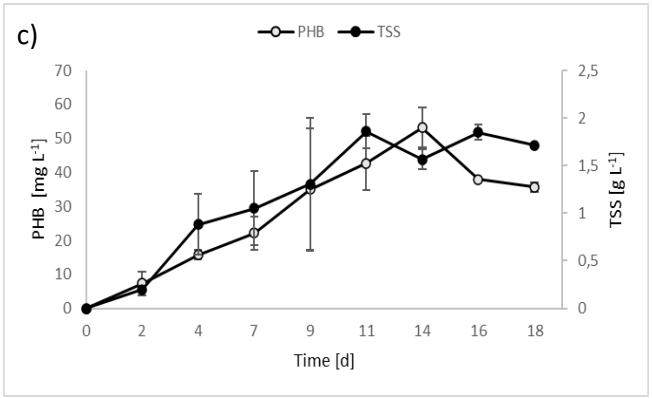

Figure 4.2. Experimental results for reactors Etoh 1. a) Hydrogen, carbon dioxide and total biogas cumulative production (standard temperature and pressure conditions). b) Ethanol and organic acids concentration. c) PHB and TSS concentration.

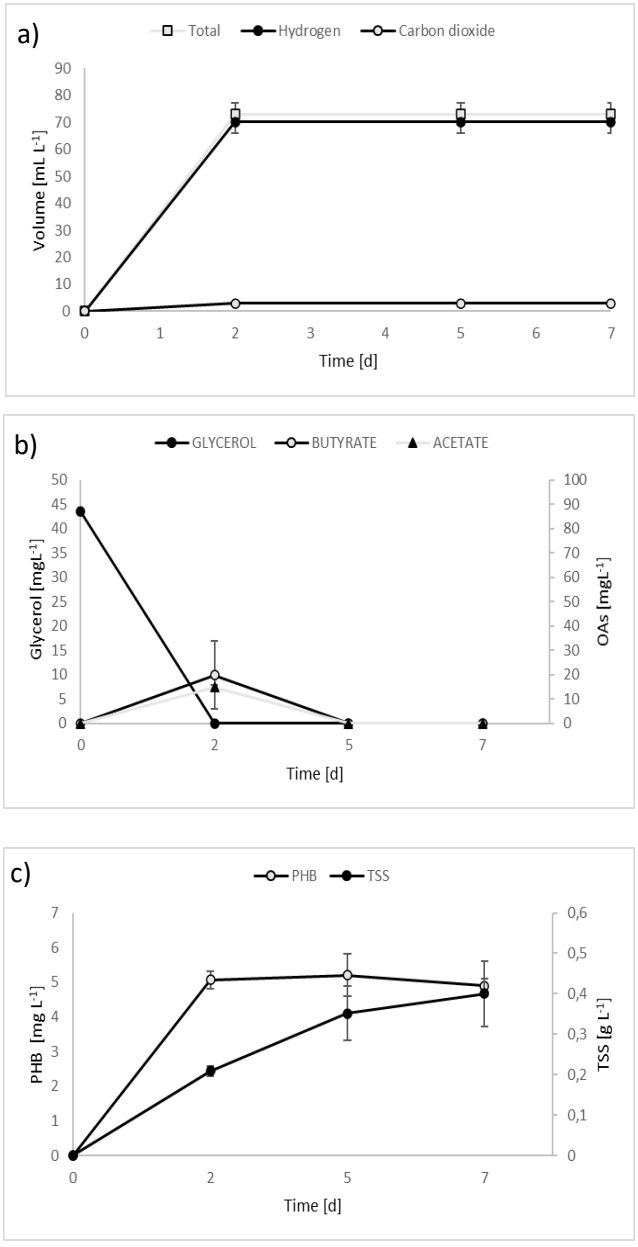

Figure 4.3. Experimental results for reactors Gly 1. a) Hydrogen, carbon dioxide and total biogas cumulative production (standard temperature and pressure conditions). b) Glycerol and organic acids concentration. c) PHB and TSS concentration.

During the initial two fermentation days, the ethanol consumption rate of the set Etoh-gly1 was lower than those observed in Etoh1, while the glycerol was completely

degraded. After the glycerol depletion, the ethanol consumption rate in the set Etoh-gly1 increased, while the rate of the Etoh1 set kept almost constant. As reported by other authors [13], the consumption rate of the main substrate increases significantly when the minor substrates are depleted when multiple substrates are present in the culture medium. Notably, in Etoh-gly1 the final cumulative volumetric hydrogen yield reached 424 $N \cdot mL \cdot H_2 \cdot L^{-1}$, while in Etoh1 it reached 458 $N \cdot mL \cdot H_2 \cdot L^{-1}$, despite the lower initial COD (**Figure 4.1**). In both experiments, acetate, butyrate, and formate were produced during the first two days of fermentation. On day 4, only acetate and formate were completely consumed in Etoh-gly1, while all the previously produced acids were consumed in Etoh1. The consumption of OAs determined a low hydrogen increase. On the other hand, acids consumption was associated to a significant increase of the biomass growth.

Afterwards, there was a gradual consumption of ethanol in both sets. Hydrogen was the main fermentation by-product. In Etoh-gly1, acetate was consumed faster than butyrate, because it represented a more favorable substrate for PNSB [14–16]. From day 7, formic and acetic acid were produced and successively consumed on day 9 and day 14, while in Etoh1 from the same day, acetic, formic, and butyric acid were produced. The first one was consumed on day 11 and the others two on day 14. Formate production was found in several photofermentative studies conducted using complex substrates such as molasses DFE [17,18] and thick juice DFE [19], as well as on lactate containing media using *Rhodobacter capsulatus* [20]. In addition, Eroğlu et al., [13] observed a relationship between formate accumulation and dark or low light intensity conditions in a study conducted using *Rhodobacter sphaeroides* with a malate containing substrate. Accumulation of formate causes the incomplete oxidation of the substrate with consequent low hydrogen production [21]. In the present study, the low accumulated amounts of formic acid (35.8 $mg \cdot L^{-1}$) avoided the above consequences.

Figures 4.4 to 4.6 illustrate the time-course profiles of the parameters monitored during the second set of experiments.

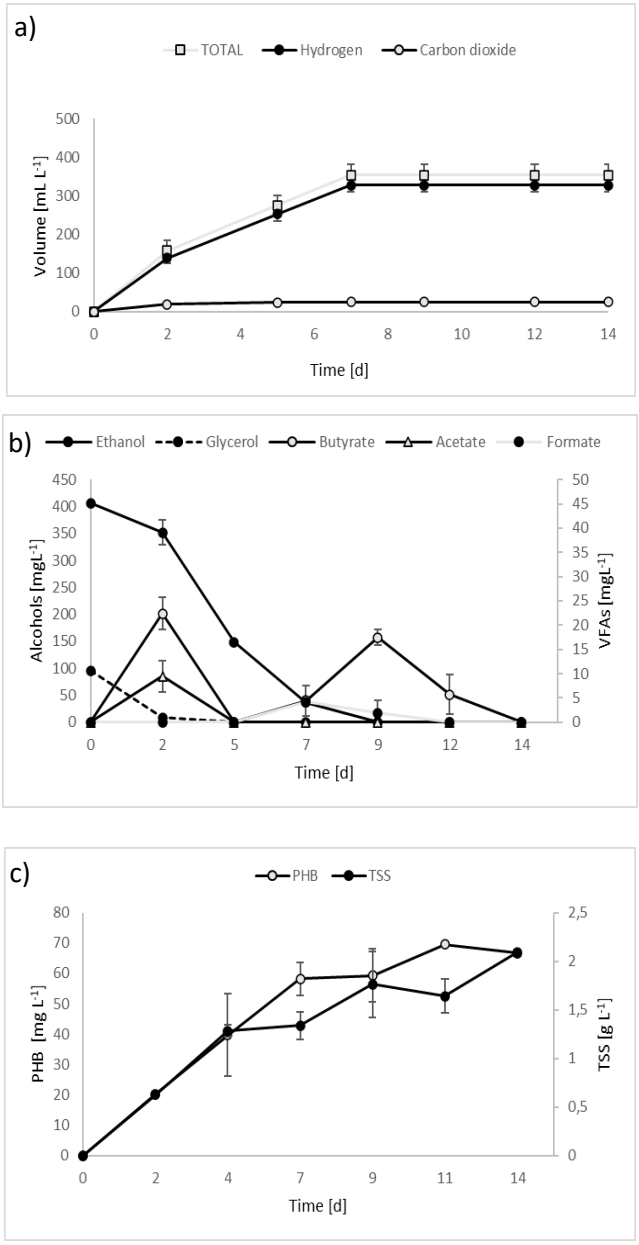

Figure 4.4. Experimental results for reactors Etoh-gly 2. a) Hydrogen, carbon dioxide and total biogas cumulative production (standard temperature and pressure conditions). b) Ethanol, glycerol and organic acids concentration. c) PHB and TSS concentration.

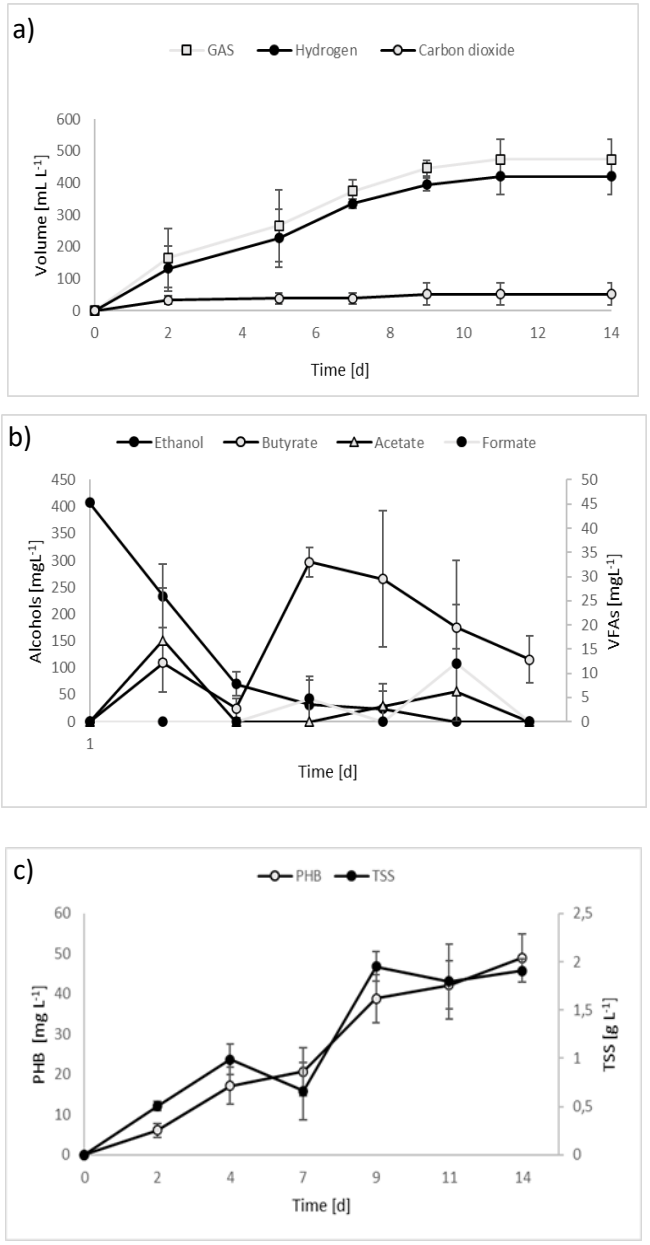

Figure 4.5. Experimental results for reactors Etoh 2. a) Hydrogen, carbon dioxide and total biogas cumulative production (standard temperature and pressure conditions). b) Ethanol and organic acids concentration. c) PHB and TSS concentration.

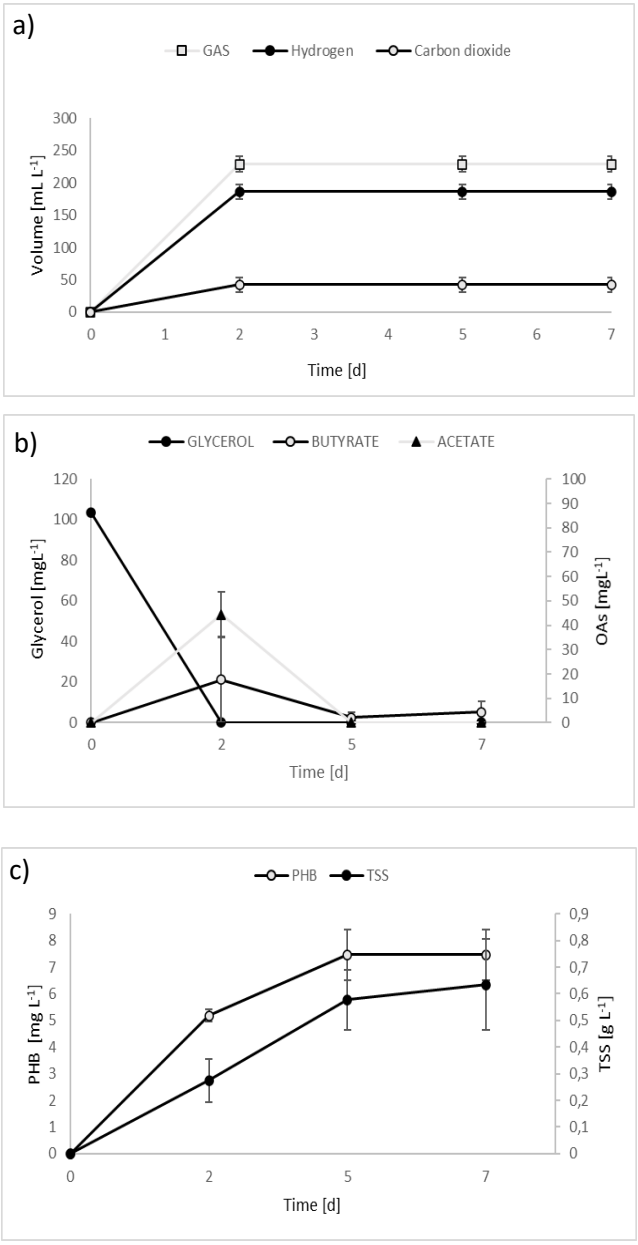

Figure 4.6. Experimental results for reactors Gly 2. a) Hydrogen, carbon dioxide and total biogas cumulative production (standard temperature and pressure conditions). b) Glycerol and organic acids concentration. c) PHB and TSS concentration.

Concerning the second set of experiments, glycerol was almost completely consumed in the first two days. The initial concentration of glycerol (105 $mg \cdot L^{-1}$) in Etoh-gly2 was higher than that observed in Etoh-gly1 (37 $mg \cdot L^{-1}$). The degradation rate of ethanol observed in the first two days was lower compared to the one achieved in the following days.

Etoh-gly2 and Etoh2 presented an overall hydrogen production of 328 $mL \cdot H_2 \cdot L^{-1}$ and 395 $mL \cdot H_2 \cdot L^{-1}$, respectively. As observed for the first set, biomass content was higher in

Etoh-gly2 (1,95 g·TSS·L^{-1}) than in Etoh2 reactors (1,70 g·TSS·L^{-1}). Furthermore, Etoh-gly2 showed a higher biomass content than Etoh-gly1 in the first two days of observation, when ethanol and glycerol coexisted. No significant hydrogen production was detected beyond the 7th day. Ethanol was completely degraded at day 9.

OAs concentration were similar to those detected in the first set of reactors. Days 7 to 9 were characterized by the increase in butyrate production and biomass growth in terms of TSS. The time-course profile of the parameters evaluated in Gly1 and Gly2 (**Figure 4.3** and **Figure 4.6**) showed that glycerol degradation by microorganisms was quite fast and the presence of the single pure substrate favoured hydrogen production. Hydrogen production from glycerol has been studied in previous works demonstrating the effectiveness of the photo fermentation process devoted to hydrogen production starting from pure or raw glycerol [22,23]. In both sets acetate and butyrate were produced during the first two days of fermentation and successively depleted.

In all reactors a considerable hydrogen percentage was detected. Indeed, about 90% of the biogas was represented by hydrogen, with peaks of 92% in Etoh-gly2. According to previous studies on mixed PNSB cultures, a partial dissolution of the carbon dioxide occurred during fermentation, which was successively used as carbon source by PNSB [24].

In all reactors, the COD removal efficiency ranged between 97% and 100%. However, these values represent a theoretical outcome, since they were computed on the final volatile fatty acids (VFAs) concentration in the effluents without considering the biomass and the presence of undetected compounds. Likewise, Ghimire et al. [25] reported such high removal efficiency, while Luongo et al. [5] obtained a COD removal efficiency of about 90% using a VFAs-based substrate and mixed PNSB cultures. Moreover, such results are generally higher than those obtained from configurations involving pure microbial culture [26].

Several other interesting considerations could be deduced from the obtained trend of the PHB concentration. It is widely known that PHB production is influenced by operational parameters such as C and N source, C/N ratio, pH and substrate concentration [27]. Notably, the accumulation of such a compound strongly depends on the characteristics of adopted PNSB species and substrates. A low PHB production is generally due to the presence of a mixed consortia devoid of accumulating PHB species [5,28]. Indeed, the

values obtained in the present study were similar to those reported by other authors, who used mixed PNSB cultures [1,25].

Higher maximum PHB concentration were reached in Etoh-gly sets. Such a result agrees with recent findings [1,5] showing the concomitant PHB accumulation and hydrogen production with the use of multiple substrates. Finally, the biomass concentration reached a higher final value in Etoh-gly than in Etoh reactors.

4.3.2. Discussion

Bioprocesses aimed at producing hydrogen and PHB are crucial to replace fossil fuels and traditional plastics. PF is one of the most attractive bioprocesses, due to its environmental-friendly characteristics and the possibility of using waste materials as substrates. However, the behaviour of phototrophic microorganisms in the presence of multiple carbon sources has not been completely elucidated. In this study, PF tests were carried out using a mixed phototrophic consortium and a synthetic substrate, simulating the real effluent deriving from the bagasse alcoholic fermentation process. To analyze the glycerol availability effect, further tests were carried out varying the ethanol to glycerol ratio and using ethanol and glycerol alone. Hydrogen cumulative production and PHB accumulation for all tested reactors are summarized in **Table 4.2**.

Table 4.2. Evaluation parameters for the two experimental sets.

Experiment #	H_2 production [mL L^{-1}]	Overlapping effects* H_2	PHB max production [mg L^{-1}]	Overlapping effects* PHB
Set 1		80%		118%
Etoh-gly 1	424±15		67±4	
Etoh 1	458±13		51±3	
Gly 1	70±4		5.7±1	
Set 2		56%		117%
Etoh-gly 2	328±14		66±1	
Etoh 2	395±18		49±6	
Gly 2	186±10		7.4±1	

**Ratio between the production of the set Etoh-gly and the sum of the production of the set Etoh plus that of the set Gly*

Despite the lower initial COD, reactors containing ethanol as sole carbon source presented a higher hydrogen production compared to those conducted using both ethanol and glycerol. By contrast, in the latter sets higher PHB concentrations were detected. The principle of overlapping effects was not respected in both sets. The sum of the hydrogen production of the Etoh and Gly reactors was higher compared to the hydrogen production

of reactors Etoh-gly. Nevertheless, the PHB production of reactors Etoh-gly was higher compared to the sum of the Etoh and Gly PHB productions. The obtained results suggest that the presence of glycerol in alcoholic effluents negatively affects hydrogen production. Indeed, part of the substrates are involved in reactions leading to biomass generation and PHB accumulation. In other words, results indicate the occurrence of the CCR phenomenon and glycerol as carbon repressor in PF of mixed substrates containing ethanol.

As reported by Ghosh et al. [9], in multi substrate environments it often occurs that one particular carbon source is used for the hydrogen production, while another one is used for the biomass generation and PHB accumulation, although both substrates could be utilized for hydrogen production. As a result of a CCR mechanism, the presence of a preferred carbon source in the culture medium [8] prevents the expression of some genes, which are necessary for the consumption of one or more carbon sources [10].

Currently, the CCR phenomenon in photo fermentation processes has been observed in mixtures of substrates containing glucose. Pattanamanee et al., [10] observed that during PF of oil palm empty fruit bunch containing glucose, xylose and acetic acid, glucose was consumed first, together with acetic acid. Xylose was consumed only after glucose depletion, once more together with acetic acid. Nonetheless acetic acid did not contribute to hydrogen production of hydrogen. Similarly, Policastro et al. [1], studying PF of winery wastewater, observed that in presence of both glucose and ethanol, PNSB showed a higher assimilation rate with glucose than with ethanol. In other studies, performed using a mixture of organic acids (e.g. acetic acid, butyric acid, propionic acid), the CCR phenomenon was not observed. Uyar et al. [15] highlighted that an organic acids mixture led to higher hydrogen conversion efficiency compared to the single acids alone. Two different mixed substrates were involved using diverse amounts of butyric, acetic, and propionic acid and none of these was chosen by microorganisms as a preferential source.

In the present study, Etoh1 and Etoh2 sets reached a similar conversion efficiency in terms of specific hydrogen production per gram of initial COD, which equalled, respectively, 479.6 $mLH_2\ g_{COD}^{-1}$ and 475.9 $mLH_2\ g_{COD}^{-1}$. However, in the presence of glycerol, the two productions dropped to 424 $mLH_2\ g_{COD}^{-1}$ for Etogly 1 and to 328 $mLH_2\ g_{COD}^{-1}$ for Etoh-gly 2, as the glycerol contained in the synthetic effluent of the bagasse fermentation acted as a carbon repressor. The ethanol to glycerol ratio also had a considerable effect on the CCR phenomenon. In particular, the higher ethanol to glycerol ratio (12.5) determined a

decrease of hydrogen production ranging around 12%, while the lower ethanol to glycerol ratio (4) led to a production drop around 32%.

Despite the lower hydrogen yield in Etoh-gly reactors, the obtained productions were comparable with values reported by Liu et al., (2015), who performed the ethanol conversion to hydrogen using *Rhodopseudomonas palustris* CGA009.

The results reported in the present study and the information available from the literature lead to some paramount considerations related to the use of mixed substrates for PF processes development. When the substrate is composed by organic acid such as acetic, butyric, and propionic acids, none of them is chosen by microorganisms as a preferential substrate. However, the presence of butyric acid as the main source is less advisable than the presence of acetic acid for hydrogen production maximization [15]. Substrates containing glucose activate the CCR phenomenon, preventing the utilisation of other carbon sources (e.g., organic acids and ethanol) for hydrogen generation. Despite the effectiveness of glycerol as sole substrate for PNSB [22,23], the availability of glycerol as secondary substrate in ethanol-rich effluents generate the CCR phenomenon. Ethanol is partially utilised as source of biomass and PHB. At high ethanol to glycerol ratios such effect is negligible. Nevertheless, an ethanol to glycerol ratio of 4 lead to a considerable reduction of the hydrogen yield. Therefore, during the ethanol production stage it is advisable to apply strategies to produce low glycerol concentrations. The most widely used approach to reduce glycerol formation is to operate the fermentation process in fed-batch mode. Such feeding mode ensure lower substrate concentrations resulting in lower osmotic stress, which limits glycerol yields [29]. The strategy is currently applied at industrial scale for the ethanol production process from sugars [12]. To further reduce the glycerol yield during the biological ethanol production process, it is possible to apply genetic engineering techniques. For instance, Jagtap et al., [12] deleted genes in the High-Osmolarity Glycerol (HOG) pathway. These genes regulated glycerol synthesis in *S. cerevisiae*. The knock-out strains showed a 35% decrease in glycerol yields.

4.4. Conclusions

This experimental study faces the lack of knowledge on the behavior of phototrophic bacteria in the presence of multiple carbon sources. Results demonstrated that the ethanol to glycerol ratio of 12.5 determined a decrease of the hydrogen production of 12%, compared to the production obtained from the fermentation of ethanol alone. Moreover, the lower ethanol to glycerol ratio of 4 led to a higher production drop (32%). As a result

of the CCR phenomenon, the presence of glycerol in ethanol-rich substrates determines a drop of the hydrogen production. Therefore, when alcoholic fermentation effluents are used as substrate in the PF process, the hydrogen yield can be maximized by limiting the concentration of glycerol, to prevent the occurrence of the CCR phenomenon. The use of mixed culture is beneficial to enhance the hydrogen yield, while mixed substrates enhance the biomass formation and the PHB accumulation.

References

[1] Policastro G, Luongo V, Fabbricino M. Biohydrogen and poly-β-hydroxybutyrate production by winery wastewater photofermentation: Effect of substrate concentration and nitrogen source. J Environ Manage 2020;271:111006. https://doi.org/10.1016/j.jenvman.2020.111006.

[2] Touloupakis E, Poloniataki EG, Ghanotakis DF, Carlozzi P. Production of Biohydrogen and/or Poly-β-hydroxybutyrate by Rhodopseudomonas sp. Using Various Carbon Sources as Substrate. Appl Biochem Biotechnol 2021;193:307–18. https://doi.org/10.1007/s12010-020-03428-1.

[3] Seifert K, Zagrodnik R, Stodolny M, Łaniecki M. Biohydrogen production from chewing gum manufacturing residue in a two-step process of dark fermentation and photofermentation. Renew Energy 2018;122:526–32. https://doi.org/10.1016/j.renene.2018.01.105.

[4] Zhang Z, Zhang H, Li Y, Lu C, Zhu S, He C, et al. Investigation of the interaction between lighting and mixing applied during the photo-fermentation biohydrogen production process from agricultural waste. Bioresour Technol 2020;312:123570. https://doi.org/10.1016/j.biortech.2020.123570.

[5] Luongo V, Ghimire A, Frunzo L, Fabbricino M, d'Antonio G, Pirozzi F, et al. Photofermentative production of hydrogen and poly-β-hydroxybutyrate from dark fermentation products. Bioresour Technol 2017;228:171–5. https://doi.org/10.1016/J.BIORTECH.2016.12.079.

[6] Dauptain K, Trably E, Santa-Catalina G, Bernet N, Carrere H. Role of indigenous bacteria in dark fermentation of organic substrates. Bioresour Technol 2020;313:123665. https://doi.org/10.1016/j.biortech.2020.123665.

[7] Ghimire A, Frunzo L, Pirozzi F, Trably E, Escudie R, Lens PNL, et al. A review on dark fermentative biohydrogen production from organic biomass: Process parameters and use of by-products. Appl Energy 2015;144:73–95. https://doi.org/10.1016/J.APENERGY.2015.01.045.

[8] Görke B, Stülke J. Carbon catabolite repression in bacteria: Many ways to make the most out of nutrients. Nat Rev Microbiol 2008;6:613–24. https://doi.org/10.1038/nrmicro1932.

[9] Ghosh S, Dairkee UK, Chowdhury R, Bhattacharya P. Hydrogen from food

processing wastes via photofermentation using Purple Non-sulfur Bacteria (PNSB) – A review. Energy Convers Manag 2017;141:299–314. https://doi.org/10.1016/J.ENCONMAN.2016.09.001.

[10] Pattanamanee W, Choorit W, Deesan C, Sirisansaneeyakul S, Chisti Y. Photofermentive production of biohydrogen from oil palm waste hydrolysate. Int J Hydrogen Energy 2012;37:4077–87. https://doi.org/10.1016/J.IJHYDENE.2011.12.002.

[11] Wang L, York SW, Ingram LO, Shanmugam KT. Simultaneous fermentation of biomass-derived sugars to ethanol by a co-culture of an engineered Escherichia coli and Saccharomyces cerevisiae. Bioresour Technol 2019;273:269–76. https://doi.org/10.1016/j.biortech.2018.11.016.

[12] Jagtap RS, Mahajan DM, Mistry SR, Bilaiya M, Singh RK, Jain R. Improving ethanol yields in sugarcane molasses fermentation by engineering the high osmolarity glycerol pathway while maintaining osmotolerance in Saccharomyces cerevisiae. Appl Microbiol Biotechnol 2019;103:1031–42. https://doi.org/10.1007/s00253-018-9532-1.

[13] Eroğlu E, Eroğlu İ, Gündüz U, Yücel M. Effect of clay pretreatment on photofermentative hydrogen production from olive mill wastewater. Bioresour Technol 2008;99:6799–808. https://doi.org/10.1016/J.BIORTECH.2008.01.076.

[14] Niño-Navarro C, Chairez I, Christen P, Canul-Chan M, García-Peña EI. Enhanced hydrogen production by a sequential dark and photo fermentation process: Effects of initial feedstock composition, dilution and microbial population. Renew Energy 2020;147:924–36. https://doi.org/10.1016/j.renene.2019.09.024.

[15] Uyar B, Eroglu I, Yücel M, Gündüz U. Photofermentative hydrogen production from volatile fatty acids present in dark fermentation effluents. Int J Hydrogen Energy 2009;34:4517–23. https://doi.org/10.1016/j.ijhydene.2008.07.057.

[16] Zong W, Yu R, Zhang P, Fan M, Zhou Z. Efficient hydrogen gas production from cassava and food waste by a two-step process of dark fermentation and photo-fermentation. Biomass and Bioenergy 2009. https://doi.org/10.1016/j.biombioe.2009.06.008.

[17] Androga DD, Özgür E, Eroglu I, Gündüz U, Yücel M. Significance of carbon to nitrogen ratio on the long-term stability of continuous photofermentative hydrogen

production. Int J Hydrogen Energy 2011;36:15583–94. https://doi.org/10.1016/J.IJHYDENE.2011.09.043.

[18] Avcioglu SG, Ozgur E, Eroglu I, Yucel M, Gunduz U. Biohydrogen production in an outdoor panel photobioreactor on dark fermentation effluent of molasses. Int J Hydrogen Energy 2011;36:11360–8. https://doi.org/10.1016/j.ijhydene.2010.12.046.

[19] Özkan E, Uyar B, Özgür E, Yücel M, Eroglu I, Gündüz U. Photofermentative hydrogen production using dark fermentation effluent of sugar beet thick juice in outdoor conditions. Int J Hydrogen Energy 2012;37:2044–9. https://doi.org/10.1016/j.ijhydene.2011.06.035.

[20] Sevinç P, Gündüz U, Eroglu I, Yücel M. Kinetic analysis of photosynthetic growth, hydrogen production and dual substrate utilization by Rhodobacter capsulatus. Int J Hydrogen Energy 2012;37:16430–6. https://doi.org/10.1016/j.ijhydene.2012.02.176.

[21] Özgür E, Mars AE, Peksel B, Louwerse A, Yücel M, Gündüz U, et al. Biohydrogen production from beet molasses by sequential dark and photofermentation. Int J Hydrogen Energy 2010;35:511–7. https://doi.org/10.1016/J.IJHYDENE.2009.10.094.

[22] Pott RWM, Howe CJ, Dennis JS. Photofermentation of crude glycerol from biodiesel using Rhodopseudomonas palustris: Comparison with organic acids and the identification of inhibitory compounds. Bioresour Technol 2013;130:725–30. https://doi.org/10.1016/j.biortech.2012.11.126.

[23] Sabourin-Provost G, Hallenbeck PC. High yield conversion of a crude glycerol fraction from biodiesel production to hydrogen by photofermentation. Bioresour Technol 2009;100:3513–7. https://doi.org/10.1016/j.biortech.2009.03.027.

[24] Adessi A, De Philippis R. Photobioreactor design and illumination systems for H2 production with anoxygenic photosynthetic bacteria: A review. Int J Hydrogen Energy 2014;39:3127–41. https://doi.org/10.1016/j.ijhydene.2013.12.084.

[25] Ghimire A, Valentino S, Frunzo L, Pirozzi F, Lens PNL, Esposito G. Concomitant biohydrogen and poly-β-hydroxybutyrate production from dark fermentation effluents by adapted Rhodobacter sphaeroides and mixed photofermentative cultures. Bioresour Technol 2016;217:157–64.

https://doi.org/10.1016/J.BIORTECH.2016.03.017.

[26] Montiel-Corona V, Revah S, Morales M. Hydrogen production by an enriched photoheterotrophic culture using dark fermentation effluent as substrate: Effect of flushing method, bicarbonate addition, and outdoor-indoor conditions. Int J Hydrogen Energy 2015. https://doi.org/10.1016/j.ijhydene.2015.05.067.

[27] Dinesh GH, Nguyen DD, Ravindran B, Chang SW, Vo DVN, Bach QV, et al. Simultaneous biohydrogen (H2) and bioplastic (poly-β-hydroxybutyrate-PHB) productions under dark, photo, and subsequent dark and photo fermentation utilizing various wastes. Int J Hydrogen Energy 2020;45:5840–53. https://doi.org/10.1016/j.ijhydene.2019.09.036.

[28] Montiel Corona V, Le Borgne S, Revah S, Morales M. Effect of light-dark cycles on hydrogen and poly-β-hydroxybutyrate production by a photoheterotrophic culture and Rhodobacter capsulatus using a dark fermentation effluent as substrate. Bioresour Technol 2017. https://doi.org/10.1016/j.biortech.2016.12.021.

[29] Bideaux C, Alfenore S, Cameleyre X, Molina-Jouve C, Uribelarrea JL, Guillouet SE. Minimization of glycerol production during the high-performance fed-batch ethanolic fermentation process in Saccharomyces cerevisiae, using a metabolic model as a prediction tool. Appl Environ Microbiol 2006;72:2134–40. https://doi.org/10.1128/AEM.72.3.2134-2140.2006.

Chapter 5

Enhancing hydrogen production by photo fermentation of ethanol rich dark fermentation effluents

This chapter has been published as: Policastro, G., Giugliano, M., Luongo, V., Napolitano, R. and Fabbricino, M. (2021). Enhancing photo fermentative hydrogen production using ethanol rich dark fermentation effluents. International Journal of Hydrogen Energy.

Enhancing photo fermentative hydrogen production using ethanol rich dark fermentation effluents

Abstract

The present study demonstrates the feasibility of a two-phase biorefinery process applied to waste substrates producing ethanol rich effluents. The process includes a dark fermentation step followed by photo fermentation and it is able to optimize hydrogen production from waste biomass. The study was conducted using winery wastewater as feedstock. The results indicate that no additional treatments are required when an appropriate dilution of the initial waste is applied. Microbial consortia contained in the winery wastewater promoted a fermentative ethanol pathway: the ethanol rich effluent was converted into hydrogen by phototrophic microorganisms. Despite the presence of inhibiting compounds, the adoption of a mixed phototrophic culture allowed to obtain good results in terms of hydrogen production. Specifically, up to 310 mLH_2 $gCOD_{consumed}^{-1}$ were obtained in the photo fermentative stage. The effectiveness of ethanol rich dark fermentation effluents for hydrogen production enhancement was demonstrated. Noteworthy, polyhydroxybutyrate was also produced during the experiments. The work faces two of the major challenges in the sequential dark fermentation and photo fermentation technology applied to real waste substrates: the minimization of pre-treatments and the enhancement of the hydrogen production yields using ethanol rich DFEs.

5.1. Introduction

Biorefinery represents an attractive sustainable route for biofuels, biochemicals and value-added compounds production from waste biomass [1]. Among various biorefinery processes, the sequential application of dark fermentation (DF) and photo fermentation (PF) is attracting increasing attention [2–4] [5]. The dark fermentation process represents a key technology for hydrogen production due to its environmentally friendly characteristics. Fermentative bacteria operating the DF process are able to convert complex organic compounds in a variety of by-products, including hydrogen (H_2), organic acids (OA), and alcohols (e.g. ethanol). However, in order to achieve proper conditions for the process scale-up from lab to pilot/full scale application, it is still necessary to enhance hydrogen yields [6]. Usually, the maximum theoretical hydrogen yield in DF ranges between 2-4 mol H_2 mol $glucose^{-1}$, when acetic acid or butyric acid are the only other end products. Thus, experimentally 2–3 mol H_2 mol $glucose^{-1}$ hydrogen

yields can be achieved, together with formation of the other organic by products [5]. As biomass conversion during DF is partly incomplete [7], the process does not allow for a complete valorisation of substrates. Consequently, dark fermentation effluents (DFEs) require an additional treatment. Different solutions involving two stage processes (e.g. dark fermentation and anaerobic digestion, dark fermentation and photo fermentation, dark fermentation and aerobic treatments) have been proposed [8–10]. In spite of producing an additional hydrogen rate and to reach a low COD value of the produced effluents, the photo fermentation process is one of the most attractive. Indeed, purple non sulphur bacteria (PNSB) are able to convert the by-products contained in the DF effluents (DFEs) operating the PF process, and they contextually synthetize an additional bio-hydrogen flow [11]. Therefore, the DF-PF integration allows to overcome the DF system bottlenecks, enhancing bio-H_2 production and total organic carbon degradation [12]. In addition, under stress conditions, PNSB are able to accumulate a biodegradable polymer used for bioplastics production, i.e. polyhydroxybutyrate (PHB), as an intracellular energy storage [13,14]. The enhancement of PHB accumulation has been observed under lack of nutrients, non-optimal pH and temperature values, osmotic shock or during adaptation to complex carbon sources. Indeed, PNSB use PHB as a carbon reserve for their growth and survival when the substrate and/or the other nutrients became scarce or to protect cells from stress conditions [15]. Even though hydrogen production and PHB accumulation have been reported to be competitive pathways, mixed cultures are able to concomitantly produce hydrogen and PHB [12].

Over the last few years, the sequential DF-PF treatment has been widely explored at lab-scale using various complex waste substrates, such as fruit and vegetable waste, rice straw, and palm oil mill [16–18]. Nonetheless, the integration between DF and PF processes still presents many challenges limiting scaled-up applications. The major challenge of using DFEs as substrates for PF processes relies on the inhibition phenomena that may occur. For instance, the presence of toxic compounds such as phenols can damage the cell membrane of bacteria [19]. Moreover, high ammonia concentrations can inhibit nitrogenase synthesis and activity. High COD or the presence of heavy metals and aromatic hydrocarbons as well as acidic pH values, may also negatively impact hydrogen production. Finally, when using pure PNSB cultures, contamination by other microorganisms should be avoided [20]. For this reason, numerous additional treatments (e.g. centrifugation, dilution, neutralization, autoclaving, adsorption) are generally required, which increase the complexity and economic costs for pilot/full scale bioreactors.

This aspect is crucial when the bioconversion begins with complex organic waste. An example is provided by winery wastewater (WWW), one of the waste streams resulting from the wine production process. Such effluent contains various by-products (e.g. ethanol, sugars, organic acids) and phenolic compounds, which are toxic for pure cultures of PNSB and have to be removed by additional pre-treatments (e.g. adsorption) [21].

In this study, a DF-PF process for winery wastewater (WWW) valorisation is presented, where only a simple dilution pre-treatment of the DFE was applied. Moreover, mixed cultures were used for the PF step to avoid sterile conditions and reduce the costs and the operative complexity of the integrated DF-PF system. Noteworthy, all the experiments were conducted using a real waste biomass as substrate. Actually, just a few studies have been conducted using real residual feedstocks for the DF-PF integrated process [22–25]. In addition, despite the ability of photo fermentative bacteria to convert organic acids rich effluents has been largely demonstrated [26,27], no studies on the photo fermentative conversion of ethanol rich effluents by mixed cultures have been published, to date.

Ethanol-rich effluents may be important for practical applications. Indeed, they are always obtained as a result of the alcoholic fermentation of sugar-rich substrates [28]. Few previous works looking into the ethanol effect on hydrogen production by pure PNSB cultures have been published. Such studies report that ethanol can exert both positive and negative effects or it is not consumed by PNSB [29–31]. Therefore, the photo conversion of ethanol rich DFEs is worth of additional research efforts.

To investigate the photo fermentative conversion of ethanol rich effluents, this study has been conducted promoting a fermentative ethanol pathway in the dark fermentation stage. The feasibility of using ethanol rich dark fermentation effluents to enhance hydrogen production in the PF step has been investigated.

5.2. Materials and Methods

5.2.1. Substrate and inoculum

Winery wastewater (WWW) was obtained from the second decanting storage of a red wine factory located in Comiziano (Naples, Italy). The sample was immediately analysed in terms of organic and inorganic compounds (Table 5.1) and stored at -20 °C to keep unaltered its characteristics until use.

Table 5.1. Winery wastewater initial characteristics

Parameter	Value
COD (g L^{-1})	265 ±1
NO_3^- (g L^{-1})	0.03 ±0.01
Total phenols (g L^{-1})	1.243 ±0.001
pH	4.5 ±0.1
Glucose (g L^{-1})	20 ±2
Ethanol (g L^{-1})	70 ±5
Lactic acid (g L^{-1})	2.0 ±0.3
Acetic acid (g L^{-1})	0.5 ±0.2
PO_4^{3-} (g L^{-1})	0.03 ±0.01
SO_4^{2-} (g L^{-1})	0.4 ±0.1

A single stage mesophilic anaerobic digestion (AD) effluent was used as inoculum. The AD plant performing the anaerobic conversion of food waste is located in Casal di Principe (Naples, Italy). The digestate was characterized in terms of total solids (TS= 79 ±1 g L^{-1}), volatile solids (VS = 52 ±1 g L^{-1}), chemical oxygen demand (COD = 77 ±2 g COD L^{-1}), and pH = 8.3.

5.2.2 Dark fermentation tests

Two different experimental sets were carried out in triplicate for the DF stage. 500 mL transparent borosilicate glass bottles (Simax, Czech Republic) were used with a 400 mL working volume.

In the first set, indicated as DF1, the digestate was added to the WWW as a supplementary source of microorganisms. Digestate was pre-heated at 105°C for 3 h to enrich the microbial consortia of H_2 producing bacteria, thus avoiding methanogenic activity. The heat shock pre-treatment temperature and time have been chosen using precautionary values, according to ranges reported in previous works [12,32,33]. No pre-treatments were carried out for WWW. The F/M ratio between substrate and biomass was kept to 1,

in terms of $gCOD_{substrate}$ $gCOD_{inoculum}^{-1}$, according to a previous work [8]. In detail, 155 mL of digestate, 45 mL of winery wastewater, and 200 mL of water were used for each reactor. In the second set, indicated as DF2, the ability of indigenous bacteria of the WWW to perform the DF process was tested by avoiding the inoculum/digestate addition. In detail, the same volume of WWW was used to prepare both DF1 and DF2 sets. However, in DF2, the inoculum/digestate volume was replaced with water.

Screw caps in PVC were properly modified with tubing to ensure gas and liquid extraction procedures. DF reactors were introduced into a water bath to keep the temperature at 35±1°C. The batch feeding strategy was adopted. Liquid and gas samples were daily analyzed to measure the organic compounds content and the biogas quantity and composition. DFEs were collected after 7 days and characterized in terms of COD, organic acids, glucose, glycerol, and ethanol concentration. The DFE containing the higher ethanol concentration was used for the PF step.

5.2.3. Photo Fermentation tests

Two different experimental sets were carried out in triplicate for the PF stage. In the first set, indicated as PF1, the real DFE obtained from the DF1 test was used. The DFE was diluted to reduce the feeding load from 22.48 g COD L^{-1} to the non-inhibiting value of 1 g COD L^{-1} [15]. In the second set, indicated as PF2, a synthetic effluent with the same concentrations of organic acids, ethanol, and glycerol contained in the diluted DFE was used. This strategy allowed to observe differences between real and synthetic substrates and to highlight the effects of additional inhibiting compounds (e.g. phenols). DFE was diluted using a specific medium and a trace elements solution reported in Ghimire et al. [6]. In detail, 9 mL of the DFE, 4 mL of the trace element solution and 387 mL of the medium were added to each PF reactor. High purity degree chemicals and bi-distilled water were used to prepare the medium and the trace element solution. The initial pH was adjusted to 6. Successively, the pH value was not controlled.

The mixed PNSB culture used as inoculum for each PF experimental test, was sampled from a lab-scale reactor used for previous PF experiments. The initial inoculum percentage of 2% v v^{-1} was adopted, corresponding to a biomass concentration of 0.025 g TSS L^{-1}. During the fermentation test, bacteria growth conferred a red color to reactors indicating the presence of purple pigments, which are typical for PNSB. PF tests were conducted in 500 mL batch reactors with a 400 mL working volume. Room temperature (25±2 °C), uncontrolled pH, and no-sterile conditions were adopted. The headspace of

the reactors was flushed with argon for 20 min before use, in order to ensure anaerobic conditions, and completely remove nitrogen gas.

Reactors were placed on magnetic stirrers, adjusting the stirring value to 250 rpm. Illumination was continuously provided by flexible LED strips, ensuring the constant illumination of 4000 lux [15].

Liquid and gaseous samples were collected for quantitative and qualitative analysis every two days.

5.2.4. Analytical methods and lab equipment

Biogas production was quantified through water displacement, as reported in [15]. Successively, gas chromatographic analysis was performed to determine the gas composition using a Varian Star 3400 gas chromatograph equipped with ShinCarbon ST 80/100 column and a thermal conductivity detector, with argon as carrier gas. The liquid fermentation products were determined with a Dionex (Sunnyvale, USA) LC 25 chromatography oven equipped with a Metrohom (Herisau, Switzerland) organic acids column (Metrosep Organic Acids - 250/7.8) and two different detectors: a Dionex (Sunnyvale, USA) UVD 340U for VFAs, and a Jasco (Cremella, Italy) RI-2031 for ethanol and sugars evaluation, respectively. The eluent (1 mM H_2SO_4) was pumped at the constant rate of 0.7 mL min^{-1} using a Dionex (Sunnyvale, USA) GD 500 gradient pump. The PHB analysis was carried out according to [35]. Samples were preliminary lyophilized and subsequently the polymer was extracted in order to determine PHB concentration. Gas chromatography and mass spectrometry (GC-MS) with a ZB Semi Volatiles Zebron column (Phenomenex, Torrance, USA) and helium as carrier gas were used. The optical density (OD) method at a 660 nm was employed for the biomass growth measurement. The OD was linked to the total suspended solids (TSS) concentration with a standard correlation curve obtained by a Photolab Spektral, WTW (Wheilheim, Germany) spectrophotometer (6600 UV vis).

Total phenolic content was measured according to the Folin and Ciocalteu method [36]. A Metrohm 761 compact ion chromatograph (Herisau, Switzerland) equipped with a Dionex IonPac AS12A 4 x 200 mm column (Sunnyvale, USA) was used for anions (NO_3^-, PO_4^{-3}, and SO_4^{-2}) evaluation. The TS and VS of the digestate and COD concentration were determined according to the standard methods [37].

5.3. Results and discussion

5.3.1. Biohydrogen production and metabolic intermediates in DF

Metabolic intermediate contents, pH, H_2 yields and gas cumulative production at the end of the two sets of the DF stage, are reported in Table 5.2.

Table 5.2. DFEs characterization

SET #	DF1	DF2
AceticaAcid (mg L^{-1})	4450 ± 790	865 ± 155
Butyric acid (mg L^{-1})	*	153
Lactic Acid (mg L^{-1})	*	259
Ethanol (mg L^{-1})	5100 ± 850	5443 ± 87
Glycerol (mg L^{-1})	500 ± 51	673 ± 72
pH	6.5 ± 0.1	3.5 ± 0.1
H_2 (mL L^{-1})	91 ± 1	38 ± 2
CO_2 (mL L^{-1})	160± 1	36± 2
H_2 (mL $gCOD^{-1}$)**	3.8 ± 0.1	3.2 ± 0.1

(*) not detected; (**) initial COD

Results showed an overall H_2 production for DF1, 2,3-times higher than DF2, as a consequence of the digestate presence, which provided an additional source of H_2-producers microorganisms. For both sets, H_2 production reached the maximum after 2 days. Successively, no significant amount of biogas was recorded.

The biohydrogen production observed was lower than previous studies. For instance, Carrillo-Reyes et al. [38] reported 528 mL H_2 L^{-1} production from winery wastewater, while [39] reported 721 mL H_2 L^{-1} production from tequila vinasses. However, an effective comparison with the data presented in these studies is not accurate due to the different initial COD concentration and reactor configurations.

The final pH values of DF1 and DF2 were 5.5 and 3.5, respectively. Such values were lower compared to the optimum pH range (7-5.5) generally suggested for fermentative hydrogen production [34]. The low pH values were due to the accumulation of acidic metabolites in the fermentation medium. Probably, the final high concentration of H^+ ions able to penetrate the microbial cell membrane had a negative effect on H_2 production, because of the interference against regular metabolic activity of the cells [40].

In terms of metabolic intermediates production, the final ethanol concentration of 5100 mg L^{-1} and 5443 mg L^{-1} were reached for DF1 and DF2, respectively. The higher ethanol concentration detected in the effluent of DF2 was attributed to the experimental set-up, which did not include any digestate addition.

Most probably, the absence of allochthonous bacteria in DF2 avoided additional competitive fermentative pathways for the substrate, which therefore evolved in the initial direction of ethanol production. Indeed, WWW is usually characterized by the presence of bacteria and yeasts conducing the alcoholic fermentation process, which convert sugars into alcohols [41]. On the contrary, allochthonous bacteria with a higher fermentation power apported by the digestate inoculum (DF1), shifted the conversion towards acetic acid production. Indeed, acetic acid production reached a final concentration of 4450 mg L^{-1} in DF1 and 865 mg L^{-1} in DF2. The high difference between acetic acid concentrations in DF1 and DF2 was not correlated with hydrogen values. From a theoretical point of view, the metabolic route from the substrate to acetate produces higher hydrogen yields compared to the other possible metabolic pathways [6]. However, acetate can also be a product of hydrogen consumers, such as homoacetogens, which are usually present in digestates. Since homoacetogenesis can occur concomitantly with biohydrogen production, probably hydrogen has been consumed to produce acetate [42].

In addition, a relevant glycerol concentration was detected at the end of DF1and DF2. The glycerol production was higher in DF2 (673 mg L^{-1}) than in DF1 (500 mg L^{-1}). Glycerol accumulation is typical in the case of sugars to ethanol conversion [43], which was the main fermentation pathway observed in DF2 set. Ethanol is usually obtained as a result of the alcoholic fermentation of sugars performed by bacteria and yeasts. The mentioned process generates ethanol as main compound and glycerol as secondary one [44]. For instance, in *S. cerevisiae* glycerol is generated from dihydroxyacetone phosphate, which is an intermediate metabolite in glycolysis pathway [45].

Additional efforts are still required to elucidate the correlation between acetate and ethanol production and H_2 generation. According to Han et al. [46], the presence of ethanol is supposed to reduce the production of acids (e.g. acetate, butyrate) and to favor a smooth production of H_2. Ren et al. [48] found that an ethanol to acetate ratio near to 1 can stabilize the fermentation process enhancing biohydrogen production ability. On the other hand, acetic pathway is also considered one of the most effective way to reach the highest H_2 yield, when fermentation takes place from carbohydrates rich substrates [34].

5.3.2. Biohydrogen production and metabolic intermediates in PF

The time-course profiles of the parameters evaluated in PF1 and PF2 are reported in Figures 5.1-5.3.

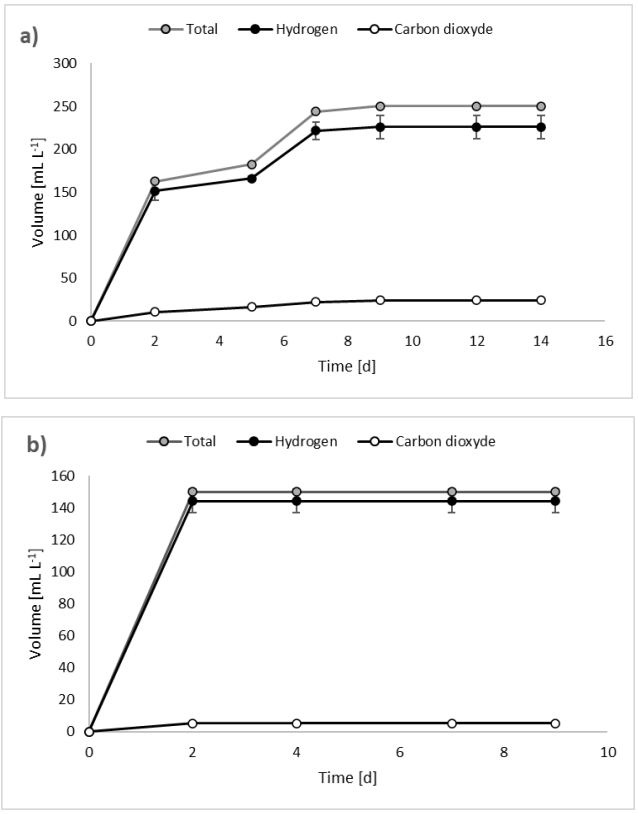

Figure 5.1. Volume of produced biogas, in terms of total biogas, hydrogen and carbon dioxide for the experimental sets PF1 (a) and PF2 (b).

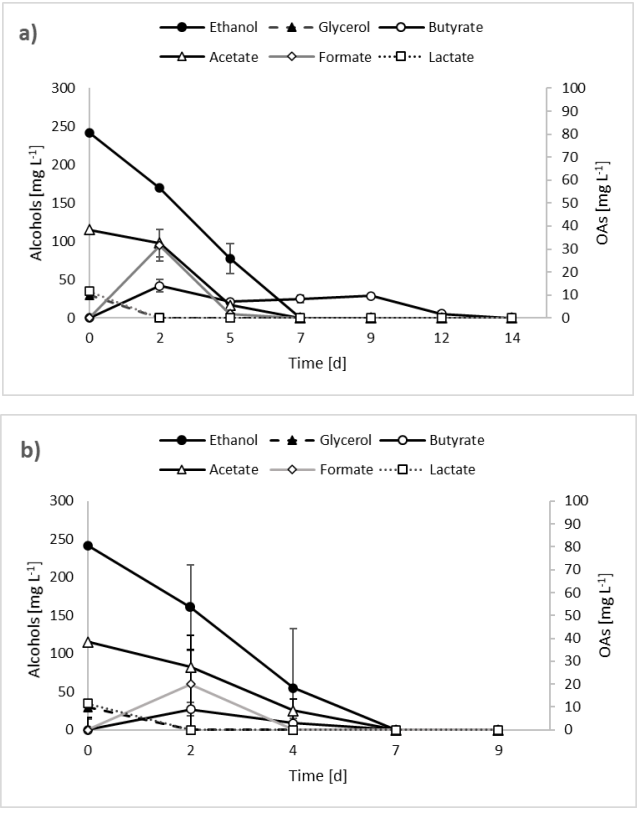

Figure 5.2. Concentration of organic acids (OAs) and alcohols for the experimental sets PF1 (a) and PF2 (b).

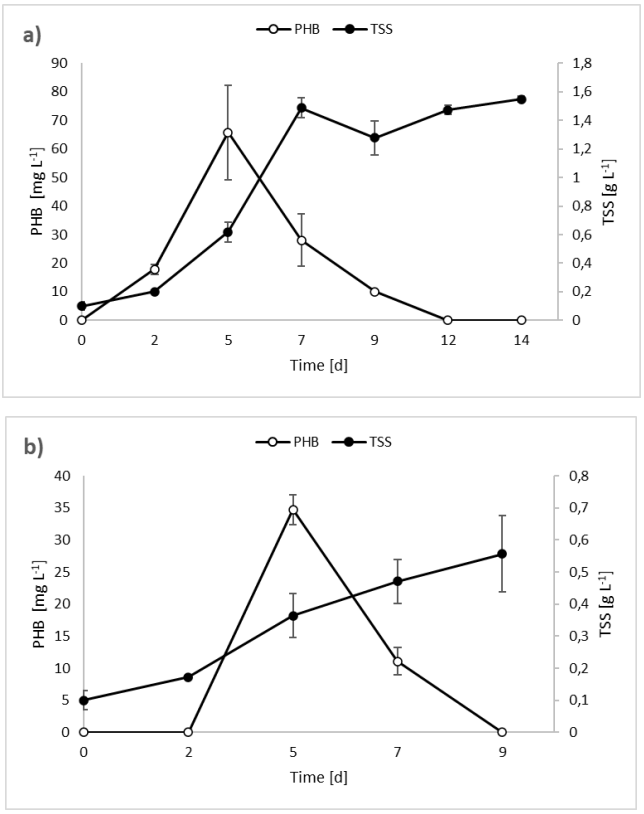

Figure 5.3. Concentration of PHB and biomass in terms of TSS for the experimental sets PF1 (a) and PF2 (b).

As it can be easily noted, in the first two days, both experimental sets were mainly subject to catabolic reactions. Indeed, during this time a slight accumulation of biomass occurred within the bioreactors. Glycerol and lactic acid were completely consumed, and the contextual formate, butyrate and hydrogen production were observed. Notably, in both sets similar hydrogen productions of about 150 mL H_2 L^{-1} was achieved. However, in terms of mLH_2 $gCOD^{-1}$, in PF2 the cumulative volumetric yield reached the highest value of 237 N mL H_2 $gCOD^{-1}$ (normal temperature and pressure conditions, 0°C, 101.3250 kPa), while in PF1 it reached only 151 N mL H_2 $gCOD^{-1}$. Nonetheless, in the successive days, hydrogen production kept increasing in PF1, and a final cumulative production of 226 mL H_2 L^{-1} was obtained. In terms of mL H_2 $gCOD^{-1}$, the cumulative hydrogen yield reached in PF1 in about 9 days (226 mL H_2 $gCOD^{-1}$) was comparable to those obtained in PF2.

For both experimental sets, glycerol and lactic acid were quickly degraded. This was associated to the promotion of metabolic activities leading to hydrogen production [16].

During the three successive days (days 2 to 5), PF1 presented a slow hydrogen production. On the contrary, no hydrogen production was detected in the set of reactors corresponding to PF2, although ethanol and VFAs consumption was observed for both tested configurations. The concomitant PHB and TSS increase, suggested that the consumed compounds were used by bacteria for biomass growth and PHB accumulation. PHB synthesis and slow hydrogen production were explained by considering the required adaptation of the biomass to different and complex carbon sources, which resulted in a stress condition for microorganisms. It is worth noting that PHB accumulation occurred due to acetate consumption. The latter had a more pronounced effect on PHB yield rather than on H_2 production in accordance to [49] and [50]. Probably, the presence of acetic acid promoted the production of acetil-coenzyme A, which represents a precursor for the synthesis of PHB [15].

As already said, hydrogen production kept increasing from day 5 in PF1. In addition, an evident biomass accumulation occurred within the bioreactors, and a contextual consumption of ethanol and acetate was observed until the complete degradation of these compounds.

The production of formate is associated with the consumption of lactate, whereas the latter is known to produce pyruvate in PNS bacteria which is converted to formate by the enzyme pyruvate formed-lyase (PFL) [51]. Formic acid does not appear to be a preferred substrate for H_2 production and PNSB growth. Interestingly, formic acid was immediately consumed in both tested experimental sets, in contrast with previous observations [15] reporting that formic acid is resistant to bioconversion. Nonetheless, in this study formic acid production did not reach very high values. Indeed, the maximum formic acid concentration of 31.6 mg L^{-1} was observed, that is lower than the value reported in the mentioned study [15].

Butyric acid persisted in the bioreactors with an almost constant concentration until day 9. Later, it was completely degraded. The observed trend was attributed to the fact that acetate was a more favorable substrate than butyrate [16,52,53], and therefore it was consumed faster by PNSB.

In PF2 set, VFAs and ethanol were completely degraded on day 7. The faster consumption of all available carbon sources detected in PF2 compared to PF1 set was probably due to the lower initial COD concentration in the synthetic culture medium (i.e. 608.46 mg L^{-1}).

Nevertheless, as said, despite the high COD gap between the two sets, the final hydrogen yield was comparable in PF1 and PF2.

PHB and biomass accumulation were considerably higher in PF1 compared to PF2. Such a result was explained considering the different nature of the real waste compared to the synthetic substrate, and the different metabolic pathways followed by PNSB in the presence of a variety of substrates [54]. Usually, WWW contains a broad range of organic compounds [55]. In this study, the wastewater and DFE theoretical COD were about 50% of the directly measured total COD. Therefore, the compounds constituting the undetected fraction of the total COD represented an aliquot of 12% of the COD consumed by bacteria. The unknown consumed organic compounds exerted a positive effect on PHB accumulation and anabolic reactions rather than on hydrogen production. Moreover, the indigenous microorganisms present in the unsterilized DFE competed with PNSB for the available COD, with a detrimental effect on H_2 production. The obtained COD removal efficiency, ranging around 73%, was comparable with the values reported in a previous PF study using WWW as substrate [15].

Table 5.3 reports previous studies relating to the photo fermentative H_2 production using VFAs rich DFEs as substrate.

Table 5.3. Adopted pretreatments and H_2 productions from photo fermentation processes conducted on DFEs

Feedstock of the DF process	Pretreatments	Strain	H_2 yields in the PF stage	Ref.
Organic fraction of municipal solid waste (OFMSW)	Centrifugation and dilution	Consortium of PNSB	233 N mL H_2 $gCOD^{-1}$	[9]
Food waste (FW)	Centrifugation and dilution	Consortium of PNSB	71.3 N mL H_2 $gCOD^{-1}$	[12]
Starch wastewater	Not reported	Consortium of PNSB	166.83 mLH_2 $gCOD_{consumed}^{-1}$	[56]
Palm oil mill effluent (POME)	Autoclaving and dilution	*Rhodopseudomonas Palustris*	44 mL H_2 $gCOD^{-1}$	[18]
Potato waste	Centrifugation, filtration and dilution	*Rhodopseudomonas Palustris*	202.8 mL H_2 $gCOD^{-1}$	[57]
Fruit and vegetable waste (FVW) and cheese whey powder (CWP)	Centrifugation, autoclaving, dilution	Consortium of PNSB	793 mL H_2 g $COD_{consumed}^{-1}$	[16]
Cassava and food waste	Centrifugation, dilution and neutralization	*Rhodobacter Sphaeroides*	827.15 mL H_2 g COD^{-1}	[52]

Sucrose	Centrifugation, dilution, autoclaving and neutralization	*Rhodobacter Sphaeroides*	420 mL H_2 g COD^{-1}	[58]
Winery Wastewater	Dilution	Consortium of PNSB	226 mL H_2 g COD^{-1}; 310 mL H_2 g $COD_{consumed}^{-1}$	This study

The H_2 yield obtained in this study was higher than those obtained in previous studies performed by using pure cultures of *Rhodopseudomonas Palustris*. For instance, Mishra et al. [18] obtained 44 mL H_2 $gCOD^{-1}$ from the DFE of palm oil mill effluent (POME), while Hitit et al. [57] observed a production of 202.8 mL H_2 $gCOD^{-1}$ from DFE of potato waste. On the other hand, higher hydrogen productions of 420 and 827.15 mLH_2 $gCOD^{-1}$ were observed in previous studies, using pure cultures of *Rhodobacter sphaeroides* [52, 58]. Such a result was attributed to the further pre-treatments adopted rather than the type of substrate. Even though ethanol has been reported to be toxic for PNSB [29], its concentration in the DFE used in this study was in non-inhibiting thresholds.

Concerning previous studies performed using mixed PNSB cultures and additional pre-treatments, the achieved H_2 productions were comparable or lower than those obtained in this study.

For instance, Ghimire et al. [12] reported a hydrogen production of 71.3 N·mL·$gCOD^{-1}$using a VFAs rich DFEs of food waste. Similarly, Luongo et al. [9] observed a production of 233 N·mL·$gCOD^{-1}$using the organic fraction of municipal solid waste as substrate in the DF step. Both authors performed the centrifugation of the DFE, in addition to dilution, prior its utilization. Finally, Nasr et al. [56], produced 166.83 mLH_2 $gCOD_{removed}^{-1}$ from acetate and butyrate contained in the DFE of starch wastewater, which was lower compared to the production observed in this study (310 mL H_2 g $COD_{removed}^{-1}$).

Overall, hydrogen yields values reported in Table 5.3 indicated that, among the organic compounds usually contained in DFE, ethanol and glycerol were among the most effective for hydrogen production. The enhanced hydrogen production from ethanol was justified considering that this substrate, rich in electrons, is a carbon source more reduced than biomass. A control experiment using the synthetic effluent of the set PF2 without ethanol confirmed that such substrate enhances the hydrogen generation (data not shown).

Probably, the availability of a high number of electrons have been exploited for hydrogen production according to Liu et al. [29]. Moreover, it has been reported that the presence of ethanol enhances the nitrogenase activity in *R. sphaeroides,* and therefore increases the consumption of reducing power [30,59].

Of course, as previously mentioned, high ethanol concentrations can also exert an inhibition effect on PNSB. Liu et al. [29] reported an ethanol inhibiting value of 1.05 M. Nevertheless, the value reached in the present study (5 mM) was in non-inhibiting thresholds, confirming the effectiveness of ethanol rich DFEs for the PF. Moreover, the high hydrogen content in the produced biogas (about 90 %) remarked that such a substrate stimulated hydrogen production, in agreement with previous findings [15]. Concerning possible conversion pathways, further studies are required. Currently, Liu et al. [29] reported a probable pathway involved in ethanol assimilation by *R. palustris*. According to the mentioned study, ethanol would be converted to acetyl-CoA through the action of alcohol dehydrogenase and acetaldehyde dehydrogenase. Acetyl-CoA would be successively fed into the citric acid cycle with conversion of some oxaloacetate to phosphoenolpyruvate by phosphoenolpyruvate carboxylase to feed gluconeogenique pathways. Of course, in the presence of mixed cultures it is possible that more complex interaction mechanisms and different pathways may be triggered.

Niño-Navarro et al. [16] observed a high hydrogen production controlling the DF stage to deviate the fermentation from VFAs production to lactate. When the substrate in the DF stage is used through the heterofermentative pathway of lactic acid bacteria, it is possible to produce lactic acid and ethanol [60,61]. According to the results achieved in the present study, this conditioning strategy for the DF stage could be used to enhance photo fermentative hydrogen productivity and optimize H_2 yields.

Results reported in Figures 5.3a and 5.3b allowed several other considerations. Biomass, in fact, reached a final concentration of about 1.55 gTSS L^{-1} in PF1 and 0.56 gTSS L^{-1} in PF2 (Figure 5.3). The characteristic exponential growth of microorganisms, limited by the self-shading phenomenon, was not observed [62]. The higher biomass growth in PF1 was attributed to the availability of higher COD content. Indeed, similar values (around 1.60 gTSS L^{-1}) were reached in a previous study conducted using an initial COD value of 1500 mg L^{-1}, and adopting similar operating conditions [15]. Moreover, TSS concentration was characterized by a slightly increasing trend at the end of the process, due to PHB consumption (Figure 5.3). Indeed, PNSB are able to consume PHB for their growth and survival when starvation condition occurs [63,64]. The maximum PHB

concentration (66 ± 16 mgPHB L^{-1}) was reached in PF1 test, whereas the lowest value (35±2 mgPHB L^{-1}) was obtained in PF2 test (Figure 5.3). As well known, PHB production depends on the operational parameters such as C/N ratio, pH, and substrate concentration. Notably, it is strongly influenced by the characteristics of adopted PNSB species. The presence of a mixed consortium is generally associated to a low PHB accumulation due to the lower presence of PHB accumulating species in PNSB microbial consortium than in pure cultures [9,23]. Indeed, the values obtained in the present study were similar to those reported by Ghimire et al. [12] (50,7 mgPHB L^{-1}), who used a mixed PNSB cultures with a diluted VFAs rich DFE.

The alternating H_2 and PHB production observed in the PF2 set were in agreement with other experimental evidences reporting that PHB synthesis and H_2 production represent two competitive metabolic pathways [9,12,65]. These metabolic routes are used by microorganisms to dissipate excess reducing power during their growth and activity [49,50]. The concomitant production of H_2 and PHB observed in PF1 was already reported under specific operating conditions, such as the utilization of complex real wastes as substrate [12,15,65].

The inhibition of the PF process due to the presence of phenolic compounds was not observed in the present study. Eroğlu et al. [66] reported a total inhibition of PF process for the treatment of mill wastewater using a pure culture of *Rhodobacter sphaeroides* O.U.001 with a phenols content of 5.8 mg L^{-1}. In the present study, the phenols content was almost constant during the fermentative processes and the initial value of 5.5 mg L^{-1} in the PF reactors did not inhibit the process. This positive result was attributed to the presence of a mixed consortia of PNSB which lead to a higher process robustness [67-69].

5.4. Conclusions

The feasibility of the enhanced H_2 production via a two-stage DF-PF process from winery wastewater was demonstrated. The process was developed using winery wastewater as initial feedstock. During the first stage of the process (DF), microbial consortia (indigenous or added inoculum) allowed controlling the production of intermediate products. These metabolites defined the H_2 production during the PF process, as ethanol enhanced H_2 yields. H_2 production was low during the DF stage due, as the metabolic pathway was deviated towards ethanol production. However, this compound, used as substrate for the PF stage, allowed an overall optimization of H_2 production. Mixed

phototrophic cultures were effective to eliminate the asepsis conditions and additional pre-treatments, usually required to avoid inhibition phenomena, such as those due to the polyphenols contained in the winery wastewater. The concomitant H_2 and PHB production by PNSB consortium was also observed. The obtained results allowed facing two of the major challenges in the sequential DF-PF technology: the minimization of pre-treatments and the enhancement of the hydrogen yields. The reduction of required pre-treatments along with the abundance of the substrate involved represent hopeful starting points for future investigations on scaling up applications.

References

[1] Vernès L, Li Y, Chemat F, Abert-Vian M. Biorefinery Concept as a Key for Sustainable Future to Green Chemistry—The Case of Microalgae, 2019. https://doi.org/10.1007/978-981-13-3810-6_2.

[2] Rai PK, Singh SP, Asthana RK, Singh S. Biohydrogen production from sugarcane bagasse by integrating dark- and photo-fermentation. Bioresour Technol 2014. https://doi.org/10.1016/j.biortech.2013.10.117.

[3] Tawfik A, El-Bery H, Kumari S, Bux F. Use of mixed culture bacteria for photofermentive hydrogen of dark fermentation effluent. Bioresour Technol 2014. https://doi.org/10.1016/j.biortech.2014.03.065.

[4] Yang H, Shi B, Ma H, Guo L. Enhanced hydrogen production from cornstalk by dark- and photo-fermentation with diluted alkali-cellulase two-step hydrolysis. Int J Hydrogen Energy 2015. https://doi.org/10.1016/j.ijhydene.2015.07.062.

[5] Pandey A, Sinha P, Pandey A. Hydrogen production by sequential dark and photofermentation using wet biomass hydrolysate of *Spirulina platensis*: Response surface methodological approach. Int J Hydrogen Energy 2021. https://doi.org/10.1016/j.ijhydene.2020.11.205.

[6] Ghimire A, Valentino S, Frunzo L, Trably E, Escudié R, Pirozzi F, et al. Biohydrogen production from food waste by coupling semi-continuous dark-photofermentation and residue post-treatment to anaerobic digestion: A synergy for energy recovery. Int J Hydrogen Energy 2015;40:16045–55. https://doi.org/10.1016/j.ijhydene.2015.09.117.

[7] Sivagurunathan P, Kuppam C, Mudhoo A, Saratale GD, Kadier A, Zhen G, et al. A comprehensive review on two-stage integrative schemes for the valorization of dark fermentative effluents. Crit Rev Biotechnol 2018. https://doi.org/10.1080/07388551.2017.1416578.

[8] Ghimire A, Sposito F, Frunzo L, Trably E, Escudié R, Pirozzi F, et al. Effects of operational parameters on dark fermentative hydrogen production from biodegradable complex waste biomass. Waste Manag 2016. https://doi.org/10.1016/j.wasman.2016.01.044.

[9] Luongo V, Ghimire A, Frunzo L, Fabbricino M, d'Antonio G, Pirozzi F, et al. Photofermentative production of hydrogen and poly-B-hydroxybutyrate from dark

fermentation products. Bioresour Technol 2017;228:171–5. https://doi.org/10.1016/j.biortech.2016.12.079.

[10] Policastro G, Panico A, Fabbricino M. Improving biological production of poly(3-hydroxybutyrate-co-3-hydroxyvalerate) (PHBV) co-polymer: a critical review. Rev Environ Sci Biotechnol 2021. https://doi.org/10.1007/s11157-021-09575-z.

[11] Reungsang A, Zhong N, Yang Y, Sittijunda S, Xia A, Liao Q. Hydrogen from photo fermentation. Green Energy Technol., 2018. https://doi.org/10.1007/978-981-10-7677-0_7.

[12] Ghimire A, Valentino S, Frunzo L, Pirozzi F, Lens PNL, Esposito G. Concomitant biohydrogen and poly-β-hydroxybutyrate production from dark fermentation effluents by adapted *Rhodobacter sphaeroides* and mixed photofermentative cultures. Bioresour Technol 2016;217:157–64. https://doi.org/10.1016/j.biortech.2016.03.017.

[13] Adessi A, Corneli E, Philippis R De. Photosynthetic purple non sulfur bacteria in hydrogen producing systems: New approaches in the use of well known and innovative substrates. Mod. Top. Phototrophic Prokaryotes Environ. Appl. Asp., 2017. https://doi.org/10.1007/978-3-319-46261-5_10.

[14] Kemavongse K, Prasertsan P, Upaichit A, Methacanon P. Poly-β-hydroxyalkanoate production by halotolerant *Rhodobacter sphaeroides* U7. World J Microbiol Biotechnol 2008. https://doi.org/10.1007/s11274-008-9712-8.

[15] Policastro G, Luongo V, Fabbricino M. Biohydrogen and poly-β-hydroxybutyrate production by winery wastewater photofermentation: Effect of substrate concentration and nitrogen source. J Environ Manage 2020;271:111006. https://doi.org/10.1016/j.jenvman.2020.111006.

[16] Niño-Navarro C, Chairez I, Christen P, Canul-Chan M, García-Peña EI. Enhanced hydrogen production by a sequential dark and photo fermentation process: Effects of initial feedstock composition, dilution and microbial population. Renew Energy 2020;147:924–36. https://doi.org/10.1016/j.renene.2019.09.024.

[17] Dinesh GH, Nguyen DD, Ravindran B, Chang SW, Vo DVN, Bach QV, et al. Simultaneous biohydrogen (H_2) and bioplastic (poly-β-hydroxybutyrate-PHB) productions under dark, photo, and subsequent dark and photo fermentation utilizing various wastes. Int J Hydrogen Energy 2020;45:5840–53.

https://doi.org/10.1016/j.ijhydene.2019.09.036.

[18] Mishra P, Thakur S, Singh L, Ab Wahid Z, Sakinah M. Enhanced hydrogen production from palm oil mill effluent using two stage sequential dark and photo fermentation. Int J Hydrogen Energy 2016;41:18431–40. https://doi.org/10.1016/j.ijhydene.2016.07.138.

[19] Campos-Esparza MR, Sánchez-Gómez MV, Matute C. Molecular mechanisms of neuroprotection by two natural antioxidant polyphenols. Cell Calcium 2009. https://doi.org/10.1016/j.ceca.2008.12.007.

[20] Keskin T, Abo-Hashesh M, Hallenbeck PC. Photofermentative hydrogen production from wastes. Bioresour Technol 2011. https://doi.org/10.1016/j.biortech.2011.04.004.

[21] Carlozzi P, Seggiani M, Capperucci A, Tanini D, Cinelli P, Lazzeri A. Hydroxytyrosol rich-mixture from olive mill wastewater and production of green products by feeding *Rhodopseudomonas* sp. S16-FVPT5 with the residual effluent. J Biotechnol 2019. https://doi.org/10.1016/j.jbiotec.2019.02.006.

[22] Seifert K, Zagrodnik R, Stodolny M, Łaniecki M. Biohydrogen production from chewing gum manufacturing residue in a two-step process of dark fermentation and photofermentation. Renew Energy 2018. https://doi.org/10.1016/j.renene.2018.01.105.

[23] Montiel Corona V, Le Borgne S, Revah S, Morales M. Effect of light-dark cycles on hydrogen and poly-β-hydroxybutyrate production by a photoheterotrophic culture and *Rhodobacter capsulatus* using a dark fermentation effluent as substrate. Bioresour Technol 2017. https://doi.org/10.1016/j.biortech.2016.12.021.

[24] Sagnak R, Kargi F. Photo-fermentative hydrogen gas production from dark fermentation effluent of acid hydrolyzed wheat starch with periodic feeding. Int J Hydrogen Energy 2011. https://doi.org/10.1016/j.ijhydene.2011.01.033.

[25] Wang R, Wen H, Cui C. Bio-hydrogen production by a new isolated strain *Rhodopseudomonas* sp. WR-17 using main metabolites of three typical dark fermentation type. Int J Hydrogen Energy 2019. https://doi.org/10.1016/j.ijhydene.2019.04.143.

[26] Elsharkawy K, Gar Alalm M, Fujii M, Afify H, Tawfik A, Elsamadony M. Paperboard mill wastewater treatment via combined dark and LED-mediated

fermentation in the absence of external chemical addition. Bioresour Technol 2020. https://doi.org/10.1016/j.biortech.2019.122312.

[27] Silva FTM, Bessa LP, Vieira LM, Moreira FS, de Souza Ferreira J, Batista FRX, et al. Dark fermentation effluent as substrate for hydrogen production from *Rhodobacter capsulatus* highlighting the performance of different fermentation systems. 3 Biotech 2019. https://doi.org/10.1007/s13205-019-1676-x.

[28] Wang L, York SW, Ingram LO, Shanmugam KT. Simultaneous fermentation of biomass-derived sugars to ethanol by a co-culture of an engineered *Escherichia coli* and *Saccharomyces cerevisiae*. Bioresour Technol 2019. https://doi.org/10.1016/j.biortech.2018.11.016.

[29] Liu Y, Ghosh D, Hallenbeck PC. Biological reformation of ethanol to hydrogen by *Rhodopseudomonas palustris* CGA009. Bioresour Technol 2015. https://doi.org/10.1016/j.biortech.2014.11.047.

[30] Kim DH, Lee JH, Kang S, Hallenbeck PC, Kim EJ, Lee JK, et al. Enhanced photo-fermentative H_2 production using *Rhodobacter sphaeroides* by ethanol addition and analysis of soluble microbial products. Biotechnol Biofuels 2014. https://doi.org/10.1186/1754-6834-7-79.

[31] Oh YK, Seol EH, Kim MS, Park S. Photoproduction of hydrogen from acetate by a chemoheterotrophic bacterium *Rhodopseudomonas palustris* P4. Int J Hydrogen Energy 2004. https://doi.org/10.1016/j.ijhydene.2003.11.008.

[32] Wang J, Wan W. Comparison of different pretreatment methods for enriching hydrogen-producing bacteria from digested sludge. Int J Hydrogen Energy 2008. https://doi.org/10.1016/j.ijhydene.2008.03.048.

[33] Spasiano D, Pirozzi F. Treatments of asbestos containing wastes. J Environ Manage 2017. https://doi.org/10.1016/j.jenvman.2017.08.038.

[34] Ghimire A, Frunzo L, Pirozzi F, Trably E, Escudie R, Lens PNL, et al. A review on dark fermentative biohydrogen production from organic biomass: Process parameters and use of by-products. Appl Energy 2015. https://doi.org/10.1016/j.apenergy.2015.01.045.

[35] Oehmen A, Keller-Lehmann B, Zeng RJ, Yuan Z, Keller J. Optimisation of poly-β-hydroxyalkanoate analysis using gas chromatography for enhanced biological phosphorus removal systems. J Chromatogr A 2005.

https://doi.org/10.1016/j.chroma.2005.02.020.

[36] Pontoni L, Panico A, Matanò A, Van Hullebusch ED, Fabbricino M, Esposito G, et al. Modified Sample Preparation Approach for the Determination of the Phenolic and Humic-Like Substances in Natural Organic Materials by the Folin Ciocalteu Method. J Agric Food Chem 2017. https://doi.org/10.1021/acs.jafc.7b04942.

[37] American Public Health Association (APHA). Standard Methods for the Examination of Water and Wastewater, 21st ed.; APHA:Washington, DC, USA, 2005. 2005.

[38] Carrillo-Reyes J, Albarrán-Contreras BA, Buitrón G. Influence of Added Nutrients and Substrate Concentration in Biohydrogen Production from Winery Wastewaters Coupled to Methane Production. Appl Biochem Biotechnol 2019. https://doi.org/10.1007/s12010-018-2812-5.

[39] Moreno-Andrade I, Moreno G, Kumar G, Buitrón G. Biohydrogen production from industrial wastewaters. Water Sci Technol 2015. https://doi.org/10.2166/wst.2014.471.

[40] Elbeshbishy E, Dhar BR, Nakhla G, Lee HS. A critical review on inhibition of dark biohydrogen fermentation. Renew Sustain Energy Rev 2017;79:656–68. https://doi.org/10.1016/j.rser.2017.05.075.

[41] Romano P, Fiore C, Paraggio M, Caruso M, Capece A. Function of yeast species and strains in wine flavour. Int J Food Microbiol 2003. https://doi.org/10.1016/S0168-1605(03)00290-3.

[42] García-Becerra M, Macías-Muro M, Arellano-García L, Aguilar-Juárez O. Bio-hydrogen production from tequila vinasses: Effect of detoxification with activated charcoal on dark fermentation performance. Int J Hydrogen Energy 2019. https://doi.org/10.1016/j.ijhydene.2019.10.059.

[43] Wang Z, Zhuge J, Fang H, Prior BA. Glycerol production by microbial fermentation: A review. Biotechnol Adv 2001. https://doi.org/10.1016/S0734-9750(01)00060-X.

[44] Policastro G, Carraturo F, Compagnone M, Giugliano M, Guida M, Luongo V, et al. A preliminary study on a novel bioaugmentation technique enhancing lactic acid production by mixed cultures fermentation. Bioresour Technol 2021;340:125595. https://doi.org/10.1016/j.biortech.2021.125595.

[45] Jagtap RS, Mahajan DM, Mistry SR, Bilaiya M, Singh RK, Jain R. Improving ethanol yields in sugarcane molasses fermentation by engineering the high osmolarity glycerol pathway while maintaining osmotolerance in *Saccharomyces cerevisiae*. Appl Microbiol Biotechnol 2019. https://doi.org/10.1007/s00253-018-9532-1.

[46] Han W, Hu Y, Li S, Huang J, Nie Q, Zhao H, et al. Simultaneous dark fermentative hydrogen and ethanol production from waste bread in a mixed packed tank reactor. J Clean Prod 2017;141:608–11. https://doi.org/10.1016/j.jclepro.2016.09.143.

[47] Ren N, Li J, Li B, Wang Y, Liu S. Biohydrogen production from molasses by anaerobic fermentation with a pilot-scale bioreactor system. Int J Hydrogen Energy 2006;31:2147–57. https://doi.org/10.1016/j.ijhydene.2006.02.011.

[48] Ren N, Li J, Li B, Wang Y, Liu S. Biohydrogen production from molasses by anaerobic fermentation with a pilot-scale bioreactor system. Int J Hydrogen Energy 2006. https://doi.org/10.1016/j.ijhydene.2006.02.011.

[49] Hustede E, Steinbüchel A, Schlegel HG. Relationship between the photoproduction of hydrogen and the accumulation of PHB in non-sulphur purple bacteria. Appl Microbiol Biotechnol 1993. https://doi.org/10.1007/BF00166854.

[50] Kim DH, Son H, Kim MS. Effect of substrate concentration on continuous Photo-fermentative hydrogen production from lactate using *Rhodobacter sphaeroides*. Int. J. Hydrogen Energy, 2012. https://doi.org/10.1016/j.ijhydene.2012.02.039.

[51] Özgür E, Peksel B. Biohydrogen production from barley straw hydrolysate through sequential dark and photofermentation. J Clean Prod 2013. https://doi.org/10.1016/j.jclepro.2013.02.035.

[52] Zong W, Yu R, Zhang P, Fan M, Zhou Z. Efficient hydrogen gas production from cassava and food waste by a two-step process of dark fermentation and photo-fermentation. Biomass and Bioenergy 2009. https://doi.org/10.1016/j.biombioe.2009.06.008.

[53] Uyar B, Eroglu I, Yücel M, Gündüz U. Photofermentative hydrogen production from volatile fatty acids present in dark fermentation effluents. Int J Hydrogen Energy 2009. https://doi.org/10.1016/j.ijhydene.2008.07.057.

[54] Ghosh S, Dairkee UK, Chowdhury R, Bhattacharya P. Hydrogen from food processing wastes via photofermentation using Purple Non-sulfur Bacteria (PNSB)

– A review. Energy Convers Manag 2017;141:299–314. https://doi.org/10.1016/j.enconman.2016.09.001.

[55] Ioannou LA, Puma GL, Fatta-Kassinos D. Treatment of winery wastewater by physicochemical, biological and advanced processes: A review. J Hazard Mater 2015. https://doi.org/10.1016/j.jhazmat.2014.12.043.

[56] Nasr M, Tawfik A, Ookawara S, Suzuki M, Kumari S, Bux F. Continuous biohydrogen production from starch wastewater via sequential dark-photo fermentation with emphasize on maghemite nanoparticles. J Ind Eng Chem 2015;21:500–6. https://doi.org/10.1016/j.jiec.2014.03.011.

[57] Hitit ZY, Zampol Lazaro C, Hallenbeck PC. Increased hydrogen yield and COD removal from starch/glucose based medium by sequential dark and photo-fermentation using *Clostridium butyricum* and *Rhodopseudomonas palustris*. Int J Hydrogen Energy 2017;42:18832–43. https://doi.org/10.1016/j.ijhydene.2017.05.161.

[58] Tao Y, Chen Y, Wu Y, He Y, Zhou Z. High hydrogen yield from a two-step process of dark- and photo-fermentation of sucrose. Int J Hydrogen Energy 2007;32:200–6. https://doi.org/10.1016/j.ijhydene.2006.06.034.

[59] Oh EK, Kim EJ, Hwang HJ, Tong X, Nam JM, Kim MS, et al. The photoheterotrophic H_2 evolution of *Rhodobacter sphaeroides* is enhanced in the presence of ethanol. Int J Hydrogen Energy 2012. https://doi.org/10.1016/j.ijhydene.2012.08.029.

[60] Luongo V, Policastro G, Ghimire A, Pirozzi F, Fabbricino M. Repeated-batch fermentation of cheese whey for semi-continuous lactic acid production using mixed cultures at uncontrolled pH. Sustain 2019;11:1–12. https://doi.org/10.3390/su10023330.

[61] Rombouts JL, Kranendonk EMM, Regueira A, Weissbrodt DG, Kleerebezem R, van Loosdrecht MCM. Selecting for lactic acid producing and utilising bacteria in anaerobic enrichment cultures. Biotechnol Bioeng 2020;117:1281–93. https://doi.org/10.1002/bit.27301.

[62] Sevinç P, Gündüz U, Eroglu I, Yücel M. Kinetic analysis of photosynthetic growth, hydrogen production and dual substrate utilization by *Rhodobacter capsulatus*. Int. J. Hydrogen Energy, 2012. https://doi.org/10.1016/j.ijhydene.2012.02.176.

[63] James BW, Mauchline WS, Dennis PJ, Keevil CW, Wait R. Poly-3-hydroxybutyrate in *Legionella pneumophila*, an energy source for survival in low-nutrient environments. Appl Environ Microbiol 1999. https://doi.org/10.1128/aem.65.2.822-827.1999.

[64] Johnson K, Jiang Y, Kleerebezem R, Muyzer G, Van Loosdrecht MCM. Enrichment of a mixed bacterial culture with a high polyhydroxyalkanoate storage capacity. Biomacromolecules, 2009. https://doi.org/10.1021/bm8013796.

[65] Montiel-Corona V, Revah S, Morales M. Hydrogen production by an enriched photoheterotrophic culture using dark fermentation effluent as substrate: Effect of flushing method, bicarbonate addition, and outdoor-indoor conditions. Int J Hydrogen Energy 2015. https://doi.org/10.1016/j.ijhydene.2015.05.067.

[66] Eroğlu E, Gündüz U, Yücel M, Türker L, Eroğlu I. Photobiological hydrogen production by using olive mill wastewater as a sole substrate source. Int J Hydrogen Energy 2004. https://doi.org/10.1016/S0360-3199(03)00110-1.

[67] Cheng J, Su H, Zhou J, Song W, Cen K. Hydrogen production by mixed bacteria through dark and photo fermentation. Int J Hydrogen Energy 2011;36:450–7. https://doi.org/10.1016/j.ijhydene.2010.10.007.

[68] Liu BF, Ren NQ, Tang J, Ding J, Liu WZ, Xu JF, et al. Bio-hydrogen production by mixed culture of photo- and dark-fermentation bacteria. Int J Hydrogen Energy 2010;35:2858–62. https://doi.org/10.1016/j.ijhydene.2009.05.005.

[69] Tiang MF, Fitri Hanipa MA, Abdul PM, Jahim JM d., Mahmod SS, Takriff MS, et al. Recent advanced biotechnological strategies to enhance photo-fermentative biohydrogen production by purple non-sulphur bacteria: An overview. Int J Hydrogen Energy 2020;45:13211–30. https://doi.org/10.1016/j.ijhydene.2020.03.033.

Chapter 6

Biohydrogen and poly-β-hydroxybutyrate production by winery wastewater photofermentation: Effect of substrate concentration and nitrogen source

This chapter has been published as: Policastro, G., Luongo, V. and Fabbricino, M. (2020). Biohydrogen and poly-β-hydroxybutyrate production by winery wastewater photofermentation: Effect of substrate concentration and nitrogen source. Journal of Environmental Management, 271, 111006.

Biohydrogen and poly-β-hydroxybutyrate production by winery wastewater photofermentation: Effect of substrate concentration and nitrogen source

Abstract

The applicability and convenience of biohydrogen and poly-β-hydroxybutyrate production through single-stage photofermentation of winery wastewater is demonstrated in the present study. Experiments are conducted using a purple non-sulfur bacteria mixed consortium, subject to variable nutrient conditions, to analyze the effect of initial chemical oxygen demand and the available nitrogen source on the metabolic response. Results show that winery wastewater is a promising substrate for photofermentation processes, despite the presence of inhibiting compounds such as phenolics. Nonetheless, the initial chemical oxygen demand must be carefully controlled to maximize hydrogen production. Up to 468 mL L^{-1} of hydrogen and 203 mg L^{-1} of poly-β-hydroxybutyrate can be produced starting from an initial chemical oxygen demand of 1500 mg L^{-1}. The used nitrogen source may direct substrate transformation through different metabolic pathways. Interestingly, the maximum production of both hydrogen and poly-β-hydroxybutyrate occurred when glutamate was used as the nitrogen source.

6.1. Introduction

Biofuel production has attracted increasing attention in recent years as a tool to reverse greenhouse gas emissions and address depletion of natural resources [1,2]. Biofuels can be obtained through several biological processes, including anaerobic digestion, dark fermentation, and photofermentation [3,4]. Among them, photofermentation (PF) is certainly one of the most promising alternatives [5], due to its potential sustainability, environmentally friendly characteristics, and the high value of the resulting product.

PF is a biological process conducted by specific anaerobic facultative species, named purple non-sulfur bacteria (PNSB). In the presence of light and absence of molecular oxygen and nitrogen, PNSB are able to convert a wide range of organic substrates to hydrogen. In addition, PNSB can store, within their own cytoplasm, poly-β-hydroxybutyrate (PHB), a promising candidate for the production of totally biodegradable plastic materials [6], perfectly fitting the biorefinery concept. The accumulation of PHB and the production of hydrogen are generally competitive metabolic pathways [7], although recent studies have shown that, under specific growth conditions, these two pathways can coexist [4,8,9].

We currently lack a complete understanding of the complex metabolism of PNSB and the consequent pathways that can be followed during the life of PNSB under different

environmental and feed conditions. This aspect is crucial when the bioconversion begins with organic waste and the PNSB consortium is composed of mixed cultures. Most studies on PF, in fact, have been conducted using synthetic substrates and/or pure cultures [7,10]. A few recent studies have described the possibility of using low-cost waste materials for the photofermentation of mixed cultures [9,11]. However, many other organic wastes could be considered as valuable sources of feedstock for the process.

A significant example is provided by winery wastewater (WWW), which is the major waste stream resulting from wine production. Every year, about 270 million hectoliters (hL) of wine are produced worldwide [12]. The produced effluent contains various by-products, including ethanol, sugars, organic acids, and several phenolic compounds [13]. Due to its high organic content, WWW is a potential source of contamination if not correctly managed [14]. On the other hand, it can be sustainably valorized through PF. Indeed, the organic molecules contained in WWW, such as alcohols and sugars (all rapidly available), represent a suitable source of carbon for PNSB. Nonetheless, PF of WWW presents some challenges due to the presence of toxic compounds, such as phenols, and the dark color of the waste, which negatively affects the penetration of light in the bioreactor [15,16]. Only a few recent studies have been conducted on WWW conversion to hydrogen via dark fermentation [17,18]. Otherwise, the single-stage photofermentation process using pure or mixed PNSB consortia has never been tested in previous studies.

The main objective of the present paper is to demonstrate the applicability of PF to WWW. The aims of the study are to add to our knowledge of the metabolic pathways that PNSB undergo in the presence of non-synthetic substrates and to address the abovementioned challenges (toxicity, color) in order to optimize the production of valuable compounds. The most relevant aspects of the study relate not only to the utilization of a waste material that has not yet been tested through the PF process, but also to the adoption of mixed cultures of PNSB (for scaling-up purposes) and to the analysis of the metabolic pathways that allow for the concomitant production of hydrogen and PHB. The study is performed under various feed conditions and tests different nitrogen sources and feeding chemical oxygen demand (COD) concentrations. In the case of waste biomass, in fact, one of the most frequent problems is the lack or incorrect distribution of macro- and micronutrients [15,19]. In particular, the type and concentration of nitrogen in the medium strongly influence the activity of nitrogenase, which is the key enzyme for hydrogen production. Similarly, the ratio between carbon

and nitrogen affects the metabolic pathway [20]. High COD values lead to the accumulation of volatile fatty acids (VFAs) and to the consequent decrease of pH, which is responsible for process inhibition [16]. All of these aspects affecting hydrogen and PHB generation have been taken into account during the experiments. These observations assume a relative value when real substrates and mixed consortia are used, as the combination of mixed consortia and substrate-related microorganisms may lead to competitive or synergistic behaviors during nutrient conversion. For instance, Luongo et al. [4] demonstrated that greater hydrogen production can be achieved by mixed PNSB consortia than by a pure *Rodobacter sphaeroides* culture using the dark fermentation effluent as photofermentation feedstock. Indeed, the present study mainly focuses on the reliability of the photofermentative conversion of WWW instead of the specific metabolic assimilation of each nutrient during the process. The obtained results constitute an important beginning step for real-scale valorization of WWW by PF.

6.2. Materials and Methods

6.2.1. Materials

WWW was obtained from a farm located in San Gregorio Magno (southern Italy) that produces white wine. Immediately after sampling, WWW was carefully characterized (Table 6.1) and stored under dark conditions at -20 °C to maintain its initial unaltered characteristics during the different PF experiments.

Table 6.1. WWW initial characteristics.

Parameter	Value
COD	282 ±1 g L^{-1}
$N\text{-}NH_4^+$	0.50 ±0.02 g L^{-1}
NO_3^-	0.005 ±0.001 g L^{-1}
Total phenols	0.6 ±0.1 g L^{-1}
pH	4.5 ±0.1
Glucose	91 ±7 g L^{-1}
Ethylic alcohol	44 ±9 g L^{-1}
Lactic acid	2.0 ± 0.3 g L^{-1}
Acetic acid	0.4 ± 0.2 g L^{-1}
PO_4^{3-}	0.002 ±0.001 g L^{-1}
SO_4^{2-}	0.007 ±0.001 g L^{-1}

As suggested by several authors [21–23], WWW was diluted prior its use so that the feeding load was kept under inhibiting threshold values. WWW was diluted using an

organic carbon-free culture medium and a specific trace element solution, prepared according to Ghimire et al. [8]. In detail, 10 mL volume of trace element solution was added to each L of culture medium. Bi-distilled water was used to prepare both the medium and the trace element solution. Differently from other investigations [22,24], no other pretreatment was used to reduce the COD content or to limit the initial total phenolic content. Due to the natural acidity of WWW, the pH of the culture medium was neutralized by fixing the initial pH to 7 with a 1 M KOH solution.

PNSB inoculum was sampled from a mixed-culture PF reactor operating at laboratory scale and fed with a synthetic wastewater rich in organic acids. Before use, the inoculum was reactivated using a synthetic glucose-based medium, and 5 mL from the previous reactor was used to inoculate the new one. Due to the high inoculum dilution, each reactor was quite transparent on day 0. During the fermentation time, PNSB growth conferred a bright red color to the reactors, which is typical for the PF process.

The chemicals used for all analytical determinations were of high purity. Only bi-distilled water was employed as the reagent water.

Before each use, the glassware was soaked overnight in a concentrated nitric acid bath (2% v/v) and rinsed several times with bi-distilled water.

6.2.2. Experimental Procedure

Experiments were conducted at room temperature (25±2 °C) and under non-sterile conditions, using 400 mL glass reactors equipped with tubing on the top for sampling and gas extraction. Tubing was also used to flush the headspace with argon gas for 20 minutes, thereby ensuring anaerobic conditions and completely removing nitrogen gas. The reactors were placed on magnetic mixers, with the rotation speed adjusted to 250 rpm to maintain completely stirred tank conditions. Light was continuously provided by flexible LED strips placed all around the bioreactors (4000 lux).

Eight sets of experiments were carried out to evaluate PF process performance with varied initial dilutions (H=high dilution, L=low dilution) and therefore initial COD concentrations (1500 mg L^{-1} and 3000 mg L^{-1}). Different nitrogen sources were used, i.e., sodium glutamate (organic nitrogen, ON), ammonium chloride (ammonia nitrogen, AN), sodium nitrate (nitric nitrogen, NN), and endogenous nitrogen (EN), as reported in Table 6.2.

Table 6.2. Experimental conditions of the different sets of reactors.

Set #	COD (mg L^{-1})	Nitrogen source	TN (mM)
H_{-ON}	1500	Sodium glutamate	2.79
H_{-AN}	1500	Ammonium chloride	2.79

H_{-NN}	1500	Sodium nitrate	2.79
H_{-EN}	1500	Endogenous nitrogen	0.22
L_{-ON}	3000	Sodium glutamate	2.79
L_{-AN}	3000	Ammonium chloride	2.79
L_{-NN}	3000	Sodium nitrate	2.79
L_{-EN}	3000	Endogenous nitrogen	0.43

Total nitrogen (TN) concentration was fixed at 2.79 mM of N for all experiments conducted using an external nitrogen source. Because of the adopted dilution, however, the experiments conducted using only the endogenous nitrogen source were characterized by initial TN concentrations of 0.22 mM for the higher dilution case (H_{-EN}) and 0.43 mM for lower dilution case (L_{-EN}). Each set was carried out in triplicate. H experiments lasted 16 days and L experiments lasted 24 days, depending on the feeding conditions. Tests were concluded when no more variations were detected in terms of hydrogen production and organic acids (OAs) concentration. Every two days, liquid and gaseous samples were collected for quantitative and qualitative analysis.

6.2.3. Analytical Methods and Instruments

Gas production was quantified through water displacement. H_2 and CO_2 contents were determined by gas chromatographic analysis conducted using a Varian Star 3400 gas chromatograph equipped with a ShinCarbon ST 80/100 column and a thermal conductivity detector, with argon as the carrier gas. OAs, sugars, and ethanol concentrations were determined by high-pressure liquid chromatography using a Dionex (Sunnyvale, USA) LC 25 Chromatography Oven equipped with a Metrohom (Herisau, Switzerland) Organic Acids column (Metrosep Organic Acids - 250/7.8). In detail, two different detectors were used: a Dionex (Sunnyvale, USA) UVD 340U for VFA determination and a Jasco (Cremella, Italy) RI-2031 for ethanol and sugar detection. The eluent (1 mM H_2SO_4) was pumped at a constant rate of 0.7 mL min^{-1} using a Dionex (Sunnyvale, USA) GD 500 Gradient Pump. The PHB concentration was determined by gas chromatography and mass spectrometry. Toward this aim, the samples were preliminarily lyophilized, and the polymers were extracted according to Oehmen et al. (2005). Gas chromatographic analysis and mass spectrometry were conducted using a GC-MS with a ZB SemiVolatiles Zebron column (Phenomenex, Torrance, USA). Helium was used as the carrier gas. Biomass growth was quantified by measuring the optical density (OD) at 660 nm referenced to the total suspended solids (TSS) concentration with a standard correlation curve. A WTW photoLab (Wheilheim, Germany) spectrophotometer (6600 UV-VIS) was utilized for the optical

density determination. COD concentration was obtained by colorimetric analysis according to standard methods (APHA, 2005). Total phenolic content was measured following the Folin and Ciocalteu Method [25]. N-NH_4^+ and TKN concentrations were measured by distillation and titration (APHA, 2005). The distillation was performed using a UDK 132 VELP (Usmate Velate, Italy) distiller. H_2SO_4 was used for titration. NO_3^-, PO_4^{3-}, and SO_4^{2-} concentrations were measured by ion chromatography, using a Metrohm 761 Compact Ion Chromatograph (Herisau, Switzerland) equipped with a Dionex IonPac AS12A 4 x 200 mm column (Sunnyvale, USA). Light intensity was checked using a Lutron-LX-107 light meter (Coopersburg, USA), and pH was measured using a Hanna pH meter (Limena, Italy).

6.3. Results

6.3.1. Organic Nitrogen Source

Figure 6.1a-f illustrates the time-course profiles of the parameters monitored during the tests conducted in the presence of ON for the two tested dilutions (1500 mg L^{-1} and 3000 mg L^{-1}).

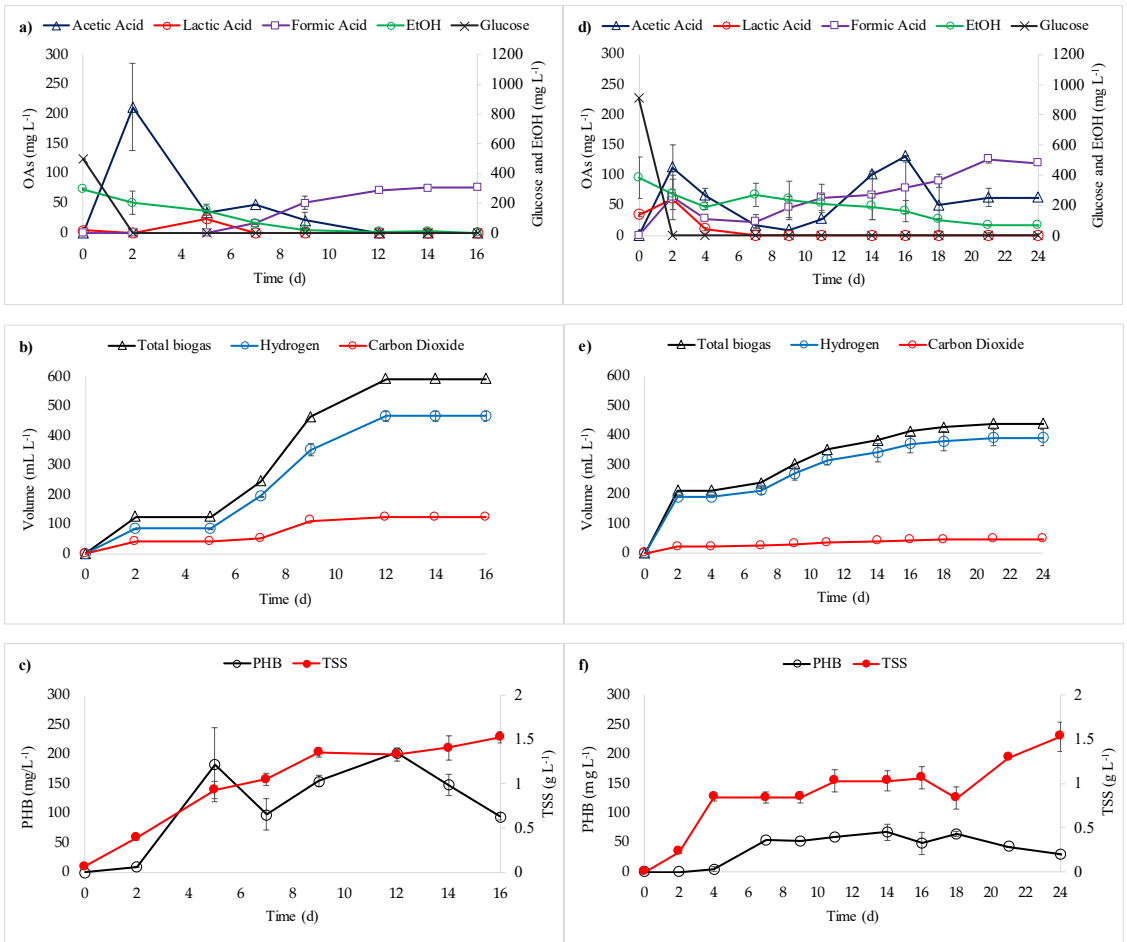

Figure 6.1. (a, b, c) Experimental results for sets H_{-ON} and (d, e, f) L_{-ON}. (a, c) The concentration of organic acids (OAs), glucose, and ethanol (EtOH). (b, e) The volume

of produced biogas, in terms of total biogas, hydrogen, and carbon dioxide. (c, f) The concentration of PHB and biomass (in terms of TSS).

For both experimental conditions (days 0 to 2), WWW was subject to catabolic and anabolic reactions according to kinetic models describing bacterial degradation of glucose and organics in anaerobic environments [26,27]. Indeed, during glucose consumption, the contextual production of acetic acid and hydrogen (catabolic reactions) and the accumulation of the biomass (anabolic reactions) were observed. For the three successive days (days 2 to 5), no hydrogen production was detected. During this time, ethanol and acetic acid were degraded and used for the biomass growth and the PHB accumulation. Over the fifth day, hydrogen production started once more. In this period, hydrogen was the main fermentation by-product. Moreover, formic acid was produced. For the set H_{-ON}, the concentration of formic acid increased from day 5 to day 12 and then was constant until the end of the process. In contrast, for the set L_{-ON}, the production of formic acid increased until day 21. Moreover, for the L_{-ON} reactors, a relevant amount of acetic acid was produced from day 10 to day 16. Residual amounts of ethanol and acetic acid were detected in the final effluent.

No differences between the two tested conditions were observed in terms of biomass growth and PHB accumulation. In both cases, in fact, the biomass reached a concentration of about 1.5 $gTSS \cdot L^{-1}$, with a slightly increasing trend at the end of the process corresponding to PHB depletion.

6.4. Ammonia Nitrogen Source

Figures 6.2 summarizes the results of the tests conducted in the presence of AN.

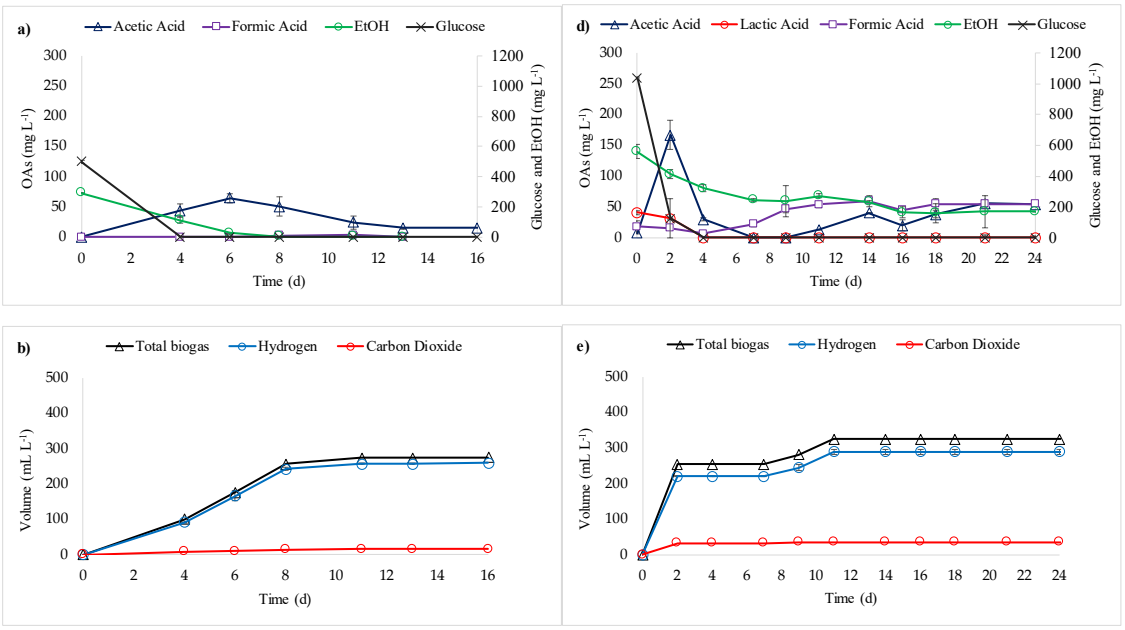

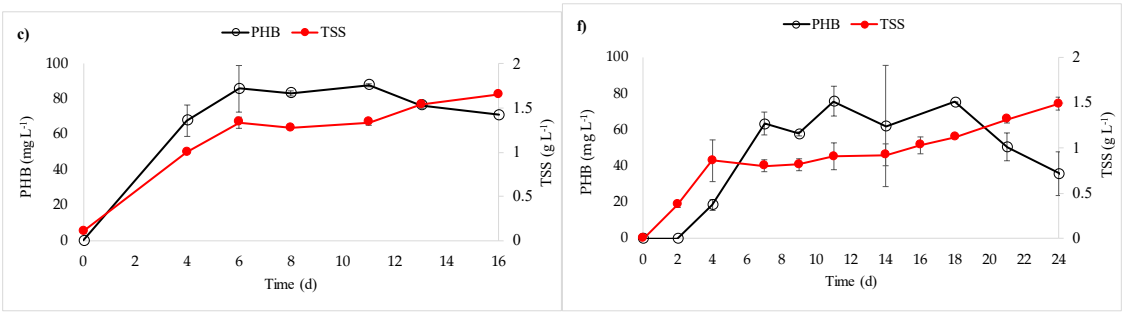

Figure 6.2. (a, b, c) Experimental results for sets H_{-AN} and (d, e, f) L_{-AN} . (a, c) The concentration of organic acids (OAs), glucose, and ethanol (EtOH). (b, e) The volume of produced biogas, in terms of total biogas, hydrogen, and carbon dioxide. (c, f) The concentration of PHB and biomass (in terms of TSS).

Set H_{-AN} revealed an interesting aspect related to nitrogen assimilation by the PNSB consortium. In fact, the use of AN in the presence of more diluted WWW avoided any formic acid production during the process. Substrate consumption led directly to hydrogen, acetic acid, and PHB production during the first six days. No PHB accumulation was detected from day 6 to day 11, and no hydrogen was produced after day 8. In the presence of the less diluted WWW (set L_{-AN}), the substrate was instead converted to acetic acid, hydrogen, and biomass during the first two days of fermentation (days 0 to 2). Furthermore, no H_2 production was observed from day 2 until day 6, ethanol and acetic acid were depleted, and the carbon was stored in the form of PHB. Past the seventh day, hydrogen, formic acid, and acetic acid were the main fermentation by-products. As observed in the reactors operated with ON (set L_{-ON}), ethanol was not completely depleted in the case of set L_{-AN}. A residual concentration of formic acid and acetic acid was measured in the final effluent. The biomass concentration reached a final value of about 1.5 $gTSS \cdot L^{-1}$, also in the presence of AN. During the last days of fermentation, the biomass growth was again associated with PHB consumption.

6.3.3. Nitric Nitrogen Source

Figures 6.3 summarizes the results of the tests conducted in the presence of NN.

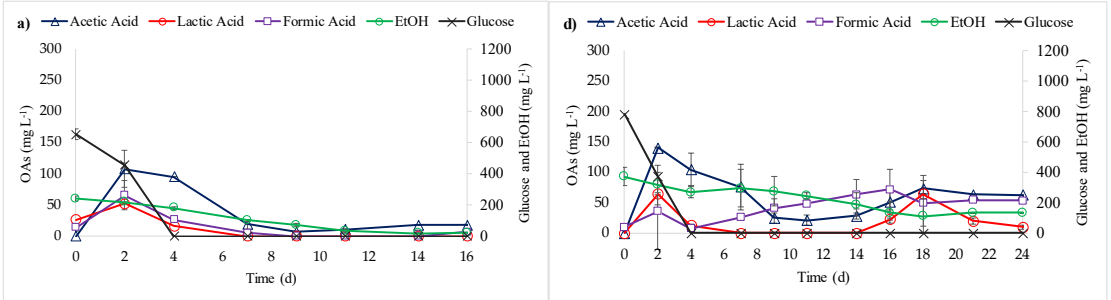

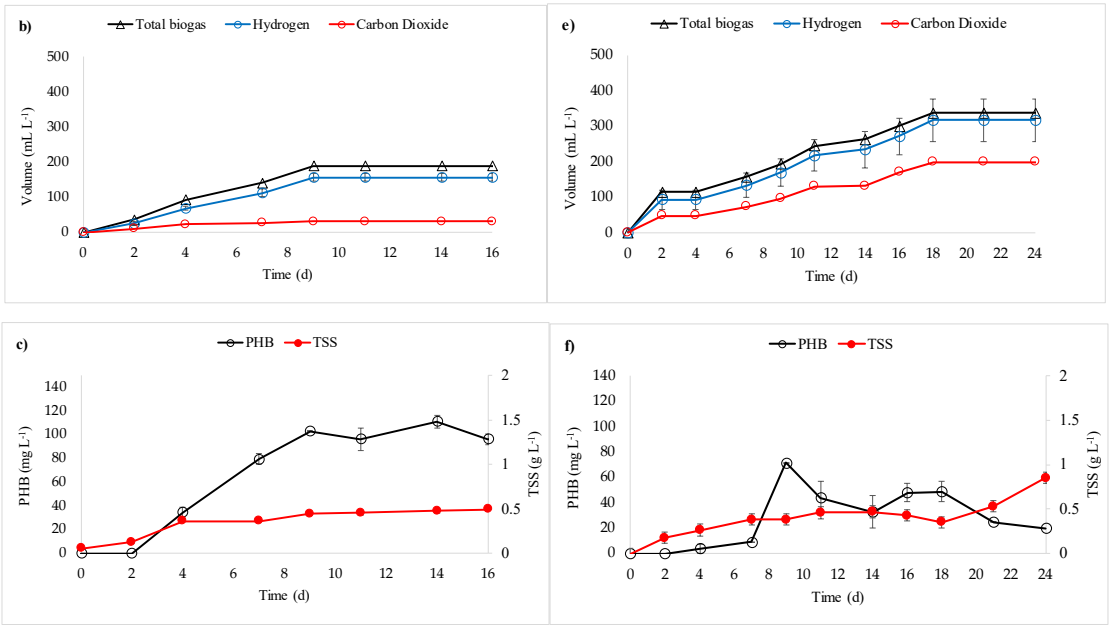

Figure 6.3. (a, b, c) Experimental results for sets H_{-NN} and (d, e, f) L_{-NN} . (a, c) The concentration of organic acids (OAs), glucose, and ethanol (EtOH). (b, e) The volume of produced biogas, in terms of total biogas, hydrogen, and carbon dioxide. (c, f) The concentration of PHB and biomass (in terms of TSS).

According to the obtained results, for both tested conditions during the first days (days 0 to 2), the substrate was principally converted to acetic, lactic, and formic acids and hydrogen. Acids were successively depleted and converted to hydrogen and PHB. In the presence of higher substrate concentrations (set L_{-NN}), lactic and formic acids were produced again during the process, and ethanol was not completely consumed at the end of the test. Hydrogen production occurred for a much longer time for the L reactors.

Biomass growth rates were slower than for the other experimental tests. The TSS value remained quite constant (around 0.5 g L^{-1}) during the whole process for the case of set H_{-NN}. A further increase after day 18 was observed instead for the case of set L_{-NN} corresponding to PHB degradation. The final biomass concentration of 0.9 g L^{-1} was reached. It is worth noting that the nitrogen source used in the experiment led to the production of 22±4 mL L^{-1} of N_2 for both sets during the first 10 days of fermentation (data not shown).

6.3.4 Endogenous Nitrogen Source

Figure 6.4a-c reports the results obtained in the presence of EN. As the endogenous nitrogen content of set H_{-EN} limited the bacterial growth, resulting in low biomass yields, no hydrogen production or PHB accumulation was detected (data not shown). Therefore, Figure 6.4a-c refers only to set L_{-EN}.

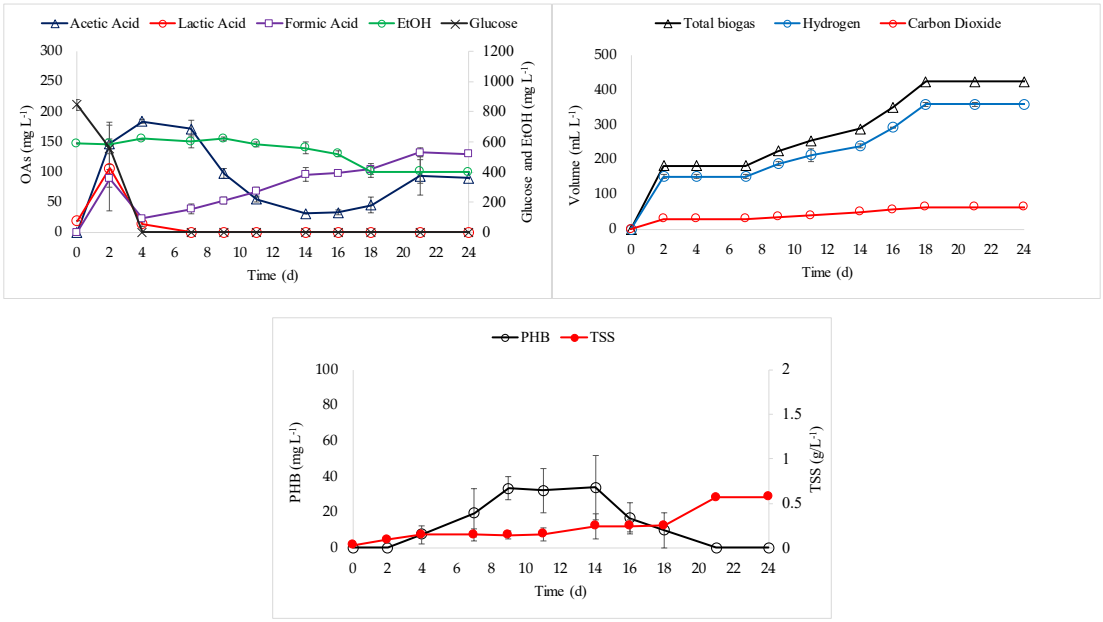

Figure 6.4. (a, b, c) Experimental results for sets L-EN. (a) The concentration of organic acids (OAs), glucose, and ethanol (EtOH). (b) The volume of produced biogas, in terms of total biogas, hydrogen, and carbon dioxide. (c) The concentration of PHB and biomass (in terms of TSS).

As it can be observed, the ethanol concentration remained constant from days 7 to 16, while acetic acid was converted to hydrogen and formic acid. During days 16–20, ethanol was depleted and converted to hydrogen, formic acid, and acetic acid. Over successive days until the end of the process, no more hydrogen or acid production was observed. Differently from the other tests, in this case, a very low amount of ethanol was used as a carbon source by microorganisms. A very low TSS value and PHB concentration were observed, suggesting that the substrate was principally used for catabolic reactions.

6.4. Discussion

6.4.1. Substrate Utilization and Biomass Growth

Substrate consumption was conditioned by the carbon catabolite repression (CCR) phenomenon. CCR takes place when a microbial consortium has access to a mixture of carbon sources, and in such a situation, the consortium may exhibit a selective pattern of substrate utilization. The presence of a preferred substrate prevents the use of other carbon sources, giving rise to CCR [19,28–30]. Glucose, which is the simplest carbohydrate, is the principal carbon catabolite repressor [30]. The obtained data are in line with the mentioned studies on CCR, and in the presence of WWW, PNSB showed a higher assimilation rate with glucose than with ethanol. Indeed, during all tests, glucose was totally consumed during the first few days of fermentation and was principally

converted to hydrogen and acetic acid. Subsequently, the biomass had to adapt to other, more complex, carbon sources. The new situation corresponded to a stress condition for the microorganisms, causing them to shift their metabolism to PHB accumulation. During the last days of fermentation, bacteria depleted the stored PHB and utilized it for their growth. In accordance with the feast-famine theory [31], PNSB used PHB as a carbon reserve for their growth and survival when the substrate and/or the other nutrients became scarce [4,32]. Correspondingly, the lowest tested nitrogen concentration (set L_{-IN}) resulted in the lowest biomass concentration, in agreement with previous findings [23]. The highest TSS content, reached in sets H_{-ON}, L_{-ON}, H_{-AN}, and L_{-AN}, indicated that the most suitable nitrogen sources for biomass growth were organic and ammonia nitrogen, whereas low biomass growth was observed instead when nitrates were used as a nitrogen source.

The highest COD removal, obtained for the set H_{-NN} (Table 6.3), was comparable with levels reported in previous PF studies conducted using mixed cultures [20].

Table 6.3. Cumulative hydrogen production, maximum PHB accumulation, and COD removal efficiency for the experimental sets.

Set #	**PHB accumulation (mg L^{-1})**	**H_2 production (mg L^{-1})**	**COD removal (%)**
H_{-ON}	203	468	74
L_{-ON}	60	391	40
H_{-AN}	88	259	76
L_{-AN}	76	317	63
H_{-NN}	103	157	80
L_{-NN}	71	289	52
H_{-EN}	-	-	-
L_{-EN}	34	358	33

At the same time, the removal was generally higher compared to studies conducted using pure cultures [20,33].

The lower level of COD removal obtained for reactors operating with AN and ON was attributed to the self-shading condition that occurred during the experiments. Indeed, the higher biomass growth observed under these conditions led to a higher TSS concentration, which negatively affected light penetration inside the reactors [33].

In addition, the reduced performance in terms of COD removal associated with L reactors compared to H reactors was likely due to the accumulation of organic acids. This is in agreement with previous studies [16,20] that reported a similar behavior in the presence of mixed cultures. More than the other acids, formic acid seemed to be

resistant to biotransformation. The concentration of this by-product principally increased when the microorganisms adopted the hydrogen production pathway. Moreover, it was detected in the effluent of the L reactors, although the residual formic acid concentration was lower (about 50%) in the presence of AN and NN (sets L_{-AN} and L_{-NN}) than in the presence of ON or EN (sets L_{-ON} and L_{-EN}). In comparison, the formic acid concentration in the effluent of the H experimental sets was very low in the presence of ON and totally absent in the presence of AN and NN. This result was in agreement with previous studies [34], attesting that the higher the ON concentration used for bacteria growth, the greater the production of formic acid during the fermentation process. In addition, the present study revealed that the higher the initial COD concentration used for the fermentation tests, the greater the production of formic acid observed in the effluents. Moreover, inorganic nitrogen compounds act as inhibiting agents in formic acid production.

6.4.2. Hydrogen Production and PHB Accumulation

In the present study, the adopted nitrogen source strongly affected hydrogen production and PHB accumulation. In detail, the utilization of ON led to the greatest hydrogen yields, which agrees with the assessment of previous studies that glutamate utilization stimulates hydrogen production [35,36]. A slightly lower value was reached in the presence of AN. Nevertheless, the value was still not negligible. In fact, $NH4^+$ is the principal inhibitor of the nitrogenase enzyme [7,37–39], which, in the presence of relevant nitrogen concentrations, can act as hydrogen consuming instead of hydrogen producing [16]. Seifert et al. [23] determined that a NH_4^+ concentration of 1.7 mM completely inhibits hydrogen generation in the presence of a pure culture of PNSB. Similarly, Özgür et al. [40] observed the complete inhibition of a pure PNSB culture during hydrogen production from substrates characterized by high AN content (2 mM of NH_4^+). In both cases, the NH_4^+ concentration was lower than those tested in the present study, suggesting that the synergistic behavior of different bacterial species, coexisting in the tested mixed consortium, had a beneficial effect on substrate utilization. This allowed for the bioconversion of a wide spectrum of organic and inorganic compounds [8].

The lowest level of hydrogen production was observed in the presence of NN. In this case, the presence of N_2 in the produced gas (data not shown) suggested that the mixed PNSB consortium mainly acted as denitrifying bacteria, converting nitrates to molecular nitrogen. Indeed, several authors [41,42] showed the possibility of using pure cultures of PNSB for NO_3 removal from wastewater. In the presence of N_2, the nitrogenase

enzyme catalyzes nitrogen fixation, producing an amount of hydrogen that is four times lower than the amount produced under nitrogen-deficient conditions [43,44]. Consequently, in the presence of NN, hydrogen production was scarce.

The initial COD concentration had a reduced effect on hydrogen production compared to the nitrogen source. As expected [45,46], an increasing C/N ratio enhanced hydrogen production. The only exception occurred in experiments conducted with glutamate as the nitrogen source. This was probably due to the very peculiar metabolic pathway followed by the biomass in this situation, leading to the concurrent production of H_2 and PHB, as detailed below. A relevant result was the high hydrogen content (about 90%) in the produced gas obtained for all tested conditions. Very low amounts of CO_2 were generated by PF of WWW compared to preliminary investigations carried out on synthetic wastewater with the same PNSB consortium (data not shown).

Notably, hydrogen production was not inhibited by the phenolic content of the substrate, even in the less diluted WWW, a countertrend from several previous studies conducted with pure PNSB cultures. For example, Eroğlu et al. [24] observed that PF of olive mill wastewater performed by *Rhodobacter Sphaeroides O.U.001* was completely inhibited by a phenol content of 5.8 $mg \cdot L^{-1}$. The phenol content was lower than the one resulting in the less diluted WWW used in the present study (6.38 $mg \cdot L^{-1}$). The positive obtained result was attributed to the beneficial effect of the mixed PNSB culture.

The maximum obtained value of hydrogen production was comparable to the one reported by Kars and Alparslan [47] during the PF of sugar beet molasses operated by a pure culture of *Rhodhobacter sphaeroides O.U.001*. On the other hand, the probable absence of specific PHB-accumulating species in the adopted PNSB consortium did not allow a high PHB concentration to be obtained [33]. The highest PHB accumulation values were lower than those found in previous studies using a pure culture of *Rodhobacter sphaeroides* AV1 but were comparable to those obtained using mixed cultures and synthetic wastewater [4]. Lower PHB concentrations were detected in L tests. In particular, the lowest value was obtained in set L_{-EN}, characterized by the minimum nitrogen content. Such a result indicated that the bioconversion was mainly driven to the hydrogen production pathway whenever the C/N ratio was sufficiently high. In this situation, a similar PHB accumulation was detected when changing the nitrogen source. In contrast, when the C/N ratio was low, the use of an ON source considerably enhanced PHB accumulation, in agreement with previous findings [48].

Generally, PHB accumulation occurred together with acetic acid consumption, confirming that the presence of acetic acid stimulated PHB accumulation [7,45,48]. As

reported by other authors [49], the different metabolic routes of substrate assimilation strongly affect PHB formation. The metabolic route of acetate provides accessible ways to generate acetyl-coenzyme A, which is the main precursor for PHB synthesis in the majority of PNSB.

The maximum PHB accumulation and the maximum hydrogen yield occurred in the same experimental set (H_{-ON}), despite the negative correlation reported in the scientific literature [7,48,50]. Indeed, both H_2 production and PHB accumulation require a reduction in power. As a consequence, H_2 production and PHB synthesis are competitive metabolic pathways. Usually, PHB synthesis occurs when microorganisms are forced to live under starvation. Consequently, when a large amount of the organic substrate is available, the metabolic pathway principally leads to hydrogen production. When the depletion of organic substrate occurs, PNSB store PHB as a carbon reserve. Nonetheless, the result was in agreement with recent findings [4,8,33] that PHB accumulation can be induced along with H_2 production when complex substrates are utilized. PHB provides different functions for PNSB; one of them is to protect bacteria from stress. A stress condition can be represented not only by carbon source scarcity but also by other nonoptimal environmental conditions (e.g., temperature or pH fluctuation, osmotic shock). In this study, after glucose depletion, the biomass spontaneously adapted to other carbon sources. Under this condition, the PHB synthesis prioritized the reduced power, despite substrate availability. Subsequently, the PHB synthesis prevented bacteria from experiencing the stress condition and retained H_2 production. Wu et al. [49] also reported that, under nonoptimal pH conditions, the PHB synthesis was beneficial to H_2 productivity, preventing the species *Rhodopseudomonas Palustris* WP3-5 from the stress of inappropriate pH and retaining H_2 productivity at an optimal pH value. It is worth noting that nitrate resulted in the most effective nitrogen source for PHB accumulation. In fact, considering the maximum PHB accumulation of cells rather than the maximum PHB concentration in the reactors, the highest value was obtained in the presence of nitrate. Indeed, the TSS concentration was about three times lower in the NN set compared to the ON and AN sets. However, further experiments are required to better clarify the relationship between nitric nitrogen and the metabolic pathways leading to PHB accumulation, focusing on the evaluation of the PHB percentage of the dry cell weight. Due to the large amounts of WWW produced worldwide and the possibility of coupling high-purity hydrogen production with PHB accumulation, it is important to conduct both laboratory-scale and pilot-scale experiments for product valorization. Moreover, the description and use of mathematical models that are able to

account for all metabolic activities occurring in photobioreactors needs to be further investigated, as this can help in designing and managing operations for real-scale applications [51,52]. The optimization of the PF process applied to WWW can lead to a more productive biorefinery system rather than the regular dark fermentation application [17,18].

6.5. Conclusions

This experimental study demonstrated that winery wastewater can be profitably used for hydrogen and PHB production through the single-stage PF. The utilization of mixed PNSB cultures is beneficial in terms of substrate utilization and hydrogen production yields, even in the presence of inhibiting ammonia and polyphenols concentration in the waste. On the other hand, to reach high COD removal efficiency and correctly manage the waste, it is necessary to use the proper initial dilution. Moreover, the formic acid concentration must be limited, as it has been shown to be resistant to biotransformation. To address this issue, the utilization of inorganic nitrogen compounds is suggested. Finally, glutamate has been revealed to enhance both PHB accumulation and hydrogen production, which means that hydrogen and PHB production are intricately related and do not simply compete for electrons and energy distribution.

List of Abbreviations

AN: ammonia nitrogen

COD: chemical oxygen demand

EN: endogenous nitrogen

H: high dilution

L: low dilution

$N\text{-}NH_4^+$: ammonia nitrogen

NN: nitric nitrogen

NO_3^-: nitrates

OAs: organic acids

ON: organic nitrogen

PF: photofermentation

PHB: poly-β-hydroxybutyrate

PNSB: purple non-sulfur bacteria

PO_4^{3-}: phosphates

SO_4^{2-} : sulfates

TKN: total Kjeldahl nitrogen

TN: total nitrogen

TSS: total suspended solids

VFAs: volatile fatty acids

WWW: winery wastewater

References

[1] Crocamo A, Di Bernardino S, Di Giovanni R, Fabbricino M, Martins-Dias S. An integrated approach to energy production and nutrient recovery through anaerobic digestion of Vetiveria zizanoides. Biomass and Bioenergy 2015;81:288–93. https://doi.org/10.1016/J.BIOMBIOE.2015.07.023.

[2] Sharma S, Basu S, Shetti NP, Aminabhavi TM. Waste-to-energy nexus for circular economy and environmental protection: Recent trends in hydrogen energy. Sci Total Environ 2020;713:136633. https://doi.org/10.1016/J.SCITOTENV.2020.136633.

[3] Ferraro A, Dottorini G, Massini G, Mazzurco Miritana V, Signorini A, Lembo G, et al. Combined bioaugmentation with anaerobic ruminal fungi and fermentative bacteria to enhance biogas production from wheat straw and mushroom spent straw. Bioresour Technol 2018;260:364–73. https://doi.org/10.1016/J.BIORTECH.2018.03.128.

[4] Luongo V, Ghimire A, Frunzo L, Fabbricino M, d'Antonio G, Pirozzi F, et al. Photofermentative production of hydrogen and poly-β-hydroxybutyrate from dark fermentation products. Bioresour Technol 2017;228:171–5. https://doi.org/10.1016/J.BIORTECH.2016.12.079.

[5] Sağır E. Photofermentative Hydrogen Production. Biohydrogen 2019:141–57. https://doi.org/10.1016/B978-0-444-64203-5.00006-X.

[6] Gouda MK, Swellam AE, Omar SH. Production of PHB by a Bacillus megaterium strain using sugarcane molasses and corn steep liquor as sole carbon and nitrogen sources. Microbiol Res 2001;156:201–7. https://doi.org/10.1078/0944-5013-00104.

[7] Kim M-S, Kim D-H, Cha J, Lee JK. Effect of carbon and nitrogen sources on photo-fermentative H2 production associated with nitrogenase, uptake hydrogenase activity, and PHB accumulation in Rhodobacter sphaeroides KD131. Bioresour Technol 2012;116:179–83. https://doi.org/10.1016/J.BIORTECH.2012.04.011.

[8] Ghimire A, Valentino S, Frunzo L, Pirozzi F, Lens PNL, Esposito G. Concomitant biohydrogen and poly-β-hydroxybutyrate production from dark fermentation effluents by adapted Rhodobacter sphaeroides and mixed photofermentative cultures. Bioresour Technol 2016;217:157–64. https://doi.org/10.1016/j.biortech.2016.03.017.

[9] Dinesh GH, Nguyen DD, Ravindran B, Chang SW, Vo DVN, Bach QV, et al.

Simultaneous biohydrogen (H2) and bioplastic (poly-β-hydroxybutyrate-PHB) productions under dark, photo, and subsequent dark and photo fermentation utilizing various wastes. Int J Hydrogen Energy 2020;45:5840–53. https://doi.org/10.1016/j.ijhydene.2019.09.036.

[10] Hakobyan L, Gabrielyan L, Trchounian A. Biohydrogen by Rhodobacter sphaeroides during photo-fermentation: Mixed vs. sole carbon sources enhance bacterial growth and H2 production. Int J Hydrogen Energy 2019;44:674–9. https://doi.org/10.1016/J.IJHYDENE.2018.11.082.

[11] Jiang D, Ge X, Lin L, Zhang T, Liu H, Hu J, et al. Continuous photo-fermentative hydrogen production in a tubular photobioreactor using corn stalk pith hydrolysate with a consortium. Int J Hydrogen Energy 2019. https://doi.org/10.1016/J.IJHYDENE.2019.06.078.

[12] Aurand J-M. Estado del mercado global en la vitivinicultura 2018.

[13] Ioannou LA, Puma GL, Fatta-Kassinos D. Treatment of winery wastewater by physicochemical, biological and advanced processes: A review. J Hazard Mater 2015;286:343–68. https://doi.org/10.1016/J.JHAZMAT.2014.12.043.

[14] Chatzilazarou A, Katsoyannos E, Gortzi O, Lalas S, Paraskevopoulos Y, Dourtoglou E, et al. Removal of polyphenols from wine sludge using cloud point extraction. J Air Waste Manag Assoc 2010;60:454–9. https://doi.org/10.3155/1047-3289.60.4.454.

[15] Adessi A, De Philippis R. Hydrogen Production: Photofermentation. In: Hallenbeck PC, editor. Microb. Technol. Adv. Biofuels Prod., Boston, MA: Springer US; 2012, p. 53–75. https://doi.org/10.1007/978-1-4614-1208-3_4.

[16] Tawfik A, El-Bery H, Kumari S, Bux F. Use of mixed culture bacteria for photofermentive hydrogen of dark fermentation effluent. Bioresour Technol 2014;168:119–26. https://doi.org/10.1016/j.biortech.2014.03.065.

[17] Buitrón G, Muñoz-Páez KM, Quijano G, Carrillo-Reyes J, Albarrán-Contreras BA. Biohydrogen production from winery effluents: control of the homoacetogenesis through the headspace gas recirculation. J Chem Technol Biotechnol 2019. https://doi.org/10.1002/jctb.6263.

[18] Carrillo-Reyes J, Albarrán-Contreras BA, Buitrón G. Influence of Added Nutrients and Substrate Concentration in Biohydrogen Production from Winery Wastewaters Coupled to Methane Production. Appl Biochem Biotechnol 2019;187:140–51. https://doi.org/10.1007/s12010-018-2812-5.

[19] Ghosh S, Dairkee UK, Chowdhury R, Bhattacharya P. Hydrogen from food

processing wastes via photofermentation using Purple Non-sulfur Bacteria (PNSB) – A review. Energy Convers Manag 2017;141:299–314. https://doi.org/10.1016/J.ENCONMAN.2016.09.001.

[20] Ghimire A, Valentino S, Frunzo L, Pirozzi F, Lens PNL, Esposito G. Concomitant biohydrogen and poly-β-hydroxybutyrate production from dark fermentation effluents by adapted Rhodobacter sphaeroides and mixed photofermentative cultures. Bioresour Technol 2016;217:157–64. https://doi.org/10.1016/J.BIORTECH.2016.03.017.

[21] Eroğlu E, Eroğlu İ, Gündüz U, Yücel M. Effect of clay pretreatment on photofermentative hydrogen production from olive mill wastewater. Bioresour Technol 2008;99:6799–808. https://doi.org/10.1016/J.BIORTECH.2008.01.076.

[22] Padovani G, Pintucci C, Carlozzi P. Dephenolization of stored olive-mill wastewater, using four different adsorbing matrices to attain a low-cost feedstock for hydrogen photo-production. Bioresour Technol 2013;138:172–9. https://doi.org/10.1016/J.BIORTECH.2013.03.155.

[23] Seifert K, Waligorska M, Laniecki M. Brewery wastewaters in photobiological hydrogen generation in presence of Rhodobacter sphaeroides O.U. 001. Int J Hydrogen Energy 2010;35:4085–91. https://doi.org/10.1016/J.IJHYDENE.2010.01.126.

[24] Eroğlu E, Gündüz U, Yücel M, Türker L, Eroğlu İ. Photobiological hydrogen production by using olive mill wastewater as a sole substrate source. Int J Hydrogen Energy 2004;29:163–71. https://doi.org/10.1016/S0360-3199(03)00110-1.

[25] Pontoni L, Panico A, Matanò A, Van Hullebusch ED, Fabbricino M, Esposito G, et al. Modified Sample Preparation Approach for the Determination of the Phenolic and Humic-Like Substances in Natural Organic Materials by the Folin Ciocalteu Method. J Agric Food Chem 2017;65:10666–72. https://doi.org/10.1021/acs.jafc.7b04942.

[26] Maharaj BC, Mattei MR, Frunzo L, van Hullebusch ED, Esposito G. ADM1 based mathematical model of trace element precipitation/dissolution in anaerobic digestion processes. Bioresour Technol 2018;267:666–76. https://doi.org/10.1016/j.biortech.2018.06.099.

[27] Maharaj BC, Mattei MR, Frunzo L, Hullebusch ED va., Esposito G. ADM1 based mathematical model of trace element complexation in anaerobic digestion processes. Bioresour Technol 2019;276:253–9.

https://doi.org/10.1016/j.biortech.2018.12.064.

[28] Brückner R, Titgemeyer F. Carbon catabolite repression in bacteria: Choice of the carbon source and autoregulatory limitation of sugar utilization. FEMS Microbiol Lett 2002;209:141–8. https://doi.org/10.1016/S0378-1097(02)00559-1.

[29] Deutscher J. The mechanisms of carbon catabolite repression in bacteria. Curr Opin Microbiol 2008;11:87–93. https://doi.org/10.1016/J.MIB.2008.02.007.

[30] Görke B, Stülke J. Carbon catabolite repression in bacteria: Many ways to make the most out of nutrients. Nat Rev Microbiol 2008;6:613–24. https://doi.org/10.1038/nrmicro1932.

[31] Johnson K, Jiang Y, Kleerebezem R, Muyzer G, Van Loosdrecht MCM. Enrichment of a mixed bacterial culture with a high polyhydroxyalkanoate storage capacity. Biomacromolecules 2009;10:670–6. https://doi.org/10.1021/bm8013796.

[32] Ghimire A, Luongo V, Frunzo L, Pirozzi F, Lens PNL, Esposito G. Continuous biohydrogen production by thermophilic dark fermentation of cheese whey: Use of buffalo manure as buffering agent. Int J Hydrogen Energy 2017;42:4861–9. https://doi.org/10.1016/j.ijhydene.2016.11.185.

[33] Montiel-Corona V, Revah S, Morales M. Hydrogen production by an enriched photoheterotrophic culture using dark fermentation effluent as substrate: Effect of flushing method, bicarbonate addition, and outdoor-indoor conditions. Int J Hydrogen Energy 2015. https://doi.org/10.1016/j.ijhydene.2015.05.067.

[34] Androga DD, Özgür E, Eroglu I, Gündüz U, Yücel M. Significance of carbon to nitrogen ratio on the long-term stability of continuous photofermentative hydrogen production. Int J Hydrogen Energy 2011;36:15583–94. https://doi.org/10.1016/J.IJHYDENE.2011.09.043.

[35] Oh Y-K, Seol E-H, Kim M-S, Park S. Photoproduction of hydrogen from acetate by a chemoheterotrophic bacterium Rhodopseudomonas palustris P4. Int J Hydrogen Energy 2004;29:1115–21. https://doi.org/10.1016/J.IJHYDENE.2003.11.008.

[36] Reungsang A, Zhong N, Yang Y, Sittijunda S, Xia A, Liao Q. Hydrogen from Photo Fermentation. In: Liao Q, Chang J, Herrmann C, Xia A, editors. Bioreact. Microb. Biomass Energy Convers., Singapore: Springer Singapore; 2018, p. 221–317. https://doi.org/10.1007/978-981-10-7677-0_7.

[37] Akköse S, Gündüz U, Yücel M, Eroglu I. Effects of ammonium ion, acetate and aerobic conditions on hydrogen production and expression levels of nitrogenase

genes in Rhodobacter sphaeroides O.U.001. Int J Hydrogen Energy 2009;34:8818–27. https://doi.org/10.1016/J.IJHYDENE.2009.08.040.

[38] Drepper T, Groß S, Yakunin AF, Hallenbeck PC, Masepohl B, Klipp W. Role of GlnB and GlnK in ammonium control of both nitrogenase systems in the phototrophic bacterium Rhodobacter capsulatus. Microbiology 2003;149:2203–12. https://doi.org/10.1099/mic.0.26235-0.

[39] Yakunin AF, Hallenbeck PC. Purification and characterization of pyruvate oxidoreductase from the photosynthetic bacterium Rhodobacter capsulatus. Biochim Biophys Acta - Bioenerg 1998;1409:39–49. https://doi.org/10.1016/S0005-2728(98)00145-5.

[40] Özgür E, Mars AE, Peksel B, Louwerse A, Yücel M, Gündüz U, et al. Biohydrogen production from beet molasses by sequential dark and photofermentation. Int J Hydrogen Energy 2010;35:511–7. https://doi.org/10.1016/J.IJHYDENE.2009.10.094.

[41] Costa S, Ganzerli S, Rugiero I, Pellizzari S, Pedrini P, Tamburini E. Potential of Rhodobacter capsulatus grown in anaerobic-light or aerobic-dark conditions as bioremediation agent for biological wastewater treatments. Water (Switzerland) 2017;9. https://doi.org/10.3390/w9020108.

[42] Cross R, Lloyd D, Poole RK, Moir JWB. Enzymatic removal of nitric oxide catalyzed by cytochrome c′ in Rhodobacter capsulatus. J Bacteriol 2001;183:3050–4. https://doi.org/10.1128/JB.183.10.3050-3054.2001.

[43] McKinlay JB, Harwood CS. Photobiological production of hydrogen gas as a biofuel. Curr Opin Biotechnol 2010;21:244–51. https://doi.org/10.1016/J.COPBIO.2010.02.012.

[44] Rupprecht J, Hankamer B, Mussgnug JH, Ananyev G, Dismukes C, Kruse O. Perspectives and advances of biological H2 production in microorganisms. Appl Microbiol Biotechnol 2006;72:442–9. https://doi.org/10.1007/s00253-006-0528-x.

[45] Pattanamanee W, Choorit W, Deesan C, Sirisansaneeyakul S, Chisti Y. Photofermentive production of biohydrogen from oil palm waste hydrolysate. Int J Hydrogen Energy 2012;37:4077–87. https://doi.org/10.1016/J.IJHYDENE.2011.12.002.

[46] Yetis M, Gündüz U, Eroglu I, Yücel M, Türker L. Photoproduction of hydrogen from sugar refinery wastewater by Rhodobacter sphaeroides O.U. 001. Int J Hydrogen Energy 2000;25:1035–41. https://doi.org/10.1016/S0360-

3199(00)00027-6.

[47] Kars G, Alparslan Ü. Valorization of sugar beet molasses for the production of biohydrogen and 5-aminolevulinic acid by Rhodobacter sphaeroides O.U.001 in a biorefinery concept. Int J Hydrogen Energy 2013;38:14488–94. https://doi.org/10.1016/J.IJHYDENE.2013.09.050.

[48] Khatipov E, Miyake M, Miyake J, Asada Y. Accumulation of poly-β-hydroxybutyrate by Rhodobacter sphaeroides on various carbon and nitrogen substrates. FEMS Microbiol Lett 1998;162:39–45. https://doi.org/10.1016/S0378-1097(98)00099-8.

[49] Wu SC, Liou SZ, Lee CM. Correlation between bio-hydrogen production and polyhydroxybutyrate (PHB) synthesis by Rhodopseudomonas palustris WP3-5. Bioresour Technol 2012;113:44–50. https://doi.org/10.1016/J.BIORTECH.2012.01.090.

[50] Hustede E, Steinbüchel A, Schlegel HG. Relationship between the photoproduction of hydrogen and the accumulation of PHB in non-sulphur purple bacteria. Appl Microbiol Biotechnol 1993;39:87–93. https://doi.org/10.1007/BF00166854.

[51] D'Acunto B, Frunzo L, Luongo V, Mattei MR. Invasion moving boundary problem for a biofilm reactor model. Eur J Appl Math 2018;29:1079–109. https://doi.org/10.1017/S0956792518000165.

[52] Frunzo L, Garra R, Giusti A, Luongo V. Modeling biological systems with an improved fractional Gompertz law. Commun Nonlinear Sci Numer Simul 2019;74:260–7. https://doi.org/10.1016/j.cnsns.2019.03.024.

Chapter 7

Mixed culture enhance hydrogen production in single stage photo fermentation processes.

Mixed culture enhance hydrogen production in single stage photo fermentation processes

Abstract

In the present chapter, (open) mixed cultures photo fermentation systems and pure cultures dark fermentation-co-photo fermentation process have been compared in terms of hydrogen production performances. In particular, different dark and photo fermentative bacteria have been isolated from an initial mixed consortium. The isolated bacteria have been tested in pure cultures systems to select the two most performant dark fermentative and photo fermentative pure species. Successively, the most performant species have been used for a dark fermentation-co-photo fermentation test. A comparison between the co-culture and the initial (open) mixed consortium has been performed. Results showed that the initial mixed consortium led to higher hydrogen yields compared to the co-fermentation test. In particular, the cumulative volumetric yields of 290 (±18) N mL H_2 L^{-1} and 65 (±3) N mL H_2 L^{-1} were obtained, respectively. Moreover, a comparison with the literature confirmed the importance of the use of mixed cultures to enhance the hydrogen production from waste substrates.

7.1. Introduction

The adverse impacts of fossil fuels, along with the scarce availability, represent one of the major concerns at global level [1]. Hydrogen is considered the best energy source to replace fossil fuels. Therefore, it is expected to highly expand in the next future [2].

However, unavailability of hydrogen gas in nature is one of the major obstacles for its wide utilization. Currently, hydrogen is produced using energy intensive processes, such as the steam reforming [3]. Therefore, researchers are focusing their attention on the low-cost hydrogen gas production by bioprocessing of inexpensive waste materials [4]. In addition, bioprocesses have the further advantage of being natural and occur under environmental temperature and pressure conditions. The most studied bioprocess is the Dark Fermentation (DF). Dark fermentative bacteria can convert complex organic compounds to a hydrogen-rich biogas. However, a variety of by-products (i.e. organic acids (OAs) and alcohols) are produced together with hydrogen, leading to an incomplete transformation of the substrate and low hydrogen yields [5].

To valorise dark fermentation effluents, many studies have been conducted on the sequential DF and Photo Fermentation (PF) process [6,7]. Indeed, photo fermentative bacteria (i.e. Purple Non Sulphur Bacteria (PNSB)) are able to convert the by-products

contained in the DF effluents (DFEs), synthetizing additional bio-hydrogen and bioplastics precursors (i.e. polyhydroxybutyrate (PHB)) [8,9,10].

In turn, pure cultures PF bacteria require the previous DF step or other pre-treatments, as PNSB are not able to degrade many complex molecules, usually present in waste substrates [11].

To date, few previous studies on Dark Fermentation-co-Photo Fermentation (DF-co-PF) processes have been conducted, where DF and PF take place simultaneously in the same reactor [1]. This configuration has been reported to be a better alternative compared to both the sequential DF-PF system and the single stage pure cultures PF [12]. However, such studies have been performed using a mix of two pure cultures of dark and photo fermentative bacteria, mainly degrading synthetic substrates (e.g. starch or glucose) [13,14].

We hypothesised that, in waste substrates-based processes, even better results can be achieved using (open) mixed cultures, due to a "contamination" of other fermentative bacteria in the reactor.

Few recent studies on the single stage PF have showed that, using (open) mixed cultures rather than pure PNSB, the degradation of complex waste substrates is possible and the hydrogen production is enhanced [15]. On the other hand, no studies have been reported on the comparison between such (open) mixed cultures systems and the pure cultures DF-co-PF process. Moreover, little is known about the interactions between populations in (open) mixed consortia and their interdependency.

The aim of this work was to study hydrogen production from winery wastewater via a single stage PF process, conducted using (open) mixed cultures containing both dark and photo fermentative bacteria. Moreover, a comparison with a pure cultures DF-co-PF experiment was performed. In particular, to look into the interactions between populations, different dark and photo fermentative bacteria have been isolated from the (open) mixed consortium. The isolated bacteria have been tested in pure cultures PF systems, to select the most performant ones. The two most performant dark fermentative and photo fermentative bacteria have been used for a DF-co-PF test and compared to the performances of the initial (open) mixed consortium. Moreover, the possibility of producing PHB along with hydrogen was investigated.

7.2. Materials and methods

7.2.1. Substrate and Initial Inoculum

For all tests, the substrate was the real winery wastewater (WWW), obtained from a red wine factory. WWW was characterized by: COD, 265 g L^{-1}; glucose, 20 g L^{-1}; ethanol, 70 g L^{-1}; lactic acid, 2 g L^{-1}; acetic acid, 0.5 g L^{-1}; total phenols, 1.243 g L^{-1}.

For all fermentation tests, the substrate was diluted to reach a COD value of 1g_{COD} L^{-1}. The dilution was performed using a nutrient-rich medium, prepared as follows: $NaC_5NO_4H_8$, 400 mg/L; $MgSO_4.7H_2O$, 200 mg/L; yeast extract, 300 mg/L; $C_6H_5FeO_7$, 24.5 mg/L; NaCl, 400 mg/L; K_2HPO_4, 600 mg/L; KH_2PO_4, 3000 mg/L; $NaHCO_3$, 700 mg/L; $CaCl_2.2H_2O$, 75 mg/L. Micronutrients were provided by adding 10 mL L^{-1} of a trace element solution to the nutrient-rich medium [16].

The initial inoculum was a mixed culture, obtained from the digestate of a full-scale plant treating buffalo manure for methane production. The culture was enriched several times under continuous illumination and using the previously mentioned culture medium. For the enrichment phases, ethanol was used as carbon source. Before use, the inoculum was characterized in terms of microbial community composition. The composition of the microbial community was: Bacteroidales, 30%; Rhizobiaceae, 25.7%; Sphingobacteriales, 19.73%; Methylophilaceae, 9,72%; Clostridiales, 5,11%; Pseudomonadaceae, 2.6%; Sphingobacteriaceae, 1,75%; Xanthomonadaceae, 1.12% Alcaligenaceae, 0,99%; Enterobacteriaceae, 0,65%; Rhodospirillales, 0,21%; Others, 3,05%.

7.2.3. Experimental set-up

Experimental activities consisted of two different steps. The first step was the isolation of bacteria from the initial inoculum and the preliminary screening. In detail, 23 different species were isolated. Among the isolated species, those belonging to genera which are able to produce hydrogen were chosen for the screening hydrogen production tests. 7 dark fermentative and 2 photo fermentative microorganisms were tested. From results of screening tests, the most performant DF specie (*Klebsiella pneumoniae strain* MF101) and the most performant PF one (*Rhodopseudomonas sp.* Strain BR0Y6) were selected for the second final step of experiments. The second step consisted of two tests: the first test was a DF-co-PF conducted using as inoculum a co-culture (1:1) of *Klebsiella*

pneumoniae strain MF101 and *Rhodopseudomonas sp.* Strain BR0Y6. The second test was performed using the initial (open) mixed culture. For simplicity, the first and the second experiments of the second step will be indicated as KR and M tests, respectively. The experimental set-up is summarized in Figure7.1:

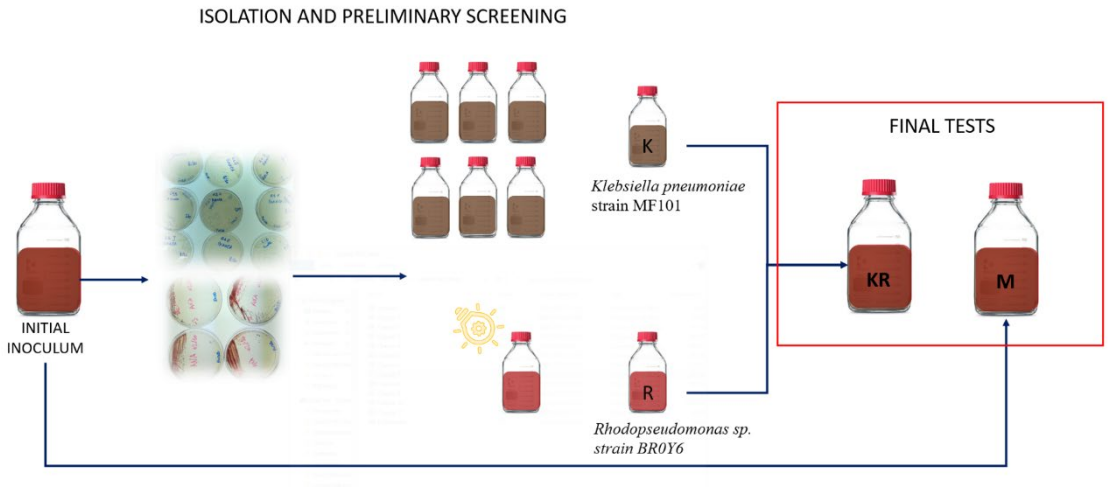

Figure 7.1. Experimental set-up

Photo bioreactors were built using transparent borosilicate glass bottles with a total volume of 500 mL and a working volume of 400 mL. Reactors were sealed hermetically with plastic caps, equipped with two tubes for gas and liquid sampling operations. Anaerobic conditions were ensured by initial flushing with argon gas. Each reactor was placed on a magnetic stirrer (250 rpm rotation speed). Temperature was kept to 25±2°C and the initial pH value was fixed to 7. The light energy was continuously provided by LED strips (4000 lux light intensity). Experiments were stopped when hydrogen was no longer produced.

7.2.4. Analytical methods and equipment

Gas production was quantified via water displacement. The biogas was sampled and analyzed via gas chromatography to determine hydrogen and carbon dioxide content. Gas chromatography was performed using a Varian Star 3400 gas chromatograph equipped with Shin Carbon ST 80/100 column. Argon was utilized as carrier gas. Organic acids (OAs), glucose, glycerol and ethanol concentrations were measured by high pressure liquid chromatography, using a Dionex (Sunnyvale, USA) LC 25 Chromatography Oven equipped with a Metrohom (Herisau, Switzerland) Organic Acids column (Metrosep Organic Acids - 250/7.8) and a Dionex (Sunnyvale, USA) GD 500 Gradient Pump. The

eluent,a 5 mM H_2SO_4 solution, was pumped at a rate of 0.7 mL/min. A Dionex (Sunnyvale, USA) UVD 340U detector was used for OAs determination and a Jasco (Cremella, Italy) RI-2031 for glucose, ethanol and glycerol detection. PHB was extracted in chloroform and successively analyzed by gas chromatography and mass spectrometry. Gas chromatography and mass spectrometry were conducted using a GC-MS with a ZB Semi Volatiles Zebron column (Phenomenex, Torrance, USA). Helium was used as carrier gas. Light intensity was measured using a Lutron-LX-107 light meter (Coopersburg, USA). Total phenolic content was measured according to the Folin and Ciocalteu Method [17]. COD concentration was determined according to the Standard Methods [18].

The chemicals used for all analytical determinations were high purity degree. Bi-distilled water was adopted as reagent water. Before use, glassware was soaked overnight in a concentrated nitric acid bath (2% v/v) and rinsed carefully.

Isolation of culturable microorganisms and microbiological analyses were performed using the Sanger protocol and the Next Generation Sequencing. The protocol for microbiological analysis and Sanger sequencing for the sample under analysis consisted in a total bacterial count (TBC), performed with the standard pour plating protocol (UNI EN ISO 6222:2001 International Standards Association, 2001); sample was additionally spread plated following serial dilutions of the specimen on PNSB medium at pH 7, supplemented with 15% agar for single colonies' isolation, for 120 h. This method allowed identifying, based on morphology, the highest number of colonies for molecular identification.

DNA extraction (by denaturing at 98 °C for 10 min and recovering supernatant following centrifugation) and amplification were performed selecting at least 5 isolated colonies of each different morphology (Chakravorty et al., 2007), using a TECHNE Prime Thermal Cycler with universal primers complementary to the V3 and V6 conserved regions of 16 S rRNA gene (700 bp amplicon size): V3f (5'-CCAGACTCCTACGGGAGGCAG-3') and V6r (5'-TCGATGCAACGCGAAGAA-3'). PCR reactions and the resulting sequences were carried out as described by Carraturo et al. [19].

Total DNA extraction for Next Generation Sequencing (NGS) analysis was performed according to Policastro et al., 2021, aiming at analysing bacterial 16S rRNA gene. An aliquot of 100 mL specimen was concentrated and subjected to CTAB extraction protocol [20].

V3 and V4 primers (V3:TCGTCGGCAGCGTCAGATGTGTATAAGAGACAGCCTACGGGNGGCWCGAG; V4: GTCTCGTGGGCTCGGAGATGTGTATAAGAGACAGGACTACHVGGGTATCTAATCC),

complementary to V3-V4 variable region of the bacterial 16S rRNA gene (500 bp) were used for the amplification. Sequences were analysed by a MiSeq Illumina platform, 2 × 300 bp paired end, 600 cycles, following the manufacturer's instructions (Illumina MiSeq, USA). Differences in the group's communities retrieved from Illumina experiment were assessed by anosim using weighted UniFrac distance, and Anova using Bray Curtis distance (Mothur) [21,22].

7.3. Results and discussion

7.3.1. Screening tests

Table 7.1 reports the results in terms of cumulative hydrogen production and maximum PHB accumulation, achieved in the preliminary screening phase.

Table 7.1. Results of the screening tests

Microorganism	Type	Hydrogen production [mL L^{-1}]	Maximum PHB concentration [mg L^{-1}]
Pseudomonas aeruginosa strain QK-6	DF	111,24	383,8
Pseudomonas aeruginosa strain Sihong 639 1	DF	27,04	455,1
Klebsiella pneumoniae strain MF101	DF	197,38	200
Pseudomonas nitroreducens strain XG-12B	DF	7,18	66,2
Uncultured Stenopseudomonas sp. Clone TOP07	DF	0,10	86,97
Rhodopseudomonas sp. Strain BR0Y6	PF	113,52	94,4
Citrobacter farmeri strain *AUSMDU00008141*	DF	32,79	40,5
Citrobacter sp. 39C.4	DF	67,67	89,1
Rhodomicrobium vannielii strain: TUT3402	PF	11,91	380,99

Among dark fermentative bacteria, *Klebsiella pneumoniae* strain MF101 was the most performant specie both in terms of hydrogen production and PHB accumulation. From previous studies, the presence of *K. pneumoniae* has been reported to efficiently produce hydrogen [23,24]. Moreover, the good performance in terms of PHB accumulation is in accordance with previous studies, as well [25].

Pseudomonas species also were found to produce high PHB concentrations, according to previous studies [26,27]. However, in terms of hydrogen production, *Pseudomonas aeruginosa* strain QK-6 led to the better results.

All the other dark fermentative species did not produce high amounts of both hydrogen and PHB. Probably, the adopted substrate was not suitable and/or exerted inhibition phenomena due to its complexity and the presence of inhibitory compounds (e.g. phenols) [7].

Concerning photo fermentative microorganisms, *Rhodopseudomonas sp. Strain BR0Y6* produced the highest hydrogen yield. This result was in agreement with previous studies. Indeed, due to their high hydrogen production potential, *Rhodopseudomonas* species are one of the most used microorganisms in photo fermentation processes [2,28]. Moreover, Mabutyana and Pott, (2021) reported that *R. palustris* CGA009 was resistant towards high phenolic concentrations and produced hydrogen in the presence of waste substrates (i.e. lignocellulosic hydrolysate).

Rhodomicrobium vannielii produced very low amounts of hydrogen. Few previous studies reported the hydrogen production capacity of this bacterium, under specific conditions and synthetic substrates [30]. However, its PHB accumulation capability has never been investigated, to date. Due to the high PHB concentration achieved in this study, it would be worth conducting further studies on this specific aspect.

Based on results obtained in this experimental phase, *Klebsiella pneumoniae* strain MF101 and *Rhodopseudomonas sp. Strain BR0Y6* were chosen for DF-co-PF hydrogen production tests.

7.3.2. Final tests

Results obtained from KR and M final tests are reported in Figure 7.2.

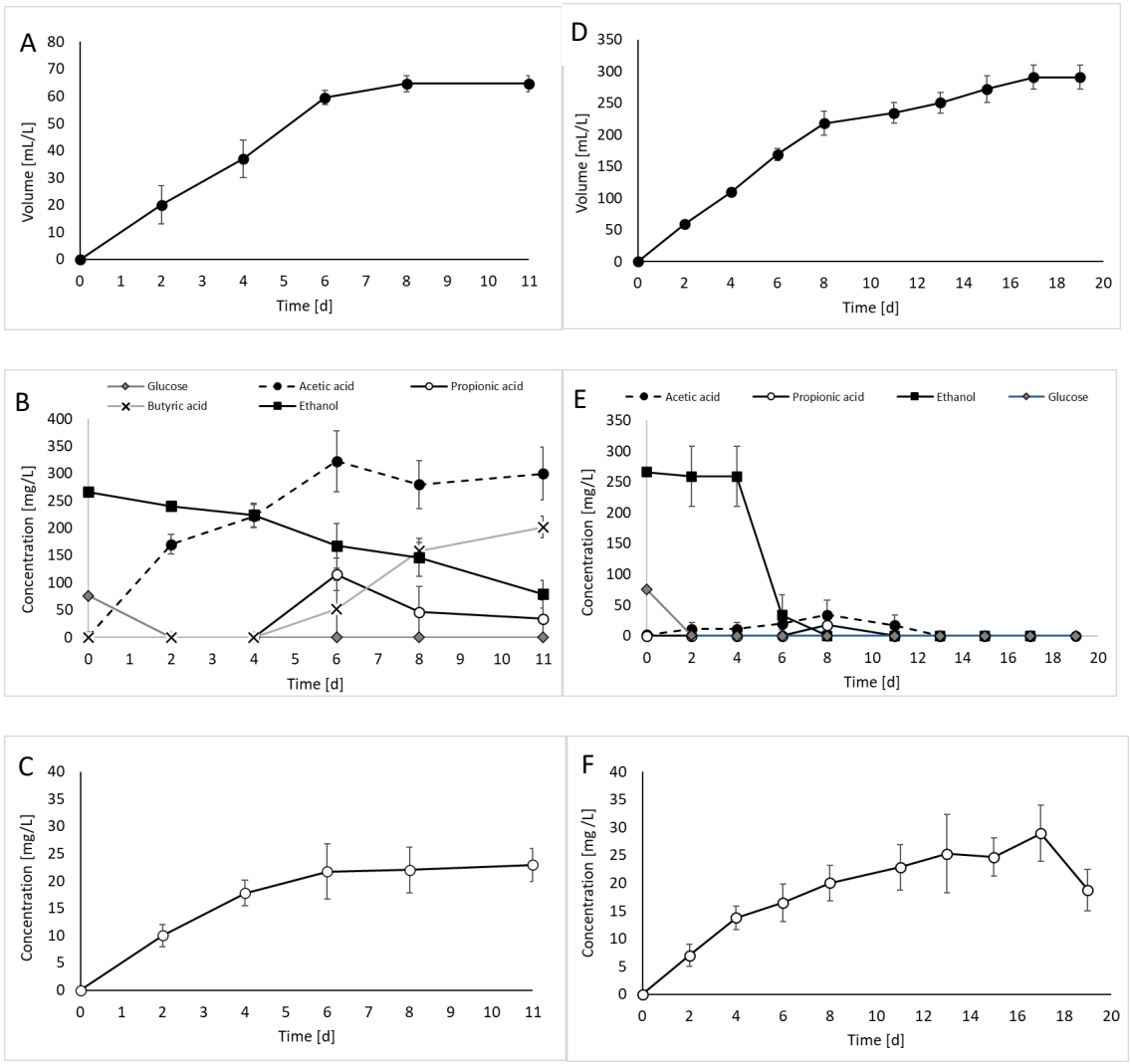

Figure 7.2 Cumulative H_2 production (A, D), organic acids, ethanol and glucose concentration (B, E), PHB concentration (C, F) in KR (A, B, C) and M (D, E, F) reactors.

As previously reported [31], glucose was consumed faster than ethanol during the initial days of fermentation. Ethanol decreased faster in M than in KR reactors and it was completely consumed in M tests. On the other hand, the residual concentration of 80 mgL^{-1} was observed in KR, after the end of the hydrogen production phase.

Low OAs concentrations were detected in M reactors. Moreover, OAs were completely consumed at the end of the process. Probably, OAs released by the DF microorganisms have been quickly metabolized by photosynthetic bacteria, resulting in low accumulation into the reactors [32]. The theoretical COD removal, calculated from organic compounds concentrations detected in the final effluent, showed a COD removal efficiency > 99%. However, as previously reported [33], the theoretical value does not take into account the production of biomass and other bacterial carotenoids, which were evidently present in the system, due to the reddish colour of the effluent.

Concerning KR reactors, acetic acid, butyric acid and propionic acid were the main by-products of the process. Due to the OAs accumulation and the incomplete ethanol conversion, a COD removal of about 10% was observed. The percentages of KR by-products, in terms of COD ($COD_{single\ product}$ /$COD_{total\ products}$) were: hydrogen, 5%; PHB, 4%; acetic acid, 44%; butyric acid, 41%; propionic acid, 45%. This distribution of the final COD between hydrogen and OAs was typical of DF processes [22]. In hybrid DF-co-PF systems, PF bacteria are supposed to convert the OAs produced by DF bacteria into additional hydrogen and PHB [12]. In this study, the high OAs accumulation suggest that, in the DF-PF co-fermentatative system, *Rhodopseudomonas sp. Strain BR0Y6* were inhibited.

Hydrogen was produced for 18 days in M reactors, while only a 9 days production period occurred for KR tests. At the end of the hydrogen production process, the cumulative volumetric yields of 65 (±3) N mL H_2 L^{-1} and 290 (±18) N mL H_2 L^{-1} were obtained for KR and M reactors, respectively. The concomitant PHB accumulation was observed in both experiments (Figure 7.2, B and E), with similar values of the maximum concentrations.

Hydrogen and PHB productions of KR reactors were lower compared to those obtained using *Klebsiella pneumoniae* strain MF101 alone (screening tests). Probably, the coexistence of the two species triggered competitive mechanisms stimulating OAs production rather than hydrogen and PHB production.

By contrast, the initial (open) mixed culture M led to higher H_2 yields compared to all the other tests performed in this study (final tests and screening tests). On the other hand, the low PHB accumulation obtained from M tests compared to both the two pure cultures alone, remarks the importance of pure cultures in PHB production [7]. This result may be due to the synergies established among different H_2 producing species, which might have enhanced the conversion of the organic substrates to H_2. For instance, in mixed cultures environments, it often happens that non-hydrogen producing bacteria indirectly enhance the productivity of hydrogen producing bacteria, for instance, favouring their aggregation [23].

Moreover, the result was due to the adaptation of the mixed culture to the adopted conditions, which established a syntrophic association between fermentative bacteria and purple phototrophic bacteria. Syntrophy in (open) mixed cultures has been previously studied in another application of PNSB, concerning the possibility of associating

fermentation and photoorganoheterotrophy processes [34]. The authors showed that mixed cultures purple phototrophic bacteria can grow on fermentation products of dark fermentative bacteria, in the same reactor. Due to the adopted conditions promoting photoorganoheterotrophy, mainly biomass and PHAs were produced. On the other hand, under unbalanced substrate uptake and growth (high C/N ratio), the PF process takes place (i.e. the excess of electrons is redirected towards H_2 synthesis) [35].

Table 7.2 reports the comparison between different studies conducted on the DF-co-PF process and this study.

Table 7.2. Studies on the DF-co-PF process

Substrate	DF microorganisms	PF microorganisms	Hydrogen yield ($molH_2\ mol_{GLUCOSEeq}^{-1}$)	Ref
Starch	Heterotrophic mixed consortium	*Rhodobacter sphaeroides*	2.6	[13]
Glucose	*Clostridium butyricum*	*Rhodopseudomonas faecalis*	2	[14]
Glucose	*Clostridium butyricum*	*Rhodopseudomonas faecalis*	4.1	[36]
Glucose	*Clostridium acetobutylicum*	*Rhodobacter sphaeroides*	6.2	[37]
Sucrose	*Clostridium acidisoli*	*Rhodobacter sphaeroides*	5	[38]
Distillery effluent	*Citrobacter freundii* , *Enterobacter aerogenes*	*Rhodopseudomonas palustris*	1.6	[39]
Ground wheat starch	*Clostridium beijerinkii* DSMZ 791	*Rhodobacter sphaeroides* RV	0.6	[40]
Ground wheat starch	anaerobic sludge	*Rhodobacter sphaeroides* NRRL B-1727 + *Rhodobacter sphaeroides* DSMZ158 + *Rhodopseudomonas palustris* DSMZ-127	0.4	[41]
Distillery waste water	Anaerobic consortia	Mixed photosynthetic consortium	1.7	[32]
Winery wastewater	*Klebsiella pneumoniae*	*Rhodopseudomonas sp.*	0.4	This study
Winery wastewater	*Mixed culture*	*Mixed culture*	2.1	This study

The H_2 yield obtained in this study from both KR and M reactors were similar or lower compared to those reached by Laurinavichene et al., Liu et al., Ding et al. and Sun et al. [13-14,34–36]. Such studies have been conducted feeding reactors with synthetic substrates (i.e. glucose, sucrose and starch). The use of a synthetic substrate might have enhanced hydrogen yields by pure cultures PNSB. However, the sustainability of hydrogen production bioprocesses strongly depends on cost effective production and easy availability of substrates. In this context, the use of waste and wastewater plays a crucial role [42].

The result obtained in KR tests was comparable with those reported by Argun et al. and Kargi et al. [40,41], who performed ground wheat starch conversion by Clostridia + *Rhodopseudomonas* and anaerobic sludge + *Rhodobacter*, respectively.

The hydrogen yield of 2 molH_2 mol$_{GLUCOSEeq}^{-1}$, which was reached in M reactors of this study, was higher compared to those reached in all previous studies conducted using waste substrates and pure cultures [32,39–41]. Nevertheless, a similar result of 1.7 molH_2 mol$_{GLUCOSEeq}^{-1}$ was obtained by Chandra et al. [32], who performed the bioconversion of distillery wastewater using mixed cultures.

Overall, hydrogen yields values reported in Table 7.2 indicate that (open) mixed cultures enhance the hydrogen yield compared to DF-co-PF pure cultures processes, when the bioconversion of a waste substrate is performed. Such results are in agreement with previous studies conducted on the PF process by Luongo et al. [7] and Montiel Corona et al. [43], who obtained higher H_2 productions from mixed consortia compared to pure PNSB cultures.

7.4. Conclusions

Investigations on microbial communities have revealed that (open) mixed cultures can lead to higher hydrogen productivities compared to a mix of DF-PF pure cultures. The synergies established among different H_2 producing species, under PF conditions, enhanced the conversion of the organic substrates to H_2, and concomitantly led to the waste substrate stabilization. Also, non-hydrogen producing bacteria might have indirectly enhanced the productivity of hydrogen producing bacteria. The present study demonstrates that “contamination”, which is considered the main risk in pure culture systems, can represent a value in the waste conversion to hydrogen by mixed cultures.

References

[1] Argun H, Kargi F, Kapdan IK. Effects of the substrate and cell concentration on bio-hydrogen production from ground wheat by combined dark and photo-fermentation. Int J Hydrogen Energy 2009;34:6181–8. https://doi.org/10.1016/j.ijhydene.2009.05.130.

[2] Touloupakis E, Poloniataki EG, Ghanotakis DF, Carlozzi P. Production of Biohydrogen and/or Poly-β-hydroxybutyrate by Rhodopseudomonas sp. Using Various Carbon Sources as Substrate. Appl Biochem Biotechnol 2021;193:307–18. https://doi.org/10.1007/s12010-020-03428-1.

[3] Kothari R, Buddhi D, Sawhney RL. Comparison of environmental and economic aspects of various hydrogen production methods. Renew Sustain Energy Rev 2008;12:553–63. https://doi.org/10.1016/j.rser.2006.07.012.

[4] Policastro G, Luongo V, Frunzo L, Fabbricino M. A comprehensive review of mathematical models of photo fermentation. Crit Rev Biotechnol 2021;41:628–48. https://doi.org/10.1080/07388551.2021.1873241.

[5] Ghimire A, Frunzo L, Pirozzi F, Trably E, Escudie R, Lens PNL, et al. A review on dark fermentative biohydrogen production from organic biomass: Process parameters and use of by-products. Appl Energy 2015;144:73–95. https://doi.org/10.1016/J.APENERGY.2015.01.045.

[6] Niño-Navarro C, Chairez I, Christen P, Canul-Chan M, García-Peña EI. Enhanced hydrogen production by a sequential dark and photo fermentation process: Effects of initial feedstock composition, dilution and microbial population. Renew Energy 2020;147:924–36. https://doi.org/10.1016/j.renene.2019.09.024.

[7] Luongo V, Ghimire A, Frunzo L, Fabbricino M, d'Antonio G, Pirozzi F, et al. Photofermentative production of hydrogen and poly-β-hydroxybutyrate from dark fermentation products. Bioresour Technol 2017;228:171–5.

[8] Reungsang A, Zhong N, Yang Y, Sittijunda S, Xia A, Liao Q. Hydrogen from Photo Fermentation. In: Liao Q, Chang J, Herrmann C, Xia A, editors. Bioreact. Microb. Biomass Energy Convers., Singapore: Springer Singapore; 2018, p. 221–317. https://doi.org/10.1007/978-981-10-7677-0_7.

[9] Policastro G, Panico A, Fabbricino M. Improving biological production of poly(3-hydroxybutyrate-co-3-hydroxyvalerate) (PHBV) co-polymer: a critical review.

vol. 20. Springer Netherlands; 2021. https://doi.org/10.1007/s11157-021-09575-z.

[10] Montiel-Corona V, Buitrón G. Polyhydroxyalkanoates from organic waste streams using purple non-sulfur bacteria. Bioresour Technol 2021;323. https://doi.org/10.1016/j.biortech.2020.124610.

[11] Ghosh S, Chowdhury R, Bhattacharya P. A review on single stage integrated dark-photo fermentative biohydrogen production: Insight into salient strategies and scopes. Int J Hydrogen Energy 2018;43:2091–107. https://doi.org/10.1016/j.ijhydene.2017.12.018.

[12] Ghosh S, Chowdhury R, Bhattacharya P. A review on single stage integrated dark-photo fermentative biohydrogen production: Insight into salient strategies and scopes. Int J Hydrogen Energy 2018;43:2091–107. https://doi.org/10.1016/J.IJHYDENE.2017.12.018.

[13] Laurinavichene T V., Laurinavichius KS, Tsygankov AA. Integration of purple non-sulfur bacteria into the starch-hydrolyzing consortium. Int J Hydrogen Energy 2014;39:7713–20. https://doi.org/10.1016/j.ijhydene.2014.03.088.

[14] Liu BF, Ren NQ, Tang J, Ding J, Liu WZ, Xu JF, et al. Bio-hydrogen production by mixed culture of photo- and dark-fermentation bacteria. Int J Hydrogen Energy 2010;35:2858–62. https://doi.org/10.1016/j.ijhydene.2009.05.005.

[15] Luongo V, Ghimire A, Frunzo L, Fabbricino M, d'Antonio G, Pirozzi F, et al. Photofermentative production of hydrogen and poly-β-hydroxybutyrate from dark fermentation products. Bioresour Technol 2017;228:171–5. https://doi.org/10.1016/J.BIORTECH.2016.12.079.

[16] Policastro G, Giugliano M, Luongo V, Napolitano R, Fabbricino M. Carbon catabolite repression occurrence in photo fermentation of ethanol-rich substrates. J Environ Manage 2021;297:113371. https://doi.org/10.1016/j.jenvman.2021.113371.

[17] Pontoni L, Panico A, Matanò A, Van Hullebusch ED, Fabbricino M, Esposito G, et al. Modified Sample Preparation Approach for the Determination of the Phenolic and Humic-Like Substances in Natural Organic Materials by the Folin Ciocalteu Method. J Agric Food Chem 2017;65:10666–72. https://doi.org/10.1021/acs.jafc.7b04942.

[18] American Public Health Association (APHA). Standard Methods for the

Examination of Water and Wastewater, 21st ed.; APHA:Washington, DC, USA, 2005. 2005.

[19] Carraturo F, Gargiulo G, Giorgio A, Aliberti F, Guida M. Prevalence, Distribution, and Diversity of Salmonella spp. in Meat Samples Collected from Italian Slaughterhouses. J Food Sci 2016;81:M2545–51. https://doi.org/10.1111/1750-3841.13430.

[20] Doyle J, Corniello A, Guida M, Stellato L, Trifuoggi M, Carraturo F, et al. Hydrochemical, isotopic and microbiota characterization of telese mineral waters (Southern Italy). Environ Geochem Health 2021;4:283–93. https://doi.org/10.1007/s10653-021-00806-4.

[21] Corniello A, Guida M, Stellato L, Trifuoggi M, Carraturo F, Del Gaudio E, et al. Hydrochemical, isotopic and microbiota characterization of telese mineral waters (Southern Italy). Environ Geochem Health 2021;4. https://doi.org/10.1007/s10653-021-00806-4.

[22] Policastro G, Carraturo F, Compagnone M, Giugliano M, Guida M, Luongo V, et al. A preliminary study on a novel bioaugmentation technique enhancing lactic acid production by mixed cultures fermentation. Bioresour Technol 2021;340:125595. https://doi.org/10.1016/j.biortech.2021.125595.

[23] Lin CY, Chang CC, Hung CH. Fermentative hydrogen production from starch using natural mixed cultures. Int J Hydrogen Energy 2008;33:2445–53. https://doi.org/10.1016/j.ijhydene.2008.02.069.

[24] Liu F, Fang B. Optimization of bio-hydrogen production from biodiesel wastes by Klebsiella pneumoniae. Biotechnol J 2007;2:374–80. https://doi.org/10.1002/biot.200600102.

[25] Valdez-Calderón A, Barraza-Salas M, Quezada-Cruz M, Islas-Ponce MA, Angeles-Padilla AF, Carrillo-Ibarra S, et al. Production of polyhydroxybutyrate (PHB) by a novel Klebsiella pneumoniae strain using low-cost media from fruit peel residues. Biomass Convers Biorefinery 2020. https://doi.org/10.1007/s13399-020-01147-5.

[26] Pan L, Li J, Wang R, Wang Y, Lin Q, Li C, et al. Biosynthesis of polyhydroxyalkanoate from food waste oil by Pseudomonas alcaligenes with simultaneous energy recovery from fermentation wastewater. Waste Manag

2021;131:268–76. https://doi.org/10.1016/j.wasman.2021.06.008.

[27] Sayyed RZ, Shaikh SS, Wani SJ, Rehman MT, Al Ajmi MF, Haque S, et al. Production of biodegradable polymer from agro-wastes in alcaligenes sp. And pseudomonas sp. Molecules 2021;26:1–16. https://doi.org/10.3390/molecules26092443.

[28] Montiel Corona V, Le Borgne S, Revah S, Morales M. Effect of light-dark cycles on hydrogen and poly-β-hydroxybutyrate production by a photoheterotrophic culture and Rhodobacter capsulatus using a dark fermentation effluent as substrate. Bioresour Technol 2017. https://doi.org/10.1016/j.biortech.2016.12.021.

[29] Mabutyana L, Pott RW. Photo-fermentative hydrogen production by Rhodopseudomonas palustris CGA009 in the presence of inhibitory compounds. Int J Hydrogen Energy 2021:1–12. https://doi.org/10.1016/j.ijhydene.2020.12.189.

[30] Hoare DS, Hoare SL. Hydrogen metabolism by Rhodomicrobium vannielii. J Bacteriol 1969;100:1124–5. https://doi.org/10.1128/jb.100.2.1124-1125.1969.

[31] Policastro G, Luongo V, Fabbricino M. Biohydrogen and poly-β-hydroxybutyrate production by winery wastewater photofermentation: Effect of substrate concentration and nitrogen source. J Environ Manage 2020;271:111006. https://doi.org/10.1016/j.jenvman.2020.111006.

[32] Chandra R, Nikhil GN, Venkata Mohan S. Single-stage operation of hybrid dark-photo fermentation to enhance biohydrogen production through regulation of system redox condition: Evaluation with real-field wastewater. Int J Mol Sci 2015;16:9540–56. https://doi.org/10.3390/ijms16059540.

[33] Ghimire A, Valentino S, Frunzo L, Pirozzi F, Lens PNL, Esposito G. Concomitant biohydrogen and poly-β-hydroxybutyrate production from dark fermentation effluents by adapted Rhodobacter sphaeroides and mixed photofermentative cultures. Bioresour Technol 2016;217:157–64. https://doi.org/10.1016/J.BIORTECH.2016.03.017.

[34] Cerruti M, Crosset-Perrotin G, Ananth M, Rombouts JL, Weissbrodt DG, Weissbrodt D. Syntrophy between fermentative and purple phototrophic bacteria 3 for carbohydrate-based wastewater treatment 4 5. BioRxiv 2021:2021.05.13.444055.

[35] Cerruti M, Ouboter HT, Chasna V, van Loosdrecht MCM, Picioreanu C, Weissbrodt DG. Effects of light / dark diel cycles on the photoorganoheterotrophic metabolism of Rhodopseudomonas palustris for differential electron allocation to PHAs and H2. BioRxiv 2020.

[36] Ding J, Liu BF, Ren NQ, Xing DF, Guo WQ, Xu JF, et al. Hydrogen production from glucose by co-culture of Clostridium Butyricum and immobilized Rhodopseudomonas faecalis RLD-53. Int J Hydrogen Energy 2009;34:3647–52. https://doi.org/10.1016/j.ijhydene.2009.02.078.

[37] Zagrodnik R, Laniecki M. The role of pH control on biohydrogen production by single stage hybrid dark- and photo-fermentation. Bioresour Technol 2015;194:187–95. https://doi.org/10.1016/j.biortech.2015.07.028.

[38] Sun Q, Xiao W, Xi D, Shi J, Yan X, Zhou Z. Statistical optimization of biohydrogen production from sucrose by a co-culture of Clostridium acidisoli and Rhodobacter sphaeroides. Int J Hydrogen Energy 2010;35:4076–84. https://doi.org/10.1016/j.ijhydene.2010.01.145.

[39] Vatsala TM, Raj SM, Manimaran A. A pilot-scale study of biohydrogen production from distillery effluent using defined bacterial co-culture. Int J Hydrogen Energy 2008;33:5404–15. https://doi.org/10.1016/j.ijhydene.2008.07.015.

[40] Argun H, Kargi F. Bio-hydrogen production from ground wheat starch by continuous combined fermentation using annular-hybrid bioreactor. Renew Energy 2010;35:6170–8. https://doi.org/10.1016/j.ijhydene.2010.03.132.

[41] Kargi F, Ozmihci S. Effects of dark/light bacteria ratio on bio-hydrogen production by combined fed-batch fermentation of ground wheat starch. Biomass and Bioenergy 2010;34:869–74. https://doi.org/10.1016/j.biombioe.2010.01.031.

[42] Ghosh S, Dairkee UK, Chowdhury R, Bhattacharya P. Hydrogen from food processing wastes via photofermentation using Purple Non-sulfur Bacteria (PNSB) – A review. Energy Convers Manag 2017;141:299–314. https://doi.org/10.1016/J.ENCONMAN.2016.09.001.

[43] Montiel-Corona V, Revah S, Morales M. Hydrogen production by an enriched photoheterotrophic culture using dark fermentation effluent as substrate: Effect of flushing method, bicarbonate addition, and outdoor-indoor conditions. Int J Hydrogen Energy 2015. https://doi.org/10.1016/j.ijhydene.2015.05.067.

Chapter 8

A comprehensive review of mathematical models of photo fermentation

This chapter has been published as: Policastro, G., Luongo, V., Frunzo, L. and Fabbricino, M. (2021). A comprehensive review of mathematical models of photo fermentation. Critical Reviews in Biotechnology, 41(4), 628-648.

A comprehensive review of mathematical models of photo fermentation

Abstract

This work aims at analysing and comparing the different modeling approaches used to date to simulate, design and control photo fermentation process for hydrogen production and/or wastewater treatment. The study is directed to researchers who approach the problem of photo fermentation mathematical modeling. It is a useful tool to address future researches in this specific field and to overcome the difficulty of modeling a complex, not totally elucidate process. We report a preliminary identification of the environmental and biological parameters, included in the models, which affect photo fermentation. Based on models features, we distinguish three different approaches, i.e. kinetic, parametric and non-ideal reactors ones. We explore the characteristics of each approach, reporting and comparing the obtained results and underlining the differences between models, together with the advantages and the limitations of each of them. The analysis of the approaches indicates that Kinetic models are useful to describe the process by the biochemical point of view, without considering the bio-reactor hydrodynamics and the spatial variations Parametric Models can be utilized to study the influence and the interaction between the operational conditions. They do not take into account the biochemical process mechanism and the influence of the reactor hydrodynamics. Quite the opposite, non-ideal reactors models focus on the reactor configuration. Otherwise, the biochemical description of purple non sulfur bacteria activities is usually simplified. The review indicates that there still is a lack of models fully describing photo fermentation process.

8.1. Introduction

The term photo fermentation (PF) refers to a biological process performed by purple non-sulfur bacteria (PNSB), a family of anaerobic facultative microorganisms, which includes several strains [1]. In presence of light and absence of molecular oxygen and nitrogen, PNSB are able to convert a wide range of organic substrates (i.e. organic acids, sugars, alcohols), which can be contained in several wastes, to molecular hydrogen and poly-β-hydroxybutyrate (PHB) [2–4]. This allows to obtain from organic waste (e.g. solid food waste, food and beverage processing wastewater, agricultural waste) energy and valuable chemicals for bio-plastic production [5–7].

The number of studies concerning PF considerably increased over last years, as it is clearly indicated by the trend of indexed papers published between 2000 and 2019, showed in **Figure 8.1**.

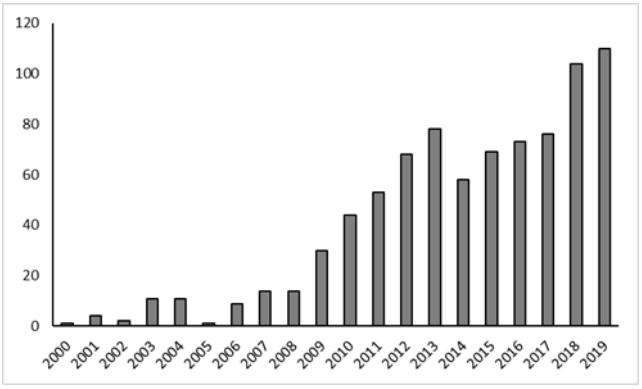

Figure 8.1 Trend of indexed papers concerning PF published between 2000 and 2019

The growing interest of the scientific community towards PF is due to the high value of the final products, and to significant value of COD removal efficiency, which helps to reduce the environmental impact of waste materials, and valorise the environmental impact of waste materials [8], in agreement with the new perspectives of circular economy.

As a result of the devoted efforts of researchers, the possibility of managing, controlling and optimizing the process has been greatly improved. Nonetheless, the complex mechanism of PF is far from being completely elucidated. Additional studies are required to clarify the behaviour of different PNSB species under different feed conditions, and to completely understand the effect of environmental conditions on the process development. Indeed, there is still a lack of pilot-scale studies and industrial scale applications. In this context, the use of mathematical models is helpful to understand how the different biological mechanisms of PF evolve, and to effectively control and design the process for scaling-up purposes. Mathematical models, in fact, can simulate the influence of different environmental and operational conditions affecting the process. Their application is crucial as it strongly decreases the time and costs required for experimental tests. In addition, they can be used as design and management tools for more efficient photo-bioreactors (PBRs) [9].

A comprehensive review of existing models of PF is therefore important to understand the potential application of the process and to address future researches in this specific field. Few previous review papers have been published on mathematical models of fermentative hydrogen production [10,11]. They principally focus on dark fermentation process and/or they only highlight specific modeling approaches applied to the PF process. Currently, a complete review of such mathematical models, applied to hydrogen production and/or to wastewater treatment, is absent in the scientific literature, and represents the object and the aim of the present chapter.

To facilitate the reading, existing models are divided into three groups:

i) Kinetic Models (KMs), developed to predict substrates degradation, biomass growth and products formation;

ii) Parametric Models (PMs), based on the experimental design strategy and machine learning methods, developed to evaluate the effect of the physico-chemical variables on process performances;

iii) Non-ideal reactor models (NIRMs), which are able to consider the spatial variability and reactor hydrodynamics and can be applied to real-scale reactors.

To better understand models benefits and limitations, a preliminary overview of the parameters affecting PF is reported, which allows identifying the main variables included in the model definitions.

8.2. Environmental factors affecting photo fermentation

As previously indicated, PF is affected by many process parameters, which have to be carefully controlled to optimize process development and efficiency (e.g. hydrogen and/or PHB production) [12,13].

PF process performance is usually evaluated in terms of COD removal efficiency, hydrogen production and PHB accumulation and it strongly depend on the bacterial strain and the organic molecules used as substrate. PNSB are able to use different organic substrates (e.g. sugars, alcohols, organic acids (OAs)) as carbon source. Some types of carbon sources stimulate hydrogen production more than PHB accumulation, while other substrates principally stimulate PHB production. At the same time, the metabolism of specific PNSB species is principally driven to the hydrogen production pathway, while the metabolism of other species is mainly driven to PHB accumulation [14]. Moreover, when waste materials or wastewater are utilized as substrate, other factors such as carbon to nitrogen ratio, presence of high ammonia ions concentrations and/or toxic compounds can strongly influence microorganisms' growth [15,16].

Substrate concentration plays a crucial role on overall PF process. Under substrate limiting conditions, PNSB shift their metabolism and accumulate intercellular granules of PHB as carbon reserve [3]. However, high substrate concentrations lead to the accumulation of organic acids in the fermentation bulk liquid, with a consequent decrease of the pH value. Conversely, low substrate concentrations lead to high pH values [17].

High acidic or alkaline pH, resulting in low ATP generation, avoid the biomass growth and affects substrate utilization and hydrogen generation [18]. On the other hand, these

pH conditions may allow PHB accumulation, which occurs when the microorganisms are forced to live under stress conditions [19]. In addition, PNSB growth rate may be inhibited by high biomass concentrations due to the limited availability of substrates and the self-shading phenomenon, which reduces the penetration of light in PBRs [20].

Light intensity is a factor of main relevance for PNSB growth. Indeed, low light intensity, resulting in low energy availability, prevents cell growth. Quite the opposite, high light intensity levels lead to the generation of an excess of energy, which has to be dissipated in form of heat, resulting in damages of the photosynthetic apparatus [21]. Moreover, as bacteria need light availability, the light distribution inside the bioreactor play an important role in the process development. Consequently, light distribution has to be taken into account in the reactor design and the choice of a suitable reactor geometry.

The incubation temperature is another relevant factor, which influences bacteria growth, hydrogen production and substrate conversion efficiency. Too high or too low temperatures result in a decrease of bacterial productivity. Moreover, when the temperature is unstable, bacteria spend too much energy in adaptation to the new condition, resulting in a decrease of productivity. Different optimal temperature values have been observed for different PNSB strains [22].

Finally, PF process strongly depends on the PBR configuration. The hydrodynamics of the reactor, linked to its specific geometry, plays a crucial role towards better process performances in terms of hydrogen production. PBRs have to be designed according to the culture requirements. Both suspension and immobilized cultures has been tested in batch or continuous mode. The most used PBRs for suspended culture are tubular reactors (e.g. vertical and horizontal and plate reactors). For immobilized cultures, gel granule packed PBRs have been widely used due to their high biomass concentration, and possibility of high fluid velocity without leading to the cell wash-out [22,23].

All these parameters have been taken into account in the revised studies. Due to the complexity of the process, each model is based on hypotheses and simplifications and deals with only some of the mentioned parameters. In reviewed studies, the authors focused on parameters they wished to dwell or on those that mostly influenced the process in the specific cases.

8.3. Kinetic models

KMs are aimed at simulating biomass growth, substrate utilization and product formation processes, taking into account their time dependence. The processes are therefore represented by a system of ordinary differential equations, coming from mass balance

equation. These can be solved through numerical integration, under suitable initial conditions and assigned kinetic and stoichiometric parameters.

An overview of KMs for PF processes is reported in **Table 8.1**. For each considered study the Table indicates the substrate and the PNSB strain used for model calibration and/or validation.

Table 8.1. Kinetic models used for photo fermentation process

PNSB strain	Substrate	Biomass growth model	Substrate consumption model	Hydrogen production model	References
R. Capsulatus IR3	Lactic acid	Monod	Michaelis-Menten	Baly, Luedeking-Piret	[25]
R. Capsulatus DSM 1710	Acetic acid, Lactic acid	Logistic model	Zero order kinetic, First order kinetic	Gompertz	[30]
R. Capsulatus DSM 1710	Acetic acid	-	First order kinetic, Second order kinetic	-	[75]
R. Sphaeroides O.U. 001	Acetic acid, Malic acid, Butyric acid	-	First order kinetic,	-	[33]
R. Capsulatus B10	Lactic acid	Monod	Michaelis-Menten	Luedeking-Piret based	[35]
R. Sphaeroides	Malic acid	Logistic model based	Luedeking-Piret based	Luedeking-Piret based	[26]
R. Palustris DSM 123	Malic Acid	Monod, Logistic model	Michaelis-Menten	Gompertz, Luedeking-Piret	[29]
PNSB consortium	Acetic acid, Butyric acid	Monod based	Luedeking-Piret based	Luedeking-Piret based	[9]
R. Sphaeroides	Malic acid	Logistic model based	Luedeking-Piret based	Luedeking-Piret based	[28]
R. Palustris WP3-5	Acetic acid, Butyric acid	-	-	Gompertz	[36]
R. Sphaeroides	Malic acid	Logistic model	First order kinetic	First order kinetic	[31]
R. Palustris	Glycerol	Droop based, Contois based	Droop based, Contois based	Droop based Contois based	[38]
Mixed PNSB culture	DFE*	-	-	Gompertz based	[37]
Mixed PPB	DW	Monod based	Michaelis-Menten based	Monod based	[39]
-	-	Monod based	Luedeking-Piret	Luedeking-Piret	[27]

*Dark Fermentation Effluent.

As for many other biological processes (e.g. anaerobic digestion, dark fermentation), the most frequently applied models used to simulate biomass growth in PBRs are based on the classical Monod's formulation, which express the growth rate as a function of the available substrate as:

$$\mu = \left(\frac{\mu_m C_s}{k_s + C_s}\right), \quad (1)$$

where μ and μ_m are the specific growth rate and the maximum specific growth rate, respectively, C_s is the substrate concentration and k_s is the half saturation constant.

The variation over time of the biomass concentration, C_x, is frequently evaluated by associating Equation (1) to a first order kinetic expression,

$$\frac{dC_x}{dt} = \mu C_x, \quad (2)$$

able to describe the biomass accumulation in bioreactors or the increase of biomass on Petri dishes and fit a wide range of experimental data [11,24,25].

To include the effect of substrate inhibition, Andrew's equation has also been applied [26]. It describes the biomass growth rate as a function of a generic j^{th} inhibiting substrate as:

$$\mu = \frac{\mu_m C_s}{K_s + C_s + C_s^2/K_{Xj}}, \; j=1,\ldots,m, \quad (3)$$

where K_{xj} is the substrate inhibition constant of cell formation related to the presence of the j^{th} substrate.

Of course, neither the classical Monod's equation, nor the Andrew's equation consider inhibition phenomena related to high/low pH values, excess/scarcity of light, and unfavourable temperature conditions. Hence, Wang et al. [27] proposed a multi-parametric modified Monod model, incorporating additional parameters, as alternative to Equation (1) and (2). In these cases, the maximum specific growth rate has been described as:

$$\mu_m = a\mu_{opt} exp\left[-b\left(\frac{I}{I_{opt}} - 1\right)^2\right] exp\left[-c\left(\frac{pH}{pH_{opt}} - 1\right)^2\right] exp\left[-d\left(\frac{T}{T_{opt}} - 1\right)^2\right], \quad (4)$$

where I is the light intensity, pH is the pH value of the substrate, T is the temperature and the subscript "opt" refers to the optimal values [27].

Logistic models have also been widely used to describe microbial growth in the case of nutrient limiting conditions, and/or high biomass concentration [28]. Several authors [24,29,30] adopted, for example, the classical logistic equation:

$$\frac{dC_x}{dt} = \mu C_x \left(1 - \frac{C_x}{C_{xm}}\right), \quad (5)$$

where C_{xm} is the maximum biomass concentration. Of course, when C_x is close to the maximum concentration C_{xm}, the biomass growth reaches a plateau and no more biomass is produced. This model, characterized by a typical sigmoidal shaped trend, well fits the entire PNSB growth curve, including the lag phase [24]. On the other hand, it is preliminary required to know the maximum biomass concentration, which strictly depends on environmental conditions (e.g. bioreactor configuration) of the specific case. Basak et al. [29] found that the logistic model was able to better fit their experimental data than the classical Monod's equation. Similarly, Akbari and Mahmoodzadeh Vaziri [28] and Koku et al. [31] found that the logistic model was better than the modified Monod's equation to simulate *Rhodobacter Sphaeroides* growth on a malic acid medium. Nonetheless, the logistic equation does not take into account the substrate inhibition effect on biomass growth, which is very important in many different situations.

To overcome this limitation, Koku et al. [31] introduced the following modification to equation (5):

$$\mu = \frac{\mu_m C_S}{k_S + C_S + C_S^2/k_{Xi}}\left(1 - \frac{C_x}{C_{xm}}\right), \quad (6)$$

and obtained a good results for data fitting.

Gadhamshetty et al. [26], in turns, proposed a modified multi-parametric version of equation (6), able to account for the effect of both light intensity and substrate inhibition. In their formulation:

$$\mu = \frac{\mu_m C_S}{K_S + C_S + C_S^2/K_{Xi}}\left(\frac{I}{K_{xI} + I + K_I I^2}\right)\left(1 - \frac{C_x}{C_{xm}}\right), \quad (7)$$

where I is the light intensity and K_I and K_{xI} are the light inhibition constant and the light saturation constant of cell formation respectively.

In some studies, Monod's equation was used to simulate substrate utilization instead of biomass growth [25,29]. In this case, it is possible to introduce the equation:

$$\frac{dC_S}{dt} = -\frac{1}{Y_{xs}}\mu C_x, \quad (8)$$

where C_s is the concentration of the substrate and Y_{xs} is the yield for substrate utilization. Nonetheless for certain specific situations, a zero-order kinetic equation or a second order kinetic equation have been found to fit the experimental data better than a first order kinetic equation. Sevinç et al. [30], for example, studied acetic acid and lactic acid consumption during PF, varying the temperature and the light intensity. The authors found that lactic acid consumption, was well approximated by a first order kinetic equation, while acetic acid degradation trend was better fitted by a zero-order kinetic equation until the last hours of the test, when the substrate was almost completely consumed. On the other hand, Özgür et al. [32] found that acetic acid was consumed

following a first order kinetic when the concentration was low, and following a second order kinetic when the concentration was high. Uyar et al. [33], instead, reported a good fitting of experimental data concerning acetic acid consumption in presence of malic acid and butyric acid, using a first order kinetic equation for all three substrates. The authors also observed that the same good fitting could not be obtained in presence of acetate alone, and was instead obtained in presence of butyrate and malate alone, in agreement with previous studies [31].

Some other studies used a conventional or modified Luedeking-Piret model to predict substrate consumption rates during photo fermentation. The conventional equation describes the relationship between substrate utilization and biomass concentration, assuming that substrate consumption is linearly dependent on both instantaneous biomass concentration and biomass growth rate:

$$\frac{dC_s}{dt} = \frac{1}{Y_{sx}}\frac{dC_x}{dt} + \mu_{sx}C_x, \quad (9)$$

where C_s is the concentration of the substrate, Y_{sx} is the yield coefficient of cells on substrate and μ_{sx} is the substrate consumption rate.

Following the approach suggested by Zhang et al. [34], Gadhamshetty et al. [26] proposed a modified version of Eq.(9) including the product term C_p and the effect of the auto-inhibition due to the substrate concentration.

$$\frac{dC_s}{dt} = \left(\frac{1}{Y_{sx}}\frac{dC_x}{dt} + \frac{1}{Y_{Ps}}\frac{dC_P}{dt} + \mu_{sx}C_x\right)\left(\frac{C_s}{k_{SA}+C_s}\right) \quad (10)$$

where C_P and Y_{Ps} are the concentration and the yield coefficient of products generated by substrate degradation, respectively, and μ_{xs} and k_{SA} are auto-inhibition constants.

The authors obtained good results in terms of model calibration and validation with using data from different bacterial strains. Conversely, they noticed a strong dependence of feeding conditions on data fitting. In particular, in presence of a mixture of substrates, they found that the interaction of different substrates was too complex to be simulated by the proposed Eq. (10).

As far as concern PF products formation, several authors [25,26,29,35] proposed to simulate hydrogen production trend either using the classical Luedeking-Piret equation:

$$\frac{dC_p}{dt} = Y_{px}\frac{dC_x}{dt} + \mu_{px}C_x, \quad (11)$$

or its modified version which takes into account also the effect of substrate concentration, light intensity and product concentration:

$$\frac{dC_p}{dt} = \left(Y_{px}\frac{dC_x}{dt} + \mu_{px}C_x\right)\left(\frac{C_s}{K_{ps}+C_s+C_s^2/K_{Pi}}\right)\left(\frac{I}{K_{PI}+I+I^2/K_{pI}}\right)\left(1-\frac{C_p}{C_{pm}}\right) \quad (12)$$

where Y_{px} is the yield coefficient of product formation due to cell growth, μ_{px} the specific product formation rate, K_{ps} is the substrate saturation constant of product formation, K_{Pi} is the substrate inhibition constant of product formation, K_{PI} is the light saturation constant of product formation, K_{pI} is the light inhibition constant of product formation, and C_{pm} is the maximum product concentration.

Another widely utilized model applied to simulate hydrogen production is the Gompertz equation [30,36]. This equation satisfactorily describes the cumulative hydrogen production in batch experiments, characterized by a slow increasing production during the first days of the process followed by a rapid increase until the attainment of an asymptotic value. The Gompertz equation is usually written as:

$$H(t) = H_m exp\left\{-exp\left[\frac{R_{m.e}}{H_m}(\lambda - t) + 1\right]\right\}, \quad (13)$$

where H(t) is the cumulative hydrogen volume, H_m the maximum cumulative hydrogen volume, R_m the maximum production rate, λ the lag time, t the incubation time and *e* the Eulero's number.

Nonetheless it does not take into account the effect of the process key variables [28].

Basak et al. [29] compared Luedeking-Piret and Gompertz models to describe PF process of *R. Palustris DSM 123* fed with malic acid as the carbon source. They found a better agreement between the model and the experimental data using Gompertz equation. Similarly, Chen et al. [36] and Sevinç et al. [30] found that Gompertz equation was able to predict well the hydrogen production under various acetate and butyrate concentrations [36], and varying temperature and light intensities values, in presence of substrate mixtures composed by acetic and lactic acid [30].

Frunzo et al. [37] introduced a modified Gompertz model by providing a fractional generalization of the law via a Caputo-like definition of the fractional derivative of a function with respect to another function. The model was successfully calibrated with experimental data describing dark and photo fermentative hydrogen production and microalgae biomass growth.

To account for the effect of light intensity, pH and temperature in batch conditions, Monroy et al. [9] developed a mechanistic model for hydrogen production supported by data-based classification models. The obtained time trajectories were similar to the experimental data when operating at optimal conditions. Akbari and Mahmoodzadeh Vaziri [28] developed a model to simultaneously account for the effect of microbial population, the H_2 amount, the substrate-limited conditions and the light intensity. They tested various models describing biomass growth, hydrogen production and substrate

consumption in combination, in order to find the best data fitting. The model MVA1, a combination of modified logistic equation (biomass growth) and modified Luedeking-Piret equations (used for substrate consumption and hydrogen production) was found to be the more accurate for the description of experimental data.

Zhang et al. [38] developed two modified models to describe PF process using *R. Palustris* on a glycerol medium. Their work describes the modification of Droop's and Contois' equation. In the first case, they completely uncoupled the growth rate from the external nutrient concentration by introducing an intercellular store of nutrients. The system of equations was written as:

$$\frac{dc_x}{dt} = \begin{cases} \mu_m . \frac{C_s}{C_s + k_s} . \frac{C_N}{C_N + k_N} . C_X, & N > 0 \\ \mu_0 . \frac{C_s}{C_s + k_s} . C_X, & q > q_{min} \\ 0, & q \leq q_{min} \end{cases} \quad (14a)$$

$$\frac{dq}{dt} = \begin{cases} Y_q . \mu_m . \frac{C_N}{C_N + k_N} - \mu_m . \frac{C_s}{C_s + k_s} . \frac{C_N}{C_N + k_N} . q, & N > 0 \\ -\mu_0 . \frac{C_s}{C_s + k_s} . q, & q > q_{min} \\ 0, & q \leq q_{min} \end{cases} \quad (14b)$$

$$\frac{dN}{dt} = -Y_N . \mu_m . \frac{C_N}{C_N + k_N} . c_x \quad (14c)$$

$$\frac{dc_s}{dt} = \begin{cases} -Y_{s1} . \frac{dCx}{dt} - Y_{s2} . C_x, & N > 0 \\ -Y^*_{s1} . \frac{dCx}{dt} - Y^*_{s2} . C_x, & q > q_{min} \\ -Y^{**}_{s2} . C_x, & q \leq q_{min} \end{cases} \quad (14d)$$

$$\frac{dH_2}{dt} = \begin{cases} Y_{H_2 1} . \frac{dCx}{dt} - Y_{H_2 2} . C_x, & N > 0 \\ Y^*_{H_2 1} . \frac{dCx}{dt} - Y^*_{H_2 2} . C_x, & q > q_{min} \\ Y^{**}_{H_2 2} . C_x, & q \leq q_{min} \end{cases} \quad (14e)$$

where N is the nitrogen source concentration, q is the normalized nitrogen quota, q_{min} the nitrogen quota threshold, Y_i are the yields during the first growth phase, Y_i* during the second growth phase and Y_i** during the stationary phase.

The second model, instead, is a variant of Monod's equation, which assumes that the growth rate is inhibited by the amount of biomass. Consequently, equations (14a), (14b) and (14c) become:

$$\frac{dc_x}{dt} = \begin{cases} \mu_m . \frac{C_s}{C_s + k_s . C_x} . \frac{C_N}{C_N + k_N . C_x} . C_x, & N > 0 \\ \mu_0 . \frac{C_s}{C_s + k_s . C_x} . C_x, & q > q_{min} \\ 0, & q \leq q_{min} \end{cases} \quad (15a)$$

$$\frac{dq}{dt} = \begin{cases} Y_q.\mu_m.\frac{C_N}{C_N+k_N.C_x} - \mu_m.\frac{C_s}{C_s+k_s.C_x}.\frac{C_N}{C_N+k_N.C_x}.q, & N > 0 \\ -\mu_0.\frac{C_s}{C_s+k_s.x}.q, & q > q_{min} \\ 0, & q \le q_{min} \end{cases} \quad (15b)$$

$$\frac{dN}{dt} = -Y_N.\mu_m.\frac{C_N}{C_N+k_N.C_x}.c_x. \quad (15c)$$

According to the authors [38], the two models are composed by several modules, each corresponding to a different phase of the process. They assumed that different growth phases are dominated by different growth mechanisms. To combine the sub-models, switch differentiable functions were utilized:

$$F(N) = \frac{N}{(N^2+\gamma^2)^{0.5}} \quad (16a)$$

$$F(q) = 0.5\frac{((q-q_{min})^2)^{0.5}+(q-q_{min})}{((q-q_{min})^2+\gamma^2)^{0.5}} \quad (16b)$$

where γ is the sharpness. The equation (16a) connected the first phase with the second phase, while the equation (16b) was used to combine the second phase with the stationary phase.

Puyol et al. [39] developed a mechanistic model for N and P recovery from domestic wastewater by a mixed consortium of purple phototrophic bacteria. They considered different microbial processes: i) hydrolysis, ii) photoheterotrophy, including acetate uptake and other organics consumption, iii) chemoheterotrophy (fermentation and anaerobic oxidation processes), iv) photoautotrophy (CO_2 fixation using hydrogen as electron donor) and v) biomass decay. The rate equations for each process are reported:

$$\left(\frac{dC_s}{dt}\right)_{hyd} = k_{hyd}C_s \quad (17a)$$

$$\left(\frac{dC_x}{dt}\right)_{act} = k_{m,ac}C_x\left(\frac{C_{ac}}{k_{s,ac}+C_{ac}}\right)I_{fa}I_{in}I_{ip}I_eI_{c\_s} \quad (17b)$$

$$\left(\frac{dC_x}{dt}\right)_{pht} = k_{m,ph}C_x\left(\frac{C_s}{k_{s,s}+C_s}\right)I_{fa}I_{in}I_{ip}I_eI_{c\_ac} \quad (17c)$$

$$\left(\frac{dC_x}{dt}\right)_{aut} = k_{m,ic}C_x\left(\frac{C_{ic}}{k_{s,ic}+C_{ic}}\right)I_{fa}I_{in}I_{ip}I_e \quad (17d)$$

$$\left(\frac{dC_x}{dt}\right)_{che} = k_{m,ch}C_x\left(\frac{C_b}{k_{s,b}+C_b}\right)I_{fa}I_{in}I_{ip} \quad (17e)$$

$$\left(\frac{dC_x}{dt}\right)_{dec} = k_{dec}C_x \quad (17f)$$

where k_{hyd} and k_{dec} are the hydrolysis and biomass decay first order constants (d^{-1}). $k_{m,ac}$, $k_{m,ph}$, $k_{m,ic}$ and $k_{m,ch}$ are specific uptake rates for acetate in photoheterotrophy, for soluble substrates in photoheterotrophy except acetate, inorganic carbon and chemoheterotrophy, respectively (mgCOD $mgCOD^{-1}d^{-1}$). $K_{s,ac}$, $K_{s,s}$, $K_{s,ic}$, $K_{s,b}$,are

saturation constants (mg L^{-1}) for acetate, soluble substrates, inorganic carbon and biomass respectively.

The terms denoted by I are limiting/inhibiting factors and are expressed as:

competitive inhibition,

$$I_{c\_s} = \left(\frac{C_{ac}}{C_{ac}+C_s}\right);\ I_{c\_ac} = \left(\frac{C_s}{C_s+C_{ac}}\right), \quad (18a)$$

nitrogen and phosphorous inhibition,

$$I_{in} = \left(\frac{C_{s,in}}{k_{s,in}+C_{s,in}}\right);\ I_{ip} = \left(\frac{C_{s,ip}}{k_{s,ip}+C_{s,ip}}\right), \quad (18b)$$

and free ammonia and light inhibition,

$$I_{fa} = \left(\frac{k_{i,fa}}{k_{i,fa}+C_{NH_3}}\right);\ I_e = \left(\frac{C_e}{k_{s,e}+C_e}\right). \quad (18c)$$

The kinetic and stoichiometric parameters were evaluated by conducting batch experiments, and the resulting kinetic expressions were used to develop a continuous photo-anaerobic membrane bioreactor model.

In Appendix A, a Table connecting all the parameters related to the reviewed models have been presented. The different approaches were divided by model equations for the specific use, e.g. for biomass growth, and the values of the available measured parameters were also reported. In some cases, different values of the same parameter were found, as the influence of bacterial strain, substrate feeding conditions and abiotic experimental conditions may vary between different experiments.

8.4. Parametric models

8.4.1 Design Of Experiments (DOE) method

PMs have been frequently proposed to evaluate and simulate the effect of a large number of process conditions on PF efficiency in terms of hydrogen production (Table 8.2). These models are based on a statistical method known as design of experiments (DOE). The easiest formulation of the DOE method is one-factor-a-time-design, which consists in the investigation of the effect of one variable a time while keeping the value of the other variables constant [11]. The advantage of the method is the ease of the experimental design and of results analysis. On the other hand, the one-factor-a-time-design does not explicitly consider the interaction between different influencing factors, which can substantially change the optimal conditions. During the last few years, a multiple-factor design approach has been introduced and widely used. Although this method is more complex than the one-factor-a-time one, it allows for studying the effect on the response (usually hydrogen production) of more factors (variables) at different levels (values). The choice of the factors to include in the experimentation, as well as the choice of the levels is a critical aspect. Of course, the higher the number of factors included in the analysis, the more the number of experiments to be conducted. For this reason, it is up to the experimenter to exclude some of the factors, according to the results of previous studies, or according to his own knowledge. Due to the versatility of PNSB bacteria, it is important to carry out the optimization study on a case-by-case basis. The relation between the response and factors is usually described using a second order polynomial model, as exemplified below:

$$Y = \beta_0 + \beta_1 X_1 + \beta_2 X_2 + \beta_{11} X_1^2 + \beta_{22} X_2^2 + \beta_{12} X_1 X_2, \quad (19)$$

where Y is the response, β_i and $\beta_{i,j}$ are the coefficients of the model and X_i are the factors considered for the specific test.

Although Equation (19) only includes two factors, it can be extended to more complicated cases, considering a higher number of them.

Results of the DOE method are usually interpreted using the response surface methodology (RSM), frequently applied for processes optimization [40,41].

An overview of PMs for PF processes is reported in **Table 8.2**.

Table 8.2 Parametric models used for photo fermentation process

PNSB strain	Substrate	Method	Investigated factors	Reference
R. Capsulatus	Acetic acid	RSM-Box-Behnken	Initial biomass concentration,	[44]

			Initial substrate concentration, light intensity	
R. Capsulatus	Acetic acid, lactic acid	Full factorial design, 3^2	Temperature, light intensity	[42]
R. Palustris	Glycerol	RSM-Box-Behnken	Substrate concentration, Nitrogen source concentration, light intensity	[46]
R. Sphaeroides	Malic acid	Full factorial design, 3^3	Substrate concentration, Nitrogen source concentration, temperature	[43]
R. Palustris	Acetic acid, Butyric acid	Central composite design	Acetate concentration, Butyrate concentration	[36]
R. Palustris	Malic acid	3^3 full factorial desig	Substrate concentration, Nitrogen source concentration, Fe concentration	[29]
R. Capsulata	VFAs	2^2 Central composite design	Nitrogen source concentration, pH	[47]
R.Palustris PBUM001	Palm oil mill effluent (POME)	5^3 RSM- Box-Behnken	Substrate concentration, inoculum concentration, initial pH, light intensity, agitation.	[45]
C. Acidisoli- R. Sphaeroides	Sucrose	Central composite design Plackett-Burman design	Substrate concentration, Inoculum ratio of C. acidisoli to R. sphaeroides, initial pH	[48]
R. Capsulatus	Wheat straw	Central composite design	Inoculum age, substrate loading, Nitrogen source concentration	[49]
R. palustris WP3-5	Butyric acid	Central composite design	Substrate concentration, Nitrogen source concentration, $FeCl_3$ concentration	[74]
PNSB consortium	Acetic acid, Butyric acid	Artificial neural networks	light intensity, pH, metals concentration	[9]
Rhodospirillum rubum	CO	hybrid fuzzy clustering-ranking approach coupled with radial basis function (RBF) neural network	agitation speed, syngas flow rate	[56]
PNSB consortium	Acetic acid, Butyric acid	Support vector machine	light intensity, pH	[57]

Two different typologies of experimental design have been used over last years: the full factorial design and the fractional factorial design. Using the first approach, all

combinations of levels have to be tested. A 3^2 full factorial design was used by Androga et al. [42] to investigate the effect of light intensity and temperature on hydrogen production from acetic and lactic acid by *R. Capsulatus*. ANOVA results showed that linear and quadratic effects of both variables were statistically significant, while the interaction between them was not significant. A 3^3 full factorial design was used by Basak et al. [29] to investigate the effect of substrate concentration (malic acid), nitrogen source (glutamate) concentration, and $FeCl_3$ concentration on hydrogen production. ANOVA analysis revealed that the linear effect of the substrate concentration was significant, as well as the quadratic effects of all the investigated variables. On the contrary, the linear effect of nitrogen concentration and Fe concentration, as well as the interactions between the selected factors, were negligible. These results were somehow in agreement with previous findings reported by Basak et al. [43] who selected, as factor of their DOE, the substrate concentration, the nitrogen concentration and the temperature.

Since a large number of experiments have to be conducted for a full factorial design approach, sometimes a fractional factorial approach can be more advisable. For PF modeling, the Box-Behnken Design (BBD), the Central Composite Design (CCD) and the Plackett-Burman design (PBD) approaches have been proposed. BBD is a three-level design strategy proposed by Box and Behnken in 1960, which is based on the combination of two-level factorial and incomplete block designs. CCD is a five-level fractional factorial design approach developed by Box and Wilson in 1951. It consists of a 2^n full factorial design, $2 \times n$ axial designs and m central designs. Finally, the Plackett-Burman design is a two-level fractional design strategy eveloped in 1946 by Robin L. Plackett and J.P. Burman. An extensive review of these methods can be found elsewhere [11].

Akman et al. [44] studied the effects of initial acetic acid concentration, light intensity and initial biomass concentration on hydrogen production in presence of *R. Capsulatus*, adopting the BBD approach. Regression analysis were performed via ANOVA. Results showed that all the investigated factors affected the response variable, especially the light intensity. In addition, the interaction among factors had a significant effect on hydrogen production. Following the same design approach and the same method of analysis, Jamil et al. [45] investigated the effects on cumulative hydrogen production by *R. Palustris* of the substrate concentration, the agitation rate, the light intensity, the pH value and the inoculum size. The first 3 factors had a significant effect on the response, while the effect of the pH value and inoculum size was not significant. Moreover, the interactions between substrate concentration and agitation rate was significant, while the light intensity interaction was negligible for low substrate concentrations. On the other hand, increasing

light intensity values had a positive effect on cumulative hydrogen production when the substrate concentration increased. The BBD approach was used also by Ghosh et al. [46] to identify the optimal condition for hydrogen production and nitrogenase activity for the photo fermentative conversion of crude glycerol by *R. Palustris*. The authors found that the substrate concentration, the nitrogen source concentration and the light intensity and their interactions strongly affected the model response. Other authors [36,47–49] used the CCD approach, instead. In details, Shi and Yu [47] evaluated the effect of the glutamate concentration and the pH value on the hydrogen yield for a single stage dark-photo fermentative process. Results, analysed through ANOVA, indicated a quadratic effect of pH on the response, and a significant interaction between pH and the initial concentration of the substrate was found. Chen et al. [36], in turns, studied the effect of carbon source composition, using a mix of acetic acid and butyric acid as organic substrate. The authors highlighted that the ratio between the two acids had an significant effect on hydrogen production. Sun et al. [48] optimized the process parameters for hydrogen production by a co-culture of *Clostridium acidisoli* and *Rhodobacter sphaeroides* from sucrose. They used the Plackett–Burman design to identify the key factors influencing the H_2 yield. Moreover, they selected the concentration of sucrose, the initial pH value, and the substrate to inoculum ratio as main influencing factors for hydrogen generation. Successively, these factors were considered for CCD and RSM analysis. The authors found that although the sucrose concentration and the pH interacted interdependently, H_2 yields were influenced by all of the key factors. Finally, Mirza et al. [49] evaluated the effect of the inoculum age, the nitrogen and the substrate concentration. They showed a quadratic effect of the inoculum age on the response and a significant interaction between all the considered factors.

Finally, explanatory mechanisms can be used to extrapolate the model to factor levels beyond the tested ranges. This can be useful to expand the optimization to not studied ranges which present difficulties in performing experiments or to reduce the number of experiments to be conducted. On the other hand, the extrapolation with polynomial models can be difficult as the curvatures in the region of data and the region of extrapolation can be different [50].

8.4.2 Machine learning methods

Machine learning methods (MLM) are advanced modelling techniques which can be manged without prior knowledge of the metabolic kinetics. These methods act increasing the model performance through the experience recorded by data [51]. MLM are low-cost

efficient tools which can be used for the real-time monitoring and prediction of the biohydrogen production. As they can approximate all kinds of non-linear functions, the application of MLM can provide a higher level of prediction accuracy compared to the DOE method [52]. On the other hand, MLM require a very large data set.

This methods have been widely used for the dark fermentation process optimization [53,54]. Despite their potentialities, also few applications have been reported for the PF to date.

Monroy et al. [55] tested the Artificial Neural Networks (ANN) algorithm as modelling technique to predict hydrogen production by a PNSB consortium. PF tests were performed under different light intensities, pH and metals concentration conditions. The model was calibrated and validated as well. The best ANN architecture provided a coefficient of correlation of 0.939.

Aghbashlo etl al. [56] proposed a novel hybrid fuzzy clustering-ranking approach coupled with radial basis function (RBF) neural network for the optimization of the syngas conversion to hydrogen process by the photo fermentative bacterium *Rhodospirillum Rhubum*. The RBF neural network was used to correlate exergetic outputs (normalized exergy destruction as well as rational and process exergetic efficiencies) to two input variables (agitation speed and syngas flow rate). The developed model predicted the exergetic performance parameters of the bioreactor with an R^2 value of 0.90, indicating a good accuracy of the method.

Finally, the support vector machines method (SVM) has been successfully applied to fault detection and diagnosis by Monroy et al. to construct data-based classification models [57]. Classification models were based on supervised learning, which consists of labelling all the experiments according to classes of faulty or undesired scenarios. The classification method can learn and train from these data so that the resulting models are expected to detect and diagnose those scenarios in further experiments. Diagnosis models were successively validated, obtaining a correct diagnosis of the undesired scenarios. The diagnosis performance indices (F1 score) indicated the reliability of the models.

8.5. Non-ideal reactor models

8.5.1 Computational Fluid Dynamic (CFD) and Lattice-Boltzmann models

A multi-scale modeling approach may be useful to provide a comprehensive view of biochemical reactions coupled with fluid flow and mass transfer phenomena, which are difficult to understand by conducting experimental studies alone. During the last few years, optimization strategies related to PBRs design have been developed, although the number of studies is quite low.

Table 8.3 summarizes different mathematical models, related to PBRs configuration, used to optimize the process. Usually, the considered model outputs are substrate consumption and hydrogen production. Velocity distribution into the PBR are also considered.

Table 8.3 Non-ideal reactor models used for photo fermentation process

PBR type	Model	Output	Reference
Annular PBR	CFD	velocity distribution, average velocity	[29]
Cylinder biofilm reactor	Lattice-Boltzmann	substrate consumption, hydrogen production	[67]
Granule-packed PBR	Lattice-Boltzmann	substrate consumption, hydrogen production	[69]
Granule-packed PBR	Lattice-Boltzmann	substrate consumption, hydrogen production	[68]
Granule-packed PBR	Multiphase-Mixture Model	substrate consumption, hydrogen production	[62]
Granule-packed PBR	Multiphase-Mixture Model	substrate consumption, hydrogen production	[64]
Tubular PBR	CFD	Temperature distribution	[58]
Baffle PBR	CFD	Temperature distribution	[59]
Tubular PBR	Matsuura and Smith's model based	Light intensity distribution, hydrogen production	[70]

As it can be deduced from the Table, three different models have been proposed, namely the computational fluid dynamic model (CFD), its modification (i.e. the multiphase mixture model (MM)) and the Lattice-Boltzmann model (LB).

CFD model allows the study of the influence of operating parameters on process development, and the process hydrodynamics at a local scale. These models define the flow pattern and characterize the reactor hydraulic behaviour. The reactor is discretized using a computational grid and the governing equations, which have to be formulated and solved, are the fundamental mass, momentum and energy conservation equations. Although CDF models are high demanding form a computational point of view and more complex than kinetic and parametric models, they can be effectively utilised for an accurate prediction of multiphase flows (i.e. fluid-fluid or fluid-solid flows). When the interphase laws are unknown or in order to simplify the model, the MM model, which is a modification of the CFD model, can be used. MM model is an alternative formulation which is able to account for multiple phases as constituents of a multiphase mixture contained in a bioreactor.

Mass conservation and momentum conservation in a generic phase 'k' and multiphase mixture are written as:

$$\nabla \cdot (\rho_k u_k) = \dot{m}_k \quad (20a)$$

$$\rho_k u_k = -\frac{K k_{rk}}{\nu_k}(\nabla \rho_k - \rho_k g) \quad (20b)$$

$$\nabla \cdot (\rho u) = \sum \dot{m}_k \quad (20c)$$

$$\rho u = -\frac{K}{\nu}\left(\nabla \rho - \gamma_\rho \rho g\right) \quad (20d)$$

where k_{rk} is the relative permeability of the phase k, g is the gravitational acceleration and ν is the cinematic viscosity. Moreover, K represents the absolute permeability and γ_ρ is the density correlation factor.

Basak et al. [29] developed a CFD study to obtain the velocity distribution and the average velocity in an annular PBR. The obtained results confirmed uniform fluid dynamics, light distribution and temperature in the PBR.

Zhiping et al. [58] used a CFD model to determine the heat transfer behaviour in a tubular photo-bioreactor. The authors considered the light radiation as the main factor affecting the temperature distribution. The small difference of temperature between the centre and edge of the reactor indicated a balanced illumination. The model was also validated with experimental data. Moreover, Zhang et al. [59] studied the influence of the inlet velocity in a baffle photo-bioreactor. They found that the inlet velocity had a marked impact on the heat transfer. The optimum inlet velocity value was found to be 0.0036 m s^{-1}. Numerical simulations were compared to experimental data, resulting in a good agreement.

When complex hydrodynamics, mass transfer and biochemical reactions are included, CFD is difficult to apply because of high computational requirements [60]. For this reason, CFD models have been used for the PF process exclusively for hydrodynamic simulations, without taking into account biochemical phenomena. However, few CFD models which couple hydrodynamics with biochemical reaction have been proposed for other biohydrogen production processes (e.g. dark fermentation) and can be adapted to the PF case [61]. The latter approach can be used for a wider range of applications than kinetic models, and includes the optimization and the control of the bioreactor for an efficient scale-up of the process. On the other hand, only simplified kinetics can be implemented because simulations are too intensive by including the high nonlinearities of kinetic expressions [51].

Liao et al. [62] and Guo et al. [63] proposed a MM model to study the interaction mechanism between biochemical reactions and transfer processes. They used similar

reactors packed with transparent gel granules in which bacterial cells were immobilized. Both models were based on the following assumptions: i) isothermal and steady-state conditions; ii) the fluid flow is one-dimensional along the height direction and it is laminar (described by Darcy's law); iii) the physical properties of the fluid are constant; iv) the biochemical reactions only occur inside the gel granules; v) hydrogen and carbon dioxide are the only gaseous products and the mole ratio is 2:1; vi) the light intensity is uniform.

The absolute permeability K and the density correlation factor γ_ρ are defined as:

$$K = \frac{\varepsilon^3 r_{gr}^2}{45(1-\varepsilon)^3} \tag{21a}$$

$$\gamma_\rho = \frac{\Sigma_k \rho_k \lambda_k}{\Sigma_k \rho_k s_k} \tag{21b}$$

where ε is the porosity of the packed bed, r_{gr} is the radius of the granule, s_k represents the saturation of phase k and λ_k is the mobility of phase k.

The conservation of species 's' in the multiphase mixture, in turns, is described as:

$$\nabla \cdot (\gamma_s \rho u \omega^s) = \nabla \cdot (\varepsilon \rho D^s \nabla \omega^s) + \nabla \cdot \{\varepsilon \textstyle\sum_k [\rho_k s_k D_k^s (\nabla \omega_k^s - \nabla \omega^s)]\} - \nabla \cdot (\textstyle\sum_k \omega_k^s j_k) - \Phi^s \tag{22}$$

where Φ^s is the substrate degradation rate, γ_s is the advection correction factor, ω is the mass fraction, D is the effective diffusion coefficient and j represents the diffusive flux. Finally, the authors modelled the gas-transfer by a diffusive law by completely neglecting the solid phase.

The mass transport inside the granules is modelled by Fick's law,

$$D_{gr}^s \frac{d^2 C_{gr}^s}{dr^2} + \frac{2D_{gr}^s}{r} \frac{dC_{gr}^s}{dr} = \frac{\Phi_{gr}^s}{M^s} \tag{23}$$

where "gr" refers to the granule and M is the molecular weight. The substrate biodegradation rate inside the granule Φ_{gr}^s is

$$\Phi_{gr}^s = \left(\frac{1}{Y_{\frac{x}{s}}} \mu + m\right) \psi C^C \tag{24}$$

where $Y_{\frac{x}{s}}$ is the cell yield, ψ is the cell density increasing coefficient, C^C defines the cell density and m is the maintenance coefficient. The specific growth rate μ is modelled by Monod's equation and the hydrogen production by the Luedeking-Piret model. The influence of light variations was not considered, as the defined kinetic growth rate and the substrate biodegradation rate are nonlinear functions of temperature and pH. Governing equations were solved numerically [62,64].

Liao et al. [62] observed that a high influent flow led to an increase of the hydrogen production, due to the improved substrate transport from the solution to the granules. Guo

et al. [64] reported that the increase of the specific area for substrate transfer due to the lower porosity of the packed bed increased the amount of substrate transferred into the granules. Consequently, more hydrogen was produced using the same feeding substrate. Nevertheless, in this model it is not considered that the lower porosity also enhances the light penetration in the reactor. Both the models were successfully calibrated and validate using real scale experimental data.

Finally, some authors used the LB model as a simplified alternative to the classical CDF. In many engineering applications, the LB model has been found to be a useful tool to simulate biochemical reactions in PBRs coupled with the hydrodynamics and the mass transfer equation. It reduces a continuum to few particles, limiting the possible spatial positions of particles and microscopic momenta, and confining the particle positions to the nodes of a lattice [65]. This model has several advantages such as the simplicity of the algorithm and of the implementation, and the capability of stable and accurate simulations [66,67]. The method is based on a simplified kinetic model for particle velocity distribution functions, which incorporate the essential physics of microscopic processes. Then, macroscopic properties, such as velocity, density, concentration and temperature, can be determined through these distribution functions [67]. Some authors used this method to describe PF process in immobilized biomass PBRs [67,68]. These authors deeply focused on the hydrodynamic characterization of the bioreactor, while they simplified the biochemical description of PSB activities. For instance, the effect of light is not accounted by the model and the biofilm is described as a stationary thin layer. Their models are based on the following simplifying assumptions: i) steady-state biofilm is formed on the support surface; ii) biochemical reactions only occur on the support surface; iii) steady-state of the flow and the reaction system; iv) biochemical reactions operate at optimal pH and temperature; v) the released heat from bioreactions can be neglected; vi) the produced hydrogen completely dissolves in the solution. A distribution function related to the flow field (f_i) and a distribution function related to the species concentration field ($g_{i,\sigma}$), were used to couple bioreactions with mass transfer and hydrodynamics (52):

$$f_i(x + e_i\delta_t, t + \delta_t) - f_i(x,t) = -\tau^{-1}\left(f_i(x,t) - f_i^{eq}(x,t)\right) \quad (25a)$$

$$g_{i,\sigma}(x + e_i\delta_t, t + \delta_t) - g_{i,\sigma}(x,t) = -\tau^{-1}\left(g_{i,\sigma}(x,t) - g_{i,\sigma}^{eq}(x,t)\right) + J_{i,\sigma}\delta_t R_\sigma \quad (25b)$$

where x is the cartesian position vector, δ_t the time space, e_i the discrete particle velocity, τ is the dimensionless relaxation time, $J_{i,\sigma}$ the specially chosen constant and R_σ the

dimensionless react source term of species σ. Finally, f_i^{eq} and $g_{i,\sigma}^{eq}$ are the corresponding equilibrium distribution functions and are expressed as:

$$f_i^{eq} = w_i \rho \left[1 + \frac{3e_i u}{c^2} + \frac{9(e_i u)^2}{2c^4} - \frac{3u^2}{2c^2}\right], \quad (26a)$$

$$g_{i,\sigma}^{eq} = c_\sigma \left(J_{i,\sigma} + k_i \frac{e_i u}{c^2}\right), \quad (26b)$$

where c is the Lattice velocity and $w_i$the weight coefficient.

ρ, u and c_σ are the macroscopic density, the fluid flow velocity and the σ-species concentration respectively. They are evaluated as follows:

$$\rho = \Sigma f_i, \quad (27a)$$

$$\rho u = \Sigma e_i f_i, \quad (27b)$$

$$c_\sigma(x,t) = \Sigma g_{i,\sigma}. \quad (27c)$$

Yang et al. (52) implemented a multi-component LB model to simulate the biochemical reaction system, the hydrodynamics and the mass transfer in a circular cylinder biofilm reactor. They obtained the velocity field by using a non-equilibrium extrapolation method for the curved boundary conditions. Obtained results showed that increasing Reynolds number led to a substrate and product concentration decrease. Then, it resulted in decreasing substrate consumption efficiency, while hydrogen yield kept constant. Indeed, substrate and by-products inhibition effects were ignored. Finally, at the back of the cylinder was possible to obtain the highest hydrogen concentration. They demonstrated the useful application of LB model to the biochemical production of hydrogen by PSB.

LB model for flow in porous media on the representative elementary volume (REV) scale was used by Liao et al. [69] to investigate the effect of operational conditions on hydrogen production in a porous granule-packed PBR. The results allowed obtaining the light intensity, which led to a maximum hydrogen yield and a maximum substrate consumption efficiency. The increasing permeability led to increasing hydrogen yields and decreasing substrate consumption efficiency, while the reverse effect was achieved increasing the porosity. Moreover, both hydrogen yield and substrate consumption efficiency decreased when the influent velocity increased.

A pore scale LB simulation method was used by Liao et al. [68] to simulate hydrogen production for a bioreactor filled with porous granule immobilized PNSB. When the porosity increased, the velocity and the substrate consumption increased, while hydrogen yield decreased. The validation model results showed a good agreement between the model and the experimental tests.

8.5.2 Light distribution models

The light intensity and the light distribution into reactors are key issues for the light conversion efficiency optimization in order to properly design and scale-up PBRs. Light intensity strongly affects PNSB growth. In particular, the inhibition effect of light on PF process needs to be accounted when modelling such process. As reported in the previous paragraphs, many kinetic and statistic models have been proposed taking into account the light intensity. On the other hand, these models are not able to account for light distribution, as the variation of light in space is completely neglected. However, as far as concern the process scale-up and the PBRs design, the light distribution inside the reactor is a key issue to be taken into account.

Zhiping et al. [58] considered the light radiation as the main factor affecting the temperature distribution in the bioreactor. The authors used a CFD model to indirectly determine the light distribution through the heat transfer. The limited temperature difference between the centre and edge of the reactor indicated a balanced illumination. The model was validated with experimental data conducted using a tubular PBR supplied by LED laps. It is worth underlining that, despite the effectiveness of the mentioned method, the heat transfer is an indirect monitoring parameter, which therefore strongly depends on the utilized light source. Moreover, the effect of light distribution on the conversion efficiency and the products formation has not been considered. Even though the light dependence is a crucial aspect of the PF process, the development of mathematical models taking into account how the light distribution influences the production process remains scarce to date.

Based on Matsuura and Smith's diffusion model (Matsuura and Smith, 1970), Katsuda et al. [70] estimated the light distribution in an externally illuminated cylindrical photo-bioreactor, which is the most popular PBR for the PF process.

The authors assumed that the incident light rays proceed in every direction and they calculated the local intensity as the sum of the light intensities. The light pass length of light L through a generic point P was calculated as follows:

$$L_{(r,\theta)} = -rcos\theta + \sqrt{R^2 - (rsin\theta)^2}, \quad (28)$$

Where r is the distance of the generic point P from the centre of the reactor O, θ is the angle between OP and L and R is the reactor radius.

The light intensity at P was calculated by integrating the light intensity at the distance *r* from the θ direction ($I_{(r,\theta)}$) from 0 to 2π as below

$$I_{(r)} = \int_0^{2\pi} I_{(L(r,\theta)} d\theta. \quad (29)$$

Since Lambert–Beer's law, which is the most diffused equation for microalgae models, was found to be not useful for explaining the decrease in the intensity, the authors used an empirical expression:

$$I_{(L)} = \frac{I_0}{(0.0216L + 1)^{1.54}(0.130CL + 1)^{1.18}}$$

Where C is the cell concentration and L is the pass length.

The model was validated using light intensities measurement from every direction, conducted in an externally illuminated cylindrical photo-bioreactor. Moreover, the light distribution was applied to estimate the hydrogen production by *R. capsulatus* ST-410 using the same photo-bioreactor. The obtained result was in good agreement with experimental data. The local specific hydrogen production rate Hr at P was calculated as $H_r = 2\pi rhC\nu_{I,}$

Where h is the height of the reactor and ν_I is the hydrogen specific production rate. The overall hydrogen production H was calculated integrating with respect to *r* from 0 to *R* as follows:

$$H = \int_0^R rC\nu_{I(r)}dr.$$

A large number of light distribution models considering other types of reactors have been proposed in the microalgae field. They concern solar irradiation systems applied to flat panel [71] and tubular PBRs [72] and artificial irradiation systems applied to both external and internal radiated reactors [71,73]. Such models could be applied to the PF process as well.

8.6. Models comparison and future perspectives

This study represents a supporting tool for researchers who approach the problem of mathematical modeling of photo fermentation process for both academic or industrial purposes. Depending on the specific application, the selection of the most appropriate model is crucial for the identification of photo fermentation dynamics and environmental factors influencing the metabolic activities. In other words, the most effective model to use strongly depends on the different aspects to highlight and on the effective purpose of the adopted photo bioreactor. **Table 8.4** summarises the possible applications, advantages and disadvantages of the reviewed modelling approaches.

Table 8.4 Models comparison

Model Type	Possible Applications	Advantages	Disadvantages
Kinetic Models			
Empirical	Analysis and Comparison	Simple	Do not take into account the process mechanism
Mechanistic	Optimization, scale-up, Bioreactor control	Take into account the process mechanism	Complex
Parametric Models			
Design Of Experiments	Analysis and Comparison, Optimization, Variables interaction analysis	Reduced number of experiments	Limited to polynomial models, Can take into account only few variables, Do not take into account the process mechanism
Artificial Neural Nethworks	Bioreactor control, Optimization	Do not require a prior specification of suitable fitting functions	Require a large data set, Do not take into account the process mechanism
Non-ideal reactor models			
Computational Fluid Dynamics	Design, Scale-up, Optimization Bioreactor Control	Real-flow conditions (multiphase), Possibility of coupling hydrodynamics with kinetics	Complexity of the algorithms
Lattice-Boltzmann	Design, Scale-up, Optimization Bioreactor Control	Simplified computational requirements, Possibility of coupling hydrodynamics with kinetics	Only simplified kinetic models can be used Less accuracy

The comparative analysis of the models proposed in the available literature for simulating, designing and controlling photo fermentation processes leads to underline some useful remarks. Kinetic models are exhaustive to describe the process from a pure biochemical point of view, without considering the influence of the bio-reactor hydrodynamics. By taking into account several environmental parameters, they allow for an accurate prediction of the hydrogen production, the biomass growth and the substrate consumption. The most frequently applied equations used to simulate biomass growth are based on the classical Monod's formulation. Other modified versions have been proposed to include the effect of additional parameters (e.g. substrate inhibition, light intensity, pH value, temperature). Moreover, the logistic models and its modifications have been widely used to describe microbial growth in case of nutrients limiting conditions, and/or high biomass concentration. For substrate consumption modeling, Michaelis Menten equation and the conventional or modified Luedeking-Piret model, which simply assumes

that substrate consumption is linearly dependent on both instantaneous biomass concentration and biomass growth rate, have also been frequently proposed. Regarding products formation, both the Luedeking Piret model, Gompertz equation and their modifications satisfactorily describes the cumulative hydrogen production. Kinetic models are useful to understand how the different biological mechanisms of PF evolve. Among them, empirical models are simpler and more manageable with respect to mechanistic models. On the other hand, mechanistic models are more complex, more refined and more realistic. They properly describe the mechanism behind the process. The development of an exhaustive mechanistic model accounting for all the crucial biochemical aspects of photo fermentation may be successfully applied to a wide range of microbiology and engineering case studies. It is noteworthy remark that kinetic models do not take into account the spatial variability. Consequently, they can be applied only to CSTR reactors and cannot be used for the bioreactor design, which requires a non-ideal reactor model.

Parametric Models are useful to study the influence and the interaction between the operational conditions. Two different methods have been used: DOE and ANN. DOE can be divided into two different approaches: full factorial design and fractional factorial design. A full factorial design approach requires a larger number of experiments, consequently, sometimes a fractional factorial approach can be more advisable. Both the Box-Behnken Design (BBD), and the Central Composite Design (CCD) approaches have been proposed. Moreover, the Analysis of Variance (ANOVA) of the regression equation can be used to identify the significant factors.

In addition, the ANN approach can provide a higher level of prediction accuracy compared to DOE and can be used for real time monitoring and bioreactor control. On the other hand, it requires a larger number of data. The disadvantages of the statistic models are that they do not take into account the biochemical process mechanism and the influence of the reactor hydrodynamics. They are generally valuable for process optimization and management, but limited to a specific examined case study. The biological system is effectively treated as a black box.

Conversely, the reactor configuration is the main object of non-ideal reactors models. These models couple biochemical reactions with fluid flow and mass transfer phenomena. They deeply focus on the hydrodynamic characterization of the photo bioreactor. Two different approaches have been proposed: the computational fluid dynamic model (CFD) and its modification (the multiphase mixture model (MM)) and the Lattice-Boltzmann model (LB). CFD model are useful to study the influence of operating parameters on

process development, and the process hydrodynamics at a local scale. The Lattice-Boltzmann approach has the advantage of a simpler algorithm compared to CFD. However, it is less realistic, as it reduces a continuum to few particles. In general, due to the complexity of the algorithms, non-ideal reactors models simplify the biochemical description of PNSB activities. This approach is therefore useful to develop optimization strategies for PBRs design but not to understand the biological mechanism.

Some of the revised models have been calibrated and validated based on laboratory-scale experiments. Majority of KMs have been calibrated. Conversely, the validation procedure was carried out only for few studies. Regarding the DOE method, optimal production values have been verified based on experimental data. Validation experiments have been conducted utilizing the optimal values of variables calculated by models. Finally, the reviewed NIRMs have been verified based on the comparison of numerical simulations with the analytical solutions or validated with experimental data. All the available information regarding calibration and validation procedures and the fitting coefficients indicating model accuracy have been reported in the APPENDIX B.

Up to date, there is still a lack of models describing exhaustively the bioconversion process occurring in photo fermentation reactors. There is not a comprehensive model able to completely take into account all the biotic and abiotic parameters affecting photo fermentation, and able to fit a wide spectrum of experimental data. Moreover, despite the presence of models on PHAs accumulation phenomenon, there are no photo fermentation models considering the contextual hydrogen production and PHB accumulation. Finally, it is important to underline that, due to the local supersaturation of the dissolved gas, gas production also results from the bubble nucleation within the liquid medium. Consequently, an interesting perspective should be the definition of a mathematical model able to account for a dispersed bubbly phase. Actually, despite the presence of dispersed phase models, no information is available in the literature regarding this approach applied to the PF process.

Further research efforts are therefore required to develop a complete model of photo fermentation in order to provide a useful tool for future engineering applications.

References

[1] Bianchi L, Mannelli F, Viti C, Adessi A, De Philippis R. Hydrogen-producing purple non-sulfur bacteria isolated from the trophic lake Averno (Naples, Italy). Int J Hydrogen Energy 2010;35:12216–23. https://doi.org/10.1016/J.IJHYDENE.2010.08.038.

[2] De Philippis R, Ena A, Guastiini M, Sili C, Vincenzini M. Factors affecting poly-β-hydroxybutyrate accumulation in cyanobacteria and in purple non-sulfur bacteria. FEMS Microbiol Lett 1992;103:187–94. https://doi.org/10.1016/0378-1097(92)90309-C.

[3] Luongo V, Ghimire A, Frunzo L, Fabbricino M, d'Antonio G, Pirozzi F, et al. Photofermentative production of hydrogen and poly-β-hydroxybutyrate from dark fermentation products. Bioresour Technol 2017;228:171–5.

[4] Sasikala CH, Ramana CHV, Rao PR. Regulation of simultaneous hydrogen photoproduction during growth by pH and glutamate in Rhodobacter sphaeroides O.U. 001. Int J Hydrogen Energy 1995;20:123–6. https://doi.org/10.1016/0360-3199(94)E0009-N.

[5] Eroğlu E, Eroğlu İ, Gündüz U, Yücel M. Effect of clay pretreatment on photofermentative hydrogen production from olive mill wastewater. Bioresour Technol 2008;99:6799–808. https://doi.org/10.1016/J.BIORTECH.2008.01.076.

[6] Ghosh S, Dairkee UK, Chowdhury R, Bhattacharya P. Hydrogen from food processing wastes via photofermentation using Purple Non-sulfur Bacteria (PNSB) – A review. Energy Convers Manag 2017;141:299–314. https://doi.org/10.1016/J.ENCONMAN.2016.09.001.

[7] Seifert K, Waligorska M, Laniecki M. Brewery wastewaters in photobiological hydrogen generation in presence of Rhodobacter sphaeroides O.U. 001. Int J Hydrogen Energy 2010;35:4085–91. https://doi.org/10.1016/J.IJHYDENE.2010.01.126.

[8] Madukasi EI, Zhang G. Microaerobic biodegradation of high organic load wastewater by phototrophic bacteria. African J Biotechnol 2010;9:3852–60. https://doi.org/10.5897/AJB2010.000-3258.

[9] Monroy I, Guevara-López E, Buitrón G. A mechanistic model supported by data-based classification models for batch hydrogen production with an immobilized photo-bacteria consortium. Int J Hydrogen Energy 2016;41:22802–11. https://doi.org/10.1016/j.ijhydene.2016.10.100.

[10] Wang J, Wan W. Kinetic models for fermentative hydrogen production: A review.

Int J Hydrogen Energy 2009;34:3313–23. https://doi.org/10.1016/j.ijhydene.2009.02.031.

[11] Nath K, Das D. Modeling and optimization of fermentative hydrogen production. Bioresour Technol 2011;102:8569–81. https://doi.org/10.1016/J.BIORTECH.2011.03.108.

[12] Ghosh D, Sobro IF, Hallenbeck PC. Optimization of the hydrogen yield from single-stage photofermentation of glucose by Rhodobacter capsulatus JP91 using response surface methodology. Bioresour Technol 2012;123:199–206. https://doi.org/10.1016/j.biortech.2012.07.061.

[13] Das D, Veziroglu TN. Advances in biological hydrogen production processes. Int J Hydrogen Energy 2008;33:6046–57. https://doi.org/10.1016/J.IJHYDENE.2008.07.098.

[14] Khatipov E, Miyake M, Miyake J, Asada Y. Accumulation of poly-β-hydroxybutyrate by Rhodobacter sphaeroides on various carbon and nitrogen substrates. FEMS Microbiol Lett 1998;162:39–45. https://doi.org/10.1016/S0378-1097(98)00099-8.

[15] Adessi A, De Philippis R. Hydrogen Production: Photofermentation. In: Hallenbeck PC, editor. Microb. Technol. Adv. Biofuels Prod., Boston, MA: Springer US; 2012, p. 53–75. https://doi.org/10.1007/978-1-4614-1208-3_4.

[16] Androga DD, Özgür E, Eroglu I, Gündüz U, Yücel M. Significance of carbon to nitrogen ratio on the long-term stability of continuous photofermentative hydrogen production. Int J Hydrogen Energy 2011;36:15583–94. https://doi.org/10.1016/J.IJHYDENE.2011.09.043.

[17] Wang X, Fang Y, Wang Y, Hu J, Zhang A, Ma X, et al. Single-stage photo-fermentative hydrogen production from hydrolyzed straw biomass using Rhodobacter sphaeroides. Int J Hydrogen Energy 2018;43:13810–20. https://doi.org/10.1016/J.IJHYDENE.2018.01.057.

[18] Lazaro CZ, Bosio M, Ferreira J dos S, Varesche MBA, Silva EL. The Biological Hydrogen Production Potential of Agroindustrial Residues. Waste and Biomass Valorization 2015;6:273–80. https://doi.org/10.1007/s12649-015-9353-8.

[19] Wu SC, Liou SZ, Lee CM. Correlation between bio-hydrogen production and polyhydroxybutyrate (PHB) synthesis by Rhodopseudomonas palustris WP3-5. Bioresour Technol 2012;113:44–50. https://doi.org/10.1016/J.BIORTECH.2012.01.090.

[20] Montiel-Corona V, Revah S, Morales M. Hydrogen production by an enriched

photoheterotrophic culture using dark fermentation effluent as substrate: Effect of flushing method, bicarbonate addition, and outdoor–indoor conditions. Int J Hydrogen Energy 2015;40:9096–105. https://doi.org/10.1016/J.IJHYDENE.2015.05.067.

[21] Adessi A, De Philippis R. Photobioreactor design and illumination systems for H2 production with anoxygenic photosynthetic bacteria: A review. Int J Hydrogen Energy 2014;39:3127–41. https://doi.org/10.1016/J.IJHYDENE.2013.12.084.

[22] Reungsang A, Zhong N, Yang Y, Sittijunda S, Xia A, Liao Q. Hydrogen from Photo Fermentation. In: Liao Q, Chang J, Herrmann C, Xia A, editors. Bioreact. Microb. Biomass Energy Convers., Singapore: Springer Singapore; 2018, p. 221–317. https://doi.org/10.1007/978-981-10-7677-0_7.

[23] Sağır E. Photofermentative Hydrogen Production. Biohydrogen 2019:141–57. https://doi.org/10.1016/B978-0-444-64203-5.00006-X.

[24] Nath K, Muthukumar M, Kumar A, Das D. Kinetics of two-stage fermentation process for the production of hydrogen. Int J Hydrogen Energy 2008;33:1195–203. https://doi.org/10.1016/J.IJHYDENE.2007.12.011.

[25] Obeid J, Magnin JP, Flaus JM, Adrot O, Willison JC, Zlatev R. Modelling of hydrogen production in batch cultures of the photosynthetic bacterium Rhodobacter capsulatus. Int J Hydrogen Energy 2009;34:180–5. https://doi.org/10.1016/j.ijhydene.2008.09.081.

[26] Gadhamshetty V, Sukumaran A, Nirmalakhandan N, Thein Myint M. Photofermentation of malate for biohydrogen production - A modeling approach. Int J Hydrogen Energy 2008;33:2138–46. https://doi.org/10.1016/j.ijhydene.2008.02.046.

[27] Wang YZ, Liao Q, Zhu X, Li J, Lee DJ. Effect of culture conditions on the kinetics of hydrogen production by photosynthetic bacteria in batch culture. Int J Hydrogen Energy 2011;36:14004–13. https://doi.org/10.1016/j.ijhydene.2011.04.005.

[28] Akbari L, Mahmoodzadeh Vaziri B. Comprehensive modeling of photo-fermentation process for prediction of hydrogen production. Int J Hydrogen Energy 2017;42:14449–57. https://doi.org/10.1016/j.ijhydene.2017.04.119.

[29] Basak N, Jana AK, Das D. CFD modeling of hydrodynamics and optimization of photofermentative hydrogen production by Rhodopseudomonas palustris DSM 123 in annular photobioreactor. Int J Hydrogen Energy 2016;41:7301–17. https://doi.org/10.1016/j.ijhydene.2016.02.126.

[30] Sevinç P, Gündüz U, Eroglu I, Yücel M. Kinetic analysis of photosynthetic growth,

hydrogen production and dual substrate utilization by Rhodobacter capsulatus. Int J Hydrogen Energy 2012;37:16430–6. https://doi.org/10.1016/j.ijhydene.2012.02.176.

[31] Koku H, Eroğlu I, Gündüz U, Yücel M, Türker L. Kinetics of biological hydrogen production by the photosynthetic bacterium Rhodobacter sphaeroides O.U. 001. Int J Hydrogen Energy 2003;28:381–8. https://doi.org/10.1016/S0360-3199(02)00080-0.

[32] Özgür E, Uyar B, Öztürk Y, Yücel M, Gündüz U, Eroğlu I. Biohydrogen production by Rhodobacter capsulatus on acetate at fluctuating temperatures. Resour Conserv Recycl 2010;54:310–4. https://doi.org/10.1016/j.resconrec.2009.06.002.

[33] Uyar B, Eroglu I, Yücel M, Gündüz U. Photofermentative hydrogen production from volatile fatty acids present in dark fermentation effluents. Int J Hydrogen Energy 2009;34:4517–23. https://doi.org/10.1016/j.ijhydene.2008.07.057.

[34] Zhang XW, Zhang YM, Chen F. Kinetic models for phycocyanin production by high cell density mixotrophic culture of the microalga Spirulina platensis. J Ind Microbiol Biotechnol 1998;21:283–8. https://doi.org/10.1038/sj.jim.2900581.

[35] Obeid J, Flaus J-M, Adrot O, Magnin J-P, Willison JC. State estimation of a batch hydrogen production process using the photosynthetic bacteria Rhodobacter capsulatus. Int J Hydrogen Energy 2010;35:10719–24. https://doi.org/10.1016/J.IJHYDENE.2010.02.051.

[36] Chen CY, Lu W Bin, Liu CH, Chang JS. Improved phototrophic H2 production with Rhodopseudomonas palustris WP3-5 using acetate and butyrate as dual carbon substrates. Bioresour Technol 2008;99:3609–16. https://doi.org/10.1016/j.biortech.2007.07.037.

[37] Frunzo L, Garra R, Giusti A, Luongo V. Modeling biological systems with an improved fractional Gompertz law. Commun Nonlinear Sci Numer Simul 2019;74:260–7. https://doi.org/10.1016/j.cnsns.2019.03.024.

[38] Zhang D, Xiao N, Mahbubani KT, del Rio-Chanona EA, Slater NKH, Vassiliadis VS. Bioprocess modelling of biohydrogen production by Rhodopseudomonas palustris: Model development and effects of operating conditions on hydrogen yield and glycerol conversion efficiency. Chem Eng Sci 2015;130:68–78. https://doi.org/10.1016/j.ces.2015.02.045.

[39] Puyol D, Barry EM, Hülsen T, Batstone DJ. A mechanistic model for anaerobic phototrophs in domestic wastewater applications: Photo-anaerobic model (PAnM).

Water Res 2017;116:241–53. https://doi.org/10.1016/J.WATRES.2017.03.022.

[40] Baş D, Boyacı İH. Modeling and optimization I: Usability of response surface methodology. J Food Eng 2007;78:836–45. https://doi.org/10.1016/J.JFOODENG.2005.11.024.

[41] Khuri AI, Mukhopadhyay S. Response surface methodology. Wiley Interdiscip Rev Comput Stat 2010;2:128–49. https://doi.org/10.1002/wics.73.

[42] Androga DD, Sevinç P, Koku H, Yücel M, Gündüz U, Eroglu I. Optimization of temperature and light intensity for improved photofermentative hydrogen production using Rhodobacter capsulatus DSM 1710. Int J Hydrogen Energy 2014;39:2472–80. https://doi.org/10.1016/J.IJHYDENE.2013.11.114.

[43] Basak N, Jana AK, Das D. Optimization of molecular hydrogen production by Rhodobacter sphaeroides O.U.001 in the annular photobioreactor using response surface methodology. Int J Hydrogen Energy 2014;39:11889–901. https://doi.org/10.1016/j.ijhydene.2014.05.108.

[44] Akman MC, Erguder TH, Gündüz U, Eroğlu I. Investigation of the effects of initial substrate and biomass concentrations and light intensity on photofermentative hydrogen gas production by response surface methodology. Int J Hydrogen Energy 2015;40:5042–9. https://doi.org/10.1016/j.ijhydene.2015.02.093.

[45] Jamil Z, Mohamad Annuar MS, Ibrahim S, Vikineswary S. Optimization of phototrophic hydrogen production by Rhodopseudomonas palustris PBUM001 via statistical experimental design. Int J Hydrogen Energy 2009;34:7502–12. https://doi.org/10.1016/j.ijhydene.2009.05.116.

[46] Ghosh D, Sobro IF, Hallenbeck PC. Stoichiometric conversion of biodiesel derived crude glycerol to hydrogen: Response surface methodology study of the effects of light intensity and crude glycerol and glutamate concentration. Bioresour Technol 2012;106:154–60. https://doi.org/10.1016/j.biortech.2011.12.021.

[47] Shi XY, Yu HQ. Optimization of glutamate concentration and pH for H2 production from volatile fatty acids by Rhodopseudomonas capsulata. Lett Appl Microbiol 2005;40:401–6. https://doi.org/10.1111/j.1472-765X.2005.01700.x.

[48] Sun Q, Xiao W, Xi D, Shi J, Yan X, Zhou Z. Statistical optimization of biohydrogen production from sucrose by a co-culture of Clostridium acidisoli and Rhodobacter sphaeroides. Int J Hydrogen Energy 2010;35:4076–84. https://doi.org/10.1016/j.ijhydene.2010.01.145.

[49] Mirza SS, Qazi JI, Zhao Q, Chen S. Photo-biohydrogen production potential of Rhodobacter capsulatus-PK from wheat straw. Biotechnol Biofuels 2013;6:2–13.

https://doi.org/10.1186/1754-6834-6-144.

[50] Okkerman PC, Vanderplassche EJ, Emans HJB, Canton JH. Validation of Some Extrapolation Methods with Toxicity Data Derived from Multiple Species Experiments. Ecotoxicol Environ Saf 1993;25:341–59. https://doi.org/https://doi.org/10.1006/eesa.1993.1031.

[51] Chezeau B, Vial C. Modeling and Simulation of the Biohydrogen Production Processes. Elsevier B.V.; 2019. https://doi.org/10.1016/b978-0-444-64203-5.00019-8.

[52] Ardabili SF, Najafi B, Shamshirband S, Bidgoli BM, Deo RC, Chau KW. Computational intelligence approach formodeling hydrogen production: A review. Eng Appl Comput Fluid Mech 2018;12:438–58. https://doi.org/10.1080/19942060.2018.1452296.

[53] Kanat G, Saral A. Estimation of Biogas Production Rate in a Thermophilic UASB Reactor Using Artificial Neural Networks. Environ Model Assess 2009;14:607–14. https://doi.org/10.1007/s10666-008-9150-x.

[54] Rosales-Colunga LM, García RG, De León Rodríguez A. Estimation of hydrogen production in genetically modified E. coli fermentations using an artificial neural network. Int J Hydrogen Energy 2010;35:13186–92. https://doi.org/https://doi.org/10.1016/j.ijhydene.2010.08.137.

[55] Monroy I, Guevara-López E, Buitrón G. Biohydrogen production by batch indoor and outdoor photo-fermentation with an immobilized consortium: A process model with Neural Networks. Biochem Eng J 2018;135:1–10. https://doi.org/10.1016/j.bej.2018.01.026.

[56] Aghbashlo M, Hosseinpour S, Tabatabaei M, Dadak A, Younesi H, Najafpour G. Multi-objective exergetic optimization of continuous photo-biohydrogen production process using a novel hybrid fuzzy clustering-ranking approach coupled with Radial Basis Function (RBF) neural network. Int J Hydrogen Energy 2016;41:18418–30. https://doi.org/10.1016/j.ijhydene.2016.08.123.

[57] Monroy I, Buitrón G. Diagnosis of undesired scenarios in hydrogen production by photo-fermentation. Water Sci Technol 2018;78:1652–7. https://doi.org/10.2166/wst.2018.435.

[58] Zhiping Z, Quanguo Z, Jianzhi Y, Lianhao L, Tian Z, Zhengbai L. CFD modeling and experiment of heat transfer in a tubular photo-bioreactor for photo-fermentation bio-hydrogen production. Int J Agric Biol Eng 2017;10:209–17. https://doi.org/10.3965/j.ijabe.20171001.2513.

[59] Zhang Z, Wu Q, Zhang C, Wang Y, Li Y, Zhang Q. Effect of inlet velocity on heat transfer process in a novel photo-fermentation biohydrogen production bioreactor using computational fluid dynamics simulation. BioResources 2015;10:469–81. https://doi.org/10.15376/biores.10.1.469-481.

[60] Liotta F, Chatellier P, Esposito G, Fabbricino M, Van Hullebusch ED, Lens PNL. Hydrodynamic mathematical modelling of aerobic plug flow and nonideal flow reactors: A critical and historical review. Crit Rev Environ Sci Technol 2014;44:2642–73. https://doi.org/10.1080/10643389.2013.829768.

[61] Wang X, Ding J, Guo WQ, Ren NQ. Scale-up and optimization of biohydrogen production reactor from laboratory-scale to industrial-scale on the basis of computational fluid dynamics simulation. Int J Hydrogen Energy 2010;35:10960–6. https://doi.org/10.1016/j.ijhydene.2010.07.060.

[62] Liao Q, Liu DM, Ye DD, Zhu X, Lee DJ. Mathematical modeling of two-phase flow and transport in an immobilized-cell photobioreactor. Int J Hydrogen Energy 2011;36:13939–48. https://doi.org/10.1016/j.ijhydene.2011.03.088.

[63] Wang CY, Cheng P. A multiphase mixture model for multiphase, multicomponent transport in capillary porous media—I. Model development. Int J Heat Mass Transf 1996;39:3607–18. https://doi.org/10.1016/0017-9310(96)00036-1.

[64] Guo CL, Cao HX, Pei HS, Guo FQ, Liu DM. A multiphase mixture model for substrate concentration distribution characteristics and photo-hydrogen production performance of the entrapped-cell photobioreactor. Bioresour Technol 2015;181:40–6. https://doi.org/10.1016/j.biortech.2015.01.022.

[65] Framework BLBM. 4 Lattice Boltzmann Models (LBMs) 4.1. Framework 1992:31–54.

[66] Chen S, Doolen GD. Lattice Boltzmann Method for Fluid Flows. Annu Rev Fluid Mech 1998;30:329–64. https://doi.org/10.1146/annurev.fluid.30.1.329.

[67] Yang Y, Liao Q, Zhu X, Wang H, Wu R, Lee DJ. Lattice Boltzmann simulation of substrate flow past a cylinder with PSB biofilm for bio-hydrogen production. Int J Hydrogen Energy 2011;36:14031–40. https://doi.org/10.1016/j.ijhydene.2011.04.026.

[68] Liao Q, Yang Y-X, Zhu X, Chen R, Fu Q. Pore-scale lattice Boltzmann simulation of flow and mass transfer in bioreactor with an immobilized granule for biohydrogen production. Sci Bull 2017;62:22–30. https://doi.org/10.1016/J.SCIB.2016.11.004.

[69] Liao Q, Yang YX, Zhu X, Chen R. Lattice Boltzmann simulation of substrate

solution through a porous granule immobilized PSB-cell for biohydrogen production. Int J Hydrogen Energy 2013;38:15700–9. https://doi.org/10.1016/J.IJHYDENE.2013.04.056.

[70] Katsuda T, Arimoto T, Igarashi K, Azuma M, Kato J, Takakuwa S, et al. Light intensity distribution in the externally illuminated cylindrical photo-bioreactor and its application to hydrogen production by Rhodobacter capsulatus. Biochem Eng J 2000;5:157–64. https://doi.org/10.1016/S1369-703X(00)00054-1.

[71] Suh IS, Lee SB. A light distribution model for an internally radiating photobioreactor. Biotechnol Bioeng 2003;82:180–9. https://doi.org/10.1002/bit.10558.

[72] Acién Fernández FG, García Camacho F, Sánchez Pérez JA, Fernández Sevilla JM, Molina Grima E. A model for light distribution and average solar irradiance inside outdoor tubular photobioreactors for the microalgal mass culture. Biotechnol Bioeng 1997;55:701–14. https://doi.org/10.1002/(SICI)1097-0290(19970905)55:5<701::AID-BIT1>3.0.CO;2-F.

[73] Cornet J-F, Dussap CG, Gros J-B, Binois C, Lasseur C. A simplified monodimensional approach for modeling coupling between radiant light transfer and growth kinetics in photobioreactors. Chem Eng Sci 1995;50:1489–500. https://doi.org/https://doi.org/10.1016/0009-2509(95)00022-W.

[74] Chen C-Y, Lu W-B, Wu J-F, Chang J-S. Enhancing phototrophic hydrogen production of Rhodopseudomonas palustris via statistical experimental design. Int J Hydrogen Energy 2007;32:940–9. https://doi.org/10.1016/J.IJHYDENE.2006.09.021.

[75] Özgür E, Mars AE, Peksel B, Louwerse A, Yücel M, Gündüz U, et al. Biohydrogen production from beet molasses by sequential dark and photofermentation. Int J Hydrogen Energy 2010;35:511–7. https://doi.org/10.1016/J.IJHYDENE.2009.10.094.

APPENDIX A

KINETIC MODELS PARAMETERS

BIOMASS GROWTH

MONOD BASED

$$\frac{dC_x}{dt} = \mu C_x\,,\ \mu = \left(\frac{\mu_m C_s}{k_s + C_s}\right)$$

Parameter	Meaning	Value	Reference
μ_m	maximum specific growth rate	0.3 h^{-1} 0.4 h^{-1} 0.0042 h^{-1} 0.012 h^{-1} (Droop model) 0.010 h^{-1} (Contois model) 1.54 d^{-1}	[25] [35] [9] [38] [38] [39]
K_S	saturation constant	10 g L^{-1} 19 g L^{-1} 5.2 0.06 g_{COD} L^{-1} 3.694 mM (Droop model) 5.425 mM (Contois model)	[25] [35] [27] [9] [38] [38]

LOGISTIC MODEL BASED

$$\frac{dC_x}{dt} = \mu C_x \left(1 - \frac{C_x}{C_{xm}}\right)$$

$$C_x = \frac{C_{xm}}{\left[1 + \exp\left(-k_c t\right)\left(1 - \frac{C_{xm}}{C_{x0}}\right)\right]}$$

Parameter	Meaning	Value	Reference
C_{xm}	maximum biomass concentration	0.5-1.9 g L^{-1} 1 g L^{-1} 1.35 g L^{-1} 0.99 g L^{-1} 0.71-1 g L^{-1}	[30] [26] [29] [28] [31]
C_{x0}	Initial biomass concentration	0.06-0.18 g L^{-1}	[30]
k_c or μ	apparent specific growth rate	0.022-0.066 h^{-1} 0.052 h^{-1} 0.060-0.144 h^{-1}	[30] [29] [31]
μ_m	maximum specific growth rate	0.17 h^{-1} 0.09 h^{-1}	[26] [28]

SUBSTRATE UTILIZATION

MICHAELIIS-MENTEN BASED

$$\frac{dC_s}{dt} = -\frac{1}{Y_{xs}}\mu C_x,$$

$$\mu = \left(\frac{\mu_m C_s}{k_s + C_s}\right)$$

Parameter	Meaning	Value	Reference
μ_m	maximum specific growth rate	0.3 h^{-1} 0.4 h^{-1}	[25] [35]
K_S	saturation constant	10 g L^{-1} 19 g L^{-1}	[25] [35]
Y_{xs}	yield for substrate utilization.	0.1 g g^{-1} 0.7 g g^{-1} 0.49 g g^{-1}	[25] (2) [9]

FIRST ORDER KINETIC

$$\frac{dC_s}{dt} = -K_1 C_s,$$

Parameter	Meaning	Value	Reference
K_1	Rate constant for a first-order reaction	0.011-0.038 h^{-1} 0.025 h^{-1} 0.001-0.026 h^{-1} 0.015-0.037 h^{-1}	[30] [32] [33] [31]

LUEDEKING-PIRET BASED

$$\frac{dC_s}{dt} = \frac{1}{Y_{sx}}\frac{dC_x}{dt} + \mu_{sx} C_x$$

Parameter	Meaning	Value	Reference
μ_{sx}	Substrate consumption rate constant	0.091 h^{-1} 0.0073 h^{-1}	[26] [28] [9]
Y_{xs}	Yield for substrate utilization	3.7 g g^{-1} 0.997 g g^{-1}	[26] [28] [9]

PRODUCT FORMATION

LUEDEKING-PIRET BASED

$$\frac{dC_p}{dt} = Y_{px}\frac{dC_x}{dt} + \mu_{px}C_x$$

Parameter	Meaning	Value	Reference
μ_{px}	Specific product formation rate	0.009 $g_{hydrogen}\ g_{biomass}^{-1}\ h^{-1}$ 0.00012 $g_{hydrogen}\ g_{biomass}^{-1}\ h^{-1}$ 12 $L_{hydrogen}L^{-1}$ 16 $L_{hydrogen}L^{-1}$	[26] [28] [9] [25] [35]
Y_{px}	Yield of product formation	0.45 g g^{-1} 3.2 g g^{-1} 0.028 g g^{-1} 1.42 $L_{hydrogen}\ g_{biomass}^{-1}$ 1 $L_{hydrogen}\ g_{biomass}^{-1}$	[26] [28] [9] [25] [35]

GOMPERTZ BASED

$$H(t) = H_m exp\left\{-exp\left[\frac{R_m.e}{H_m}(\lambda - t) + 1\right]\right\}$$

Parameter	Meaning	Value	Reference
R_m	Maximum cumulative hydrogen volume	0.14-0.5 mmol $L^{-1}h^{-1}$ 7 mL $L^{-1}h^{-1}$ 17.06-38.05 mL h^{-1}	[30] [29] [36]
H_m	cumulative hydrogen volume	23-58 mmol L^{-1} 700 mL L^{-1} 1506-3101 mL	[30] [29] [36]
λ	Lag time	17-128 h 14h	[30] [29]

CFD MODELS PARAMETERS

Parameter	Meaning	Value	Reference
ρ	solution density	1125 kg m^{-3}	[29,58,59]
ν	viscosity	1.3×10-3 $kgm^{-1}s^{-1}$	[29,58,59]
cp	specific heat	5.167 KJ $Kg^{-1}K^{-1}$	[58,59]
λ	thermal conductivity	0.63 W $m^{-1}K^{-1}$	[58,59]

MULTIPHASE MIXTURE MODEL PARAMETERS

Parameter	Meaning	Value	Reference
X_{cell}	Initial cell density	0.76 Kg m^{-3}	[62],[64]
C_{s0}	Inlet substrate concentration	10.8 Kg m^{-3} 60mM	[62] [64]
C_{H2}	Hydrogen concentration	0.05952 Kg m^{-3} 29.76 mM	[62] [64]

D_s	Substrate diffusion coefficient in gel granules	$7.94\ 10^{-10}\ m^2\ s^{-1}$ $2.86\ 10^{-5}\ m^2\ h^{-1}$	[62] [64]
D_{H2}	Hydrogen diffusion coefficient in gel granules	$6.36\ 10^{-10}\ m^2\ s^{-1}$ $2.29\ 10^{-5}\ m^2\ h^{-1}$	[62] [64]
D_{H2l}	Hydrogen diffusion coefficient in the liquid phase	$1.68\ 10^{-9}\ m^2\ s^{-1}$ $6.06\ 10^{-5}\ m^2\ h^{-1}$	[62] [64]
ν_l	Liquid phase viscosity	$0.801\ 10^{-6}\ m^2\ s^{-1}$	[62],[64]
ν_g	Gas phase viscosity	$9.89\ 10^{-5}\ m^2\ s^{-1}$	[62],[64]
ρ_g	Gas phase density	$0.7143\ Kg\ m^{-3}$	[62],[64]
σ_l	Surface tension of the liquid phase	$0.0728\ N\ m^{-2}$	[62],[64]
φ_x	Cell density increasing coefficient	1.97	[62],[64]

APPENDIX B

MODELS CALIBRATION AND VALIDATION

KINETIC MODELS

Calibration	Validation	References
Yes	-	[25]
Calibration performed using a program (Curve Expert 1.3) r = 0.95- 1 (biomass) R^2 = 0.84-0.99 (substrate)	-	[30]
Yes R^2 = 0.86-0.99	-	[33]
Yes	-	[35]
Yes Parameters from literature or determined by fitting the model to batch mode laboratory scale data	Yes	[26]
Logistic parameters were obtained fitting the experimental data of biomass concentration vs. time in Origin Pro software (version 8.5) R^2 = 97.99% (biomass) R^2 = 99.5% (substrate) R^2 = 99.9% P (Products, Gompertz) R^2 = 96.6% P (Products, Luedeking-Piret)	-	[29]
Yes Parameters determined by fitting the model to batch mode laboratory scale data)	Yes	[9]
Yes Parameters determined trough non-linear regression (nlinfit, Matlab) or adapted from literature	Yes Sum of squared errors: 0.0113	[28]
Parameters determined via Sigma Plot 8.0	-	[36]
Yes R^2 = 98% (biomass)	-	[31]
Parameters were either calculated by an explicit Euler method or obtained from literature	-	[38]. 2015
Yes The normalized root mean square error (nRMSE), the index of agreement (IoA), and the modeling efficiency (ME) were calculated. nRMSE=0.0792 IoA =0.9961 ME =0.9835		[37]
Yes	Yes	[39]

Yes Relative maximum errors: 36.8 % (biomass) 37.1 % (substrate) 48.6 % (products)	Yes	[27]

PARAMETRIC MODELS

Optimal values	**Validation**	**Reference**
Max rate H_2: 1.04 mmol/Lreactor·h Initial substrate concentration =35.35 mM initial biomass concentration =0.27 g VSS L^{-1} light intensity= 263.6 W/m2 (3955 lux) Lack of fit = 0.001	-	[44]
Max rate H_2: 0.566 mmol H_2/L/h, Max yield H_2: 0.326 mol H2/mol substrate Temperature: 27.5 °C Light Intensity: 287 W/m2 Lack of fit = 0.172-0.130	Max yield: H_2: 0.32 mol H2/mol substrate	[42]
Max yield H_2: 6.35 mol H2/mol glycerol Nitrogenase activity: 205 nmol of C2H4/ml/min Substrate concentration: 35 mM Nitrogen source concentration: 4.5 mM Light intensity: 175 W/m2 Lack of fit = 0.998-0.127	Max yield: H_2: 6.69 mol H2/mol glycerol Nitrogenase activity: 228 nmol of C2H4/ml/min	[46]
Average rate H_2: 7.97 mL H2 L^{-1} h^{-1}, Temperature: 32 °C, Substrate concentration: 15 mM, Nitrogen source concentration: 2 Mm Lack of fit = 0.0167	Measured average rate H_2: 7.92 mL H2 L^{-1} h^{-1}	[43]
Max rate H_2: 31.6 ml h^{-1} Acetate concentration = 2400 mg COD L^{-1} Butyrate concentration = 2900 mg COD L^{-1} Regression coefficient = 0.793	Max rate H_2: 39.5 ml h^{-1}	[36]
Average rate H_2: 6.885 mL H_2 L^{-1} h^{-1}, $FeCl_3$ concentration: 0.312 mM, Substrate concentration: 20 mM, Nitrogen source concentration: 4 mM Lack of fit = 0.027	Average rate H_2: 6.9 mL H_2 L^{-1} h^{-1}	[29]
Max rate H_2: 19.1 mL g^{-1} Nitrogen source concentration:7.01 mmol L^{-1} pH:7.31	R^2= 0.953	[47]
Max yield H_2: 1.05 mL mL^{-1} substrate; COD reduction: 31.71% Substrate concentration: 100% (v/v), Initial pH: 6, Light intensity: 4000 lux Inoculum concentration: 10% (v/v)	Max yield H_2: 0.66 mL mL^{-1} substrate COD reduction: 30.54%.	[45]

Agitation: 250 rpm Lack of fit = 0.004		
Max substrate conversion efficiency: 10.16 mol H2 mol substrate $^{-1}$ Substrate concentration: 11.43 g L^{-1} initial pH: 7.13 inoculum ratio of *C. acidisoli* to *R. sphaeroides*: 0.83	Max substrate conversion efficiency: 10.70 mol H2 mol substrate $^{-1}$	[48]
Max yield H_2: 598 ml L^{-1} Inoculum age: 48h, Substrate loading: 2 g, Nitrogen concentration: 300 mg L^{-1}	Error calculated comparing actual and predicted production: 0.21%-1.1%	[49]
Max rate H_2: 24.9 mL L^{-1} h^{-1} Substrate concentration: 20.8 mM, Nitrogen source concentration: 4.13 mM, FeCl3 concentration: 0.330 mM R^2= 0.963 (regression coefficient)	Max rate H_2: 24.7 mL L^{-1} h^{-1}	[74]
-	R^2= 0.939	[9]
-	R^2= 0.90	[56]
-	Validation using mechanistic model derived data and experimental lab scale data. F1 score = 55%-100%	[57]

NON-IDEAL REACTOR MODELS

Validation/Verification	**Reference**
-	[29]
Comparison of the numerical simulation with the analytical solution	[67]
Comparison of the numerical simulation with the analytical solution	[69]
Comparison between the hydrogen production achieved with the LB model and experimental results. Error: 5.4%-5.9%	[68]
Comparison between model results and experimental data of the hydrogen production and substrate consumption along time. Error: 2.8% -29.2%	[62]
Comparison between model results and experimental data of the hydrogen production and substrate consumption along time. Error: 9.6% -22.7%	[64]
Simulated and experimental temperature distribution were compared	[58]
Simulated and experimental temperature distribution were compared	[59]
Simulated and experimental overall hydrogen production rate and light intensity were compared	[70]

PART 3

Other biorefinery processes

Chapter 9

Improving biological production of poly(3-hydroxybutyrate-co-3-hydroxyvalerate) (PHBV) co-polymer: a critical review

This chapter has been published as: Policastro, G., Panico, A. and Fabbricino, M. (2021). Improving biological production of poly (3-hydroxybutyrate-co-3-hydroxyvalerate)(PHBV) co-polymer: a critical review. Reviews in Environmental Science and Bio/Technology, 1-35.

Improving biological production of poly(3-hydroxybutyrate-co-3-hydroxyvalerate) (PHBV) co-polymer: a critical review

Abstract

Although poly(3-hydroxybutyrate-co-3-hydroxyvalerate) (PHBV) is the most promising biopolymer for petroleum-based plastics replacement, the low processes productivity as well as the high sale price represent a major barrier for its widespread usage. The present work examines comparatively the existing methods proposed to enhance the yield of the PHBV co-polymer biological production processes and/or reduce their costs. The study is addressed to researchers working on the development of new biological production methods and/or the improvement of those currently used. At this aim, the authors have considered the analysis of some crucial aspects related to substrates and microorganism's choice. The production strategies have been individuated, presented and discussed, either based on a single aspect (type of substrate or microorganism) or based on combined aspects (type of substrate and microorganism). Operating conditions have been discussed as well. The analysis indicates that the addition of 3HV precursors is able to dramatically enhance the hydroxyvalerate fraction in the produced polymers. On the other hand, due to the high costs of the 3HV precursors, the utilization of wild bacterial species able to produce the hydroxyvalerate fraction from unrelated carbon sources (i.e no 3HV precursors) can also be considered a valuable strategy for costs reduction. Metabolic engineering techniques, in turn, can be successfully used to promote 3HV precursors-independent biosynthesis pathways and enhance the process productivity. The use of mixed cultures or extremophile bacteria avoids the need of sterile reaction environments, and therefore favours the process scale-up. The utilization of organic waste as substrate plays a key role for a sharp reduction of production costs. The selection of the most suitable substrate-microorganism combination cannot be separated by the adoption of an appropriate choice regarding the reactor configuration and the abiotic factors.

9.1.Introduction

The discovery of polyhydroxyalkanoates (PHAs) dates back to 1888, when Martinus W. Beijerinck, one of the cofounders of the environmental microbiology, observed, for the first time, PHAs granules in microorganisms' cytoplasm [1]. Over the next 80 years, scientists kept studying the microbial synthesis of various PHAs as an academic concern [2]. Only in the last few decades, due to the need of finding biodegradable materials able to replace conventional plastics, the studies on PHAs production have assumed a primary

interest. Indeed, from an environmental perspective, PHAs are the most suitable biopolymers for the production of biodegradable plastic materials [3]. Such conclusion has been deduced through different Life Cicle Assessment (LCA) studies, performed on various types of bioplastics and conventional plastics. Results from these analyses showed that, in terms of energy demand and greenhouse gases emissions, production and use of all bioplastics is more advantageous than conventional plastics. Conversely, bioplastics, such as those based on starch and corn, have a strong impact on the environment resulting in soil acidification and surface waters eutrophication because of fertilizers and chemicals used to cultivate the raw materials [4]. Among the different types of bioplastics, PHAs have the advantage to be produced from waste materials [5], thus avoiding the occurrence of the mentioned soil acidification and surface waters eutrophication phenomena.

Currently, researchers are focusing their attention on the enhancement of PHAs properties to promote their use in various applications [6]. It has been demonstrated, in fact, that different species of microorganisms are able to incorporate hydroxyvalerate (3HV) units into the PHB molecule, which is the most studied compound among the family of PHAs [7,8]. The result is a co-polymer, the poly(3-hydroxybutyrate-co-3-hydroxyvalerate), widely known with the acronym of PHBV, that owns better thermal and mechanical properties compared to PHB and all other PHAs. Due to enhanced physical and chemical characteristics, such as better mechanical flexibility and strength, shorter chain packing and lower toughness, PHBV is gaining attention from many researchers [9]. Compared to other PHAs, PHBV has become the most promising biopolymer to replace petroleum-based plastics in a wide range of applications (e.g. tissue engineering, biomaterial applications, everyday disposable objects and high mechanical resistance objects production) [10]. Moreover, due to its superior characteristics compared to other PHAs and other biopolymers, PHBV is particularly attractive for biomedical applications as well [9].

However, the high sale price of PHBV still represents a major barrier to its widespread diffusion [11]. On the base of techno-economic analysis, the PHBV production costs strongly depend on specific process conditions [12]. Therefore, it is necessary to address further efforts to enhance the production process efficiency as well as reduce the final cost of the product. A comprehensive review of the existing methods used to optimize the PHBV production is certainly relevant to provide a starting point to better address future investigations. An updated and critical analysis of such strategies is currently absent in

the literature and represents the object of the present paper. Therefore, this work is aimed at reducing the economic gap between PHBV and traditional plastics.

In particular, the paper contains the analysis of strategies concerning the enhancement of the productivity as well as those related to the reduction of costs, individuated on the basis of the available techno-economic analysis. In more details, the paper presents a comprehensive review of a massive number of published studies on strategies to improve the biological production of the co-polymer PHBV. The relevant information on the processes used to produce PHBV have been pointed out and compared. The peculiarities and the effectiveness of the adopted microbial species and substrates have been analysed. The efficiency of microorganisms, substrates and the microorganism-substrate combination have been assessed in terms of PHBV accumulation and hydroxyvalerate (3HV) monomer fraction. The most significant production strategies have been critically presented and discussed, highlighting, for each of them, the advantages as well as the disadvantages, in order to guide any reader towards a reasoned decision that might be suitable for his specific scope.

To facilitate the analysis, the reviewed studies are divided into two main groups. The first group includes all strategies based on microorganisms' selection, either the use of wild microorganisms or those metabolic engineered. The second group, instead, includes all strategies based on substrate selection and/or substrate pre-treatment/modifications (i.e. 3HV precursors co-substrates addition). Operative conditions and combinations of different strategies have been discussed as well. A final discussion on all presented strategies is critically conducted, with the aim of focusing the most performing. The study is, therefore, of great concern for researchers interested in developing new methods to produce PHBV and/or improve those currently used, with the aim of achieving optimal operating conditions, effective and efficient enough to promote an economically convenient full-scale production of PHBV.

9.2. PHBV biosynthesis processes, characteristics and applications

PHBV, also indicated as PHBHV or P(3HB-*co*-3HV), is a thermoplastic bio-polyester that structurally originates from the insertion of a 3HV unit into the PHB polymer structure (Figure 9.1).

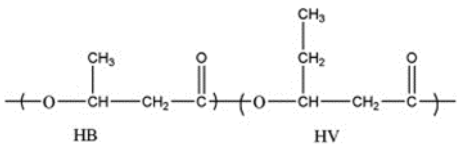

Figure 9.1 PHBV chemical structure

PHBV, as all the other PHAs, is the product of biosynthesis of a wide variety of both gram-positive and gram-negative bacteria [10]. Among wild microbes, the most used specie has been *Ralstonia eutropha*, also known as *Cupriavidus necator* or *Alcaligenes eutrophus* [13–17]. This bacterial strain can accumulate high PHBV amounts under unbalanced growth conditions (i.e. lack of nitrogen, phosphorus or sulfur). Recently, the archea *Haloferax Mediterranei,* an extremely halophilic microrganism, has gained a greater attention, due to its faster growth, its high PHBV productivity and its capacity of producing high quality products [18]. Different species of *Bacillus, Methilobacterium, Pseudomonas* and *Rhodospirillacee* have been also tested on various substrates [8,19–22]. Finally, even though less studied if compared to the previous mentioned microorganisms, *Alcaligenes*, *Comamonas*, *Halomonas* and *Rhodococcus* have been found to be capable to produce PHBV [23-26]. Microorganisms store PHAs in form of intracellular granules, with the aim of using them as energy reserve. PHAs accumulation is a strategy of microorganisms to increase their chance of survival under adverse environmental conditions [5]. Specifically, microorganisms can follow the metabolic pathway that results in PHAs production whenever one or more of the following specific conditions occur [27]: i) environmental signals, such as nutrient starvation, that leads to the activation of the PHA-gene expression; ii) presence of specific metabolic intermediates or cell components that activate the PHA synthetic enzymes; iii) enrichment of the required intermediates for PHA synthesis due to the inhibition of competing metabolic pathways.

Metabolic pathways promoting PHBV biosynthesis principally depend on the characteristics of the bacterial strain. The majority of PHBV accumulating bacterial

species store the biopolymer under nutrient (e.g. nitrogen, phosphorous or sulphur) starvation with excess of carbon source [10].

Figure 9.2 shows the simplified PHBV production pathway from glucose and propionic acid.

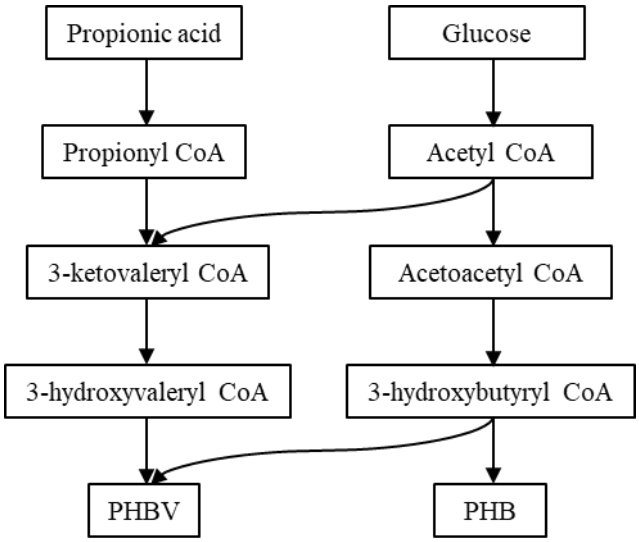

Figure 9.2 PHB and PHBV production pathways

As reported in Figure 9.2, the PHBV biosynthesis is catalysed by two key enzymes: the 3-hydroxybutyl-CoA (3HBCoA) and the 3-hydroxyvaleryl-CoA (3HVCoA). While the 3HBCoA can be obtained from a wide range of substrates by a large variety of bacteria, the majority of PHBV accumulating bacteria require the presence of precursors of the 3HV fraction (e.g. valerate and propionate) to synthetize the 3HVCoA.

Concerning the properties of PHBV, they have been extensively reviewed by Laycock et al. [28]. To sum them up, the 3HV fraction determines the defection of the PHB lamellae crystals, thus leading to the disruption of the PHB crystallinity [28]. The result is a more flexible structure of the bio-copolymer compared to the structure of polyhydroxybutirate-PHB. Such an improved flexibility is responsible for a general enhancement of all its mechanical properties [29]. A comparison of the main properties among PHBV, PHB and the widest diffused traditional plastic (low density polyethylene) are reported in Table 9.1.

Table 9.1 PHBV, PHB and low density polypropylene properties (Adapted from Strong et al. (2016)).

Polymer	Melting Temperature (°C)	Glass-Transition Temperature (°C)	Young's Modulus (GPa)	Tensile Strenght (MPa)	Elongation to Break (%)
PHB	180	4	3.5	40	5
P(3HB-co-20mol%£HV)	145	-1	0.8	20	50
Low density polypropylene	130	-30	0.2	10	620

PHBV is tougher and more elastic than PHB. The lower melting temperature of PHBV makes it easier and less expensive to be processed if compared to PHB. Moreover, as it can be easily noticed from Table 9.1, comparing PHB and PHBV properties, PHBV is more similar to the traditional low density polypropylene [30,31]. Compared to conventional plastic materials, PHBV shows similar physical and mechanical properties with the advantage of being totally biodegradable and biocompatible with a wide variety of cells [32]. In addition, it is non-toxic, and resistant to ultraviolet radiation as well as to several alcohols, fats, and oils [32]. Finally, at the end of its life cycle, PHBV based polymers can be conveniently valorised as renewable energy and/or material source. At this aim, both mechanical recycling, conducted through extrusion, and chemical recycling, conducted thorough pyrolysis, result to be effective [33,34]. Alternatively the bio-copolymer can be used as substrate for biofuels production, through anaerobic digestion or dark fermentation [29].

Currently, PHBV is the most commonly used copolymer to prepare high-performance biopolymers [35]. Without further modifications, PHBV can be used for various applications (e.g. controlled release of drugs, medical implants and repairs, packaging, orthopedic devices, everyday disposable objects, etc…). Moreover, combining the copolymer with other natural materials (e.g. fibres, other polymers, carbon nanomaterials) allows producing a wide spectrum of biomaterials with different structures and enhanced mechanical properties [10]. The physical and mechanical properties of PHBV greatly depend on the 3HV content in the copolymer. Indeed, the increasing 3HV content enhances the biodegradability and reduces the crystallinity and melting point of the bio-copolymer. Therefore, according to the required application, a suitable 3HV fraction should be reached by modifying the operational conditions of the process [10].

9.3.Techno-economic analysis and production strategies

Currently, the production costs of PHBV have been approximately estimated to range between 1.50 and 10 $/Kg$_{PHA}$, depending on the production plant location and, principally, on the adopted operating conditions [12, 36].

The analysis of the PHAs production costs is of primary concern for the selection of strategies aimed at enhancing the process performance. Usually, a techno-economic analysis considers fixed capital and annual operating costs. Fixed capital costs include both direct and indirect plant costs and other costs such as contractor's fee and contingency. The annual operating costs regards the management of the direct fixed capital-dependent items as well as labor-dependent items, the administration and overhead expense, the raw materials purchase, the utilities and waste treatment/disposal costs [38]. All these costs are strongly dependent on production factors.

First of all, equipment-related costs considerably increase when the productivity decreases. Indeed, for the production of the same amount of PHA per year, the process with lower productivity (g_{PHA}/L/h) requires larger both reactor size and equipment [39]. Moreover, the PHA content and the PHA yield in terms of used carbon source affect the biopolymer recovery process efficiency. Indeed, higher PHA content requires less digesting agents to separate granules from cells. For instance, Choi and Lee estimated a recovery cost of 4.8$/kg$_{PHA}$ when the PHA content in cells was 50%. Nevertheless, the cost decreased to 0.92$/kg$_{PHA}$ with 88% PHA content in cells. In addition, low PHA yields cause a large amount of carbon substrate to be wasted. Koller et al. [40] performed the techno-economic analysis in producing PHAs by comparing different species of microorganisms. They estimated that the polymers produced by *P. hydrogenovora* and *H. mediterranei* could be manufactured at the prices of 10.5 and 2.82 euros per Kg$_{PHA}$, respectively. The lower costs achieved using *H. Mediterranei* were due to the higher PHBV concentration and productivity. In addition, as *H. mediterranei* do not require sterile conditions, energy demanding sterility precautions was restricted to an absolute minimum.

The cost of the carbon source also contributes significantly to the overall production costs. Chanprateep [41] calculated that raw material accounts for 30–40% of the total costs. Also, Choi and Lee estimated that the cost of the carbon source was 38% of the total operating costs when the production amounts to 100 000 tonnes/year. Further details were provided by Choi et al. [42], who performed a sensitivity analysis. The PHA production

costs depended significantly on changes in feedstock price. When the substrate cost was reduced from 55$/Mg to22 $/Mg, the PHA cost was reduced to 0.05$/$kg_{PHA}$. When the substrate cost increased to 88$/Mg, the PHA cost increased by 115%. Similarly, Bhattacharyya et al. [12] observed that the raw material costs proposed in their study accounted only for 20% the costs estimated by Garcia et al. for PHBV production in similar operating conditions. The carbon source required in the process proposed by Garcia et al. costed 0.22$/$kg_{PHA}$. This value significantly affected the final production price. On the other hand, the stillage used as substrate by Bhattacharyya et al. [12] had no cost, because it was a waste. Moreover, such waste already contained a propionate concentration of 0.65 g/l, therefore PHBV production did not require additional costs due to PHBV precursor supply. Indeed, for most practical uses of PHBV, the 3HV fraction of the biopolymer should be at least in the range of 10 to 20 % (m/m) [36] and to achieve such 3HV fraction, usually precursors (e.g. propionate and valerate) are required to be added [36]. On the other hand, the use of waste substrates could require additional high equipment costs due to pre-treatments, as reported by Garcia et al., who performed extrusion of rice/wheat bran and corn starch prior to starting the PHBV production phase.

Concerning the costs of operational conditions, providing sufficient oxygen to maintain aerobic conditions can be potentially costly [43]. Indeed, prevention of oxygen limitation generally requires a pressurized vessel, high mixing energy and oxygen-enriched air feeds. Therefore, the production costs increase significantly [39]. Moreover, Akiyama et al. [44] proved that the effect of aeration rate was more significant on costs compared to the effect of the temperature.

The combination of different processes that can generate both energy and PHAs could significantly reduce the global costs. For instance, Choi et al. [42] performed the sensitivity analysis concerning costs of combined processes producing PHAs and hydrogen. The production costs of PHAs was significantly influenced by changes in the hydrogen market price: reducing the hydrogen market price from 2.0$/kg to 0.8$/kg, the PHA production costs increased by 191% to 6.46$/$kg_{PHA}$. A higher hydrogen market price of 3.2$/kg resulted in a decrease of the PHA production costs up to 3.15$/$kg_{PHA}$. Similar result could be reached by increasing the hydrogen productivity.

Based on economic analysis and the techniques used to produce PHBV in the published papers, different production strategies have been considered promising.

The addition of precursors has been widely used and has been therefore individuated as a strategy aimed at PHBV productivity enhancement and 3HV fraction control. Alternatively, it has been successfully tested the utilization of bacterial species that do not require precursors. The use of specific bacterial strains has also been supported when this practice is able to reduce the costs of sterilization and/or ensures a higher productivity. Finally, metabolic engineering techniques have been tested and proposed, obtaining interesting results: *Ralstonia eutropha*, *Haloferax Mediterranei* and *Alcaliges* species have been modified to enhance their productivity [23; 45;46]. Moreover, other species such as *Escherichia coli, Halomonas, Aeromonas* and *Salmonella enterica,* which do not produce biopolymers, have been engineered to produce PHBV [47–50].

As far as concern the choice of the most appropriate substrate to be used, both primary and waste substrates have been tested. The majority of studies have been carried out using pure substrates (e.g. glucose, glycerol, starch, methane, oils and volatile fatty acids) with high nutritional value and/or prize. However, in PHAs production processes, due to the intracellular respiration and the production of other metabolites, less than half of the carbon source is directed towards PHAs accumulation [36]. Consequently, carbon supply largely affects PHAs production costs. Clearly, the utilization of waste materials as feedstock is a strategy of main importance as it considerably reduces both costs related to substrates supply and waste disposal issues. Therefore, over the last few years, researchers have tested several waste materials to verify their PHBV production efficiency [51–53]. Due to the complexity of real substrates, in most cases, the use of waste material requires the adoption of appropriate pre-treatment techniques. The aim of pre-treatments is to facilitate the degradation process and/or avoid the possible inhibition of microorganisms' activity. On the other hand, pre-treatments also require additional costs. Table 9.2 reports a summary of the most relevant studies that have developed and tested the most promising strategies reported in the present work. All the strategies have been presented and discussed in the following sections.

Table 9.2. Summary of the most relevant studies on biological PHBV production

Strategy	Substrate/s and Microorganism	System configuration and feeding condition	Operating conditions	PHBV production	PHBV properties	Reference
Wild strains	*Glucose; Haloferax mediterranei.*	Two stage reactor; Fed-batch feeding.	V= 10 L; T= 41 °C; pH= 6.8-7.4 (controlled); Aeration= 10 L/min air; 20% O_2; Agitation= 300-650 rpm.	Concentration= NDR; Productivity= 0.21 g/Lh M.f.= 13.02% CDM; 3HV f.= NDR.	Melting temperature=150.8°C e 158.9 °C; Molecular weight=1057 kDa.	[54]
	Glucose; Haloferax mediterranei.	One stage reactor; Batch feeding.	V= 6 L; T= 37 °; pH= 7 (controlled); Aeration= 100% O_2; 10 L/min air; Agitation=800 rpm.	Concentration= 85.8 g/L; Productivity= NDR; M.f.= NDR; 3HV f. = NDR.	Melting temperature=131.1 – 144.3°C.	[55]
	Acetate; Activated sludge.	Fed-batch feeding.	V= 1.25-200 L; T= 30°C; pH=4-6 (uncontrolled); Aeration= NDR Agitation= NDR.	Concentration= NDR; Productivity= NDR; M.f.= 0.25 (m/m as COD); 3HV f.= 35-54% 3HV.	Melting temperature= 55-157°C; Glass transition temperature= -10.9-12.5°C; Polydispersivity index:1.9-5.6; Molecular weight x 10^5 g/mol= 2.8-5.4.	[56]
	Butyrate; *Ralstonia eutropha*	Two stage reactor; Fed-batch feeding.	V= 2-5 L; T= 30°C; pH= 7.0 (controlled); Aeration= NDR; 20% O_2; Agitation= NDR.	Concentration= 58 g/L; Productivity= 0.65 g/Lh; M.f.= 88% CDM; 3HV f.= 32-50% 3HV.	NDR.	[13]
	Fructose; *Rhodospirillum Rhubum.*	Two stage reactor; Batch feeding.	V= NDR; T= 26°C; pH= 7 Aeration= NAA Agitation= 170 rpm.	Concentration= NDR; Productivity= NDR; M.f= NDR; 3HV f.= 20% 3HV.	Melting temperature= 173.5°C; Degradation temperature= 279.2°C. Cristallization temperature=96.15 °C; Polydisperivity index=1.08; Molecula weight x 10^5 g/mol= 5.13.	[57]
	Maltose; *Halomonas campisalis.*	Single stage reactor; Batch feeding.	V=250 mL T= 25-55°C pH= 6-11; Aeration= NDR; Agitation = NDR.	Concentration= NDR; Productivity=NDR; M.f.= 45-81 %CDM; 3HV f. = NDR.	Melting temperature= 143.7°C; Cristallinity= 38.3%.	[25]
	Fructose;	Two stage reactor;	V= 7 L;	Concentration= 3.6 g/L;	NDR.	[16]

	Ralstonia eutropha KHB-8862.	Batch feeding.	T= 30 °; pH= 7.0 (controlled); Aeration= 1 vvm air; NDR; Agitation= 360 rpm.	Productivity= NDR; M.f.= 69% CDM; 3HV f.= 7% 3HV		
	Destrose; *Bacillus circulans (MTCC 8167).*	Two stage reactor; Batch feeding.	V= 250 ml; T= 37 ° C; pH= 7.0 (controlled); Aeration= NAA Agitation=180 rpm.	Concentration= NDR; Productivity= NDR; M.f. = NDR; 3HV f.= NDR..	Poly dispesivity index=1.21; Molecular mass= $5.1*10^4$ Da; Cristallinity= 65%	[58]
	Glucose; *Bacillus cereus FA11.*	Two stage reactor; Batch feeding.	V= 200 ml ; T= 30 ° C; pH= 7.0 (controlled); Aeration= NAA; Agitation=150 rpm.	Concentration= 3.9 g/L; Productivity= NDR; M.f.= 48.43% CDM; 3HV f.= 15% 3HV.	NDR.	[59]
	Glucose; *Bacillus flexus.*	Single stage reactor; Batch feeding.	V=6.6L T=28.3-37°C; pH= 7.5 (controlled); Aeration= 0.5-1 vvm; 40-70% O_2 Agitation= 300-700 rpm.	Concentration= 4-9.7 g/L; Productivity= NDR; M.f.= 32% CDM; 3HV f.= 2% 3HV.	NDR.	[60]
	Methane; *Methane-utilizing mixed cultures.*	Two stage reactor; Fed-batch feeding.	V=250 mL; T=25°C pH=6-7 (controlled); Aeration= 100 mL/d O_2; Agitation= 160 rpm.	Concentration= NDR; Productivity= NDR; M.f.= 52% CDM; 3HV f.= 33% 3HV.	NDR.	[61]
	Acetate; *Rhodobacter sphaeroides U7.*	Batch feeding.	V=5 L T=30°C pH= NDR; Aeration= 0-1.5 vvm air; Agitation= 0-300 rpm.	Concentration= 2.5 g/L; Productivity= NDR; M.f.= 65% CDM 3HV f.= 15.2 % 3HV.	Melting temperature=166°C; Glass transition temperature= -5.8°C; Crystallization temperature= 121°C; Cristallinity= 66.84 %.	[62]
Engineered strains	Glucose/Glycerol; *Escherichia coli.*	Two stage reactor; Batch feeding.	V= 125 mL; T= 30-37° C; pH= 7 (controlled); Aeration= NAA; Agitation= 280 rpm.	Concentration= 3.71 g_{HV}/L; Productivity= NDR; M.f.= NDR; 3HV f.= 24.1% 3HV.	NDR.	[47]
	Glycerin; *Salmonella enterica.*	Two stage reactor; Batch feeding.	V= 7 L; T= 37° C; pH= 7 (controlled); Aeration= NAA;	Concentration=NDR; Productivity= NDR; M.f.= 18-34 %CDM; 3HV.f.= 5-30% 3HV	NDR.	[50]

			Agitation= 200 rpm.			
	Glycerol; *Salmonella enterica.*	Two stage reactor; Batch feeding.	V= NDR; T= NDR; pH= NDR; Aeration= NDR; Agitation= NDR.	Concentration= NDR; Productivity= NDR; M.f.= 34.2% CDM; 3HV.f.= 14.2% 3HV.	NDR.	[63]
	Glucose; *Haloferax mediterranei.*	Two stage reactor; Batch feeding.	V= 7 L; T= 37° C; pH= 7 (controlled); Aeration= NDR;100% O_2; Agitation= 300 rpm.	Concentration= 21.28 g / L; Productivity= NDR; M.f.= 45-50% CDM; 3HV.f.=NDR.	NDR.	[46]
	Glucose; *Corynebacterium glutamicum* WM001.	Two stage reactor; Batch/Fed-batch feeding.	V= 0.5-3 L; T= 30° C; pH= 7 (controlled); Aeration= 1 L/min O_2; Agitation= 200-800 rpm.	Concentration= 15 g/L; Productivity= NDR; M.f.= NDR; 3HV.f.= 72.5% 3HV.	NDR.	[64]
	Glucose/Sodium gluconate; *Halomonas bluephagenesis.*	Single stage reactor; Batch feeding.	T= 37° C; pH= 8.5 (controlled); Aeration= NAA; Agitation= 200 rpm.	Concentration= 6.3 g/L; Productivity= NDR; M.f.= 65% CDM; 3HV f.= 25% 3HV.	Melting temperature= 177.4-136.8C; Glass transition temperature= -7.34- 0.5°C.	[65]
	Sucrose/maltose/ fructose/glycerol; *Halomonas* TD01	Batch feeding.	V= NDR; T=37°C; pH= 9 (controlled); Aeration= NAA; Agitation= 200 rpm.	Concentration= 3.2-8.6 g/L; Productivity= NDR; M.f.= 47.4-70.4% CDM 3HV f.= 1-6% 3HV.	NDR.	[66]
	Acetate; *Aeromonas hydrophilia.*	Batch feeding.	V=500; T=30°C; pH= NDR; Aeration= NAA; Agitation= 200 rpm.	Concentration= 0.5 g/L; Productivity= NDR; M.f.= 15% CDM; 3HV f.=4% 3HV.	NDR.	[49]
Precursors addition	Methane; Valerate; Mixed culture containing methanotrophic bacteria.	Single stage reactor; Batch feeding.	V= NDR; T= 30 ° C; pH= 7.0 (controlled); Aeration= NAA; Agitation=150 rpm.	Concentration= NDR; Productivity= NDR; M.f.= 27-45% CDM; 3HV f.= 18-40% 3HV.	Melting temperature= 151-136 °C; Glass transition temperature= -2- -6°C.	[67]
	Butyric acid; Valerate;	Single stage reactor; Batch feeding;	V= 3 L; T= 30 ° C; pH= 6.9 (controlled);	Concentration= NDR; Productivity= NDR; M.f.= 40% CDM;	Melting temperature= 178-180 °C; Molecular weight x10^6 g/mol= 0.9-1.2; Polydispersivity index= 3.	[68]

Ralstonia eutropha DSM 428.		Aeration =NDR; 20% O_2. Agitation=150 rpm.	3HV f.= 62% 3HV.		
Glucose; Valerate; *Delftia acidovorans* JCM 10181.	Two stage reactor; Batch feeding.	V= 50 ml; T= 30 ° C; pH= 7.0 (controlled); Aeration= NAA; Agitation= 150 rpm.	Concentration= NDR; Productivity= NDR; M.f.= 35 % CDM; 3HV f.= 0-90% 3HV.	NDR.	[69]
Glucose; Valerate; *Haloferax mediterranei* ES1.	Single stage reactor; Fed-batch feeding.	V= 7 L T= 37 ° C; pH= 7.0 (controlled); Aeration= NDR; 20% O_2; Agitation= 450 rpm.	Concentration= 0.2-5.4 g/l; Productivity= NDR; M.f.= 32.4-50 CDM; 3HV f.= 8.9-60.3% 3HV.	Melting Temperature= 140.4-151.2 °C; Glass transition temperature= -10.1-2.25 °C; Crystallization temperature= 59.8-77.8 °C; Cristallinity= 9.6-47.8%.	[70]
Glucose; Propionate; *Ralstonia eutropha.*	Two stage reactor; Continuous feeding.	V= 3 L; T= 30 ° C; pH=7.0 (controlled); Aeration= NDR; 2-20% O_2; Agitation= NDR.	Concentration= 2.71 g/L; Productivity=0.252 g/Lh M.f.= 78 % CDM; 3HV f.= 60% 3HV.	NDR.	[71]
Glucose; Propionate; *Bacillus aryabhattai* PHB10.	Single stage reactor; Batch feeding.	V= 500 ml; T= 28-40 ° C; pH= 5-9 (controlled); Aeration= NAA; Agitation=180 rpm.	Concentration= 2.8 g / L; Productivity= NDR; M.f.= 71.15% CDM; 3HV f.= NDR.	Melting temperature: 90 °C; Initial and final decomposition temperature= 220-225 °C; Tensile strength= 10.3 MPa; Elongation at break= 13.3%.	[19]
Acetate; Propionate; *Ralstonia eutropha* H16.	Two stage reactor; Batch feeding-	V= 100 cm^3; T= 30 ° C; pH= 7.0 (controlled); Aer= NDR; Aeration=NDR; Agitation=NDR.	Concentration= NDR; Productivity= NDR; M.f.= 50 % CDM; 3HV f.= 45% 3HV.	NDR.	[72]
Glucose; Propionate; *Bacillus Thuringiensis* R-510.	Two stage reactor; Batch feeding.	V=5L; T=33°C; pH= 6.0 (controlled); Aeration= NAA; Agitation= 350 rpm.	Concentration= NDR; Productivity= NDR; M.f.= 5.3-38.7% CDM; 3HV f.= 34-84% 3HV.	NDR.	[73]
Butyrate; Propionate; *Ralstonia eutropha.*	Two stage reactor; Fed-batch feeding.	V=2-5 L; T=30°C; pH= 7.0 (controlled); Aeration= NDR; 20% O_2;	Concentration= 58 g/L; Productivity= NDR; M.f.= 88% CDM; 3HV f.= 32-50% 3HV.	Melting temperature= 171°C; Cristallinity= 51%.	[13]

			Agitation= NDR.			
	Methane; Valerate/pentanol; *Methylocystis* WRRC1.	Single stage reactor; Fed-batch feeding.	V= NDR; T= 30 ° C; pH= 7.0 (controlled); Aeration= NAA; Agitation=300 rpm.	Concentration= 0.32g_{HV}/L; Productivity= M.f.= 78% CDM; 3HV f.= 58% 3HV.	Melting temperature= 161-170°C Cristallinity= 5-23%.	[74]
	Methanol; Pentanol; *Methylobacterium extorquens* G10.	Two stage reactor; Batch feeding.	V= 4 L; T= 30 ° C; pH= 6.85 (controlled); Aeration= NAA; Agitation=180 rpm.	Concentration= NDR; Productivity= NDR; M.f.= 30-53% CDM; 3HV f.= 0-50%.	Melting temperature= 162-172°C Cristallinity= 8-63%. Molecular weight=196-1500 kDa; Elongation at break= 4-230%.	[75]
	Fructose; Levulinic acid; *Ralstonia eutropha* KHB-8862;.	Two stage reactor; Batch feeding.	V=7 L; T=30°C; pH= 7 (controlled); Aeration= NAA; Agitation= 360 rpm.	Concentration= 3.6 g/L; Productivity= NDR; M.f.= 69% CDM; 3HV f.= 40% 3HV.	NDR.	[16]
	Valine; *Alcaligenes* SH-69.	Two stage reactor; Batch feeding.	V= 2.5 L; T= 37° C; pH= 7 (controlled); Aeration= NAA; Agitation= 420 rpm.	Concentration= 7.3 g/L; Productivity= M.f.=52.4% CDM; 3HV f.= 14.8% 3HV.	NDR.	[45]
Waste substrates	Madhuca indica flower extract; Pre-treatment= Extraction with hot chloroform; *Ralstonia eutropha*.	Batch feeding.	V= 250 L; T= 35 °; pH= 7 (controlled); Aeration= NAA; Agitation= 150 rpm.	Concentration= 1.44 g/L; Productivity= NDR; M.f.= 49.4% CDM; 3HV f.= 27.82% 3HV.	Melting temperature= 136°C-140.69°C.	[76]
	Digested food wastes; Pre-treatment= Digestion; *Ralstonia eutropha* ATCC 17699.	Two stage reactor; Fed-batch feeding.	V= 1.6 L T= 30 °; pH= 7.5 (controlled); Aeration. =20% oxygen; Agitation=600 rpm.	Concentration= 22.7 g/L; Productivity= NDR; M.f.= 72.6 %CDM; 3HV f.= 2.8% 3HV	NDR.	[53]
	Wastewater from biodiesel industry; Pre-treatment=NDR; *Pseudomonas mendocina* (PSU)	Two stage reactor; Batch feeding.	T= 35° C; pH= 7.0 (controlled); Aeration= NAA Agitation=150 rpm.	Concentration= NDR; Productivity= NDR; M.f.= 43.6 % CDM; 3HV f.= 8.6% 3HV.	Melting temperature= 170°C; Molecular weigth x10^5 g/mol=1.07-1.60; Polydisperivity index= 1.20-1.61.	[21]

Waste glycerol; Pre-treatment=NDR; *Ralstonia eutropha.*	Fed-batch feeding.	V=2L; T=34°C; pH=6.8; Aeration= 3.6 L_{air}/min; Agitation= 200-1500 rpm.	Concentration= 9.7-11 g/L; Productivity= 0.21-0.35 g/Lh; M.f.= 14.8-36.9% CDM; 3HV f.= 5.6-9.8% 3HV.	NDR.	[77]
Crop waste from date palm fruit; Pre-treatment= Mechanical and thermal carbohydrates extraction; *Haloferax Mediterranei.*	Fed-batch feeding.	V=5L; T=37°C; pH=7.2; Aeration= NDR; 20% O_2 Agitation= 200-800 rpm.	Concentration= 18 g/L; Productivity= NDR; M.f.= 25 % CDW; 3HV f.= 18% 3HV.	Melting temperature= 148.1 °C; Molecular weight= 746.0 kDa; Polydispersity index=1.5; Cristallinity: 26.5%.	[78]
Rice straw; Pre-treatment=Acid digestion; *Ralstonia eutropha.*	Two stage reactor; Batch feeding.	V=NDR; T=NDR; pH=6.8; Aeration= NDR; Agitation= NDR.	Concentration= 0.5-3.9 g/L; Productivity= 0.011 g_{HV}/Lh; M.f.= 39% CDM; 3HV f.= 23% 3HV	NDR.	[79]
Madhuca flowers; Pre-treatment= Thermal with water, Filtration; *Bacillus* sp-256.	Single stage reactor; Batch feeding.	V=3 L; T= 30°C; pH=7; Aeration= 1v/v air; Agitation= NDR.	Concentration= 2.7 g/L Productivity= NDR; M.f.= 54 %CDM; 3HV f.= 10% 3HV.	NDR.	[80]
Cheese whey permeate; Pre-treatment=NDR; *Bacillus megaterium.*	Single stage reactor; Batch feeding.	V=3 L; T = NDR; pH=7.2; Aeration= NDR; Agitation= NDR.	Concentration= 3.64 g/L; Productivity= NDR; M.f.= 86.6%CDM; 3HV f.= 16.6% 3HV.	Melting temperature= 116.6 °C; Crystallization temperature= 108.92°C; Glass transition temperature= 87.88°C; Tensile strength= 4.41 MPa.	[81]
Organic waste; Pre-treatment= Fermentation; *Ralstonia eutropha.*	Single stage reactor; Batch feeding.	V=1 L; T= 30°C; pH=8; Aeration= 2.4 mL_{air}/min; Agitation= NDR.	Concentration= 1.1 g/L; Productivity= M.f.= 40% CDM; 3HV f.= 30% 3HV.	NDR.	[82]
Palm oil mill effluent;	Single stage reactor; Fed-batch feeding.	V=2-7 L; T= NDR; pH=7-8.4;	Concentration= 7.3 g/L; Productivity= NDR; M.f.= 73 % CDM;	NDR.	[83]

	Pre-treatment= Fermentation; *Comamonas* sp EB 172.		Aeration= 1 -8 vvm air Agitation= 200-1200 rpm.	3HV f.= 13% 3HV.		
Wild strains, waste substrate and precursors addition	Whey lactose; Valerate; *Haloferax mediterranei*.	Single stage reactor; Fed-batch feeding.	V = 40L; T = 37 ° C; pH = 7.0 (controlled); Aeration= NDR; 50% O_2; Agitation= NDR.	Concentration= 12.2 g/L; Productivity= 0.09 g/Lh; M.f.= 73% CDM; 3HV f.= 6% 3HV.	Melting temperature= 150.8-158.9°C; Molecular weight= 1057 kDa; Polydisperivity index= 1.5.	[84]
	Plant oils; Valerate/propionate; *Ralstonia eutropha* H16.	Single stage reactor; Batch feeding.	V=250 mL; T= 30 °C; pH= NDR; Aeration= NAA Agitation= 200 rpm.	Concentration= 6.8 g/L; Productivity= M.f.= 61-90% CDM 3HV f.= 0-23% 3HV.	Melting temperature= 113-170°C; Molecular weight= 1,400,000 - 3,100,000 Da.	[14]
	Jatroba oil; Valerate/propionate; *Ralstonia eutropha*.	Two stage reactor; Batch feeding.	V= 250 mL; T= 30°C; pH= NDR Aeration= NDR; Agitation= NDR.	Concentration= 3.8-8.3 g/L; Productivity= NDR; M.f.= 69-90 % CDM; 3HV f.= 27-41% 3HV	Melting temperature= 131-164 °C; Decomposition temperature= 251-254 °C; Glass transition temperature= -6.1-1.8 °C; Molecular weigth x10^5 g/mol=9.0-18.4.	[15]
Precursors addition and waste substrate	Gluconate/VFAs/food starches; Valerate; *Caldimonas taiwanensis.*	Two stage reactor; Batch feeding.	V= 250 ml ; T= 55 ° C; pH= 7.0 (controlled); Aeration= NAA; Agitation=200 rpm.	Concentration= 2.15 g/l; Productivity= NDR; M.f.= 42-67% CDM; 3HV f.= 10-85% 3HV.	NDR.	[85]
Wild strains and precursors addition	Acetate;/lactate; Propionate; Activated sludge.	Single stage reactor; Batch feeding.	V=2L; T=25°C; pH= 7.5 (controlled); Aeration= NDR; Agitation= 900 rpm.	Concentration= NDR; Productivity= 0.14 g_{PHA}/ L h. M.f.= 50% CDM; 3HV f.= 31% 3HV.	NDR.	[86]
	Glucose; Propionate; *Ralstonia eutropha.*	Two stage reactor; Fed-batch feeding.	V= 800 mL; T= 34 °C; pH= 6.8 (controlled); Aeration= NDR; 20% O_2; Agitation= 1000 rpm.	Concentration=117 g/L; Productivity= NDR; M.f. = 74 % CDM; 3HV f.= 4.3% 3HV.	NDR.	[17]
	Fructose; Levulinic acid; *Ralstonia eutropha* H16.	Two stage reactor; Batch feeding.	V=250 Ml; T=30°C; pH=7 Aeration= NAA; Agitation=180 rpm.	Concentration= 0-5g/L; Productivity= NDR; M.f.=0-55.4% CDM; 3HV f.= 0-20.6% 3HV.	Melting temperature= 164.7-168-2 °C; Polydispersivity index= 1.05-1.07; Molecular weight= 0-726 kDa.	[87]
	Glucose;	Two stage reactor;	V=5 L;	Concentration= 8 g/L;	NDR.	[23]

Engineered strains and precursors addition	Levulinic acid; *Alcaligens* SH 69.	Batch feeding.	T=37°C; pH=7; Aeration= NAA; Agitation=360 rpm.	Productivity= NDR; M.f.= 38% CDM; 3HV f.= 74.5% 3HV.		
	Glucose; *Escherichia coli.*	Single stage reactor; Batch feeding.	V= 100 mL; T= 30° C; pH= 6.8 (controlled); Aeration= NAA; Agitation= 200 rpm.	Concentration= 5g/L; Productivity= NDR; M.f.= 54-45.4% CDM; 3HV f.= 22.81% 3HV.	Melting temperature= 162. 99 - 150.3°C.	[88]
	Aceetate; *Escherichia coli.*	Single stage reactor; Fed-batch feeding.	V= 6.6 L; T= 30° C; pH= 6.9 (controlled); Aeration= NAA; Agitation= 1000 rpm.	Concentration= 158 g/L; Productivity= 2.88 g/Lh M.f.= 78.2% CDM; 3HV f.= 10.6 % 3HV.	NDR.	[89]
	Glucose; *Escherichia coli.*	Single stage reactor; Batch feeding.	V=100; T=37°C; pH= 6.8 (controlled); Aeration= NAA; Agitation= 200 rpm.	Concentration= NDR; Productivity=NDR; M.f.= 55% CDM; 3HV f.= 80% 3HV.	NDR.	[90]
Wild strains and waste substrate	Olive mill wastewater; *Haloferax mediterranei*.	One stage reactor; Batch feeding.	V= 250 mL; T= 25-45 °; pH= 7 (controlled); Aeration= NAA Agitation= 100-220 rpm.	Concentration= 0.2 g/L; Productivity= NDR; M.f.= 43% CDM; 3HV f= 6.5% 3HV.	Melting temperature= 140.1-154.4 ° C; Glass transition temperature= 2.6 °C.	[91]
	Cheese whey; *Haloferax mediterranei*.	One stage reactor; Batch feeding.	V= 2 L; T= 37 °; pH= 7.2 (controlled); Aeration= NDR; 80% O_2; Agitation=200-800 rpm.	Concentration= 7.9 g/L; Productivity= 4.04 g/Ld M.f.= 54% CDM; 3HV f.=1.5% 3HV.	Melting temperature: 128.7-160.78 ° C.	[51]
	Raw glycerol; *Haloferax mediterranei*.	Two stage reactor; Fed-batch feeding.	V= 10 L; T= 37 °; pH= 7.0 (controlled); Aeration= NDR; 20% O_2.; Agitation NDR.	Concentration= 16.2 g/L; Productivity= 0.12 g/Lh M.f.= 76% CDM; 3HV f.=10% 3HV.	Melting temperature= 128.7 -138.8 ° C; Glass transition temperature= 7.0°C; Molecular weight= 253 kDa; Polydispersivity index= 2.7.	[36]
	Cornstarch; *Haloferax mediterranei*.	Two stage reactor; Fed-batch feeding.	V= 6 L; T= 37 °; pH= 7.0 (controlled); Aeration= 10 L/min air; 100% O_2;	Concentration= 20 g/L; Productivity= NDR; M.f.= 50.8% CDM; 3HV f.=10.4% 3HV.	Melting temperature= 129.1-144°C; Glass transition temperature= -1.2°C.	[92]

		Agitation= 800 rpm.			
Vinasse; *Haloferax mediterranei*.	One stage reactor; Batch feeding.	V= 250 mL; T= 37 °; pH= 7.2 (controlled); Aeration= NAA; Agitation= 180 rpm.	Concentration= 19.7 g/L; Productivity= 0.21 g/Lh M.f.= 70% CDM; 3HV f.= 12.36-14.09% 3HV.	Melting temperature= 144.63 °C.	[52]
Rice bran/cornstarch; *Haloferax mediterranei.*	Two stage reactor; Repeated-batch feeding.	V= 5 L; T= 37 °; pH= 6.9-7.1 (controlled); Aer= NDR; 20% O_2; Agitation=800 rpm.	Concentration = 77.8 g/L; Productivity= NDR; M.f.= 55.6 % CDM; 3HV f. = NDR.	NDR.	[93]
Rice-based ethanol stillage; *Haloferax mediterranei*.	Two stage reactor; Batch feeding.	V=250 mL; T= 37°C; pH=7.2; Aeration= NAA Agitation=180 rpm.	Concentration= 16.42 g/L; Productivity= 0.17 g/Lh; M.f.= 71% CDM; 3HV f.= 15.4% 3HV.	NDR.	[94]
Poplar; Activated sludge.	Batch feeding.	V= 2-7 L; T= 28°C pH= 7; Aeration= NAA Agitation= 300 rpm.	Concentration= 637.6 mg/L; Productivity= M.f.= NDR; 3HV f.= NDR.	NDR.	[95]
Condensed corn solubles; *Rhodospirillum rhubum*.	Batch feeding.	V= 4 L; T= NDR; pH= 7 (controlled); Aeration= 1vvm air; 30% O_2; Agitation= 250-500 rpm.	Concentration= NDR; Productivity= M.f.=36 % CDM; 3HV f.= NDR.	NDR.	[22]
Glucose/whey/ starch/bagasse/rice bran; *Bacillus OU40^T*.	Two stage reactor.	V= NDR; T=30°C; pH= NDR; Aeration= NAA; Agitation= 150 rpm.	Concentration= 3-3.5 g/L; Productivity= NDR; M.f.= 45-71.9 % CDM; 3HV f.= 5.27-15.60% 3HV.	Melting temperature= 160°C; Cristallinity=40.4%; Poly dispesivity index= 1.76.	[96]
Crude glycerol/fructose corn syrup; *Yangia ND199*.	Single stage reactor; Batch/fed-batch feeding.	V=2L; T=30°C; pH= 7; Aeration= NDR; Agitation = NDR.	Concentration= NDR; Productivity= NDR; M.f.= 52.8-56%wCDM 3HV f.= 2.9% 3HV.	NDR.	[97]

3HV f= fraction of HV in PHBV molecule (m/m);
M.f.= fraction of PHBV in cell or PHA (m/m);
CDM= Cell Dry Mass (g)

NAA: Not artificially aerated
NDR = no data reported
NP= Not performed (dilution and sterilization are excluded);
pH= initial pH;
T= Process temperature (°C)
V= working volume (L).

9.4.Microorganisms as production strategy

As previously said, a wide range of both gram-positive and gram-negative bacteria have been found to be able to produce PHBV.

To enhance the process productivity and contextually reduce the costs, the choice of microorganisms represents a crucial aspect, and therefore it can be considered as a production strategy. For this reason, in this section are reviewed and compared results of research studies, which have used different bacterial species, including those that have tested metabolic engineering techniques.

9.4.1. Wild species

According to the Table 9.2, the gram-negative bacterium *Ralstonia eutropha* is one of the most frequently tested microorganisms. *Ralstonia eutropha* can degrade a wide variety of substrates, including aromatic compounds. Moreover, it is resistant to potential toxic elements (PTE) such as mercury [98]. It can utilize wastes containing sugars, alcohols and volatile fatty acids (e.g. acetic, propionic, and butyric acids) as sole carbon and energy source for growing and synthesizing PHB as well [99,100]. On the other hand, it can produce PHBV only with the addition of precursors containing the 3HV fraction.

Results obtained using *Ralstonia eutropha* indicate that this microorganism can accumulate up to 80% of PHBV in cell dry mass (CDM) when fed with fructose or butyrate [13,16] and more than 90 % when fed with jatropha oil and other plant oils [14,15]. In terms of PHAs concentration, *Ralstonia eutropha* was found to be able to produce 117 g/L of PHAs using glucose as substrate [17], which is the highest production observed in all the reviewed studies.

To maximize the 3HV fraction in the PHBV polymer, other species of microorganisms have been found to be performant as well. For instance, the bacteria *Delftia acidovorans* and *Caldimnia taiwanensis*, fed with valerate, produced PHBV containing a 3HV fraction higher than 90% [69,85].

Rhodospirillaceae, known as purple non sulfur bacteria (PNSB), belong to one of the most versatile family of microrganisms in terms of metabolism. PNSB have attracted increasing attention as they are capable to produce concomitantly hydrogen and PHB

from a wide variety of substrates [5]. Nevertheless, with the addition of precursors, the specie *Rhodobacter Sphaeroides U7* was found to be able to produce PHBV from volatile fatty acids (VFAs) [62].

Obviously, the use of bacteria which do not require costly precursors is advisable to reduce production costs. The absence of precursors results also in important advantages in terms of process management, as precursors have been proved to be harmful to cell growth [69,86], and therefore, to keep their concentration in non-inhibiting thresholds, the process needs a strict control.

Various microorganisms have been studied using the main substrate without any precursors addition. Different species of *Bacillus* such as *Bacillus circulans*, *Bacillus cereus*, *Bacillus Flexus* and *Bacillus OU40T* produced PHBV when fed with sugars or industrial wastes [58–60,96]. *Pseudomonas aeruginosa*, *Yangia ND199* and *Halomonas campisalis* showed the same interesting capacity [25,97,101]. Nonetheless, in all mentioned studies, PHBV productions were not very high.

Nevertheless, it has been demonstrated that the PNSB *Rhodospirillum Rubum* synthetizes PHBV from sugars and wastes without the need of precursors supply [22,57]. In particular, in a study from Liu et al. [57], a 3HV fraction of 46.5% was observed, which was the highest obtained in all the reviewed studies from unrelated carbon sources.

Recently, different studies on open mixed cultures have been conducted with the aim of lowering production costs. Open mixed cultures do not require sterile conditions and are able to adapt to a very wide variety of complex and inexpensive waste feedstock, thus resulting more interesting in the perspective of a process scale-up.

Arcos-Hernandez et al. [56] and Dionisi et al. [86] tested the biomass from activated sludge wastewater treatment plants, obtaining PHBV from a mix of organic acids and using propionic acid as precursor. Activated sludge was also successfully used to produce PHBV from poplar waste, by Yin et al. [95]. Fergala et al. [61] investigated the feasibility of enriching methane-utilizing mixed cultures from the anaerobic digestion process: the mixed consortium showed the capability to accumulate PHBV when fed with a mixture of methane and valerate.

In order to avoid sterile conditions, extremophile microorganisms, such as *Haloferax Mediterranei* can be used. *Haloferax Mediterranei* belongs to the class of halobacteria, the extremely halophilic branch of the Archaea domain. This specie tolerates high salinity and requires a concentration of 2–5 M NaCl for its growth [91]. The required highly saline environment avoids the growth of other microorganisms in non-sterile conditions, thus significantly reducing process costs. Moreover, *Haloferax Mediterranei* grows faster compared to the majority of other microorganisms and it is capable of accumulating high amount of PHBV [102]. Finally, *Haloferax Mediterranei* can convert a wide variety of substrates, such as sugars and VFAs [55,103,104]. For such feature, *Haloferax Mediterranei* has been used for the conversion of different organic waste materials, as follow: whey [51,84]; raw glycerol [36]; cornstarch [92,93]; vinasse and stillage [52,94]; rice bran [93]; crop waste [78].

Due to its high robustness, stability and capacity to degrade complex molecules, *Haloferax Mediterranei* can produce high PHBV amount even without substrate pre-treatments, thus further reducing process costs, as demonstrated by Bhattacharyya et al. [94], who used this specie for PHBV production with stillage without any pre-treatment. Similar results were obtained by Hermann-Krauss et al. [36], who performed only dilution of waste glicerol (10-20 g/L). Alsafadi & Al-Mashaqbeh [91] investigated the conversion of olive mill wastewater (OMD), 5%, 15%, 25%, 50%, 75% in volume, respectively, to PHBV by *Haloferax Mediterranei*. They demonstrated the feasibility of producing PHAs in one-stage cultivation process without the need of pre-treatments, as phenols contained in OMW had no inhibitory effect on the growth of the biomass. An additional advantage of using *Haloferax Mediterranei* is the absence of need to add precursors for PHBV production.

The major bottleneck in the industrial application of *Haloferax Mediterranei* is the high quantity of required salts and the production of a high saline effluent, which after has to be correctly disposed, even though 96 % of the medium salts can be reused and recovered as reported by Bhattacharyya et al. [94]. Another strategy related to microorganisms is the adoption of engineered strains, as reported in the following sub-section.

9.4.2. Metabolic engineering strategies

The results achieved in molecular-genetic research and the detailed investigations on the PHBV synthesis have found a convergent point in the study of recombinant strains, which have proven to be efficient in enhancing the production of biopolymers [102] Different approaches have been proposed to use metabolic engineering as a strategy to produce and/or increase the accumulation of PHBV.

As previously said, due to the lack of propionyl-CoA in most microorganisms, PHBV production is often hindered by the high costs associated to the supplementation of precursors. Therefore, various studies on metabolic engineering have been conducted with the aim of promoting precursors-independent pathways to produce PHBV. I. S. Aldor et al. [50] engineered the specie *Salmonella enterica*: the obtained mutant produced propionyl-CoA without the presence of propionate in the culture medium. A recombinant strain of *Salmonella enterica serovar Typhimurium* (mutant in propionate-activation activity) was metabolically engineered by I. Aldor & Keasling [63] to control the composition of the polymer. A gene (prpE) encoding propionyl-CoA synthetase was placed under the control of the IPTG-inducible taclacUV5 promoter (PtaclacUV5) while the PHA synthesis operon (phaBCA) from *Acinetobacter sp. RA3849* was co-expressed under the control of the arabinose-inducible araBAD promoter (PBAD).

Other authors reported the derivation of engineered *Escherichia coli* strains for PHBV production from unrelated carbon sources. Miscevic et al. [47] enabled the intracellular formation of non-native propionyl-CoA and investigated various enzymes involved in 3HV biosynthetic pathway from different microorganisms. The engineered *Escherichia coli* strains produced PHBV from glucose and glycerol as sole carbon sources.

Ma et al. [64] inserted the phaCAB gene cluster into the bacteria *Corynebacterium glutamicum WM001* to enhance the level of intracellular propionyl-CoA. The recombinant strain produced high concentrations of PHBV from glucose with high 3HV fraction.

Some enzymes converting propionic acid to propionyl-CoA have been used to engineer *Escherichia coli* strains for PHBV production using propionic acid singularly or combined with other substrates. Usually, mutant strains harbouring other microorganisms genes have been used. For instance, Yang et al. [90] inserted propionyl- CoA transferase

(Pct) into *Escherichia coli* and produced PHBV containing >80 wt% 3HV content. To impart PHA production in *Escherichia coli* strains, the authors used the acetoacetyl-CoA reductase (phaB), PHA synthase (phaC) and a b-ketothiolase gene (bktB) from *Ralstonia eutropha*.

Other authors, instead, investigated strategies for high cell density PHBV production by a recombinant *Escherichia coli* harbouring the *Alcaligens latus* PHA biosynthesis genes. The mutant produced a large amount of PHBV with a higher productivity compared to recombinant *Escherichia coli* harbouring *Ralstonia eutropha* PHA biosynthesis genes [89]. Finally, to increase the 3HV fraction, Horng et al. [88] cloned the *prpE* gene encoding propionyl-CoA synthase, the *vgb* gene encoding bacterial hemoglobin (VHb) and the PHAs synthesis operon (phaCAB) in a plasmid transformed into *Escherichia coli XL1-blue*. The recombinant specie produced PHBV with increased 3HV fraction and molecular weight.

Another strategy resulting in propionyl-CoA formation has been the induction of the intracellular generation, or over- production, of propionyl-CoA precursors amino acids (e.g. threonine). In the study by Tan et al. (2014), the overexpression of the threonine synthesis pathway and threonine dehydrogenase made a recombinant *Halomonas TD01* specie able to produce PHBV using carbohydrates as sole carbon source. Metabolic engineering of the threonine biosynthetic pathway was used by Choi et al. [23]. The authors studied a threonine overproducing mutant of *Alcaligenes sp. SH-69* which was able to produce from glucose an amount of PHBV approximately six folds higher than that achieved by the wild type under the same culture conditions.

The engineering of the tricarboxylic acid (TCA) cycle in *Halomonas bluephagenesi* has been proposed as well. Y. Chen et al. [65] performed the study hampering the 3HV consumption pathways, thus increasing flux to 3HV precursor synthesis and activating ED pathway to reduce NADH/NAD^+ ratio for promoting TCA cycle activity via over-expressing bacterial hemoglobin gene vgb. This engineered specie produced PHBV with different 3HV fractions (0–25 mol%) from glucose. Shi et al. [49] proposed a metabolic engineering strategy to produce PHBV from acetate rather than lauric acid with the specie *Aeromonas hydrophila*. The engineered specie was capable to overexpress b-ketothiolase, acetoacetyl-CoA reductase, and acetyl-CoA synthetase and it was found able to produce high PHBV amounts.

A finally strategy to increase the PHBV production has been the conveyance of the substrate conversion towards the PHAs synthesis rather than other metabolites. Zhao et al. [46] identified a gene cluster involved in EPS biosynthesis in *Haloferax mediterranei*. Inactivating the genes, they eliminated EPS synthesis. The deficiency in EPS biosynthesis in the mutant strain remarkably increased PHBV accumulation. The productivity of the mutant strain was 20 folds increased compared to that of the wild strain. To sum up, different types of microorganisms with different peculiarities can be used to enhance the PHBV production process performance. However, the choice of microorganisms cannot be decoupled from the adoption of appropriate substrates.

9.5.Strategies related to substrates

The microorganism-substrate combination plays an important role in the process effectiveness. PHBV producing bacteria can utilize a wide variety of organic molecules as substrates, principally sugars, alcohols and organic acids. As previously said, to enhance the process productivity and/or increase the 3HV fraction, the addition of co-substrates (precursors) is a strategy of main relevance. Many studies investigating the effect of different types of precursors as well as the required precursor dosage in the medium, have been performed, although, as expected, the precursors utilization results in a considerable increase of the production costs. Therefore, the use of waste organic material is reasonably more advisable, as it allows moving the process towards a biorefinery scenario fed with abundant and inexpensive materials. Moreover, the utilization of pre-treatments which generate precursors from wastes has been also proposed as a promising production strategy.

9.5.1. Addition of 3HV fraction precursors

As mentioned above, the majority of bacteria are able to produce PHBV instead of PHB only if specific precursors are available. The presence of precursors is also fundamental to adjust the 3HV monomer fraction in PBHV and, consequently, modify the polymer properties. Therefore, several studies have been addressed to verify the effect of a large number of synthetic carbon sources (e.g. methane, glucose, fructose), linked to these precursors (Table 9.2). These studies have confirmed that methanotrophic bacteria, *Ralstonia eutropha, Pseudomonas* species and *Hydrogenophaga pseudoflava* were able to produce only PHB when fed with the main substrate solely [17,21,67,68,74] while the

specie *Ralstonia eutropha DSM 545* was able to produce PH3HB4HB when fed with sole glycerol [77]. In turn, the addition of precursors led, in all cases, to PHBV production.

Valeric acid and propionic acid have been the most studied precursors. Valeric acid is clearly a precursor of the 3HV monomer as it leads to the formation of the 3HV-CoA enzyme, which is successively polymerized [70]. Moreover, valerate concentration in the culture medium strongly affects the 3HV fraction of the PHBV biopolymer. Myung et al. [67] tested various combination of CH_4 and valerate using a methanotrophic consortium. The authors observed that the 3HV fraction increased when the valerate concentration as well as the fraction of the oxidized methane were increased. Inn et al. [68] reached similar results using the bacterium *Ralstonia eutropha* and butyrate as principal carbon source: a maximum 3HV fraction of 62% was reached when a valerate fraction of 100% was used in the culture medium. Moreover, Sheu et al. [85] showed that the modification of the valerate concentration in a sugar rich medium could be used to produce the desired 3HV fraction (10%-90%) using the thermophilic bacterium *Caldimonas taiwanensis*.

The addition of valerate and, therefore, the increase of the 3HV fraction is relevant as it enhances the quality of the final product. For instance, Koller et al. [84] observed that the polymer produced through valerate addition presented better thermal properties compared to the polymer obtained without the precursor addition. According to their analysis, the product quality was appropriate for melt extrusion and film blowing technologies. In the study conducted by Inn et al. [68], the analysis of the characteristics of the produced polymers showed that increasing the 3HV fraction led to a decrease of the melting and glass transition temperatures while the polymer composition did not substantially influence the molecular weight distribution. It is worth noticing that the accumulation of high concentrations of acids in the culture medium can result in bacteria inhibition. To induce the reduction of free protons generation in the cell cytoplasm and avoid the acid accumulation in the medium, Loo & Sudesh [69] converted the valeric acid into its salt form prior to feeding cells, thus obtaining a reduced inhibitory effect.

Concerning the use of propionic acid as precursor, it was used in 1970 by Imperial Chemical Industries Ltd. to produce PHBV for the first time. In that case, the 3HV-CoA was obtained from condensation of acetyl-CoA and propionyl-CoA to 3-ketovaleryl-CoA and the subsequent reduction of the condensation product to 3HV-CoA. These two reactions were catalysed by β-ketothiolases and acetoacetyl-CoA reductases, respectively

[27]. In the following years, various authors tested different propionate concentrations dissolved in the culture medium. For instance, S. T. Yu et al. [71] used culture media containing glucose and three propionate concentrations (5, 7 and 15 g/L) with the strain *Ralstonia eutropha.* The tested media led to increasing 3HV fractions in PBHV (respectively 30%, 40% and 60 %). Similarly, Doi et al. [72] showed that increasing the propionate concentration increased the 3HV fraction in the produced biopolymer (from 22% to 45%) using the bacteria *Ralstonia eutropha* H16.

Kim et al. [17] studied the effect of three different propionic acid to glucose mole ratios (0.17, 0.35, and 0.52) using *Ralstonia eutropha* NCIMB 11599. The final PBHV concentrations of 117, 74, and 64 g /L with 3HV fractions of 74%, 57%, and 56.5% respectively, were obtained. Propionate concentration in a glucose medium was also investigated by Park at al. (1997) in presence of *Bacillus thuringiensis* R-510. The 3HV fraction increased from 0% to 85%, increasing propionate concentration from 0% to 0.8% (w/v). A minimum melting temperature of 65°C was measured when the polymer presented a 3HV fraction of 35%.

Other authors tested propionic acid addition to culture media and observed that without the addition of the precursor, only PHB was produced. Conversely, the use of propionic acid as co-substrate led to the production of a PHBV polymer with better thermal and mechanical properties. In particular, the melting temperature, thermal stability, tensile strength and elongation at break were found to be, respectively, 90°C, 220°C, 10.3MPa and 13.3% [19]. On the other hand, the same side effect responsible for culture inhibition produced by high valerate concentrations occurs with high propionate concentrations. In particular, propionic acid was even found to be more toxic compared to valeric acid. Indeed, Loo & Sudesh [69] observed that the inhibitory effects of the 3HV precursors increased in the following order: valerate salt < valeric acid < propionate salt. The formation of Acetyl-Coa from propionic acid was found to be the rate-limiting step in HVCoA formation, reducing the substrate consumption rate, when propionate was tested as single substrate. Dionisi et al. [86] tested lactate, acetate and propionate as single substrates and their mixture. The authors found that when Acetyl-CoA was formed from acetic or lactic acid instead of being formed from sole propionate, higher fractions of the 3HV monomer were achieved. Moreover, the uptake rate of the propionic acid increased. The importance of using propionic acid as co-substrate rather than as sole carbon source

was also underlined by Grousseau et al. [13]. They showed that the simultaneous availability of a second carbon source (butyric acid) led to higher conversion rate of propionic acid into 3HV, in presence of *Ralstonia eutropha*.

Due to the high costs of both valeric and propionic acids, during the last few years, alternative less costly compounds have been tested. For instance, pentanol, which can be oxidized via valeraldehyde to valeric acid and then, converted to the 3HV monomer. It has been demonstrated that increasing pentanol fraction by 20% in a methanol-pentanol medium resulted in a valerate increase of 50% and in the stimulation of the PHBV production. Conversely, higher pentanol concentration resulted to be toxic for microorganisms [75]. Despite the reduced costs of the process, pentanol is less effective for PHBV production compared to valerate. Indeed, Cal et al. [74] tested methanotrophic bacteria fed with sole methane, a mixture of methane with valerate and a mixture of methane with pentanol, by changing the co-substrates concentration. The authors found that the 3HB/3HV molar ratio in PBHV was directly related to the valerate concentration in the culture medium. The same strain (i.e. *Methylocystis* WRRC1) produced pure PHB when the process was fed with sole methane and 50% lower amount of PHBV when it was fed with a mixture of methane with pentanol rather than valerate.

In addition, levulinic acid, the most inexpensive precursor among all others considered, has been tested to increase the 3HV fraction in PBHV. However, mechanisms leading to PHBV production from levulinic acid have not been clarified yet. Novackova et al. [87] studied the adaptation of the bacteria *Ralstonia eutropha* to levulinic acid: the analysis of the PHBV into cells showed higher content of 3HV when the mentioned precursor was used. The influence of levulinic acid on PHBV production by *Ralstonia eutropha* was also investigated by Chung et al. [16]: the precursor addition greatly increased the molar fraction of 3HV from 7 to 75.l% by increasing the levulinic acid concentration from 0.5 to 4.0 g/L in a culture medium containing fructose as main carbon source.

A comparison between the utilization of propionic acid, valeric acid and levulinic acid was performed by Choi et al. [23]. They added precursors to a glucose medium using the bacterium *Alcaligens* SH 69. Precursors greatly increased the molar fraction of 3HV to 38–77%. The higher 3HV fraction of 77% was reached adding levulinic acid.

Also, a few studies reported that PHBV could be synthesized through the propionate pathway when some amino acids like threonine, valine and isoleucine act as precursors for propionyl CoA [45,105].

Finally, a very interesting and convenient option is neither the use of waste substrates containing precursors or the adoption of waste pre-treatments generating precursors. Indeed, the use of wastes and wastewater is a strategy of main relevance for the reduction of process costs.

9.5.2. Waste substrates and pre-treatments used to enhance the productivity

Over the last few years, various organic wastes and wastewaters have been used as feedstock for PHBV production.

One of the most widely used waste has been the crude glycerol, which is the main by-product of biodiesel industry [21,36,77,97]. Crude glycerol is particularly suitable for PHAs accumulating species. Indeed, carbon atoms are higher reduced in glycerol than in any other molecule (e.g. carbohydrates). Consequently, cells using glycerol are in a more reduced physiological state, which favours intracellular polymer synthesis [36].
It is worth to underline that pure glycerol is actually an expensive material. However, biodiesel manufacturing produces about 10 Kg of crude glycerol per 100 L of produced biodiesel. Biodiesel and related by-products industry is growing annually, causing a sharp decrease of the crude glycerol cost compared to the pure one [36,106].

Van-Thuoc et al. [97] tested, comparatively, glucose, maltose, xylose, sucrose, fructose, dextrin and glycerol as substrates for PHBV production, obtaining the best results with glucose and glycerol in terms of PHA content and with maltose and glycerol in terms of 3HV fraction. Hermann-Krauss et al. [36] compared the utilization of crude glycerol and pure glycerol to feed *Haloferax mediterranei.* The authors pointed out that the amount of the polymer produced and its characteristics were almost the same in the two investigated cases. Therefore, due to the abundance of crude glycerol and the limited costs of its production, its use results more convenient than the use of the pure glycerol.

By-products from the ethanol industry have been tested as well. Smith et al. [22] used a condensed corn solubles (CCS) medium to feed *Rhodospirillum Rhubum*. CCS is a coproduct of corn ethanol production and contains organic acids (lactic acid, succinic acid

and acetic acid), glycerol, glucose, maltose, higher dextrins, microelements, phosphorus and a small amount of free nitrogen. Therefore, it represents a suitable source of nutrients for different species of bacteria. Bhattacharyya et al. [52, 94], in turn, tested vinasse and stillage, highly polluting wastes of the ethanol industry. Results showed that both substrates were effective for PHBV production, and they could be degraded easily during the process, thus obtaining an important lowering of the organic load at the end of the processes.

Agricultural wastes also represent abundant and inexpensive organic sources. Due to the high carbohydrates content in their hemicellulose and cellulose structures, they can be used for PHBV production.

C. W. Chen et al. [92] showed that cornstarch, which is rich in sugars, can be successfully used. Poplar hydrolysate has been positively used as well [95], and the use of madhuca flowers from India, which contain a large quantity of sugars, proteins, mineral nutrients and organic acids, has been proposed which success [76,80].

Among others, rice straw is worldwide the most abundant agricultural waste (approximately 700–800 million tons generated every year). Therefore, it can be a potential candidate for the industrial PHA production [79,107]. Indeed, rice wastes have been widely tested. Nagamani & Mahmood [96] used rice straw to feed *Ralstonia eutropha*, obtaining better results in terms of PHBV productivity and 3HV fraction compared to pure glucose, whey, starch and bagasse. Rice bran was compared with wheat bran to replace part of the pure starch in the culture broth by Huang et al. [93]. Both waste substrates increased the cell concentration and the PHBV accumulation. However, the maximum cell concentration, PHBV concentration and its content were achieved when rice bran was used as co-substrate with starch, setting a waste to starch mass ratio of 1:8 (w/w).

Due to their high organic load, organic wastes and wastewaters from food industry represent further potentially effective substrates for PHAs accumulating bacteria. A widely utilized waste has been cheese whey, the major by-product from the cheese industry [81, 96, 51]. The application of cheese whey for PHBV production in presence of *Haloferax mediterranei* has revealed to be interesting due to the high salinity requirement of the mentioned bacteria. Indeed, as various types of cheese require the

addition of large quantities of salt, the obtained waste is a high saline cheese whey which already contains the quantity of salt required by *Haloferax mediterranei* [51]. Fruit and vegetable processing wastewastes represent, certainly, inexpensive and abundant substrates, rich in sugars and nutrients. Vegetable waste has been used as sole carbon source by Ganzeveld et al. [82]. Du & Yu [53], instead, coupled anaerobic digestion of food scraps with PHB and PHBV production using the digested food waste as substrate for the PHAs production step. Alsafadi et al. [91] tested date palm, one of the most successful and vital crops in Middle East region as well as in other arid and semiarid regions, to feed *Haloferax mediterranei*.

Finally, wastes from vegetable oils production, such as olive mill wastewater as well as jatropha, sunflower, palm and coconut oils have revealed to be effective for PHBV production [14, 15, 83, 91]. Results obtained from the jatropha oil conversion to PHBV revealed that the quality of the produced copolymer was essentially the same as that produced from other pure carbon sources, such as sugars [15].

It has to be highlighted that the use of waste substrates requires usually appropriate pre-treatments, aimed at neither reducing the size and/or the molecular complexity of the used organic waste, or eliminating toxic compounds.

As it can be noticed from **Table 9.2**, physical, chemical or biological pre-treatments can be successfully used. The physical pre-treatment, based on thermal or mechanical processes, are aimed at reducing the waste size or extracting simpler molecules. Kerketta & Vasanth [76] dried, boiled and filtered madhuca flowers to extract macro and micronutrients. In the study of Alsafadi et al. [78], both mechanical and thermal pre-treatments were applied to date palm fruit waste: fruit seeds were firstly removed manually, then dates were sliced to small pieces (1 cm × 1 cm × 0.5 cm). Successively, carbohydrates extraction was performed using a thermal pre-treatment. The thermal extraction was investigated by testing different conditions (e.g. temperature and extraction times). The maximum carbohydrates concentration (210 g /L) was obtained using 6 h extraction time and 40°C temperature. Another widely used pre-treatment is the extrusion. Extruders are used to mix and considerably reduce the waste size, in order to facilitate the metabolic activity of bacteria. This treatment was applied to cornstarch by C. W. Chen et al. [92] and rice bran by Huang et al. [93]. Both studies compared the

utilization of extruded waste and raw waste obtaining better results using the extrudates as carbon source.

Thermal pre-treatments have been also coupled with hydrolysis. Yin et al. [95] studied hot compressed water method for delignification and promoting the successive enzymatic saccharification of poplar wood. Hot water pre-treatment increased the efficiency of cellulase enzymatic hydrolysis and the yield of reducing sugars. The optimized pre-treatment conditions resulted in being the use of hot water at 200 °C for 30 min, and the enzymatic hydrolysis at 45 °C for 3 days. In addition, the conversion of enzymatically hydrolyzed cheese whey into PHBV by *Haloferax mediterranei* was investigated by Martin Koller et al. [84], while Pais et al. [51] performed the cheese whey chemical hydrolysis using the same microbial strain. Results obtained using the enzymatic hydrolysis were better in terms of PHBV productivity. However, the study was conducted with precursors addition.

Chemical hydrolysis has been reported to be less expensive than that enzymatic. Moreover, chemical hydrolysis of cheese whey, requiring alkali addition for hydrolysate neutralization, results in a saline substrate, which is an advantage whenever *Haloferax mediterranei* is utilized as microbial strain. Pais et al. [51] tested different HCl concentrations (0.4, 0.7 and 1.0 M) and different reaction times (30, 60, 90 minutes). The most efficient lactose hydrolysis (96%) with no appreciable degradation of glucose (3.6%) and galactose (0.9%) was obtained using 1.0 M HCl and 90 minutes reaction time [51].

Ahn et al. [79] studied the effect of thermal pre-treatment and chemical hydrolysis on PHBV production, using rice straw. The pre-treatments conditions strongly affected the substrate composition and the process productivity. The increasing sulfuric acid concentration from 2% to 6% generated a larger PHBV production while the 3HV fraction decreased. To obtain a higher 3HV fraction, an additional heating process of 60 min was conducted following 2% sulfuric acid digestion. In such a condition the highest 3HV mole fraction (22.9%) was achieved. On the other hand, shorter or longer thermal pre-treatment time resulted in a lower 3HV fraction. The obtained results were attributed to the generation of both sugars and levulinic acid, which are precursors of the 3HV fraction.

PHAs production can be coupled with biofuels generation if biological anaerobic processes are conducted as substrate pre-treatment. These processes are inexpensive and environmental-friendly and lead to organic acids generation as soluble products [108].

Du & Yu [53] developed a new technology to couple anaerobic digestion of food scraps with PHBV production. The food wastes were digested in an anaerobic reactor producing acetic, propionic, butyric, and lactic acid. The produced acids were successively transferred through membranes via molecule diffusion into an air-bubbling reactor and utilized to produce PHBV. Mumtaz et al. [83], in turn, used anaerobic fermentation as pre-treatment to obtain a mixture of acetic, butyric and propionic acid, which was successively used for PHBV production by *Comamonas*.

Bhattacharyya et al. [52] used, instead, a different process, i.e. adsorption on activate carbon, to pretreat vinasse. This pretreatment was aimed at removing polyphenolic compounds that are toxic to microorganisms.

Obviously, the convenience of any pre-treatment has to be evaluated by considering the costs/benefits balance. Generally, the use of a substrate rich in simple macro and micro nutrients as well as free of toxic compounds is advisable. For instance, Bhattacharyya et al. [94] compared the use of stillage with the use of vinasse. The authors reported an increase in the 3HV fraction using stillage. The improvement was possibly due to the higher amount of available organic acids in stillage, including 3HV precursors. Moreover, stillage did not require any pre-treatment, while vinasse has to be treated through adsorption, as previously mentioned. Consequently, stillage was more cost effective than vinasse for PHBV production.

9.6. Combination of different strategies

Most of the studies on PHBV production have been conducted using a combination of two or more strategies, as reported in **Table 9.2**.

The use of both precursors addition and waste substrates results in a concomitant reduction of process costs and enhancement of the 3HV fraction. For instance, Sheu et al. [85] demonstrated that up to 95% 3HV can be accumulated in the produced polymer using food starches and providing a suitable valerate concentration in the culture medium. A further productivity enhancement in terms of polymer concentration/mass fraction can be

reached using the previously mentioned performant wild strains, in addition to precursors utilization and waste substrates. For instance, the combination of plant oils and 3HV precursors as substrate was evaluated for the biosynthesis of PHBV by *Ralstonia eutropa*. This combination was suitable for the biosynthesis of high PHBV concentration with high 3HV fraction [14,15]. Similar results were achieved by Koller et al. [84], who performed the conversion of whey lactose and valerate to PHBV by *Haloferax mediterranei*. As previously mentioned, in this case the combination of this specific waste and *Haloferax mediterranei* further reduced process costs. Indeed, whey contains a high salt concentration, which is required by *Haloferax mediterranei*. The absence of salt in the waste substrate would have determined an additional cost due to the salt supply. The combination of cheese whey and *Haloferax Mediterranei* have been tested by Pais et al. [51], as well, without the addition of precursors. The authors obtained promising results in terms of PHBV production, even though the production was lower compared to that obtained by Koller et al. [84], using valerate.

Based on the used strain, in combination with precursors supply, the reduction of costs or the enhancement of the productivity can be reached. For instance, when precursors are used with mixed cultures, such as activated sludge, it is possible to enhance the 3HV fraction and avoid sterilization costs [86]. Otherwise, the use of precursors and pure cultures leading to high PHV accumulation (e.g. *Ralstonia eutropha*) results in the concomitant PHBV accumulation and 3HV fraction enhancement [17]. Moreover, precursors such as levulinic acid, can be used as a stress factor that favors the selection of microorganisms with desired phenotype. Compared to the parental strain, *Ralstonia eutropha* species, adapted to levulinic acid, have shown a better growth rate in presence of the mentioned precursor and a higher PHBV accumulation [87].

Another approach concerns the use of precursors in combination with metabolic engineering. For instance, Choi et al. [23] studied the threonine overproducing mutant of *Alcaligenes sp. SH-69* using levulinic acid as precursor. The use of metabolic engineering resulted in the enhancement of the PHBV accumulation, while levulinic acid enhanced the 3HV fraction of the produced polymer. Moreover, as previously mentioned, some enzymes converting propionic acid to propionyl-CoA have been used to engineer *Escherichia coli* strains for PHBV production, using precursors singulalrly or combined with other substrates [89-90].

Various studies have been conducted by combining the utilization of waste substrates and wild strains which do not require precursors availability to produce the 3HV fraction. Combining these two strategies, rather than add precursors, led to further costs reduction.

In particular, the utilization of waste substrates and pure wild species (i.e. *Rhodospirillum rhubum*, *Bacillus OU40T, Yangia ND199*) resulted in the reduction of process costs related to precursors supply [22,96,97]. Moreover, the utilization of waste substrates and mixed consortia (i.e. acivated sludge) avoided sterilization costs, as well [95]. On the other hand, in this case the production was lower compared to studies performed using pure cultures. Finally, the utilization of organic wastes in combination with the pure specie *Haloferax mediterranei* led to high PHBV productions in concomitance with low process costs [36,51,52,92–94].

9.7.Operating Conditions

In addition to the dependence on the strain and substrate selection, PHBV production processes are strongly affected by other factors such as pH, temperature, aeration conditions, bioreactor design and process regime. Such factors are among the most decisive, especially in the process upscaling. Various bioreactors of different sizes and types have been tested for single stage or multi stage processes under different feeding regimes, extensively reviewed by Koller et al. [109] and Raza et al. [2].

The cylindrical stirred tank reactor (STR) apparatus has been used in all studies. This system can be operated discontinuously (batch, repeated batch, fed batch) or continuously (CSTR).

The batch cultivation mode has been found to be the most used. There are two different approaches developed for batch processes: one-stage cultivation and two-stage cultivation. The choice of the number of stages strongly depends on the selected strain [109]. It is noteworthy that most bacteria produce PHAs under nutritionally unbalanced conditions. In this case, the biomass growth and PHA accumulation have to be conducted in two different phases. The first one is conducted under nutrient-rich conditions and it is characterized by the increase of the microbial biomass concentration. The second one is conducted under the running out of an essential nutrient (e.g. nitrogen, phosphorous, sulphur) and it is characterized by an almost constant biomass concentration and an increasing PHAs percentage inside cells. PHAs concentration increases until the external carbon source is depleted [110]. On the other hand, other strains can accumulate PHAs

already under nutritionally balanced conditions. Moreover, PHA-producers with typically clearly separated phases of biomass and PHAs formation can also contain significant amounts of PHA even without nutrient limitation. In these cases, it is possible to use one stage processes, in which cell growth and PHA accumulation occur simultaneously, allowing for costs reduction [91].

The batch feeding mode is simple in operations, but the productions are intrinsically low. Indeed, the maximum allowed concentration of nutrients at the beginning of the process is restricted by the physiological conditions of the used strain [109]. A simple alternative to the batch cultivation is the repeated batch mode. It consists in conducting a batch cultivation and then periodically removing a fixed fraction of the fermentation broth that will be replaced by the same volume of fresh cultivation medium [111]. For instance, Huang et al. [93] performed a repeated batch fermentation of *Haloferax mediterranei* on extruded rice bran and cornstarch under pH-stat control strategy. The reached high volumetric productivity can be considered an advantage of this strategy over simple batch processes. Moreover, the repeated batch approach saves non-productive time occurring between individual batches.

The same advantage can be obtained using the more common fed batch mode. In this case substrate is added via substrate pulses when its concentration drops below a critical value, without removing the effluent [109]. The fed batch method generally produces higher cell densities compared to the simple batch method. Consequently, it reduces the overall manufacturing cost and allows for the easier management of the process (Rhee et al., 1993). Both reactor configurations have been tested by Ma et al. [64]. The authors achieved higher PHBV production with a higher 3HV fraction for fed batch cultures compared to batch ones.

On the other hand, the major drawback of fed batch cultivation systems is that the addition of the feeding solution during the process increases the fermentation volume, causing a concomitant dilution of the fermentation broth [109].

An alternative fed batch process is to operate the cell-recycling mode by coupling a membrane module directly with the bioreactor. This type of reactor has been used by Lorantfy et al. (2014), who installed a microfiltration unit for high productive biosynthesis of PHBV. The authors observed a ten-fold increase of volumetric productivity for the fed batch cell recycle system compared to a continuous chemostat [112]. Another approach is the continuous fed batch mode, used by Du and Yu [53]. In this case the medium was permanently supplied as a response to the substrate

concentration gradient. The authors coupled anaerobic fermentation with PHBV production. The organic acids produced by the acidogenic consortium in the first anaerobic stage were recycled through a tubular membrane module immersed in the fermentation broth of the aerobic reactor. The membrane enabled the permeation of organic acids into the culture broth of the aerobic stage but retained biomass. Using a silicon rubber membrane, only butyrate and acetate passed through, resulting in PHB accumulation. Nevertheless, using a dialysis membrane also enabled the passing through of lactate and propionate, allowing for PHBV production.

Continuous fed batch processes have been conducted in the case of gaseous substrates as well. For instance, López et al. [113] coupled anaerobic digestion with PHBV production by the methylotrophic bacterium *Methylocystis hirsuta* using biogas and VFAs as substrates. Cal et al. [74] also obtained high 3HV content using the same reactor configuration with methanotrophic consortia fed with methane and valerate or pentanol. Similarly, purple non sulphur bacteria have been tested in these systems to produce PHBV from CO [22,114].

Other authors conduced continuous processes (CSTR) which, often, are used in the same meaning as "chemostat" processes ("chemical environment remaining static"). Continuous processes are characterized by steady state conditions as process parameters like concentrations, pH-value, dissolved oxygen tension (pO2), working volume, nutrient supply, etc., are kept constant. The most decisive parameter for the process is the "dilution rate" (D), which is ratio between flow rate (influent and effluent volume per time) and working volume. Too low D values will lead to insufficient substrates supply while too high D values will lead to the "wash out" condition [109]. The one-stage chemostat has been used for the first time in PHBV production by Ramsay et al. [115] using *Ralstonia eutropha* fed with glucose and propionate and setting a D value of 0.15 1/h. However, the one stage mode, without the separation of growth and accumulation phases, was not competitive with fed batch setups.

To increase the PHBV accumulation and the substrate consumption, a two- stage process is advisable. For instance, Du and Yu [53] selected a drastically higher retention time in the second stage than in the first to boost intracellular PHBV accumulation. Moreover, Ramsay et al. [115] performed sucrose and propionic acid conversion to PHBV using two-stages setups operated at D = 0.15 1/h in both stages. Nitrogen source and propionate were completely utilized in the first stage, while the residual sucrose was used in the second stage to produce an additional PHBV aliquot.

Generally, in bioreactors, controlled conditions of pO_2, pH-value, and temperature are adopted.

Based on the gaseous needs of microorganisms, it is necessary to use different culture systems.

From the analysis of the reviewed studies, it emerged that 96% of them were conducted under aerobic conditions. To ensure the aerobic environment, reactors have to be equipped with aeration and/or agitation systems. Usually, air/oxygen rate and agitation speed are adjusted to ensure a dissolved oxygen value of 20-30% during both the growth phase and the accumulation phase. However, Vollbrecht and Schlegel [116] discovered that mutant strains of *Ralstonia eutrophus* accumulated different PHBV concentrations at different aeration rates. Moreover, Mumtaz et al. [83] observed that it is possible to obtain higher cell dry weight and yield by establishing oxygen excess conditions in the growth phase and oxygen-limited conditions during the production phase. Such results are of primary concern in the optimization of process costs, as well. Indeed, aeration has been demostrated to be significative on costs [44].

To investigate the optimal oxygen supply for the synthesis of PHBV from organic waste, Ganzeveld et al. [82] performed a series of experiments varying the airflow during the oxygen limited step. The airflow was varied between 2.4 and 16.8 ml/min. Optimum air flow was found to be 5.1. Also, Wagle et al. [60] lowered the agitation and air inflow (rpm from 700 to 350 and vvm from 1 to 0.5) and increased the temperature from 28 to 37°C to favor PHBV production. The strategy resulted in an appreciable 36% increase in PHBV production and better substrate utilization.

Other experiments were conducted adjusting the agitation speed to ensure the oxygen availability.

Cavalheiro et al. [77], for instance observed an increase in PHBV accumulation and 3HV fraction when the dissolved oxygen value was set to 2% rather than 20% during the growth phase by adjusting agitation and aeration rate. Moreover, Alsafadi and Al-Mashaqbeh [91] investigated the effect of agitation
(100-220 rpm) and found that the best condition for PHBV accumulation was 170 rpm.

The growth of microorganisms is influenced by other environmental parameters such as temperature and pH. The temperature influences chemical reactions, metabolism and, consequently, PHBV accumulation. The pH, instead, influences the activity of proteins and enzymes. In almost all studies on PHBV production, the temperature and pH

conditions were set in the ranges of 30-35 ° C and 7-7.5, respectively. However, some authors tested different values to optimize T and pH conditions.

For instance, to study the effect of temperature and pH on PHBV production by *Bacillus* species, Balakrishna Pillai et al. [19] varied the incubation temperature between 28 °C and 40 °C and the initial pH between 5 and 9. The optimum temperature and pH values for PHBV accumulation were 31 °C and 7, respectively. Similarly, optimal values of 30° C and 7 were observed by Masood et al. [59] for the specie *Bacillus cereus.* Moreover, PHBV production by engineered *Escherichia coli* at a temperature value of 30°C was found to be significantly higher than those of 37°C [47].

The only observed exception is the *Haloferax Mediterranei* specie, which have been found to accumulate higher PHBV amounts at higher temperatures. Indeed, Alsafadi and Al-Mashaqbeh [91] studied different temperature conditions (25- 45 °C) and observed that the optimal value was 37°C. Moreover, majority of studies on *Haloferax mediterranei* species have been conducted using the temperature value of 37°C, obtaining good results in terms of PHBV accumulation [52,92–94]. Pais et al. [51], instead, used the higher temperature of 45°C while Koller et al. [54] settled the temperature value to 41°C .

Regarding exceptions in pH optimal values, the species *Halomonas campisalis*, examined by Kulkarni et al. [24] produced PHBV at the higher value of 9. Moreover, Ganzeveld et al. [82] found that a pH of 8, instead of the formerly applied 7, resulted in faster growth of the bacterium *Ralstonia eutrophus*. Shimizu et al. (1993) and Vollbrecht and Schlegel [116] also showed that a pH value around 8 considerably stimulates PHBV production by the same species. Finally, Loo and Sudesh [69] varied the initial pH of the medium from 5 to 8 to study optimal values for the bacterium *Delftia acidovorans*. The Highest PHBV accumulation was detected when the pH was set to 7-7.5 while the maximum HV fraction was reached when the pH was set to 5. However, the effect of the pH value on PHBV accumulation, was more beneficial compared to that observed on the HV fraction.

9.8.Discussion

As stated several times in this manuscript, PHBV owns better environmental, thermal and mechanical properties compared to all other bioplastics. However, PHBV high costs and low productivity are still a challenge to be properly faced. Therefore, this review was aimed at reducing the economic gap between PHBV and traditional plastics.

Different strategies for PHBV process productivity enhancement and costs reduction have been analyzed and discussed. In particular, two different approaches have been individuated: the first is related to microorganisms and the second to substrates. Concerning substrates, the discussed strategies have been the addition of precursors of the 3HV fraction or the use of pre-treated waste materials. Concerning microorganisms, the first discussed strategy has been the use of wild performant species, while the second strategy has been the use of metabolic engineering techniques. Finally, combinations of different strategies and operating conditions have been analyzed. In this section, it is presented a critical discussion on all different strategies. The discussion is conducted with the aim of highlighting the most performing strategy or combination of strategies to address future researches.

All revised production methods have revealed to be effective to enhance the PHBV productivity and/or reduce costs. In particular, the selection of the most suitable wild microorganisms resulted of primary concern. Among the different species of microorganisms, an interesting option is the selection of bacteria that produce high amounts of PHBV in presence of precursors. Based on results, *Ralstonia eutropha* is the most performant among others. However, in absence of precursors, this group of bacteria produces exclusively PHB. It is therefore necessary to choose the most convenient precursor to be used as co-substrate. In this case, different suitable possibilities can be considered. In particular, when the addition of synthetic solutions has to be performed, the use of levulinic acid or pentanol is more convenient than other precursors, due to related costs. In particular, excellent results in terms of 3HV fraction enhancement can be obtained by using levulinic acid. Moreover, levulinic acid is competitive with traditional precursors, such as valerate and propionate. However, the addition of synthetic precursors leads to additional costs and increases the difficulties in the process management. Alternatively, it is possible to use waste substrates already containing precursors (e.g. stillage) or to adopt convenient pre-treatments capable to generate precursors (e.g. fermentation).

Another strategy is the use of microorganisms able to convert unrelated carbon sources (not containing precursors) to PHBV, such as the wild specie *Rhodospirillum Rhubum.* Moreover, metabolic engineering techniques can be used to promote precursors-independent pathways in a wide range of microorganisms (e.g. *Escherichia coli* and

Salmonella enterica). On the other hand, the limitation of this option is that the absence of precursors does not allow controlling the 3HV fraction of the produced PHBV. Furthermore, all the mentioned microorganisms are pure species which require a sterile environmental conditions.

The requirement of non-sterile conditions in the reaction environment, is crucial for the process scale-up. Consequently, open mixed cultures (e.g. activate sludges), which are able to adapt to complex unsterile waste substrates, can be used for PHBV production. Alternatively, it can be used *Haloferax mediterranei* which does not require sterile conditions. This bacterium is one of the most performant specie, due to its high robustness, its stability and its capacity of degrading complex molecules. Moreover, *Haloferax Mediterranei* can produce high PHBV amount without substrate pre-treatments and without precursors addition. Due to the requirement of a high saline environment, waste substrates containing high salts concentrations such as cheese whey, are preferable. To further enhance the PHBV productivity by *Haloferax mediterranei*, metabolic engineering techniques can be used to inactivate the gene cluster of the EPS biosynthesis.

The last interesting option to avoid sterilization costs and the global process costs is to focus on a combined biorefinery approach. In particular, the combined production of energy and materials from waste is gaining great attention. This new approach can replace fossil fuels with organic matter as a source of both biofuels and bioplastics.

For instance, the utilization of anaerobic processes as organic waste pre-treatment for PHBV production processes makes reliable to guarantee precursors availability, and therefore enhance the 3HV fraction without supplying the process with costly synthetic co-substrates. Anaerobic cultures can convert organic waste to biofuels and a mix of organic acids, including 3HV precursors. Performing a double stage anaerobic digestion process can lead to the production of organic acids mixture containing valerate in the first stage and biogas in the second stage. It is possible to recover the produced biogas and use the organic acids mixture for the PHBV production step. Alternatively, both biogas and organic acids can be used in the PHBV production step, when the conversion to PHBV is performed by methanotrophic species.

Also, it is possible to carry out the dark fermentation process in the first anaerobic stage. In this case, it is possible to generate hydrogen and a mixture of organic acids containing propionate. Such a mixture can be successively used for PHBV production in the second aerobic step. Hydrogen recovery from the dark fermentation process represents an important added value. Indeed, hydrogen is the most attractive alternative to fossil fuels due to its high energy content and clean combustion properties.

Finally, the choice of the most suitable substrate-microorganism combination cannot be decoupled from the adoption of appropriate operating conditions, such as reactor configuration and abiotic factors. Concerning the reactor configuration, the most effective feeding mode is the continuous fed-batch or the fed-batch system with cell-recycling. In the case of continuous reactors, a two-stage process which separates the growth phase and the accumulation phase promote a productivity increase. Abiotic factors such as temperature, pH and agitation have to be settled in order to establish favourable conditions for the microorganisms. Finally, in aerobic processes, oxygen excess conditions in the growth phase followed by oxygen-limited conditions during the production phase result in higher PHBV yields and simultaneously lower production costs.

The mentioned single strategies and their suggested combinations can be successfully studied in future researches on PHBV production. As majority of the reviewed works have been performed on bench scale reactors, it would be worth testing pilot-plants, in order to move forward the process scale-up.

9.9.Conclusions

PHBV is the most promising biopolymer candidate to replace petroleum-based plastics in a wide range of application. However, even though it owns environmental advantages and more suitable properties compared to other bioplastics, the PHBV wide utilization is still limited by its high production costs and low productivity. Therefore, the current challenge for researchers is the implementation of efficient and low-cost PHBV production processes. In the present work, based on techno-economic analysis, the authors individuated and presented various production strategies, capable to enhance the PHBV productivity and reduce its costs. The critical evaluation of such strategies suggests the following remark:

a reasoned combination of strategies related to the selection of microorganisms and substrates as well as the optimization of operative conditions and the adoption of a combined biorefinery approach can be the right direction to enhance the economic competitiveness of PHBV compared to petroleum-based plastics. Therefore, further research efforts in the process scale-up could make PHBV the most convenient polymer for the production of totally biodegradable and high performant plastics materials.

References

[1] Khanna S, Srivastava AK. Recent advances in microbial polyhydroxyalkanoates. Process Biochem 2005;40:607–19. https://doi.org/10.1016/J.PROCBIO.2004.01.053.

[2] Raza ZA, Tariq MR, Majeed MI, Banat IM. Recent developments in bioreactor scale production of bacterial polyhydroxyalkanoates. Bioprocess Biosyst Eng 2019;42:901–19. https://doi.org/10.1007/s00449-019-02093-x.

[3] Li Z, Yang J, Loh XJ. Polyhydroxyalkanoates: Opening doors for a sustainable future. NPG Asia Mater 2016;8:1–20. https://doi.org/10.1038/am.2016.48.

[4] Gironi F, Piemonte V. Bioplastics and petroleum-based plastics: Strengths and weaknesses. Energy Sources, Part A Recover Util Environ Eff 2011;33:1949–59. https://doi.org/10.1080/15567030903436830.

[5] Policastro G, Luongo V, Fabbricino M. Biohydrogen and poly-β-hydroxybutyrate production by winery wastewater photofermentation: Effect of substrate concentration and nitrogen source. J Environ Manage 2020;271:111006. https://doi.org/10.1016/j.jenvman.2020.111006.

[6] Zheng Y, Chen J-C, Ma Y-M, Chen G-Q. Engineering biosynthesis of polyhydroxyalkanoates (PHA) for diversity and cost reduction. Metab Eng 2020;58:82–93. https://doi.org/10.1016/J.YMBEN.2019.07.004.

[7] Byrom D. copolymers 1992;103:247–50.

[8] Zuñiga C, Morales M, Revah S. Polyhydroxyalkanoates accumulation by Methylobacterium organophilum CZ-2 during methane degradation using citrate or propionate as cosubstrates. Bioresour Technol 2013;129:686–9. https://doi.org/10.1016/j.biortech.2012.11.120.

[9] Tebaldi ML, Maia ALC, Poletto F, de Andrade FV, Soares DCF. Poly(-3-hydroxybutyrate-co-3-hydroxyvalerate) (PHBV): Current advances in synthesis methodologies, antitumor applications and biocompatibility. J Drug Deliv Sci Technol 2019;51:115–26. https://doi.org/10.1016/j.jddst.2019.02.007.

[10] Rivera-Briso AL, Serrano-Aroca Á. Poly(3-Hydroxybutyrate-co-3-Hydroxyvalerate): Enhancement strategies for advanced applications. Polymers (Basel) 2018;10:1–28. https://doi.org/10.3390/polym10070732.

[11] Yu L, Dean K, Li L. Polymer blends and composites from renewable resources. Prog Polym Sci 2006;31:576–602. https://doi.org/10.1016/J.PROGPOLYMSCI.2006.03.002.

[12] Bhattacharyya A, Jana K, Haldar S, Bhowmic A, Mukhopadhyay UK, De S, et al. Integration of poly-3-(hydroxybutyrate-co-hydroxyvalerate) production by Haloferax mediterranei through utilization of stillage from rice-based ethanol manufacture in India and its techno-economic analysis. World J Microbiol Biotechnol 2015;31:717–27. https://doi.org/10.1007/s11274-015-1823-4.

[13] Grousseau E, Blanchet E, Déléris S, Albuquerque MGE, Paul E, Uribelarrea J-L. Phosphorus limitation strategy to increase propionic acid flux towards 3-hydroxyvaleric acid monomers in Cupriavidus necator. Bioresour Technol 2014;153:206–15. https://doi.org/https://doi.org/10.1016/j.biortech.2013.11.072.

[14] Lee WH, Loo CY, Nomura CT, Sudesh K. Biosynthesis of polyhydroxyalkanoate copolymers from mixtures of plant oils and 3-hydroxyvalerate precursors. Bioresour Technol 2008;99:6844–51. https://doi.org/10.1016/j.biortech.2008.01.051.

[15] Ng KS, Wong YM, Tsuge T, Sudesh K. Biosynthesis and characterization of poly(3-hydroxybutyrate-co-3- hydroxyvalerate) and poly(3-hydroxybutyrate-co-3-hydroxyhexanoate) copolymers using jatropha oil as the main carbon source. Process Biochem 2011;46:1572–8. https://doi.org/10.1016/j.procbio.2011.04.012.

[16] Chung SH, Choi GG, Kim HW, Rhee YH. Effect of Levulinic Acid on the Production of Poly(3-hydroxybutyrate-co-3-hydroxyvalerate) by Ralstonia eutropha KHB-8862. J Microbiol 2001;39:79–82.

[17] Kim BS, Lee SC, Lee SY, Chang HN, Chang YK, Woo SI. Production of poly(3-hydroxybutyric-co-3-hydroxyvaleric acid) by fed-batch culture of Alcaligenes eutrophus with substrate control using on-line glucose analyzer. Enzyme Microb Technol 1994;16:556–61. https://doi.org/10.1016/0141-0229(94)90118-X.

[18] Hou J, Feng B, Han J, Liu H, Zhao D, Zhou J, et al. Haloarchaeal-type β-ketothiolases involved in poly(3-hydroxybutyrate-co-3-hydroxyvalerate) synthesis in Haloferax mediterranei. Appl Environ Microbiol 2013;79:5104–11. https://doi.org/10.1128/AEM.01370-13.

[19] Balakrishna Pillai A, Jaya Kumar A, Kumarapillai H. Biosynthesis of poly(3-hydroxybutyrate-co-3-hydroxyvalerate) (PHBV) in Bacillus aryabhattai and cytotoxicity evaluation of PHBV/poly(ethylene glycol) blends. 3 Biotech 2020;10:1–10. https://doi.org/10.1007/s13205-019-2017-9.

[20] Ueda S, Matsumoto S, Takagi A, Yamane T. Synthesis of poly(3-hydroxybutyrate-co-3-hydroxyvalerate) from methanol and n-amyl alcohol by the methylotrophic

bacteria Paracoccus denitrificans and Methylobacterium extorquens. Appl Environ Microbiol 1992;58:3574–9. https://doi.org/10.1128/aem.58.11.3574-3579.1992.

[21] Martla M, Umsakul K, Sudesh K. Production and recovery of poly(3-hydroxybutyrate-co-3-hydroxyvalerate) from biodiesel liquid waste (BLW). J Basic Microbiol 2018;58:977–86. https://doi.org/10.1002/jobm.201800279.

[22] Smith RL, West TP, Gibbons WR. Rhodospirillum rubrum: Utilization of condensed corn solubles for poly-(3-hydroxybutyrate-co-3-hydroxyvalerate) production. J Appl Microbiol 2008;104:1488–94. https://doi.org/10.1111/j.1365-2672.2007.03685.x.

[23] Choi GG, Kim MW, Kim JY, Rhee YH. Production of poly(3-hydroxybutyrate-co-3-hydroxyvalerate) with high molar fractions of 3-hydroxyvalerate by a threonine-overproducing mutant of Alcaligenes sp. SH-69. Biotechnol Lett 2003;25:665–70. https://doi.org/10.1023/A:1023437013044.

[24] Zakaria MR, Ariffin H, Abd-Aziz S, Hassan MA, Shirai Y. Improved Properties of Poly(3-hydroxybutyrate- co -3-hydroxyvalerate) Produced by Comamonas sp. EB172 Utilizing Volatile Fatty Acids by Regulating the Nitrogen Source. Biomed Res Int 2013;2013. https://doi.org/10.1155/2013/237806.

[25] Kulkarni SO, Kanekar PP, Nilegaonkar SS, Sarnaik SS, Jog JP. Production and characterization of a biodegradable poly (hydroxybutyrate-co-hydroxyvalerate) (PHB-co-PHV) copolymer by moderately haloalkalitolerant Halomonas campisalis MCM B-1027 isolated from Lonar Lake, India. Bioresour Technol 2010;101:9765–71. https://doi.org/10.1016/j.biortech.2010.07.089.

[26] Williams DR, Anderson AJ, Dawes EA, Ewing DF. Production of a co-polyester of 3-hydroxybutyric acid and 3-hydroxyvaleric acid from succinic acid by Rhodococcus ruber: biosynthetic considerations. Appl Microbiol Biotechnol 1994;40:717–23. https://doi.org/10.1007/BF00173334.

[27] Steinbüchel A, Lütke-Eversloh T. Metabolic engineering and pathway construction for biotechnological production of relevant polyhydroxyalkanoates in microorganisms. Biochem Eng J 2003;16:81–96. https://doi.org/10.1016/S1369-703X(03)00036-6.

[28] Laycock B, Halley P, Pratt S, Werker A, Lant P. The chemomechanical properties of microbial polyhydroxyalkanoates. Prog Polym Sci 2014;39:397–442. https://doi.org/10.1016/j.progpolymsci.2013.06.008.

[29] Vu DH, Åkesson D, Taherzadeh MJ, Ferreira JA. Recycling strategies for

polyhydroxyalkanoate-based waste materials: An overview. Bioresour Technol 2020;298. https://doi.org/10.1016/j.biortech.2019.122393.

[30] Strong P, Laycock B, Mahamud S, Jensen P, Lant P, Tyson G, et al. The Opportunity for High-Performance Biomaterials from Methane. Microorganisms 2016;4:11. https://doi.org/10.3390/microorganisms4010011.

[31] Poltronieri P, Kumar P. Polyhydroxyalcanoates (PHAs) in Industrial Applications BT - Handbook of Ecomaterials. In: Martínez LMT, Kharissova OV, Kharisov BI, editors., Cham: Springer International Publishing; 2017, p. 1–30. https://doi.org/10.1007/978-3-319-48281-1_70-1.

[32] Bugnicourt E, Cinelli P, Lazzeri A, Alvarez V. Polyhydroxyalkanoate (PHA): Review of synthesis, characteristics, processing and potential applications in packaging. Express Polym Lett 2014;8:791–808. https://doi.org/10.3144/expresspolymlett.2014.82.

[33] Zembouai I, Bruzaud S, Kaci M, Benhamida A, Corre YM, Grohens Y. Mechanical Recycling of Poly(3-Hydroxybutyrate-co-3-Hydroxyvalerate)/Polylactide Based Blends. J Polym Environ 2014;22:449–59. https://doi.org/10.1007/s10924-014-0684-5.

[34] Morikawa H, Marchessault RH. Pyrolysis of bacterial polyalkanoates. Can J Chem 1981;59:2306–13. https://doi.org/10.1139/v81-334.

[35] Ashori A, Jonoobi M, Ayrilmis N, Shahreki A, Fashapoyeh MA. Preparation and characterization of polyhydroxybutyrate-co-valerate (PHBV) as green composites using nano reinforcements. Int J Biol Macromol 2019;136:1119–24. https://doi.org/10.1016/J.IJBIOMAC.2019.06.181.

[36] Hermann-Krauss C, Koller M, Muhr A, Fasl H, Stelzer F, Braunegg G. Archaeal production of polyhydroxyalkanoate (PHA) Co- and terpolyesters from biodiesel industry-derived by-products. Archaea 2013;2013. https://doi.org/10.1155/2013/129268.

[37] García IL, López JA, Dorado MP, Kopsahelis N, Alexandri M, Papanikolaou S, et al. Evaluation of by-products from the biodiesel industry as fermentation feedstock for poly(3-hydroxybutyrate-co-3-hydroxyvalerate) production by Cupriavidus necator. Bioresour Technol 2013;130:16–22. https://doi.org/10.1016/j.biortech.2012.11.088.

[38] Choi J Il, Lee SY. Process analysis and economic evaluation for poly(3-hydroxybutyrate) production by fermentation. Bioprocess Eng 1997;17:335–42.

https://doi.org/10.1007/s004490050394.

[39] Choi J, Lee SY. Factors affecting the economics of polyhydroxyalkanoate production by bacterial fermentation. Appl Microbiol Biotechnol 1999;51:13–21. https://doi.org/10.1007/s002530051357.

[40] Koller M, Hesse P, Bona R, Kutschera C, Atlić A, Braunegg G. Potential of various archae- and eubacterial strains as industrial polyhydroxyalkanoate producers from whey. Macromol Biosci 2007;7:218–26. https://doi.org/10.1002/mabi.200600211.

[41] Chanprateep S. Current trends in biodegradable polyhydroxyalkanoates. J Biosci Bioeng 2010;110:621–32. https://doi.org/10.1016/j.jbiosc.2010.07.014.

[42] Choi D, Chipman DC, Bents SC, Brown RC. A techno-economic analysis of polyhydroxyalkanoate and hydrogen production from syngas fermentation of gasified biomass. Appl Biochem Biotechnol 2010;160:1032–46. https://doi.org/10.1007/s12010-009-8560-9.

[43] Wegen RJVAN, Ling Y, Member APJM. Polyhydroxyalkanoates Using Escherichia Coli : an Economic Analysis 1998;76.

[44] Akiyama M, Tsuge T, Doi Y. Environmental life cycle comparison of polyhydroxyalkanoates produced from renewable carbon resources by bacterial fermentation. Polym Degrad Stab 2003;80:183–94. https://doi.org/10.1016/S0141-3910(02)00400-7.

[45] Yoon JS, Kim JY, Rhee YH. Effects of amino acid addition on molar fraction of 3-hydroxyvalerate in copolyester of 3-hydroxybutyrate and 3-hydroxyvalerate synthesized by Alcaligenes sp. SH-69. J Ferment Bioeng 1995;80:350–4. https://doi.org/10.1016/0922-338X(95)94203-4.

[46] Zhao D, Cai L, Wu J, Li M, Liu H, Han J, et al. Improving polyhydroxyalkanoate production by knocking out the genes involved in exopolysaccharide biosynthesis in Haloferax mediterranei. Appl Microbiol Biotechnol 2013;97:3027–36. https://doi.org/10.1007/s00253-012-4415-3.

[47] Miscevic D, Srirangan K, Kefale T, Kilpatrick S, Chung DA, Moo-Young M, et al. Heterologous production of 3-hydroxyvalerate in engineered Escherichia coli. Metab Eng 2019. https://doi.org/10.1016/j.ymben.2019.11.005.

[48] Wu SC, Liou SZ, Lee CM. Correlation between bio-hydrogen production and polyhydroxybutyrate (PHB) synthesis by Rhodopseudomonas palustris WP3-5. Bioresour Technol 2012;113:44–50. https://doi.org/10.1016/J.BIORTECH.2012.01.090.

[49] Shi LL, Da YY, Zheng WT, Chen GQ, Li ZJ. Production of polyhydroxyalkanoate from acetate by metabolically engineered Aeromonas hydrophilia. J Biosci Bioeng 2020;xxx. https://doi.org/10.1016/j.jbiosc.2020.05.003.

[50] Aldor IS, Kim SW, Jones Prather KL, Keasling JD. Metabolic engineering of a novel propionate-independent pathway for the production of poly(3-hydroxybutyrate-co-3-hydroxyvalerate) in recombinant Salmonella enterica serovar typhimurium. Appl Environ Microbiol 2002;68:3848–54. https://doi.org/10.1128/AEM.68.8.3848-3854.2002.

[51] Pais J, Serafim LS, Freitas F, Reis MAM. Conversion of cheese whey into poly(3-hydroxybutyrate-co-3-hydroxyvalerate) by Haloferax mediterranei. N Biotechnol 2016;33:224–30. https://doi.org/10.1016/j.nbt.2015.06.001.

[52] Bhattacharyya A, Pramanik A, Maji S, Haldar S, Mukhopadhyay U, Mukherjee J. Utilization of vinasse for production of poly-3-(hydroxybutyrate-co-hydroxyvalerate) by Haloferax mediterranei. AMB Express 2012;2:34. https://doi.org/10.1186/2191-0855-2-34.

[53] Du G, Yu J. Green technology for conversion of food scraps to biodegradable thermoplastic polyhydroxyalkanoates. Environ Sci Technol 2002;36:5511–6. https://doi.org/10.1021/es011110o.

[54] Koller M, Chiellini E, Braunegg G. Study on the production and re-use of poly(3-hydroxybutyrate-co-3-hydroxyvalerate) and extracellular polysaccharide by the archaeon Haloferax mediterranei strain DSM 1411. Chem Biochem Eng Q 2015;29:87–98. https://doi.org/10.15255/CABEQ.2014.2058.

[55] Don TM, Chen CW, Chan TH. Preparation and characterization of poly(hydroxyalkanoate) from the fermentation of Haloferax mediterranei. J Biomater Sci Polym Ed 2006;17:1425–38. https://doi.org/10.1163/156856206778937208.

[56] Arcos-Hernandez M V., Pratt S, Laycock B, Johansson P, Werker A, Lant PA. Waste activated sludge as biomass for production of commercial-grade polyhydroxyalkanoate (PHA). Waste and Biomass Valorization 2013;4:117–27. https://doi.org/10.1007/s12649-012-9165-z.

[57] Liu J, Zhao Y, Diao M, Wang W, Hua W, Wu S, et al. Poly(3-hydroxybutyrate-co-3-hydroxyvalerate) Production by Rhodospirillum rubrum Using a Two-Step Culture Strategy. J Chem 2019;2019. https://doi.org/10.1155/2019/8369179.

[58] Phukon P, Saikia JP, Konwar BK. Bio-plastic (P-3HB-co-3HV) from Bacillus

circulans (MTCC 8167) and its biodegradation. Colloids Surfaces B Biointerfaces 2012;92:30–4. https://doi.org/10.1016/j.colsurfb.2011.11.011.

[59] Masood F, Hasan F, Ahmed S, Hameed A. Biosynthesis and characterization of poly (3-hydroxybutyrate-co-3- hydroxyvalerate) from Bacillus cereus FA11 isolated from TNT-contaminated soil. Ann Microbiol 2012;62:1377–84. https://doi.org/10.1007/s13213-011-0386-3.

[60] Wagle AR, Dixit YM, Vakil B V. Scale Up Studies for Polyhydroxyalkanoate Production by a Bacillus flexus Strain with Industrial Potential. Indian J Microbiol 2019;59:383–6. https://doi.org/10.1007/s12088-019-00807-z.

[61] Fergala A, Alsayed A, Khattab S, Ramirez M, Eldyasti A. Development of Methane-Utilizing Mixed Cultures for the Production of Polyhydroxyalkanoates (PHAs) from Anaerobic Digester Sludge. Environ Sci Technol 2018;52:12376–87. https://doi.org/10.1021/acs.est.8b04142.

[62] Kemavongse K, Prasertsan P, Upaichit A, Methacanon P. Poly-β-hydroxyalkanoate production by halotolerant Rhodobacter sphaeroides U7. World J Microbiol Biotechnol 2008;24:2073–85. https://doi.org/10.1007/s11274-008-9712-8.

[63] Aldor I, Keasling JD. Composition in Recombinant Salmonella enterica Serovar Typhimurium. Biotechnology 2001.

[64] Ma W, Wang J, Li Y, Yin L, Wang X. Poly(3-hydroxybutyrate-co-3-hydroxyvalerate) co-produced with l-isoleucine in Corynebacterium glutamicum WM001. Microb Cell Fact 2018;17:1–12. https://doi.org/10.1186/s12934-018-0942-7.

[65] Chen Y, Chen XY, Du HT, Zhang X, Ma YM, Chen JC, et al. Chromosome engineering of the TCA cycle in Halomonas bluephagenesis for production of copolymers of 3-hydroxybutyrate and 3-hydroxyvalerate (PHBV). Metab Eng 2019;54:69–82. https://doi.org/10.1016/j.ymben.2019.03.006.

[66] Tan D, Wu Q, Chen JC, Chen GQ. Engineering Halomonas TD01 for the low-cost production of polyhydroxyalkanoates. Metab Eng 2014;26:34–47. https://doi.org/10.1016/j.ymben.2014.09.001.

[67] Myung J, Galega WM, Van Nostrand JD, Yuan T, Zhou J, Criddle CS. Long-term cultivation of a stable Methylocystis-dominated methanotrophic enrichment enabling tailored production of poly(3-hydroxybutyrate-co-3-hydroxyvalerate). Bioresour Technol 2015;198:811–8.

https://doi.org/10.1016/j.biortech.2015.09.094.

[68] Inn Z, Eilenmann W, Any H, Chmid S, Gli E. of Poly ([R] -3-hydroxybutyrate-co-3-hydroxyvalerate) (PHB / HV) in Ralstonia eutropha DSM 428 2003;23:309–16.

[69] Loo CY, Sudesh K. Biosynthesis and native granule characteristics of poly(3-hydroxybutyrate-co-3-hydroxyvalerate) in Delftia acidovorans. Int J Biol Macromol 2007;40:466–71. https://doi.org/10.1016/j.ijbiomac.2006.11.003.

[70] Han J, Wu LP, Hou J, Zhao D, Xiang H. Biosynthesis, characterization, and hemostasis potential of tailor-made poly(3-hydroxybutyrate- co -3-hydroxyvalerate) produced by Haloferax mediterranei. Biomacromolecules 2015;16:578–88. https://doi.org/10.1021/bm5016267.

[71] Yu ST, Lin CC, Too JR. PHBV production by Ralstonia eutropha in a continuous stirred tank reactor. Process Biochem 2005;40:2729–34. https://doi.org/10.1016/j.procbio.2004.12.023.

[72] Doi Y, Kunioka M, Nakamura Y, Soga K. Biosynthesis of Copolyesters in Alcaligenes eutrophus H16 from13C-Labeled Acetate and Propionate. Macromolecules 1987;20:2988–91. https://doi.org/10.1021/ma00178a006.

[73] Park_1997.pdf n.d.

[74] Cal AJ, Sikkema WD, Ponce MI, Franqui-Villanueva D, Riiff TJ, Orts WJ, et al. Methanotrophic production of polyhydroxybutyrate-co-hydroxyvalerate with high hydroxyvalerate content. Int J Biol Macromol 2016;87:302–7. https://doi.org/10.1016/j.ijbiomac.2016.02.056.

[75] Ezhov VA, Doronina N V., Trotsenko YA. Biosynthesis of polyhydroxybutyrate/valerate with different molecular weights during the growth of Methylobacterium extorquens G-10 on a methanol-pentanol mixture. Appl Biochem Microbiol 2013;49:150–3. https://doi.org/10.1134/S0003683813020038.

[76] Kerketta A, Vasanth D. Madhuca indica flower extract as cheaper carbon source for production of poly (3-hydroxybutyrate-co-3-hydroxyvalerate) using Ralstonia eutropha. Process Biochem 2019;87:1–9. https://doi.org/10.1016/j.procbio.2019.09.013.

[77] Cavalheiro JMBT, Raposo RS, de Almeida MCMD, Teresa Cesário M, Sevrin C, Grandfils C, et al. Effect of cultivation parameters on the production of poly(3-hydroxybutyrate-co-4-hydroxybutyrate) and poly(3-hydroxybutyrate-4-hydroxybutyrate-3-hydroxyvalerate) by Cupriavidus necator using waste glycerol.

Bioresour Technol 2012;111:391–7. https://doi.org/10.1016/j.biortech.2012.01.176.

[78] Alsafadi D, Ibrahim MI, Alamry KA, Hussein MA, Mansour A. Utilizing the crop waste of date palm fruit to biosynthesize polyhydroxyalkanoate bioplastics with favorable properties. Sci Total Environ 2020;737:139716. https://doi.org/https://doi.org/10.1016/j.scitotenv.2020.139716.

[79] Ahn J, Jho EH, Kim M, Nam K. Increased 3HV Concentration in the Bacterial Production of 3-Hydroxybutyrate (3HB) and 3-Hydroxyvalerate (3HV) Copolymer with Acid-Digested Rice Straw Waste. J Polym Environ 2016;24:98–103. https://doi.org/10.1007/s10924-015-0749-0.

[80] Anil Kumar PK, Shamala TR, Kshama L, Prakash MH, Joshi GJ, Chandrashekar A, et al. Bacterial synthesis of poly(hydroxybutyrate- co-hydroxyvalerate) using carbohydrate-rich mahua (Madhuca sp.) flowers. J Appl Microbiol 2007;103:204–9. https://doi.org/10.1111/j.1365-2672.2006.03221.x.

[81] Suhazsini P, Keshav R, Narayanan S, Chaudhuri A, Radha P. A Study on the Synthesis of Poly (3-hydroxybutyrate-co-3-hydroxyvalerate) by Bacillus megaterium Utilizing Cheese Whey Permeate. J Polym Environ 2020;28:1390–405. https://doi.org/10.1007/s10924-020-01687-x.

[82] Ganzeveld KJ, Van Hagen A, Van Agteren MH, De Koning W, Uiterkamp AJMS. Upgrading of organic waste: Production of the copolymer poly-3-hydroxybutyrate-co-valerate by Ralstonia eutrophus withorganic waste as sole carbon source. J Clean Prod 1999;7:413–9. https://doi.org/10.1016/s0959-6526(99)00159-6.

[83] Mumtaz T, Abd-Aziz S, Rahman NA, Yee PL, Shirai Y, Hassan MA. Fed-batch production of P(3HB-co-3HV) copolymer by Comamonas sp EB 172 using mixed organic acids under dual nutrient limitation. Eur J Sci Res 2009;33:374–84.

[84] Koller M, Atlić A, Gonzalez-Garcia Y, Kutschera C, Braunegg G. Polyhydroxyalkanoate (PHA) biosynthesis from whey lactose. Macromol Symp 2008;272:87–92. https://doi.org/10.1002/masy.200851212.

[85] Sheu DS, Chen WM, Yang JY, Chang RC. Thermophilic bacterium Caldimonas taiwanensis produces poly(3-hydroxybutyrate-co-3-hydroxyvalerate) from starch and valerate as carbon sources. Enzyme Microb Technol 2009;44:289–94. https://doi.org/10.1016/j.enzmictec.2009.01.004.

[86] Dionisi D, Majone M, Papa V, Beccari M. Biodegradable Polymers from Organic

Acids by Using Activated Sludge Enriched by Aerobic Periodic Feeding. Biotechnol Bioeng 2004;85:569–79. https://doi.org/10.1002/bit.10910.

[87] Novackova I, Kucera D, Porizka J, Pernicova I, Sedlacek P, Koller M, et al. Adaptation of Cupriavidus necator to levulinic acid for enhanced production of P(3HB-co-3HV) copolyesters. Biochem Eng J 2019;151:107350. https://doi.org/10.1016/j.bej.2019.107350.

[88] Horng Y-T, Chien C-C, Huang C-T, Wei Y-H, Chen S-Y, Lan JC-W, et al. Biosynthesis of poly(3-hydroxybutyrate-co-3-hydroxyvalerate) with co-expressed propionate permease (prpP), beta-ketothiolase B (bktB), and propionate-CoA synthase (prpE) in Escherichia coli. Biochem Eng J 2013;78:73–9. https://doi.org/https://doi.org/10.1016/j.bej.2012.12.016.

[89] Choi J Il, Lee SY. High-level production of poly(3-hydroxybutyrate-co-3-hydroxyvalerate) by fed-batch culture of recombinant Escherichia coli. Appl Environ Microbiol 1999;65:4363–8. https://doi.org/10.1128/aem.65.10.4363-4368.1999.

[90] Yang YH, Brigham CJ, Song E, Jeon JM, Rha CK, Sinskey AJ. Biosynthesis of poly(3-hydroxybutyrate-co-3-hydroxyvalerate) containing a predominant amount of 3-hydroxyvalerate by engineered Escherichia coli expressing propionate-CoA transferase. J Appl Microbiol 2012;113:815–23. https://doi.org/10.1111/j.1365-2672.2012.05391.x.

[91] Alsafadi D, Al-Mashaqbeh O. A one-stage cultivation process for the production of poly-3-(hydroxybutyrate-co-hydroxyvalerate) from olive mill wastewater by Haloferax mediterranei. N Biotechnol 2017;34:47–53. https://doi.org/10.1016/j.nbt.2016.05.003.

[92] Chen CW, Don TM, Yen HF. Enzymatic extruded starch as a carbon source for the production of poly(3-hydroxybutyrate-co-3-hydroxyvalerate) by Haloferax mediterranei. Process Biochem 2006;41:2289–96. https://doi.org/10.1016/j.procbio.2006.05.026.

[93] Huang TY, Duan KJ, Huang SY, Chen CW. Production of polyhydroxyalkanoates from inexpensive extruded rice bran and starch by Haloferax mediterranei. J Ind Microbiol Biotechnol 2006;33:701–6. https://doi.org/10.1007/s10295-006-0098-z.

[94] Bhattacharyya A, Saha J, Haldar S, Bhowmic A, Mukhopadhyay UK, Mukherjee J. Production of poly-3-(hydroxybutyrate-co-hydroxyvalerate) by Haloferax

mediterranei using rice-based ethanol stillage with simultaneous recovery and re-use of medium salts. Extremophiles 2014;18:463–70. https://doi.org/10.1007/s00792-013-0622-9.

[95] Yin F, Li D, Ma X, Zhang C. Pretreatment of lignocellulosic feedstock to produce fermentable sugars for poly(3-hydroxybutyrate-co-3-hydroxyvalerate) production using activated sludge. Bioresour Technol 2019;290. https://doi.org/10.1016/j.biortech.2019.121773.

[96] Nagamani P, Mahmood S. International Journal of Pharma and Bio Sciences ISSN 6299 PRODUCTION OF POLY (3-HYDROXYBUTYRATE-CO-3-HYDROXYVALERATE) BY A NOVEL BACILLUS OU40 T FROM INEXPENSIVE CARBON SOURCES. Int J Pharma Biosci 2013;4:182–93.

[97] Van-Thuoc D, Huu-Phong T, Minh-Khuong D, Hatti-Kaul R. Poly(3-Hydroxybutyrate-co-3-Hydroxyvalerate) Production by a Moderate Halophile Yangia sp. ND199 Using Glycerol as a Carbon Source. Appl Biochem Biotechnol 2015;175:3120–32. https://doi.org/10.1007/s12010-015-1479-4.

[98] Pérez-Pantoja D, De La Iglesia R, Pieper DH, González B. Metabolic reconstruction of aromatic compounds degradation from the genome of the amazing pollutant-degrading bacterium Cupriavidus necator JMP134. vol. 32. 2008. https://doi.org/10.1111/j.1574-6976.2008.00122.x.

[99] Verlinden RAJ, Hill DJ, Kenward MA, Williams CD, Piotrowska-Seget Z, Radecka IK. Production of polyhydroxyalkanoates from waste frying oil by cupriavidus necator. AMB Express 2011;1:1–8. https://doi.org/10.1186/2191-0855-1-11.

[100] Cavalheiro JMBT, de Almeida MCMD, Grandfils C, da Fonseca MMR. Poly(3-hydroxybutyrate) production by Cupriavidus necator using waste glycerol. Process Biochem 2009;44:509–15. https://doi.org/10.1016/j.procbio.2009.01.008.

[101] Ali I, Jamil N. Biosynthesis and genetics of polyhydroxyalkanoates by newly isolated Pseudomonas aeruginosa IFS and 30N using inexpensive carbon sources. Int J Environ Sci Technol 2017;14:1879–88. https://doi.org/10.1007/s13762-017-1268-4.

[102] Koller M, Hesse P, Bona R, Kutschera C, Atlić A, Braunegg G. Biosynthesis of high quality polyhydroxyalkanoate Co- And terpolyesters for potential medical application by the archaeon haloferax mediterranei. Macromol Symp 2007;253:33–9. https://doi.org/10.1002/masy.200750704.

[103] Ferre-Guell A, Winterburn J. Production of the copolymer poly(3-hydroxybutyrate-co-3-hydroxyvalerate) with varied composition using different nitrogen sources with Haloferax mediterranei. Extremophiles 2017;21:1037–47. https://doi.org/10.1007/s00792-017-0964-9.

[104] Ferre-Guell A, Winterburn J. Increased production of polyhydroxyalkanoates with controllable composition and consistent material properties by fed-batch fermentation. Biochem Eng J 2019;141:35–42. https://doi.org/10.1016/j.bej.2018.10.004.

[105] Steinbüchel A, Pieper U. Production of a copolyester of 3-hydroxybutyric acid and 3-hydroxyvaleric acid from single unrelated carbon sources by a mutant of Alcaligenes eutrophus. Appl Microbiol Biotechnol 1992;37:1–6. https://doi.org/10.1007/BF00174193.

[106] Ghosh D, Sobro IF, Hallenbeck PC. Stoichiometric conversion of biodiesel derived crude glycerol to hydrogen: Response surface methodology study of the effects of light intensity and crude glycerol and glutamate concentration. Bioresour Technol 2012;106:154–60. https://doi.org/10.1016/j.biortech.2011.12.021.

[107] Ahn J, Jho EH, Nam K. Effect of acid-digested rice straw waste feeding methods on the 3HV fraction of bacterial poly(3-hydroxybutyrate-co-3-hydroxyvalerate) production. Process Biochem 2016;51:2119–26. https://doi.org/10.1016/j.procbio.2016.09.014.

[108] Pagliano G, Ventorino V, Panico A, Pepe O. Integrated systems for biopolymers and bioenergy production from organic waste and by-products: A review of microbial processes. Biotechnol Biofuels 2017;10:1–24. https://doi.org/10.1186/s13068-017-0802-4.

[109] Koller M. A review on established and emerging fermentation schemes for microbial production of polyhydroxyalkanoate (PHA) biopolyesters. Fermentation 2018;4. https://doi.org/10.3390/fermentation4020030.

[110] Kourmentza C, Plácido J, Venetsaneas N, Burniol-Figols A, Varrone C, Gavala HN, et al. Recent advances and challenges towards sustainable polyhydroxyalkanoate (PHA) production. Bioengineering 2017;4:1–43. https://doi.org/10.3390/bioengineering4020055.

[111] Luongo V, Policastro G, Ghimire A, Pirozzi F, Fabbricino M. Repeated-Batch Fermentation of Cheese Whey for Semi-Continuous Lactic Acid Production Using Mixed Cultures at Uncontrolled pH. Sustainability 2019;11:3330.

https://doi.org/10.3390/su11123330.

[112] Lorantfy B, Ruschitzka P, Herwig C. Investigation of physiological limits and conditions for robust bioprocessing of an extreme halophilic archaeon using external cell retention system. Biochem Eng J 2014;90:140–8. https://doi.org/https://doi.org/10.1016/j.bej.2014.06.004.

[113] López JC, Arnáiz E, Merchán L, Lebrero R, Muñoz R. Biogas-based polyhydroxyalkanoates production by Methylocystis hirsuta: A step further in anaerobic digestion biorefineries. Chem Eng J 2018;333:529–36. https://doi.org/https://doi.org/10.1016/j.cej.2017.09.185.

[114] Do YS, Smeenk J, Broer KM, Kisting CJ, Brown R, Heindel TJ, et al. Growth of Rhodospirillum rubrum on synthesis gas: Conversion of CO to H2 and poly-β-hydroxyalkanoate. Biotechnol Bioeng 2007;97:279–86. https://doi.org/10.1002/bit.21226.

[115] Ramsay BA, Lomaliza K, Chavarie C, Dube B, Bataille P, Ramsay JA. Production of Poly- (P-Hydroxybutyric-Co-3-Hydroxyvaleric) Acids 1990;56:2093–8.

[116] Vollbrecht D, Schlegel HG. Excretion of metabolites by hydrogen bacteria II. Influences of aeration, pH, temperature, and age of cells. Eur J Appl Microbiol Biotechnol 1978;6:157–66. https://doi.org/10.1007/BF00504427.

[117] Shimizu H, Tamura S, Shioya S, Suga K. Kinetic study of poly-d(−)-3-hydroxybutyric acid (PHB) production and its molecular weight distribution control in a fed-batch culture of Alcaligenes eutrophus. J Ferment Bioeng 1993;76:465–9. https://doi.org/https://doi.org/10.1016/0922-338X(93)90242-Z

Chapter 10

A chemostat enrichment system to induce lipids accumulation in microalgae

The present chapter reports preliminary results of a study in progress, which is part of an international collaboration with the "Delft University of Technology (Delft, The Netherlands)".

A chemostat enrichment system to induce lipids accumulation in microalgae

Abstract

In this study we tested a dual-limited chemostat system to induce lipid accumulation in mixed cultures microalgae. We adopted light intensity and nitrogen concentration as the limiting factors to induce lipids accumulation. Different nitrogen loading rates were tested, from nitrogen limiting to nitrogen excess or light excess to light limiting conditions. Moreover, we performed a medium manipulation to enrich the phototrophic lipid storing community. In particular, the medium was supplied with a vitamin trace solution and silicate. Preliminary results show that the medium manipulation allowed to enrich a mixed culture which stored lipids. Moreover, the dual limitation (both nitrogen and light limitation) enhanced lipids concentration in the effluent. A maximum lipids concentration of 429.6 mg L^{-1} d^{-1} was achieved, which is a very high value compared to previous studies performed on pure culture chemostat systems.

10.1. Introduction

The finding of clean and renewable energy sources is one of the most debated and challenging problems to be faced globally. Many countries and regions have established targets for CO_2 reduction, in order to meet the goals of environmental protocols. Currently, in European Union (EU), the transportation and energy sectors are the major anthropogenic sources of greenhouse gas (GHG) emissions [1]. Therefore, an important goal is the finding of measures able to reduce transportation emissions, such as the gradual replacement of fossil fuels by biofuels. Biofuels can offer a huge contribution to the decarbonisation of transportation fuels and to the increase of the energy supply sustainability. They are mainly produced from biomass and contribute to lower combustion emissions (compared to fossil fuels) per equivalent power output [2]. The most common biofuels are biodiesel and bio-ethanol, which can replace diesel and gasoline, respectively. These biofuels can be used in existing systems, with little or none modifications of vehicle engines [3].

Currently, among the various possibilities being investigated to produce biofuels, one of the most interesting is represented by the third generation biorefining systems based on microalgae [4]. The main advantages of using microalgae-derived biofuels include high growth rates, ease of cultivation, the possibility of CO_2 sequestration, and wastewater treatment. Indeed, large-scale cultivation of microalgae may be 20 times more productive than biofuels crops on a per hectare base, without competing for food production [5]. Via the photosynthesis process, microalgae can convert CO_2 into organic compounds with high energy content [6]. Moreover, it is possible to couple biofuels production with

tertiary wastewater treatment as microalgae can use nitrogen and phosphorous contaminants as nutrients for their growth [3]. The major bottlenecks hindering the commercial production of microalgal derived biofuels are the high costs and the low productivity. Pure culture cultivation of microalgae requires aseptic inflows and carefully controlled conditions, resulting in high investments and operating costs. Conversely, open mixed cultures do not require sterilization of the inflow wastewater and confer more stability and robustness to the process [7].

During their growth, microalgae are able to accumulate value-added organic compounds, such as starch and lipids which are precursors of bioethanol and biodiesel, respectively. Lipids production is a preferable option due to the higher energy density, lower downstream energy costs [8] as well as higher value compared to sugar production. Over the last few years, the induction of lipids accumulation in microalgae has been intensively studied. Under optimal growth conditions, large amounts of biomass are produced, with relatively low lipid content. Conversely, microalgae switch their biosynthetic pathways from biomass generation towards the accumulation of lipids under stress conditions [9]. To this aim, different stress conditions have been applied, such as non-optimal light irradiance, nutrition starvation, non-optimal culture pH and temperature, and other non-optimal operating conditions [4,10]. In this context, nitrogen starvation has been reported as the most successful lipid accumulation inducing technique. Nitrogen is the most growth-limiting factor for eukaryotic microalgae and nitrogen starvation is relatively easy to apply. Moreover, while the response to other stress factors is strain specific, all the microalgal species studied so far seem to increase lipids production under nitrogen stress [9]. This makes this approach particularly suitable for mixed culture cultivations. Nitrogen starvation for lipids accumulation by microalgae is usually performed in two-step batch processes. First, algae are grown under optimal conditions to enhance the photosynthetic activity and the biomass concentration. Then, lipids accumulation is induced by arresting the growth using nitrogen deprivation [11]. Using this strategy, high lipids content can be reached after prolonged nitrogen starvation [12]. During the initial period of the second step carbohydrate polymers are the main by-products. Successively, lipids production occurs due to *de novo* fatty acid synthesis or due to the conversion of the sugar polymers [13]. However, the exposition to unfavourable conditions for relatively long time dramatically limits the biomass growth. Consequently, the maximum lipids productivity is only reached within the first days of cultivation, when the biomass concentration is high and the cellular lipids content is still low [14].

Continuous microalgae cultivation in a chemostat culture mode would offer many advantages, such as stable productivity and higher process control compared to the batch feeding mode [15]. When steady-state conditions are reached at a specific dilution rate, the biomass productivity and the intracellular biochemical composition remain constant [11]. Therefore, operational conditions can be studied and optimized to reach the highest lipids productivity [16]. A trade-off between microalgae growth and storage metabolites production should be carefully analysed to optimize the nutrient manipulation strategy. Maintaining photosynthetic activity in a prolonged period of nitrogen starvation could result in improved lipid productivity, which contributes to improved process economics [17].

Egli and Quayle [18] studied the effect of the carbon (C) to nitrogen (N) ratio on polyhydroxybutyrate (PHB) accumulation by a yeast in chemostat systems. The authors identified three different growth zones: i) a C limitation zone at low C/N ratios, ii) a N limitation zone at high C/N ratios, and iii) a transient zone, which is characterized by the complete consumption of both nutrients. The existence of this dual nutrient limitation (DNL) growth zone relies on the ability of microorganisms to adjust their cellular composition to different nutrient limitation conditions. The authors observed that the PHB accumulation improved under DNL conditions. This observation was later confirmed by other authors, whose studies focused on C and N [19,20] or C and P limitations [21].

Inspired by these approaches, in this study we hypothesized that a dual-limited (DL) chemostat system can efficiently induce lipid accumulation in mixed cultures microalgae along with biomass generation. We adopted light intensity and nitrogen concentration as the limiting factors to induce lipids accumulation. Moreover, we performed a medium manipulation to enrich our phototrophic lipid storing community. In particular, the medium was supplied with a vitamin trace solution, which have been reported to dramatically enhance lipid concentration in a mixed culture batch study [22].

10.2. Materials and methods

10.2.1. Feed composition and photobioreactor set up

A mix of samples from different water bodies in Delft (Netherlands) was used as inoculum. The mixed culture was enriched for four weeks in a 500 mL batch reactor. The working volume (400 mL) consisted of a modified f/2 medium and the inoculum (20% v/v). The composition of the medium was the following (mg L^{-1}): NH_4Cl (477.0) $MgSO_4$ $.7H_2O$ (394.4); KCl (18.2); K_2HPO_4 (156.8); $CaCl_2.2H_2O$ (22.0); $FeCl_3.6H_2O$ (38.0);

NaEDTA.2H_2O (150.5); H_3BO_3 (46.4); $NaSiO_3.9H_2O$ (85.3); allylthiourea (70); 1 mL L^{-1} trace element solution and 1 mL L^{-1} vitamin trace solution. The final trace elements concentrations in the medium were: (mg L^{-1}): $ZnSO_4.7H_2O$ (2.20); $MnSO_4$ (4.32); $CuSO_4.5H_2O$ (1.57); $CoCl_2.6H_2O$ (1.61); $Na_2MoO_4.2H_2O$ (2.18). The final vitamins concentrations were (mg L^{-1}): Vitamin B_1(1.00); vitamin B_7 (0.49); vitamin B_{12} (0.53); vitamin B_5 (4.38).

The enriched inoculum was used to start up a 3 L photobioreactor (Applikon Biotechnology, the Netherlands).

The medium (2 L working volume) was the same which was used in the enrichment phase. 200 mL of enriched inoculum were centrifugated and wet pellets were harvested to inoculate the reactor.

The continuous illumination of 350 µmol.m^{-2} s^{-1} was provided by LED strips, controlled via a Photo Biosym (Designinnova, India). The reactor was aerated with CO_2 (6%, v/v in air) at the flow rate of 500 mL min^{-1}, using a mass flow controller (Brooks Instruments, Ede, the Netherlands). The off-gas stream was cooled to 4 °C and analyzed for carbon dioxide and oxygen percentages detection. The speed of the stirrer, pH, and temperature were maintained at 150 rpm, 7.5, and 30 °C, respectively. A Masterflex pump (Cole-Parmer, Vernon Hills, IL, USA) with two heads was used at inflow and outflow rate of 0.69 mL min^{-1} to provide the constant dilution rate of 0.5 d^{-1} and HRT of 2 d. A Biocontroller ADI 1030 (Applikon, The Netherlands) continuously measured pH and DOT (Dissolved Oxygen Tension). All data were stored by PC with MFCS_win software (Sartorius Stedim Systems, Germany).

The photobioreactor was run in batch mode until the OD was higher than 1.8 [14]. Successively, the feeding mode was switched to continuous. All experiments were conducted under non-sterile conditions.

10.2.2. Experimental tests and analytical methods

Four different conditions were tested, using different NLRs. The different loading rates were settled in order to test the culture both under nitrogen limitation and nitrogen excess conditions (or light excess and light limitation). **Table 1** reports NLRs and NH_4Cl concentrations used during five different experimental tests.

Test	N1	N2	N3	N4	N5

NLRs (mgN $L^{-1}d^{-1}$)	20	32.5	42	63	n.a.
NH_4Cl (mg L^{-1})	150	246	318	477	n.a.

* n.a. not available as in progress.

Each NLR was tested until the steady state condition was reached (i.e. oxygen and carbon dioxide in the off-gas did not vary of more than the 10% for three consecutive HRTs).

OD_{680} and the off-gas were measured every day, using a DR 3900 spectrophotometer (Hach, the Netherlands) and a Rosemount NGA off-gas analyzer (Emerson, USA), respectively.

When the steady state was reached, samples were collected to measure the biomass and the residual nitrogen concentration in the effluent. Moreover, lipids and starch content in cells were quantified.

The content of nitrogen was measured spectrophotometrically using Dr. Lange Ammonium cuvette tests (Hach Lange, Germany).

To measure VS content, a sample of 50 mL of effluent was dried overnight in a pre-weighed aluminum foil container at 104 °C. Ash content was determined by drying the sample at 550 °C for 3 hours. The following equation was used to estimate the biomass productivity:

$$\text{Biomass Productivity (mg } L^{-1} d^{-1}) = \text{VS (mg } L^{-1}) \times D\ (d^{-1}) \quad (1)$$

where VS and D are volatile solids and dilution rate, respectively.

Lipids were extracted using a modified PHB extraction protocol [30]. In digestion tubes, 1.5mL of 1-propanol: hydrochloric acid (4:1 v/v), and 1.5 mL of 1,2-dichloroethane were added to weighed freeze-dried biomass. The tubes were placed in a digester block at 100 °C for 2 h. 1 mL bi-distilled water was added to facilitate the separation of the two phases. The lower layer, containing the organic phase, was extracted from tubes. Successively, total lipids were measured according to Coelho et al. [31]. In particular, the organic solvent was evaporated and the remaining material (total lipids) was left in the oven at 50 °C, cooled down until room temperature and weighted until constant weight.

Starch extraction was performed as follows: 5 mL of 0.6 M HCl were added to 4-mg freeze-dried biomass. Digestion tubes were heated with for 3 h at 100 °C. After centrifugation, the total carbohydrates content was measured using the colorimetric

method according to standard methods (APHA, 2005). The productivity of starch and lipids were calculated according to the following equations:

Starch Productivity (mg L^{-1} d^{-1}) = Starch Content (mg L^{-1})×D(d^{-1}) (2)

Lipid Productivity (mg L^{-1} d^{-1}) = Lipid Content (mg L^{-1})×D(d^{-1}) (3)

Finally, a Zeiss microscope (Carl Zeiss, Germany) was used to observe the culture and the staining of cells. 4 µl BODIPY 505/515 (4,4-difluoro-1,3,5,7-tetramethyl-4-bora-3a,4a-diazasindacene) in anhydrous dimethyl sulfoxide (DMSO; 1 mg mL^{-1}) was added to 0.2 mL of algal culture for visualizing the lipids droplets in the cells. The excitation and emission wavelengths for monitoring BODIPY 505/515 fluorescence were 488 and 515 nm, respectively.

10.3. Results and discussion

Figure 10.1a shows the observed results related to nitrogen depletion and biomass production in terms of VS, in Figure 10.1b starch and lipids productivity are reported.

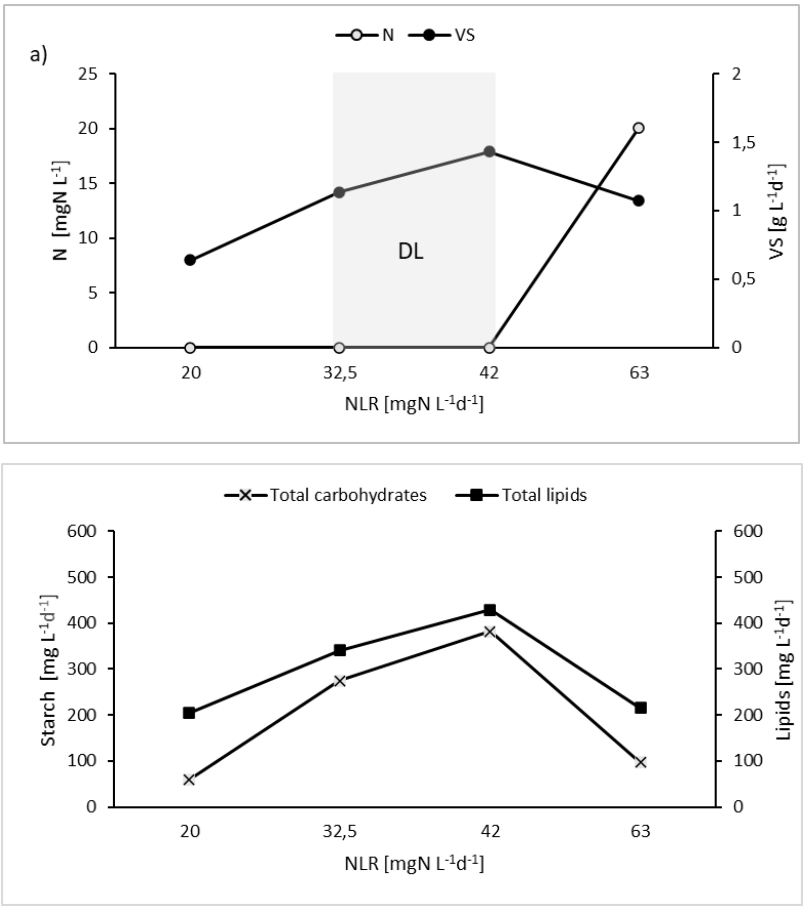

Figure 10.1. Preliminaryresults at the steady state under different NLRs. a) Nitrogen concentration in the effluent and biomass productivity. b) Starch and total lipids productivity.

At the highest NLR of 63 mgN L^{-1} d^{-1}, the microalgae enrichment did not consume all the nitrogen supplied to the reactor. In this case, the light was the limiting factor due to the high biomass concentration and the self-sheading phenomenon. The nitrogen concentration in the effluent was below the detection limit for the nitrogen loading rates (NLR) of 20, 32.5 and 42 mgN L^{-1} d^{-1}: confirming nitrogen was a limiting substrate. To evaluate the DL growth zone, the biomass growth under light limitation was assumed as a reference value. In particular, the VS concentration of 1.07 $g_{VS}L^{-1}d^{-1}$, was considered as the reference value. The biomass growth achieved at the NLR of 20 mgN L^{-1} d^{-1} was lower than this reference value. Therefore, we assumed nitrogen as the only limiting factor of the specific NLR condition. On the other hand, the cultures characterized by the NLRs of 32.5 and 42 mgN L^{-1} d^{-1} achieved similar or even higher VS values compared to the target value, and therefore experienced a nitrogen and light limitation. The higher VS concentration achieved in the DL growth zone (Figure 10.1a) was attributed to the carbon compounds storage, which was confirmed by the increased CO_2 consumption observed from off-gas measurements.

The highest lipids productivity of 429.6 mg L^{-1} d^{-1}, corresponding to 18% of the total dry weight, was achieved under the NLR of 42 mgN L^{-1} d^{-1}. The enhanced lipids accumulation detected under the DL condition was confirmed by the observation of lipid bodies by fluorescence microscopy (Figure 10.2).

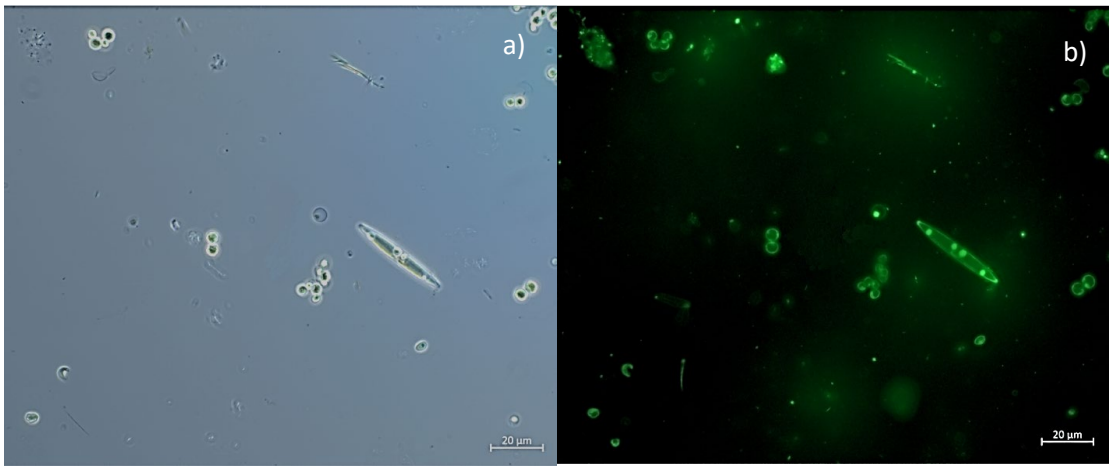

Figure 10.2. Microscopic pictures of microalgae present in the culture at the steady state under DL conditions. a) Normal light, b) fluorescence light.

Besides lipids also the content of starch in the chemostat increased under the DL condition. Nevertheless, lipids accumulation was higher compared to starch for all the tested NLRs. This result suggests that all environmental conditions used during the enrichment phase stimulated the selection of lipids accumulating species. According to Mooij et al. [23], lipids production is higher in diatoms dominated systems than in green microalgae dominated systems. In our experiments, microscope observations revealed a

consistent presence of diatoms, which was likely due to the silicate availability in the medium. Silicate is an essential nutrient for the development of the diatoms' silica shell**.** To reach each steady state, the culture was subjected to a prolonged period of nitrogen starvation. This could have resulted in improved lipid productivities, as suggested in a recent work [13].

Finally, most likely the supplementation of vitamins played a role in the enzymatic activity of lipid biosynthesis in microalgae, providing a selective environment in which species with higher lipid production capability were enriched [22]. A comparison between our initial results and those achieved in previous studies on lipids production by microalgae in continuous systems is reported in Table 10.1.

Table 10.1. Algal cultivation for improved biomass growth and lipid content in continuous mode

Specie	Reactor	Carbon	Nitrogen	Dilution rate	Lipids productivity	Other conditions	Lipids production strategy	Ref
D. tertiolecta	Type= Cylinder; V= 6 L; d= NR.	4% v/v CO_2-enriched air; Gas flow rate = 30mL min^{-1}; Other sources= no.	Source= $NaNO_3$; [N]= 1.64 mg L^{-1}.	0.17-0.74 d^{-1} (0.42 optimal value).	9.8 $mgL^{-1}d^{-1}$ 10.8% DW	T= 25°C; pH= initial 7.8, not controlled; Mechanical agitation= 600 rpm; Incident irradiance= 50 µmol m^{-2} s^{-1}.	Optimization of dilution rate; Vitamin B_{12} addition.	[24])
Chlorella pyrenoidosa XQ-20044	Type= Cylinder; V=2 L; d=10 cm.	1% v/v CO_2-enriched air; Gas flow rate = 2 L min^{-1}; Other sources= Na_2CO_3 (0.18 mM).	Source= $NaNO_3$; [N]= 3.29, 6.59, 9.88, 13.2, 16.4, 31.3 and 49.4 mg L^{-1} (9.88 optimal value)	0.24-2.4 d^{-1} (0.48 optimal value).	144 $mgL^{-1}d^{-1}$ 34.69 %DW	T= 30°C; pH= 7-8; Mechanical agitation= NP; Incident irradiance= 600 µmol m^{-2} s^{-1}.	Optimization of nitrogen concentration and dilution rate.	[16]
Choricystis minor B. Fott	Type= Cylinder; V= 3.5 L; d=17.8 cm.	1.58% v/v CO_2-enriched air; Gas flow rate = 4.7 L min^{-1}; Other sources= Na_2CO_3 (0.009 mM).	Source= $NaNO_3$; [N]= 252 mg L^{-1}.	0.12-4.8 d^{-1} (0.33 optimal value).	82 $mgL^{-1}d^{-1}$ 29.7% DW	T=10-30°C, optimal value= 25°C; pH= 6; Mechanical agitation= 200 rpm; Incident irradiance= 500 µmol m^{-2} s^{-1}.	Optimization of dilution rate and temperature; Investigation on the lipids extraction method.	[25])
Parachlorella kessleri UTEX2229	Type= Flat panel; V= 1 L; d=3 cm (thickness).	Air; Gas flow rate = 100 mL min^{-1}; 100% CO_2 was injected to control the pH. Other sources= $NaHCO_3$ (0.005 mM).	Source= $NaNO_3$; [N]= 214, 69.1, 51, 31.2, 14 mg L^{-1} (51 optimal value).	0.24 d^{-1}.	85.8 $mgL^{-1}d^{-1}$ 20% DW	T= 22 °C; pH= 8; Mechanical agitation= NP; Incident irradiance= 250 µmol m^{-2} s^{-1}.	Optimization of the nitrogen concentration	[11]
Neochloris oleoabundans	Type= Flat panel; V= 1.7 L; d= 2 cm (thickness).	2% v/v CO_2-enriched N_2; Gas flow rate = 1.2 L min^{-1}; Other sources= $NaHCO_3$ (10 mM).	Source= $NaNO_3$; [N]= 19.7, 5.76, 3.46, and 2.14 mg $L^{-1}d^{-1}$ for Low Light and 33.9, 11.5, 9.05, 5.76 (optimal) and 3.46 g $L^{-1}d^{-1}$ for High Light.	0.18-1.15 d^{-1}.	46 $mgL^{-1}d^{-1}$ 12.4% DW	T= 30 °C; pH=7.5; Mechanical agitation= NP; Incident irradiance= Low Light - 200 µmol m^{-2} s^{-1}, High Light - 500 µmol m^{-2} s^{-1} (optimal value).	Optimization of the nitrogen concentration and the incident irradiance; Constant energy intake by turbidostat operation.	[14]

Acutodesmus obliquus starchless mutant	Type= Flat panel; V= 1.7 L; d= 2 cm (thickness).	1% v/v CO_2-enriched N_2; Gas flow rate = 1 L min^{-1}; Other sources= $NaHCO_3$ (10 mM).	Nitrates Optimal: 7 ± 1 mgN $mol_{photons}^{-1}$	Not reported	157 $mgL^{-1}d^{-1}$ 33% DW	T= 27.5 °C; pH=7; Mechanical agitation= NP; Incident irradiance= 500 µmol m^{-2} s^{-1} ,16 h light and 8 h dark.	Nitrogen limitation under light/dark cycles; Vitamins addition (B_1, B_7, B_{12}).	[17]
Chlorella sp. A2	Type= NR; V= 4 L; d= NR.	Air; Gas flow rate =NR; Other sources= Na_2CO_3 (0.009 mM).	Source= CH_4N_2O; [N]= First mode: 2.1, 4.2, 9.4, 4.2x Int (OD_{680}/2.5+1) mg L^{-1} (optimal). It means that 4.2 mgN L^{-1} were added daily if OD<2.5 and additional 4.2 for every increase in OD_{680} 2.5 Second mode: 8.4 mgN L^{-1} daily (optimal), every 2,3 or 4 days.	Not reported	29.9 $mgL^{-1}d^{-1}$ 22.7 %DW	T= outdoor temperature; pH= NR; Mechanical agitation= NP; Incident irradiance= Natural light at a light intensity > 6000 lux.	Minimal nitrogen supply.	[26]
*Chlorella*PY-ZU	Type= Cylinder; V= NR; d= NR.	15% v/v CO_2-enriched N_2; Gas flow rate = 0.1 vvm; Other sources= Na_2CO_3 (0.009 mM).	Source= $NaNO_3$; [N]=First stage - 247 mg L^{-1}, second stage - 0 gL^{-1}.	Not reported	191.3 $mgL^{-1}d^{-1}$ 42.10% DW	T= 27 °C pH= NR; Mechanical agitation= NP; Incident irradiance= Light intensity of approximately 8500 lux, 16 h light and 8 h dark	Two steps process: First step-nitrogen sufficient, second step-nitrogen starvation and phosphorous addition.	[27]
Ettlia sp. YC001	Type= Cylinder; V= 0.8 L; d= 9.5 cm.	10% v/v CO_2-enriched air; Gas flow rate = 150 mL min^{-1}; Other sources= no.	Source= $NaNO_3$; [N]=252 mg L^{-1}.	0.2-0.8 d^{-1} (0.79 optimal value).	291.4 $mgL^{-1}d^{-1}$ 23.1% DW	T= 25-28 °C; pH= 6.5-10.5 (optimal value 6.5); Mechanical agitation= NP; Incident irradiance= 260-1500 µmol m^{-2} s^{-1} (1500 optimal value).	Optimization of pH, light intensity and dilution rate.	[15]

Chlorella vulgaris OW-01	Type= Cylinder; V: 3 L; d: 17 cm.	Air, 3% v/v CO_2-enriched air (optimal); Gas flow rate = 600 mL min^{-1}; Other sources= Na_2CO_3 (0.009 mM).	Source= $NaNO_3$; [N]=247 mg L^{-1}.	0.08-1.5 d^{-1} (0.75 optimal value).	270 $mgL^{-1}d^{-1}$ 32% DW	T: 25°C; pH= not controlled; Mechanical agitation= 120 rpm; Incident irradiance= 500 µmol m^{-2} s^{-1}.	Two steps process: First step- compensation of limiting growth factors to reach the highest biomass productivity, second step- optimization of the dilution rate.	[28]
Ettilia sp. YC001	Type= Cylinder; V: 5 L; d: 25 cm.	10% v/v CO_2-enriched air (optimal); Gas flow rate = 1 L min^{-1} at 5 s intervals; Other sources= Na_2CO_3 (0.009 mM).	Source= $NaNO_3$; [N]=247 mg L^{-1}.	0.2 d^{-1}.	49.7 $mgL^{-1}d^{-1}$ 51% DW	T= 25 °C; pH= 6.5, 8.5 (optimal value), 10.5; Mechanical agitation= NP; Incident irradiance= 500 µmol m^{-2} s^{-1}.	pH control via CO_2 rather than chemical pH control.	[15]
Scenedesmus obliquus	Type= Flat panel; V: 0.25 L; d:1.2 cm.	CO_2-enriched air; Other sources= Na_2CO_3 (0.009 mM).	Source= $NaNO_3$; [N]=247 mg L^{-1}.	0.31 d^{-1}.	318 $mgL^{-1}d^{-1}$ 39% DW	T= 23 °C; pH= 8; Mechanical agitation= NP; Incident irradiance= 100 µmol m^{-2} s^{-1}.	Investigation on biomass recycle (optimal condition without recycle).	[29]
Mixed culture	Type= Cylinder; V: 2 L; d:12 cm	6% v/v CO_2-enriched air; Other sources= no.	Source= NH_4Cl; [N]=42 mg L^{-1}.	0.5 d^{-1}.	429.6 $mgL^{-1}d^{-1}$ 18% DW	T= 30 °C; pH= 7.5; Mechanical agitation= 150 rpm; Incident irradiance= 350 µmol m^{-2} s^{-1}.	Vitamins addition; Dual limitation (nitrogen and light) strategy.	This study

N.R.= Not reported
N.P.= Not performed

From the analysis of the considered works it emerged that all authors studied pure cultures to produce lipids. One of the most used strategies to enhance the lipids accumulation was nitrogen limitation, using a continuous low nitrogen loading rate [11,14,16]. Chu et al. [27] adopted a two-step strategy. The first step was conducted under non-limiting nitrogen conditions while the second one was under complete nitrogen starvation (0 $mgL^{-1}d^{-1}$). Remmers et al. [17] adopted an alternating light/dark strategy (500 µmol m^{-2} s^{-1}, 16 h light and 8 h dark) to induce the stress condition. In the same study, vitamins addition (B_1, B_7, B_{12}) was performed to enhance the productivity. The latter strategy was adopted by Tang et al. [24], as well.

The comparison between our initial results with literature reveals that the lipids content (%DW) in our study was similar or lower compared to those of pure cultures. On the other hand, the overall lipids productivity achieved in our chemostat was higher than other studies due to the higher biomass accumulation. These results underline that the DL chemostat enrichment conditions is a promising methodology to select lipid producing microalgae and enhance the lipids productivity.

10.4. Conclusions

Lipids production in a chemostat based enrichment system was studied in this work. The presented ecology-based method effectively enriched microalgae with a higher lipids production capability over starch. The supplementation of vitamins and silicate to the medium provided a selective environment in which species with higher lipid production capability were enriched. Moreover, the dual limitation strategy further enhanced the lipids accumulation and contextually avoided the loss in biomass formation, which is usually associated with nitrogen limitation as the sole stress inducing condition. Currently, we are performing further investigations to validate the reported preliminary results. Nonetheless, we believe that our findings may represent a step forward in the large-scale microalgae cultivation.

References

[1] Mandl Nicole (EEA), Pinterits Marion (EEA), Mandl N (ETAC), Pinterits M (ETC). Annual European Union greenhouse gas inventory 1990-2018 and inventory report 2020 2020:977.

[2] Ebadian M, van Dyk S, McMillan JD, Saddler J. Biofuels policies that have encouraged their production and use: An international perspective. Energy Policy 2020;147:111906. https://doi.org/10.1016/j.enpol.2020.111906.

[3] Mata TM, Martins AA, Caetano NS. Microalgae for biodiesel production and other applications: A review. Renew Sustain Energy Rev 2010;14:217–32. https://doi.org/10.1016/j.rser.2009.07.020.

[4] Behera B, Unpaprom Y, Ramaraj R, Maniam GP, Govindan N, Paramasivan B. Integrated biomolecular and bioprocess engineering strategies for enhancing the lipid yield from microalgae. Renew Sustain Energy Rev 2021;148:111270. https://doi.org/10.1016/j.rser.2021.111270.

[5] Rawat I, Ranjith Kumar R, Mutanda T, Bux F. Biodiesel from microalgae: A critical evaluation from laboratory to large scale production. Appl Energy 2013;103:444–67. https://doi.org/10.1016/j.apenergy.2012.10.004.

[6] Mooij PR, Stouten GR, Tamis J, Van Loosdrecht MCM, Kleerebezem R. Survival of the fattest. Energy Environ Sci 2013;6:3404–6. https://doi.org/10.1039/c3ee42912a.

[7] Kleerebezem R, van Loosdrecht MC. Mixed culture biotechnology for bioenergy production. Curr Opin Biotechnol 2007;18:207–12. https://doi.org/10.1016/j.copbio.2007.05.001.

[8] Li T, Gargouri M, Feng J, Park JJ, Gao D, Miao C, et al. Regulation of starch and lipid accumulation in a microalga Chlorella sorokiniana. Bioresour Technol 2015;180:250–7. https://doi.org/10.1016/j.biortech.2015.01.005.

[9] Sharma KK, Schuhmann H, Schenk PM. High lipid induction in microalgae for biodiesel production. Energies 2012;5:1532–53. https://doi.org/10.3390/en5051532.

[10] Sibi G, Shetty V, Mokashi K. Enhanced lipid productivity approaches in microalgae as an alternate for fossil fuels – A review. J Energy Inst 2016;89:330–4. https://doi.org/10.1016/j.joei.2015.03.008.

[11] Kandilian R, Taleb A, Heredia V, Cogne G, Pruvost J. Effect of light absorption rate and nitrate concentration on TAG accumulation and productivity of Parachlorella kessleri cultures grown in chemostat mode. Algal Res 2019;39:101442. https://doi.org/10.1016/j.algal.2019.101442.

[12] Hu Q, Sommerfeld M, Jarvis E, Ghirardi M, Posewitz M, Seibert M, et al. Microalgal triacylglycerols as feedstocks for biofuel production: Perspectives and advances. Plant J 2008;54:621–39. https://doi.org/10.1111/j.1365-313X.2008.03492.x.

[13] Mooij PR. On the use of selective environments in microalgal cultivation. 2016.

[14] Klok AJ, Martens DE, Wijffels RH, Lamers PP. Simultaneous growth and neutral lipid accumulation in microalgae. Bioresour Technol 2013;134:233–43. https://doi.org/10.1016/j.biortech.2013.02.006.

[15] Seo SH, Ha JS, Yoo C, Srivastava A, Ahn CY, Cho DH, et al. Light intensity as major factor to maximize biomass and lipid productivity of Ettlia sp. in CO2-controlled photoautotrophic chemostat. Bioresour Technol 2017;244:621–8. https://doi.org/10.1016/j.biortech.2017.08.020.

[16] Wen X, Geng Y, Li Y. Enhanced lipid production in Chlorella pyrenoidosa by continuous culture. Bioresour Technol 2014;161:297–303. https://doi.org/10.1016/j.biortech.2014.03.077.

[17] Remmers IM, Hidalgo-Ulloa A, Brandt BP, Evers WAC, Wijffels RH, Lamers PP. Continuous versus batch production of lipids in the microalgae Acutodesmus obliquus. Bioresour Technol 2017;244:1384–92. https://doi.org/10.1016/j.biortech.2017.04.093.

[18] Egli T, Quayle JR. Influence of the carbon: Nitrogen ratio of the growth medium on the cellular composition and the ability of the methylotrophic yeast Hansenula polymorpha to utilize mixed carbon sources. J Gen Microbiol 1986;132:1779–88. https://doi.org/10.1099/00221287-132-7-1779.

[19] Durner R, Witholt B, Egli T. Accumulation of poly[(R)-3-hydroxyalkanoates] in Pseudomonas oleovorans during growth with octanoate in continuous culture at different dilution rates. Appl Environ Microbiol 2000;66:3408–14. https://doi.org/10.1128/AEM.66.8.3408-3414.2000.

[20] Poblete-Castro I, Escapa IF, Jäger C, Puchalka J, Chi Lam CM, Schomburg D, et al. The metabolic response of P. putida KT2442 producing high levels of polyhydroxyalkanoate under single- and multiple-nutrient-limited growth: Highlights from a multi-level omics approach. Microb Cell Fact 2012;11:1–21. https://doi.org/10.1186/1475-2859-11-34.

[21] Cavaillé L, Albuquerque M, Grousseau E, Lepeuple AS, Uribelarrea JL, Hernandez-Raquet G, et al. Understanding of polyhydroxybutyrate production under carbon and phosphorus-limited growth conditions in non-axenic continuous culture. Bioresour Technol 2016;201:65–73. https://doi.org/10.1016/j.biortech.2015.11.003.

[22] Fazeli Danesh A, Mooij P, Ebrahimi S, Kleerebezem R, van Loosdrecht M. Effective role of medium supplementation in microalgal lipid accumulation. Biotechnol Bioeng 2018;115:1152–60. https://doi.org/10.1002/bit.26548.

[23] Mooij PR, de Jongh LD, van Loosdrecht MCM, Kleerebezem R. Influence of silicate on enrichment of highly productive microalgae from a mixed culture. J Appl Phycol

2016;28:1453–7. https://doi.org/10.1007/s10811-015-0678-2.

[24] Tang H, Chen M, Simon Ng KY, Salley SO. Continuous microalgae cultivation in a photobioreactor. Biotechnol Bioeng 2012;109:2468–74. https://doi.org/10.1002/bit.24516.

[25] Sobczuk TM, Chisti Y. Potential fuel oils from the microalga Choricystis minor. J Chem Technol Biotechnol 2010;85:100–8. https://doi.org/10.1002/jctb.2272.

[26] Zhu J, Chen W, Chen H, Zhang X, He C, Rong J and Wang Q. Improved productivity of Neutral Lipids in Chlorella sp. A2 by Minimal Nitrogen Supply. Frontoers in Microbiology, 2016. https//doi.org/10.3389/fmicb.2016.00557.

[27] Chu F, Cheng J, Zhang X, Ye Q, Zhou J. Enhancing lipid production in microalgae Chlorella PY-ZU1 with phosphorus excess and nitrogen starvation under 15% CO2 in a continuous two-step cultivation process. Chem Eng J 2019;375:121912. https://doi.org/10.1016/j.cej.2019.121912.

[28] Cho DH, Ramanan R, Heo J, Shin DS, Oh HM, Kim HS. Influence of limiting factors on biomass and lipid productivities of axenic Chlorella vulgaris in photobioreactor under chemostat cultivation. Bioresour Technol 2016;211:367–73. https://doi.org/10.1016/j.biortech.2016.03.109.

[29] Sforza E, Enzo M, Bertucco A. Design of microalgal biomass production in a continuous photobioreactor: An integrated experimental and modeling approach. Chem Eng Res Des 2014;92:1153–62. https://doi.org/10.1016/j.cherd.2013.08.017.

[30] Johnson K, Jiang Y, Kleerebezem R, Muyzer G, Van Loosdrecht MCM. Enrichment of a mixed bacterial culture with a high polyhydroxyalkanoate storage capacity. Biomacromolecules 2009;10:670–6. https://doi.org/10.1021/bm8013796.

[31] Coelho RS, Vidotti ADS, Reis ÉM, Franco TT. High cell density cultures of microalgae under fed-batch and continuous growth. Chem Eng Trans 2014;38:313–8. https://doi.org/10.3303/CET1438053.

Chapter 11

Conclusions and perspectives

Conclusions and perspectives

This thesis deals with waste biomass valorisation via mixed cultures biological processes. From the study of the state of the art, it emerged that one of the main drawbacks to the scale-up of innovative biological systems (e.g. dark and photo fermentation) is the wide use of pure cultures, which require aseptic environments and carefully controlled conditions. Nonetheless, focusing on a desired characteristic rather than on a specific strain, the issue of contamination can become a value. Mixed cultures with the desired metabolic capacity confer higher robustness and lower costs to processes. However, little is known about the operational conditions to be applied to obtain suitable selective environments for the mentioned bioprocesses and the effectiveness of such technologies. Therefore, the leading research question of this work was:

How to efficiently apply the use of mixed cultures to produce energy and valuable chemicals via dark and photo fermentation of waste biomass?

To answer this question, different dark and photo fermentation applications, including lactic acid, hydrogen and PHAs production have been studied, using both experimental and modelling approaches and under different cultivation modes. Moreover, further processes (e.g. PHBV production processes and microalgal systems) have been investigated. Results achieved in this thesis represent a contribution to the paradigm shift which is occurring, showing that waste-based processes, performed using mixed cultures, can achieve similar or higher productivities compared to pure culture processes. Suitable operational conditions to be applied to select the desired culture and optimize productivities have been found. Therefore, the results of this thesis filled many knowledge gaps in the mixed cultures applications of the dark and photo fermentation processes. The main findings of the work are following reported:

In Chapter 1 and Chapter 2 of this thesis, different approaches to select lactic acid producing cultures have been studied. In particular, in Chapter 1, the semi-continuous lactic acid production from cheese whey, under uncontrolled pH, was investigated. The best results indicated that the LA productivity was enhanced when the indigenous community contained in the cheese whey substrate was used as inoculum. The selective environment, due to the uncontrolled pH, favoured the LA production by cheese whey bacteria. Conversely, the use of an external inoculum (i.e. digestate) decreased the LA productivity and purity. The improved productivity by indigenous cultures has been

demonstrated for the ethanol fermentative production, as well (Chapter 5). Ethanol production during the DF of winery wastewater, can be enhanced by the use of indigenous substrate cultures rather than an external digestate inoculum. These evidences underline that the choice of the waste substrate is paramount in fermentation processes, not only for the contained carbon compounds. Indeed, the waste characteristics can create a selective environment, allowing for the presence of suitable microbial communities.

When different substrates have to be used, it is necessary to select a community owing the desired functionality from external inocula. Chapter 2 demonstrates that it is possible to select lactic acid producing microorganisms from digestate via a bioaugmentation technique. The adopted technique was based on pH sudden variations, occurring in sequential batch steps. The bioaugmentation process allowed to increase the percentage of bacteria belonging to the genus Bacillus, which consistently enhanced the LA effluent purity.

Results from the PF stage of a sequential DF-PF process, applied to winery wastewater, showed that real ethanol-rich DFEs can be effectively converted into hydrogen by phototrophic microorganisms (Chapter 5). However, indeep investigations on the conversion of such effluents demonstrated that the process was affected by the Carbon Catabolite Repression phenomenon, due to the presence of glycerol (Chapter 4). Indeed, in the presence of both ethanol and glycerol, part of the ethanol source was converted to biomass and PHB, rather than to hydrogen. The hydrogen drop percentage was strongly affected by the ethanol to glycerol ratio. The mixed culture PF process is effective as a single stage process, as well. Indeed, as demonstrated in Chapter 6, good hydrogen and PHB productivities can be reached using winery wastewater as substrate. Concerning the most suitable operational conditions, the adoption of organic nitrogen sources and suitable dilution factors are essential to improve both the hydrogen and the PHB productivity. Comparing results obtained from the single stage PF (Chapter 6) and the double-stage DF-PF process (Chapter 5) in similar conditions, PF performances are enhanced by the addition of a previous DF stage. However, future investigations and economic analysis are required to assess whether the enhanced productivity justify the costs of two different reactors.

The use of mixed cultures has revealed to be advantageous in all performed studies on the PF process. Indeed, mixed cultures avoided pre-treatments, usually applied in

previous pure studies using DFEs or other waste as substrates. Also, mixed cultures allowed to obtain good results in terms of hydrogen and PHB production, despite the presence of inhibiting compounds (e.g. phenols, ammonium) in the culture media. Investigations on microbial communities have revealed that (open) mixed cultures can lead to higher hydrogen productivities compared to pure cultures and dark-photo co-cultures. The synergies established among different dark fermentative and photo fermentative H_2 producing species, under PF conditions, enhanced the conversion of the organic substrates to H_2, and concomitantly led to the waste substrate stabilization. Also, non-hydrogen producing bacteria might have indirectly enhanced the productivity of hydrogen producing bacteria (Chapter 7).

Mathematical models can simulate the influence of different environmental and operational conditions affecting the PF process, decreasing the need of experimental tests. The analysis of the approaches used to date to model the PF process indicates that Kinetic models are useful to describe the process by the biochemical point of view, without considering the bio-reactor hydrodynamics. Parametric Models can be utilized to study the influence and the interaction between the operational conditions. They do not take into account the biochemical process mechanism and the influence of the reactor hydrodynamics. Quite the opposite, non-ideal reactor models focus on the reactor configuration. Otherwise, the biochemical description of purple non sulfur bacteria activities is simplified. To, date there still is a lack of models considering the contextual hydrogen production and PHB accumulation (Chapter 8).

In Chapter 9, a literature study on strategies to improve the PHBV production process has been performed. The comparative examination of the existing methods to enhance the PHBV production and/or reduce the process costs indicated that one of the most interesting option is a combined biorefinery approach. In particular, the mixed cultures combined production of energy and PHBV from waste could replace fossil fuels with organic matter as a source of both biofuels and bioplastics. The adoption of the dark fermentation process as first step could be particularly interesting, due to the presence of 3HV precursors in DFEs. Indeed, the addition of precursors is capable to dramatically enhance the 3HV fraction in the produced biopolymers, resulting in enhanced mechanical and thermic characteristics. On the other hand, currently, the wide use of pure cultures and the high costs of precursors avoid the spread of large-scale applications.

The study in progress on lipids accumulation in microalgae, which is reported in Chapter 10, is giving promising preliminary results. The observed data show that lipids productivity in the adopted chemostat system is higher compared to those of other continuous reactors, operated using pure cultures. The enhanced lipids productivity is mainly due to the high biomass generation, achieved using a dual nutrient limitation strategy, rather than the nitrogen starvation only. Moreover, the presence of vitamins in the culture medium and other adopted operational conditions (e.g. silicate availability, continuous feeding mode) effectively enriched microalgae with a high lipids production capability. Future investigations include the analyses of further key factors and the microbial community structure to better understand the lipid accumulation mechanisms.

Contamination is considered the main risk in pure culture systems. However, the main focus of biotechnological processes should be the maintenance of a functionality, rather than a certain species. To this aim, contamination can represent a value to the production processes, as demonstrated in this thesis. The findings of this thesis represent interesting starting points for many possible future research directions. Further developments are required to enable the processes scale-up. In particular, perspectives include techno-economic analyses and the increase of the experiments size to pilot-scale plants.